THE
PHYSICAL REVIEW

A journal of experimental and theoretical physics established by E. L. Nichols in 1893

SECOND SERIES, VOL. 78, NO. 2 APRIL 15, 1950

A Reinterpretation of the Electron Spectra of Radioactive Ytterbium and Tantalum*

J. M. CORK, H. B. KELLER, W. C. RUTLEDGE, AND A. E. STODDARD
University of Michigan, Ann Arbor, Michigan

(Received December 8, 1949)

Highly purified ytterbium, on irradiation in the pile, yields radioactivities whose half-lives are found to be 32.4 days, 4.2 days, and 6.7 days, in addition to the 2.4-hour activity known to exist. The 32.4-day activity is assigned to Yb 169 which decays by *K*-capture to excited Tm 169, yielding no general beta-radiation, but about 30 electron conversion lines which are interpreted as due to 10 gamma-rays. Many of the gamma-rays fit into a simple level scheme. The 4.2-day activity is assigned to Yb 175 and in addition to a strong beta-radiation shows conversion electron lines indicative of 4 gamma-rays. It is shown that the 6.7-day activity is a daughter product in lutecium 177, growing from a radioactive ytterbium 177 which is presumably the well-known 2.4-hour activity.

A re-interpretation of the approximately 40 electron conversion lines in radioactive tantalum 182 leads to 18 gamma-rays, all of which fit well a proposed energy level scheme.

IN previous investigations, specimens of ytterbium and tantalum, irradiated in the Oak Ridge pile, were each found[1] to yield an exceedingly complicated electron spectrum. Continued study of these results has led to interpretations somewhat different from that originally reported.

YTTERBIUM

Ytterbium exists in nature as seven stable isotopes whose percentages of abundance are shown in Fig. 1. An available specimen supposedly chemically pure, gave numerous electron lines some of which showed *K–L–M* differences indicative of impurities, particularly erbium. A later specimen, of high purity, was prepared and kindly made available to us by Dr. F. H. Spedding, of Iowa State College. To check the purity of the two specimens both were examined in a Siegbahn vacuum x-ray spectrometer. The former sample showed clearly the presence of many impurities including erbium, while the Spedding sample gave no trace of neighboring elements as shown in Fig. 2.

Surprisingly, however, the pure ytterbium specimen gave most of the same electron lines that had been observed with the impure sample. Moreover, the *K–L–M* differences of certain of the groups were characteristic of thulium ($Z=69$), as would have been expected following beta-emission from a radioactive erbium. Other electron lines had *K–L–M* differences characteristic of hafnium and were recognized as exactly those due to the 6.7-day activity in radioactive lutecium. These observations may now be completely reconciled to an initially pure ytterbium. The electron lines are shown in column 1, Table I, together with their interpretation.

No long-lived activity (>100 days) as found in the impure specimen was observed in the Spedding sample. This activity has now been shown to be the 120-day emitter, thulium 170, which is formed as shown in Fig. 1. The decay curve of the pure ytterbium is shown in Fig. 3 and except for the well-known short-period activity (2.4 hour), may be resolved into three distinct activities whose half-lives are 32.4 day, 4.2 day, and 6.7 day. It had been proposed[2] by Bothe that the 33-day activity existed in Yb 169 and that it decayed by *K*-capture. Since this isotope would be made by neutron

ELEMENT		MASS									
		168	169	170	171	172	173	174	175	176	177
THULIUM	69		100 AK								
YTTERBIUM	70	0.06	32d	4.2	14.2	21.5	17.0	29.8	4.20 Yb	13.4	2.4h
LUTECIUM	71								97.5	2.5	6.7d
HAFNIUM	72							0.2		5.3	18.5 Yb

FIG. 1. The stable and radioactive isotopes of ytterbium.

* Supported by ONR and AEC.

[1] Cork, Keller, Rutledge, Stoddard, and Sazynski, Phys. Rev. 75, 1133 (1949); 75, 1778 (1949).

[2] W. Bothe, Zeits. f. Naturforschung 4, 173 (1946).

TABLE I. Electron energies from irradiated ytterbium.

Electron energy	Interpretation and energy sum Thulium	Lutecium	Hafnium	Electron energy	Interpretation and energy sum Thulium	Lutecium	Hafnium
34.0	K^2 93.5 kev			117.8	K^5 177.3 kev		
39.0	Auger L			120.9	$L_{1,2}{}^4$ 130.8		
or	$L_{1,2}{}^a$ 49.0			122.0	$L_3{}^4$ 130.6		
40.5	$L_3{}^a$ 49.1			128.5	M^4 130.8		
46.9	Auger M			130.0	N^4 130.5		
or	M^a 49.2			138.7	K^5 198.2		
50.2	K^3 109.7			143.5			K^2 208.9
52.8	$L_{1,2}{}^1$ 62.7			167.0	$K_{1,2}{}^5$ 176.9		
54.3	$L_3{}^1$ 62.9			168.2	$L_3{}^5$ 176.8		
58.5	L^b 68.4			174.6	M^5 176.8		
or	K^b 118.0			176.4	N^5 176.9		
60.7	M^1 63.0			188.2	$L_{1,2}{}^6$ 198.1		
62.5	N^1 63.0			195.6	M^6 197.9		
71.0	K^4 130.5			or		K^a 259.0	
74.1		K^1 137.5		197.3	N^6 197.3		
83.5	$L_{1,2}{}^2$ 93.4			219.2		K^2 282.6	
85.0	$L_3{}^2$ 93.6			248.2	K^7 307.7		
91.3	M^2 93.6			or		$L_{1,2}{}^a$ 258.8	
99.8	L^3 109.7			297.8	L^7 307.7		
102.3			$L_{1,2}{}^1$ 113.3	304.5	M^7 306.8		
107.5	M^3 109.8			333.0		K^3 396.4	
109.5	N^3 110.0			385.5		$L_{1,2}{}^3$ 396.2	
110.8			M^1 113.4				

capture in the pile from Yb 168, whose abundance is only 0.06 percent the assignment might have been doubted. The present investigation, however, unquestionably confirms this interpretation indicating an enormously large cross section for neutron capture in Yb 168.

In fact, about 30 of the more than 40 observed electron lines shown in Table I decay with the 32.4-day half-life and all fit the K–L differences of thulium ($Z=69$). Since no ytterbium exists in the initial specimen, and stable thulium exists only as mass 169, then the excited states in thulium could only follow K-capture in Yb 169. The electron groups thus indicate about 10 gamma-rays for thulium 169, most of which fit well the level scheme proposed in Fig. 4.

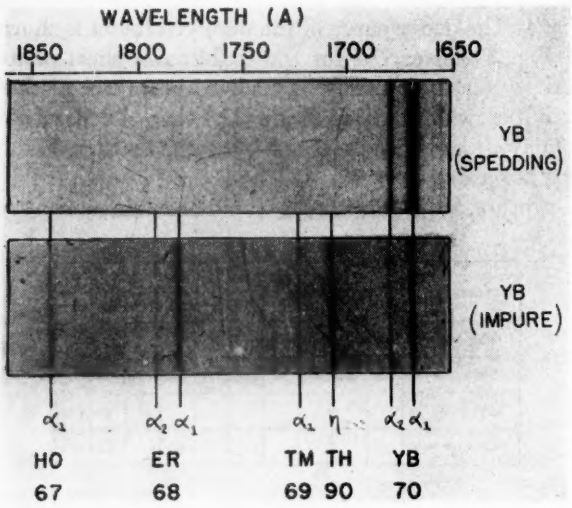

FIG. 2. Test for impurities in ytterbium by x-ray analysis using a Siegbahn vacuum spectrometer, showing the L series lines.

A relatively small number of the electron lines are satisfied by K–L differences in lutecium and are thus really due to a radioactive ytterbium decaying by beta-emission. These lines die out with the 4.2-day half-life and indicate the existence of four gamma-rays. These gamma-energies may be related by some scheme as suggested in Fig. 5, and are undoubtedly associated with the isotope of mass 175 as will be shown.

By neutron capture in the pile, Yb 176 might be expected to produce radioactive Yb 177. This could decay only by successive beta-emissions through lutecium 177 (well known),[3] to hafnium 177. A question might arise (Fig. 1) as to the assignment of the 4.2-day and the 2.4-hour activities to the isotopes of mass 175 and 177. From the decay curve it is apparent that the initial activity of the 4.2-day emitter is enormously

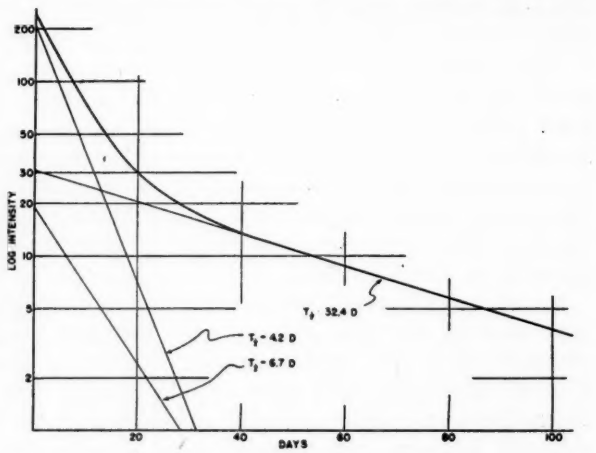

FIG. 3. Decay curve of irradiated ytterbium, resolved into its three components.

[3] Cork, Keller, and Stoddard, Phys. Rev. **76**, 986 (1949).

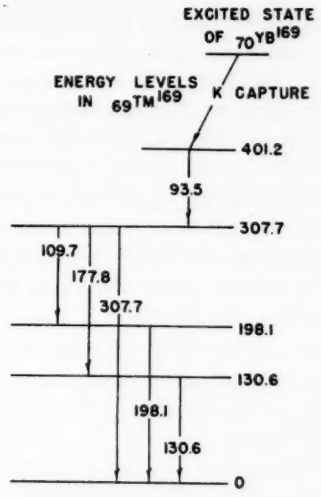

FIG. 4. Energy levels (kev) in thulium 169, following K-capture in ytterbium 169.

greater than that of the 6.7-day lutecium. Had the latter isotope grown as a daughter product from the 4.2-day activity, then it would have been relatively stronger when first examined, which was not the case. Hence, it is highly probable that the 4.2-day activity is made from Yb 174 which must also have a relatively large cross section to account for the strong yield. This would then reasonably leave the 2.4-hour emitter to be Yb 177, from which the daughter product Lu 177 is derived by beta-emission.

No continuous beta-emission for the 32.4-day activity is apparent on the photographic plates, which is as would be expected in the K-capture process, whereas a very dense general blackening accompanies the electron lines due to the 4.2-day emitter. The upper limit of this beta-radiation as determined by the Feather rule

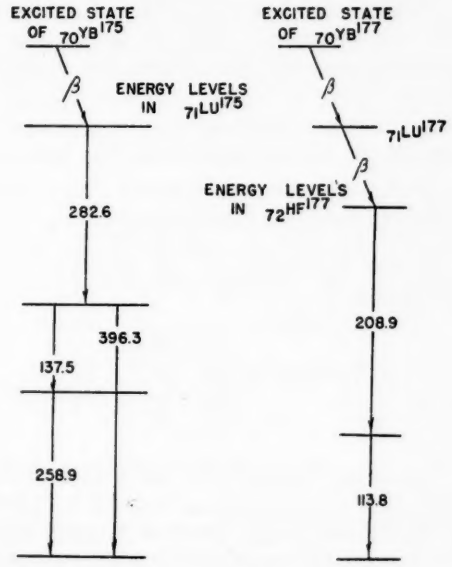

FIG. 5. Level schemes (kev) for Lu 175 following beta-emission from Yb 175 and for Hf 177 following successive beta-emissions from Yb 177.

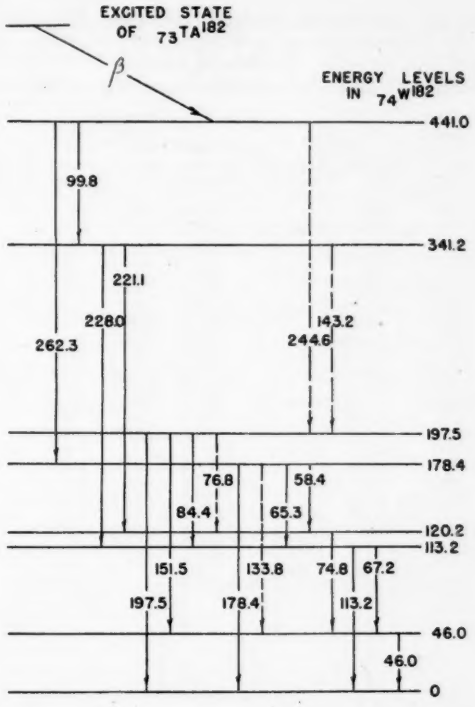

FIG. 6. Excited levels (kev) in W 182 following beta-emission from Ta 182.

from absorption in aluminum is about 0.39 Mev. The gamma-energies from each of the three radioactive isotopes are tabulated in Table II.

TANTALUM

The electron spectrum from irradiated tantalum, consisting as it does of around 40 lines, has been rephotographed many times, leading to some slight adjustment in the reported energy of each line. It is now known that the fine structure of the L lines is in some cases resolved on the photographic plates. This process was originally thought to be too unlikely to be visible. As a result, it is now possible to re-interpret the observed electron lines shown collectively in Table III, so as to yield the gamma-energies shown in columns 4 and 8. Certain less distinct lines previously reported,

TABLE II. Summary of gamma-energies (kev) derived from ytterbium.

Arbitrary line no.	Yb 169 (32.4 day)	Yb 175 (4.2 day)	Lu 177 (6.7 day)
1	63.0	137.5	113.4
2	93.5	282.6	208.9
3	109.7	396.3	
4	130.6		
5	176.8		
6	198.1		
7	307.7		
a	49.1	258.9	
b	68.4 or 118.0		

TABLE III. The electron energies (kev) from radioactive tantalum 182. (Superscripts are arbitrary numbers assigned to the gamma-rays in the order of increasing energy.)

Electron energy	Proposed interpretation	Energy sum	Gamma-energy	Electron energy	Proposed interpretation	Energy sum	Gamma-energy
30.5	K^7	99.8		81.7	K^9	151.0	
33.9	$L_1{}^1$	46.0	46.0(1)	88.3	$L_{1,2}{}^7$	99.8	
43.9	K^8	113.2		89.6	$L_3{}^7$	99.8	99.8(7)
47.0	$L_{1,2}{}^2$	58.4		97.0	M^7	99.8	
48.2	$L_2{}^2$	58.4	58.4(2)	99.1	N^7	99.7	
53.6	$L_{1,2}{}^3$	65.1		101.2	$L_{1,2}{}^8$	113.3	
55.3	$L_3{}^3$	65.4	65.3(3)	102.8	$L_3{}^8$	113.0	113.2(8)
	$L_{1,2}{}^4$	66.9		109.2	K^{10}	178.5	
	M^3	58.3		110.3	M^8	113.1	
57.2	$L_2{}^4$	67.4	67.2(4)	128.2	K^{11}	197.5	
62.5	$L_1{}^5$	74.6		139.9	$L_1{}^9$	152.0	151.5(9)
	M^3	65.3		151.8	K^{12}	221.1	
64.7	$L_3{}^5$	74.9	74.8(5)	158.7	K^{13}	228.0	
	M^4	67.5		166.2	$L_1{}^{10}$	178.3	178.4(10)
	($L_1{}^a$)	(76.8)	76.8(a)	175.3	M^{10}	178.1	
	(K^b)	(133.8)	133.8(b)		K^d	244.6	244.6(d)
66.7	N^4	67.3		185.5	$L_1{}^{11}$	197.6	197.5(11)
72.1	M^5	74.9		193.0	K^{14}	262.3	
	$L_{1,2}{}^6$	84.2		209.5	$L_{1,2}{}^{12}$	221.2	221.1(12)
74.0	$L_3{}^6$	84.4	84.4(6)	216.1	$L_{1,2}{}^{13}$	228.1	228.0(13)
	(M^a)	(76.8)		225.1	M^{13}	227.9	
	(K^c)	(143.2)	143.2(c)	250.6	$L_{1,2}{}^{14}$	262.4	262.3(14)
81.7	M^6	84.5		259.5	M^{14}	262.3	

probably exist, but since they cannot be evaluated with the same certainty, they are omitted in this report.

All fourteen of the strong gamma-rays indicated by this interpretation fit well a proposed level scheme as shown in Fig. 6. Among other possible transitions, gamma-rays of energy 76.8, 133.8, 143.2, and 243.9 kev would also be expected. On critically examining the electron energies, it may be noted that a double interpretation of certain electron lines would in fact yield these gamma-rays. These four gamma-values are shown by arbitrary letters a, b, c, and d instead of numbers in Table III and are indicated as dotted lines in Fig. 6.

Additional high energy gamma-rays are known[4] to exist in tantalum with energies of about 1.12, 1.19, and 1.234 Mev.

This investigation was made possible by the support of the ONR and the AEC.

[4] C. H. Goddard and C. S. Cook, Phys. Rev. **76**, 1419 (1949); W. Rall and R. G. Wilkinson, Phys. Rev. **71**, 321 (1947).

PHYSICAL REVIEW VOLUME 78, NUMBER 2 APRIL 15, 1950

Quantum Electrodynamics: The Self-Energy Problem*

HARTLAND S. SNYDER
Brookhaven National Laboratories, Upton, Long Island, New York
(Received December 5, 1949)

In this paper it will be shown that the limiting processes by means of which the integrals of the Hamiltonian of the interacting electron-positron field with the electromagnetic field are defined, may be carried out so that the self-energies of the electrons and photons are zero.

I. INTRODUCTION

FIELD theories have been plagued by the appearance of divergent expressions for the self-energies of the elementary particles. The purpose of this paper is to show that by the use of appropriate limiting processes for the integrals which define the Hamiltonian of the interacting fields, one can in fact obtain the value zero for the self-energy integrals. Although we will work here only with the electron-positron field in interaction with the electromagnetic field, I believe that the technique used here will also enable one to eliminate the self-energy problem in other cases as well.

This work will be carried out in a momentum space representation. In this representation the Hamiltonian for the interacting electron-positron field and the electromagnetic field, may be written

$$H=\int d\mathbf{p}d\mathbf{p}'\delta(\mathbf{p}-\mathbf{p}')e_{\mathbf{p}s}(\alpha_{\mathbf{p}s}{}^{+}\alpha_{\mathbf{p}'s})+\int d\mathbf{k}d\mathbf{k}'\delta(\mathbf{k}-\mathbf{k}')ka_{\mathbf{k}\lambda}{}^{+}a_{\lambda\mathbf{k}'}-\frac{e}{2\pi}\int d\mathbf{p}d\mathbf{p}'d\mathbf{k}\frac{\delta(\mathbf{p}-\mathbf{p}'-\mathbf{k})}{(k)^{\frac{1}{2}}}$$

$$\times\{(\alpha_{\mathbf{p}s}{}^{+}\alpha_{\mathbf{p}'s'})a_{\lambda\mathbf{k}}(\mathbf{p}s|\boldsymbol{\varepsilon}_{\lambda\mathbf{k}}\cdot\boldsymbol{\alpha}|\mathbf{p}'s')+(\alpha_{\mathbf{p}'s'}{}^{+}\alpha_{\mathbf{p}s})a_{\mathbf{k}\lambda}{}^{+}(\mathbf{p}'s'|\boldsymbol{\varepsilon}_{\lambda\mathbf{k}}\cdot\boldsymbol{\alpha}|\mathbf{p}s)\}+\frac{e^2}{(2\pi)^2}\int\frac{d\mathbf{p}d\mathbf{p}'d\mathbf{p}''d\mathbf{p}'''}{|p-p'|^2}\delta(\mathbf{p}-\mathbf{p}'+\mathbf{p}''-\mathbf{p}''')$$

$$\times(\alpha_{\mathbf{p}s}{}^{+}\alpha_{\mathbf{p}'s'})(\alpha_{\mathbf{p}''s''}{}^{+}\alpha_{\mathbf{p}'''s'''})(\mathbf{p}s|1|\mathbf{p}'s')(\mathbf{p}''s''|1|\mathbf{p}'''s'''). \quad (1)$$

At this point remarks concerning the notation used in (1) are appropriate. I am using units such that $\hbar=c=1$, $e^2\simeq 1/137$. Symbols printed in bold face type are vectors, $d\mathbf{p}$ is a small volume of momentum space. $\boldsymbol{\alpha}$ is the Dirac vector with 4×4 matrix components α_1, α_2, α_3, which satisfy the relation $\alpha_i\alpha_j+\alpha_j\alpha_i=2\delta_{ij}$. The other Dirac matrix β satisfied $\beta\alpha_i+\alpha_i\beta=0$, $\beta^2=1$, with 1 the 4×4 unit matrix. By the symbol $(\mathbf{p}s|A|\mathbf{p}'s')$

* Work performed at the Brookhaven National Laboratory, under the auspices of the AEC.

is understood $\sum_{\alpha\beta} U_\alpha^*(\mathbf{p}s)A_{\alpha\beta}U_\beta(\mathbf{p}'s')$ in which $U_\beta(\mathbf{p}'s')$ is the βth component of the Dirac spin function corresponding to an electron of momentum $\mathbf{p}'$ and spin state s'. The spin function $U(\mathbf{p}s)$ satisfies $H_\mathbf{p}U(\mathbf{p}s)=e_{\mathbf{p}s}U(\mathbf{p},s)$ with $H_\mathbf{p}=\boldsymbol{\alpha}\cdot\mathbf{p}+m\beta$, with m the mass of the electron. The spin functions are normalized so that $(\mathbf{p}s|1|\mathbf{p}s')=\delta_{ss'}$. $U_\alpha^*(\mathbf{p}s)$ is the complex conjugate of $U_\alpha(\mathbf{p}s)$. $a_{\lambda\mathbf{k}}$ is the annihilation operator and $a_{\lambda\mathbf{k}}^+$ is the creation operator for a photon of momentum $\mathbf{k}$ and direction of polarization $\boldsymbol{\varepsilon}_{\lambda\mathbf{k}}$. λ takes on the values 1 and 2, and $\boldsymbol{\varepsilon}_{1\mathbf{k}}\cdot\mathbf{k}=\boldsymbol{\varepsilon}_{2\mathbf{k}}\cdot\mathbf{k}=\boldsymbol{\varepsilon}_{1\mathbf{k}}\cdot\boldsymbol{\varepsilon}_{2\mathbf{k}}=0$. The commutation relations satisfied by the $a_{\lambda\mathbf{k}}$ and $a_{\lambda\mathbf{k}}^+$ are

$$[a_{\lambda\mathbf{k}}, a_{\lambda'\mathbf{k}'}]=0, \quad [a_{\lambda\mathbf{k}}, a_{\lambda'\mathbf{k}'}^+]=\delta_{\lambda\lambda'}\delta(\mathbf{k}-\mathbf{k}'). \quad (2)$$

By $\delta(\mathbf{p}-\mathbf{p}')$ is meant the three-dimensional Dirac δ-function, and $\delta_{\lambda\lambda'}$ is the Kronecker δ. $\alpha_{\mathbf{p}s}$ is the annihilation operator for an electron of momentum $\mathbf{p}$ if s refers to a positive energy state; if s refers to a negative energy state then $\alpha_{\mathbf{p}s}$ is the creation operator of a positron of momentum $-\mathbf{p}$. $\alpha_{\mathbf{p}s}^+$ either creates an electron or destroys a positron according as s refers to positive or negative energy states. The commutation relations satisfied by the $\alpha_{\mathbf{p}s}^+$ and $\alpha_{\mathbf{p}s}$ are

$$[\alpha_{\mathbf{p}s}, \alpha_{\mathbf{p}'s'}]_+=0, \quad [\alpha_{\mathbf{p}s}, \alpha_{\mathbf{p}'s'}^+]_+=\delta_{ss'}\delta(\mathbf{p}-\mathbf{p}'). \quad (3)$$

The plus sign is placed on the bracket to indicate an anticommutator. Whenever a parenthesis is placed around a combination of α- and α^+-operators, it is understood that all creation operators are to be written on the left of the annihilation operators whenever this makes a difference. For example, $(\alpha_{\mathbf{p}s}^+\alpha_{\mathbf{p}'s'})=\alpha_{\mathbf{p}s}^+\alpha_{\mathbf{p}'s'}$ if either or both s or s' refer to positive energy states but $(\alpha_{\mathbf{p}s}^+\alpha_{\mathbf{p}'s'})=-\alpha_{\mathbf{p}'s'}\alpha_{\mathbf{p}s}^+$ when both s and s' refer to negative energy states. Due care must be taken as to sign so as to be consistent with the anticommutation relations (3) as in the above example. The above convention as to the meaning of $(\alpha_{\mathbf{p}s}^+\alpha_{\mathbf{p}'s'})$ then insures that the Hamiltonian (1) is the Hamiltonian of electron-positron theory.

II. THE COULOMB SELF-ENERGY

The last term of (1) gives the Coulomb interaction of the electrons and positrons with themselves and each other, and includes also the Coulomb self-energy effects to order e^2. We now observe that

$$(\alpha_{\mathbf{p}s}^+\alpha_{\mathbf{p}'s'})(\alpha_{\mathbf{p}''s''}^+\alpha_{\mathbf{p}'''s'''})$$

may be written as

$$(\alpha_{\mathbf{p}s}^+\alpha_{\mathbf{p}'s'}\alpha_{\mathbf{p}''s''}^+\alpha_{\mathbf{p}'''s'''})$$

plus additional terms. It is the additional terms which give rise to the positron and electron self-energy. We also wish to point out that the integrals which define Coulomb energy are in fact divergent and that the value of the self-energy parts of the Coulomb energy depends strongly on the limiting process by means of which such integrals over infinite domains are always defined. In considering the last term of (1) we shall suppose that the integrals over $\mathbf{p}$, $\mathbf{p}'$, $\mathbf{p}''$, and $\mathbf{p}'''$ are to be integrated over a finite region. However, for different values of the spin indices s, s', s'', and s''' these regions will in general be different. Actually, of course, because of the presence of $\delta(\mathbf{p}-\mathbf{p}'+\mathbf{p}''-\mathbf{p}''')$ in the integrand these integrals are effectively over a nine-dimensional space. One condition which we impose on these regions is that the resulting operator must be Hermitian. Another condition which we impose is that the operator shall be symmetric under the interchange of positive and negative energy states. We may now abstract from (1) the self-energy of the electrons and positrons which may be written by using projection operators for positive and negative energy states as

$$H_{cs}=\frac{e^2}{(2\pi)^2}\int d\mathbf{p}d\mathbf{p}'\delta(\mathbf{p}-\mathbf{p}') \times(\alpha_{\mathbf{p}s}^+\alpha_{\mathbf{p}'s'})(\mathbf{p}s|M_{cs}(\mathbf{p})|\mathbf{p}'s') \quad (4)$$

in which

$$\begin{aligned}M_{cs}(\mathbf{p})=&\int_{I(\mathbf{p})}\frac{d\mathbf{k}}{k^2}\Big\{\frac{e_\mathbf{p}+H_\mathbf{p}}{2e_\mathbf{p}}\frac{e_{\mathbf{p}-\mathbf{k}}+H_{\mathbf{p}-\mathbf{k}}}{2e_{\mathbf{p}-\mathbf{k}}}\frac{e_\mathbf{p}+H_\mathbf{p}}{2e_\mathbf{p}}\\&-\frac{e_\mathbf{p}-H_\mathbf{p}}{2e_\mathbf{p}}\frac{e_{\mathbf{p}-\mathbf{k}}-H_{\mathbf{p}-\mathbf{k}}}{2e_{\mathbf{p}-\mathbf{k}}}\frac{e_\mathbf{p}-H_\mathbf{p}}{2e_\mathbf{p}}\Big\}\\&+\int_{II(\mathbf{p})}\frac{d\mathbf{k}}{k^2}\Big\{\frac{e_\mathbf{p}-H_\mathbf{p}}{2e_\mathbf{p}}\frac{e_{\mathbf{p}-\mathbf{k}}+H_{\mathbf{p}-\mathbf{k}}}{2e_{\mathbf{p}-\mathbf{k}}}\frac{e_\mathbf{p}-H_\mathbf{p}}{2e_\mathbf{p}}\\&-\frac{e_\mathbf{p}+H_\mathbf{p}}{2e_\mathbf{p}}\frac{e_{\mathbf{p}-\mathbf{k}}-H_{\mathbf{p}-\mathbf{k}}}{2e_{\mathbf{p}-\mathbf{k}}}\frac{e_\mathbf{p}+H_\mathbf{p}}{2e_\mathbf{p}}\Big\}\\&+\int_{III(\mathbf{p})}\frac{d\mathbf{k}}{k^2}\Big\{\frac{e_\mathbf{p}+H_\mathbf{p}}{2e_\mathbf{p}}\frac{e_{\mathbf{p}-\mathbf{k}}+H_{\mathbf{p}-\mathbf{k}}}{2e_{\mathbf{p}-\mathbf{k}}}\frac{e_\mathbf{p}-H_\mathbf{p}}{2e_\mathbf{p}}\\&+\frac{e_\mathbf{p}-H_\mathbf{p}}{2e_\mathbf{p}}\frac{e_{\mathbf{p}-\mathbf{k}}+H_{\mathbf{p}-\mathbf{k}}}{2e_{\mathbf{p}-\mathbf{k}}}\frac{e_\mathbf{p}+H_\mathbf{p}}{2e_\mathbf{p}}\\&-\frac{e_\mathbf{p}-H_\mathbf{p}}{2e_\mathbf{p}}\frac{e_{\mathbf{p}-\mathbf{k}}-H_{\mathbf{p}-\mathbf{k}}}{2e_{\mathbf{p}-\mathbf{k}}}\frac{e_\mathbf{p}+H_\mathbf{p}}{2e_\mathbf{p}}\\&-\frac{e_\mathbf{p}+H_\mathbf{p}}{2e_\mathbf{p}}\frac{e_{\mathbf{p}-\mathbf{k}}-H_{\mathbf{p}-\mathbf{k}}}{2e_{\mathbf{p}-\mathbf{k}}}\frac{e_\mathbf{p}-H_\mathbf{p}}{2e_\mathbf{p}}\Big\}. \quad (5)\end{aligned}$$

In (5) the three different integrals carry the subscripts $I(\mathbf{p})$, $II(\mathbf{p})$, and $III(\mathbf{p})$ which indicates the finite regions in the $\mathbf{k}$ space over which the integrals are to be evaluated. These three regions depend on $\mathbf{p}$ and are not necessarily the same, as one can readily see that each term is Hermitian and invarient under the interchange of positive and negative energy states. The expression (5) for the Coulomb self-energy may

be simplified to the following form

$$M_{cs}(\mathbf{p})=\frac{H_{\mathbf{p}}}{2e_{\mathbf{p}}}\int_{I(\mathbf{p})}\frac{d\mathbf{k}}{k^2}\left(1+\frac{e_{\mathbf{p}}^2-\mathbf{p}\cdot\mathbf{k}}{e_{\mathbf{p}}e_{\mathbf{p}-\mathbf{k}}}\right)$$
$$-\frac{H_{\mathbf{p}}}{2e_{\mathbf{p}}}\int_{II(\mathbf{p})}\frac{d\mathbf{k}}{k^2}\left(1-\frac{e_{\mathbf{p}}^2-\mathbf{p}\cdot\mathbf{k}}{e_{\mathbf{p}}e_{\mathbf{p}-\mathbf{k}}}\right)$$
$$+\int_{III(\mathbf{p})}\frac{d\mathbf{k}}{k^2e_{\mathbf{p}-\mathbf{k}}}\left(\frac{\mathbf{p}\cdot\mathbf{k}}{e_{\mathbf{p}}^2}H_{\mathbf{p}}-\boldsymbol{\alpha}\cdot\mathbf{k}\right). \quad (6)$$

Define the following integrals

$$A_I(\mathbf{p})=\frac{1}{2}\int_{I(\mathbf{p})}\frac{d\mathbf{k}}{k^2e_{\mathbf{p}}};\qquad A_{II}(\mathbf{p})=\frac{1}{2}\int_{II(\mathbf{p})}\frac{d\mathbf{k}}{k^2e_{\mathbf{p}}}$$
$$B_I(\mathbf{p})=\frac{1}{2}\int_{I(\mathbf{p})}\frac{d\mathbf{k}}{k^2e_{\mathbf{p}-\mathbf{k}}};\qquad B_{II}(\mathbf{p})=\frac{1}{2}\int_{II(\mathbf{p})}\frac{d\mathbf{k}}{k^2e_{\mathbf{p}-\mathbf{k}}} \quad (7)$$
$$C_I(\mathbf{p})=\frac{1}{2}\int_{I(\mathbf{p})}\frac{d\mathbf{k}(\mathbf{p}\cdot\mathbf{k})}{k^2e_{\mathbf{p}-\mathbf{k}}e_{\mathbf{p}}^2};\qquad C_{II}(\mathbf{p})=\frac{1}{2}\int_{II(\mathbf{p})}\frac{d\mathbf{k}(\mathbf{p}\cdot\mathbf{k})}{k^2e_{\mathbf{p}-\mathbf{k}}e_{\mathbf{p}}^2}$$
$$C_{III}(\mathbf{p})=\frac{1}{2}\int_{III(\mathbf{p})}\frac{d\mathbf{k}(\mathbf{p}\cdot\mathbf{k})}{k^2e_{\mathbf{p}-\mathbf{k}}e_{\mathbf{p}}^2}.$$

Then if the integral with respect to $\mathbf{k}$ is carried out with azimuthal symmetry with respect to $\mathbf{p}$ we obtain

$$M_{cs}(\mathbf{p})=H_{\mathbf{p}}\{A_I(\mathbf{p})-A_{II}(\mathbf{p})+B_I(\mathbf{p})+B_{II}(\mathbf{p})-C_I(\mathbf{p})$$
$$-C_{II}(\mathbf{p})+2C_{III}(\mathbf{p})\}-2\boldsymbol{\alpha}\cdot\mathbf{p}e_{\mathbf{p}}^2C_{III}(\mathbf{p})/\mathbf{p}^2. \quad (8)$$

By inspection of (7) one can see that $A_I(\mathbf{p})$ and $A_{II}(\mathbf{p})$ are positive and diverge linearly with respect to the integration on $\mathbf{k}$. $B_I(\mathbf{p})$ and $B_{II}(\mathbf{p})$ are positive and diverge logarithmically with respect to integration on $\mathbf{k}$. The integrals $C_I(\mathbf{p})$, $C_{II}(\mathbf{p})$, and $C_{III}(\mathbf{p})$ may be made positive or negative or zero and in general diverge linearly with the size of the region of $\mathbf{k}$ integration. In particular we may take region $III(\mathbf{p})$ so that $C_{III}(\mathbf{p})=0$. Further, the relative shape and size of regions $I(\mathbf{p})$ and $II(\mathbf{p})$ may be taken arbitrarily many ways so that $A_I(\mathbf{p})-A_{II}(\mathbf{p})+B_I(\mathbf{p})+B_{II}(\mathbf{p})-C_I(\mathbf{p})-C_{II}(\mathbf{p})=0$, because the terms $A_I(\mathbf{p})$ and $A_{II}(\mathbf{p})$ diverge linearly while $B_I(\mathbf{p})$ and $B_{II}(\mathbf{p})$ diverge only logarithmically. This shows that the Coulomb self-energy of order e^2 may be made zero when a suitable limiting process is used to define Coulomb interaction terms of the Hamiltonian.

III. THE ELECTROMAGNETIC SELF-ENERGY OF THE ELECTRON

The interaction between the electron-positron current and the transverse electromagnetic field, as given by the third term of Eqs. (1), gives rise to an electromagnetic electron self-energy. An easy way to exhibit this self-energy is to eliminate the third terms of (1) by means of a unitary transformation.

We now transform H by means of a unitary transformation of the form e^{iS_1} in which S_1 is Hermitian, $S_1^+=S_1$. The transformed Hamiltonian, H', is given by

$$H'=e^{-iS_1}(H_0+H_1+H_2)e^{iS_1}$$
$$=H_0+\{H_1-i[S_1,H_0]\}$$
$$+\{H_2-i[S_1,H_1]-\tfrac{1}{2}[S_1,[S_1,H_0]]\}+\cdots. \quad (9)$$

The second term of (9) is of order e and will be taken to be zero by an appropriate choice of S_1. The third term of (9) is then of order e^2 and contains the electrodynamic self-energy to order e^2. We now obtain

$$[S_1,H_0]=-iH_1, \quad (10)$$

then

$$H'=H_0+H_2-(i/2)[S_1,H_1]+\cdots. \quad (11)$$

A solution of (10) for S_1 is

$$S_1=-\frac{ie}{2\pi}\int\frac{dpdp'd\mathbf{k}\delta(\mathbf{p}-\mathbf{p}'-\mathbf{k})}{(k)^{\frac{1}{2}}(e_{\mathbf{p}s}-e_{\mathbf{p}'s'}-k)}$$
$$\times\{(\alpha_{\mathbf{p}s}+\alpha_{\mathbf{p}'s'})a_{\lambda\mathbf{k}}(\mathbf{p}s|\boldsymbol{\varepsilon}_{\lambda\mathbf{k}}\cdot\boldsymbol{\alpha}|\mathbf{p}'s')$$
$$-(\alpha_{\mathbf{p}'s'}+\alpha_{\mathbf{p}s})a_{\lambda\mathbf{k}}^+(\mathbf{p}'s'|\boldsymbol{\varepsilon}_{\lambda\mathbf{k}}\cdot\boldsymbol{\alpha}|\mathbf{p}s)\}. \quad (12)$$

Using this value of S_1 we compute the electrodynamic part of H' of order e^2

$$H_{1,1}=-\frac{i}{2}[S_1,H_1]=\frac{e^2}{8\pi^2}\int\frac{dpdp'dp''dp'''d\mathbf{k}d\mathbf{k}'\delta(\mathbf{p}-\mathbf{p}'-\mathbf{k})\delta(\mathbf{p}''-\mathbf{p}'''-\mathbf{k}')}{(kk')^{\frac{1}{2}}(e_{\mathbf{p}s}-e_{\mathbf{p}'s'}-\mathbf{k})}$$
$$\times[(\alpha_{\mathbf{p}s}+\alpha_{\mathbf{p}'s'})a_{\lambda\mathbf{k}}(\mathbf{p}s|\boldsymbol{\varepsilon}_{\lambda\mathbf{k}}\cdot\boldsymbol{\alpha}|\mathbf{p}'s')-(\alpha_{\mathbf{p}'s'}+\alpha_{\mathbf{p}s})a_{\lambda\mathbf{k}}^+(\mathbf{p}'s'|\boldsymbol{\varepsilon}_{\lambda\mathbf{k}}\cdot\boldsymbol{\alpha}|\mathbf{p}s),$$
$$(\alpha_{\mathbf{p}''s''}+\alpha_{\mathbf{p}'''s'''})\alpha_{\lambda'\mathbf{k}'}(\mathbf{p}''s''|\boldsymbol{\varepsilon}_{\lambda'\mathbf{k}'}\cdot\boldsymbol{\alpha}|\mathbf{p}'''s''')+(\alpha_{\mathbf{p}'''s'''}+\alpha_{\mathbf{p}''s''})a_{\lambda'\mathbf{k}'}^+(\mathbf{p}'''s'''|\boldsymbol{\varepsilon}_{\lambda'\mathbf{k}'}\cdot\boldsymbol{\alpha}|\mathbf{p}''s'')]. \quad (13)$$

Evaluating the commutator in (13) we obtain

$$H_{1,1}=-\frac{e^2}{8\pi^2}\Bigg[\int\frac{dpdp'dp''dp'''\delta(\mathbf{p}-\mathbf{p}'+\mathbf{p}''-\mathbf{p}''')}{|\mathbf{p}-\mathbf{p}'|(e_{\mathbf{p}s}-e_{\mathbf{p}'s'}-|\mathbf{p}-\mathbf{p}'|)}(\alpha_{\mathbf{p}s}+\alpha_{\mathbf{p}'s'})(\alpha_{\mathbf{p}''s''}+\alpha_{\mathbf{p}'''s'''})$$
$$\times(\mathbf{p}s|\boldsymbol{\varepsilon}_{\lambda\mathbf{p}-\mathbf{p}'}\cdot\boldsymbol{\alpha}|\mathbf{p}'s')(\mathbf{p}''s''|\boldsymbol{\varepsilon}_{\lambda\mathbf{p}-\mathbf{p}'}\cdot\boldsymbol{\alpha}|\mathbf{p}'''s''')+\text{C.C.}\Bigg]$$
$$+\frac{e^2}{8\pi^2}\Bigg[\int\frac{dpdp'dkdk'}{(kk')^{\frac{1}{2}}}\delta(\mathbf{p}-\mathbf{p}'-\mathbf{k}-\mathbf{k}')\alpha_{\mathbf{p}s}^+\alpha_{\mathbf{p}'s'}a_{\lambda\mathbf{k}}a_{\lambda'\mathbf{k}'}$$

$$\times\Big(ps\Big|\frac{\varepsilon_{\lambda k}\cdot\alpha(e_{p-k}+H_{p-k})\varepsilon_{\lambda' k'}\cdot\alpha}{2e_{p-k}(e_{ps}-e_{p-k}-k)}+\frac{\varepsilon_{\lambda k}\cdot\alpha(e_{p-k}-H_{p-k})\varepsilon_{\lambda' k'}\cdot\alpha}{2e_{p-k}(e_{ps}+e_{p-k}-k)}$$

$$-\frac{\varepsilon_{\lambda' k'}\cdot\alpha(e_{p'+k}+H_{p'+k})\varepsilon_{\lambda k}\cdot\alpha}{2e_{p'+k}(e_{p'+k}-e_{p's'}-k)}-\frac{\varepsilon_{\lambda' k'}\cdot\alpha(e_{p'+k}-H_{p'+k})\varepsilon_{\lambda k}\cdot\alpha}{2e_{p'+k}(-e_{p'+k}-e_{p's'}-k)}\Big|p's'\Big)+\text{C.C.}\Big]$$

$$+\frac{e^2}{8\pi^2}\Big[\int\frac{dpdp'dkdk'}{(kk')^{\frac{1}{2}}}\delta(p-p'+k'-k)\alpha_{ps}{}^{+}\alpha_{p's'}a_{\lambda' k'}{}^{+}a_{\lambda k}$$

$$\times\Big(ps\Big|\frac{\varepsilon_{\lambda k}\cdot\alpha(e_{p-k}+H_{p-k})\varepsilon_{\lambda' k'}\cdot\alpha}{2e_{p-k}(e_{ps}-e_{p-k}-k)}+\frac{\varepsilon_{\lambda k}\cdot\alpha(e_{p-k}-H_{p-k})\varepsilon_{\lambda' k'}\cdot\alpha}{2e_{p-k}(e_{ps}+e_{p-k}-k)}$$

$$-\frac{\varepsilon_{\lambda' k'}\cdot\alpha(e_{p'+k}+H_{p'+k})\varepsilon_{\lambda k}\cdot\alpha}{e_{p'+k}(e_{p'+k}-e_{p's'}-k)}-\frac{\varepsilon_{\lambda' k'}\cdot\alpha(e_{p'+k}-H_{p'+k})\varepsilon_{\lambda k}\cdot\alpha}{2e_{p'+k}(-e_{p'+k}-e_{p's'}-k)}\Big|p's'\Big)+\text{C.C.}\Big]. \quad (14)$$

As was the case in my earlier discussion of the Coulomb self-energy, we consider the integral defining H_1 to be integrated over a certain finite region in $(\mathbf{p}, \mathbf{p}')$ space which region will ultimately be taken in the limit to include all the $(\mathbf{p}, \mathbf{p}')$ space. The particular way in which this limit is taken, strongly influences the value which $H_{1.1}$ approaches. There is no loss in supposing that if the point $(\mathbf{p}, \mathbf{p}')$ is in this finite region then the point $(-\mathbf{p}, -\mathbf{p}')$ is also in this region. To preserve the charge symmetry of the theory we may now take the region for $(e_{ps}>0;\ e_{p's'}>0)$ to be the same as the region $(e_{ps}<0;\ e_{p's'}<0)$ and label this region, $I(\mathbf{p}, \mathbf{p}')$; we must also take the region for $(e_{ps}<0;\ e_{p's'}>0)$ to be the same as the region for $(e_{ps}>0;\ e_{p's'}<0)$ and label this region, $II(\mathbf{p}, \mathbf{p}')$.

The electromagnetic self-energy may now be obtained from (14) and is

$$H_{ems}=\frac{e^2}{2(2\pi)^2}\int dpdp'(\alpha_{ps}{}^{+}\alpha_{p's'})(ps|M_{ems}(p)|p's')\delta(p-p'), \quad (15)$$

in which

$$M_{ems}(p)=\int_{A(p)}\frac{dp'}{|p-p'|}\Big\{\frac{e_p+H_p}{2e_p}\varepsilon_{\lambda p-p'}\cdot\alpha\frac{e_{p'}+H_{p'}}{2e_{p'}}\varepsilon_{\lambda p-p'}\cdot\alpha\frac{e_p+H_p}{2e_p}$$

$$\frac{-e_p-H_p}{2e_p}\varepsilon_{\lambda p-p'}\cdot\alpha\frac{e_{p'}-H_{p'}}{2e_{p'}}\varepsilon_{\lambda p-p'}\cdot\alpha\frac{e_p-H_p}{2e_p}\Big\}\frac{1}{e_p-e_{p'}-|p-p'|}$$

$$+\int_{B(p)}\frac{dp'}{|p-p'|}\Big\{\frac{e_p-H_p}{2e_p}\varepsilon_{\lambda p-p'}\cdot\alpha\frac{e_{p'}+H_{p'}}{2e_{p'}}\varepsilon_{\lambda p-p'}\cdot\alpha\frac{e_p-H_p}{2e_p}$$

$$-\frac{e_p+H_p}{2e_p}\varepsilon_{\lambda p-p'}\cdot\alpha\frac{e_{p'}-H_{p'}}{2e_{p'}}\varepsilon_{\lambda p-p'}\cdot\alpha\frac{e_p+H_p}{2e_p}\Big\}\frac{1}{-e_p-e_{p'}-|p-p'|}$$

$$+\int_{C(p)}\frac{dp'}{|p-p'|}\Big\{\frac{e_p+H_p}{2e_p}\varepsilon_{\lambda p-p'}\cdot\alpha\frac{e_{p'}+H_{p'}}{2e_{p'}}\varepsilon_{\lambda p-p'}\cdot\alpha\frac{e_p-H_p}{2e_p}$$

$$-\frac{e_p+H_p}{2e_p}\varepsilon_{\lambda p-p'}\cdot\alpha\frac{e_{p'}-H_{p'}}{2e_{p'}}\varepsilon_{\lambda p-p'}\cdot\alpha\frac{e_p-H_p}{2e_p}\Big\}\frac{1}{e_p-e_{p'}-|p-p'|}$$

$$+\int_{D(p)}\frac{dp'}{|p-p'|}\Big\{\frac{e_p-H_p}{2e_p}\varepsilon_{\lambda p-p'}\cdot\alpha\frac{e_{p'}+H_{p'}}{2e_{p'}}\varepsilon_{\lambda p-p'}\cdot\alpha\frac{e_p+H_p}{2e_p}$$

$$-\frac{e_p-H_p}{2e_p}\varepsilon_{\lambda p-p'}\cdot\alpha\frac{e_{p'}-H_{p'}}{2e_{p'}}\varepsilon_{\lambda p-p'}\cdot\alpha\frac{e_p+H_p}{2e_p}\Big\}\frac{1}{-e_p-e_{p'}-|p-p'|}+\text{C.C.} \quad (16)$$

In (16) the region $A(\mathbf{p})$ over which $\mathbf{p}'$ is integrated is the region common to $I(\mathbf{p}, \mathbf{p}')$ and $I(\mathbf{p}', \mathbf{p})$ for fixed $\mathbf{p}$. The integration region, $B(\mathbf{p})$ for $\mathbf{p}'$ is the region common to $II(\mathbf{p}, \mathbf{p}')$ and $II(\mathbf{p}', \mathbf{p})$ with fixed $\mathbf{p}$. The integration region, $C(\mathbf{p})$, for $\mathbf{p}'$ is the region common to $I(\mathbf{p}, \mathbf{p}')$ and $II(\mathbf{p}', \mathbf{p})$ with fixed $\mathbf{p}$. The integration region, $D(\mathbf{p})$, for $\mathbf{p}'$ is the region common to $II(\mathbf{p}, \mathbf{p}')$ and $I(\mathbf{p}', \mathbf{p})$ with fixed $\mathbf{p}$. As was the case for the Coulomb self-energy we may write here

$$M_{em s}(\mathbf{p}) = A(\mathbf{p}) H_{\mathbf{p}} + \mathbf{B}(\mathbf{p}) \cdot \boldsymbol{\alpha}. \tag{17}$$

Here $A(\mathbf{p})$ is composed of the sum of two logarithmically divergent integrals plus the difference between two linearly divergent integrals, plus some indefinite linearly divergent integrals. The vector $\mathbf{B}(\mathbf{p})$ of (17) is an indefinite linearly divergent integral. Thus, we see that by an appropriate choice of the regions $I(\mathbf{p}, \mathbf{p}')$ and $II(\mathbf{p}, \mathbf{p}')$ both $A(\mathbf{p})$ and $\mathbf{B}(\mathbf{p})$ may be made to vanish.

IV. THE PHOTON SELF-ENERGY

We have already computed the expression (14) from which the self-energy of the photon may be obtained. To make the self-energy vanish it is not necessary to have the two regions $I(\mathbf{p}, \mathbf{p}')$ and $II(\mathbf{p}, \mathbf{p}')$ different. Since making these two regions the same results in considerable simplification in the expression for the photon self-energy, and does not alter the character of divergent integrals in terms of which it is expressed, we make this simplification even though it is not consistent with (16). The self-energy of the photons may now be written:

$$\begin{aligned} H_{phs} = \frac{e^2}{2\pi^2}\Bigg[\int \frac{d\mathbf{k} d\mathbf{k}'}{k} a_{\lambda\mathbf{k}} a_{\lambda'\mathbf{k}'} \delta(\mathbf{k}+\mathbf{k}') \Bigg\{ \int_{E(\mathbf{k})} d\mathbf{p}\ \mathrm{spur} \Bigg[\boldsymbol{\varepsilon}_{\lambda\mathbf{k}} \cdot \boldsymbol{\alpha} \frac{1}{-e_{\mathbf{p}} - H_{\mathbf{p}-\mathbf{k}} - k} \boldsymbol{\varepsilon}_{\lambda'\mathbf{k}'} \cdot \boldsymbol{\alpha} \frac{e_{\mathbf{p}} - H_{\mathbf{p}}}{2e_{\mathbf{p}}} \Bigg] \\ - \int_{F(\mathbf{k})} d\mathbf{p}\ \mathrm{spur} \Bigg[\boldsymbol{\varepsilon}_{\lambda'\mathbf{k}'} \cdot \boldsymbol{\alpha} \frac{1}{H_{\mathbf{p}+\mathbf{k}} + e_{\mathbf{p}} - k} \boldsymbol{\varepsilon}_{\lambda\mathbf{k}} \cdot \boldsymbol{\alpha} \frac{e_{\mathbf{p}} - H_{\mathbf{p}}}{2e_{\mathbf{p}}} \Bigg] \Bigg\} + \mathrm{C.C.} \Bigg] + \frac{e^2}{8\pi^2} \int \frac{d\mathbf{k} d\mathbf{k}'}{k} a_{\lambda'\mathbf{k}'} + a_{\lambda\mathbf{k}} \delta(\mathbf{k}'-\mathbf{k}) \\ \times \Bigg[\int_{E(\mathbf{k})} d\mathbf{p}\ \mathrm{spur} \Bigg\{ \boldsymbol{\varepsilon}_{\lambda\mathbf{k}} \cdot \boldsymbol{\alpha} \frac{1}{-e_{\mathbf{p}} - H_{\mathbf{p}-\mathbf{k}} - k} \boldsymbol{\varepsilon}_{\lambda'\mathbf{k}'} \cdot \boldsymbol{\alpha} \frac{e_{\mathbf{p}} - H_{\mathbf{p}}}{2e_{\mathbf{p}}} + \frac{e_{\mathbf{p}} - H_{\mathbf{p}}}{2e_{\mathbf{p}}} \boldsymbol{\varepsilon}_{\lambda'\mathbf{k}'} \cdot \boldsymbol{\alpha} \frac{1}{-e_{\mathbf{p}} - H_{\mathbf{p}-\mathbf{k}} - k} \boldsymbol{\varepsilon}_{\lambda\mathbf{k}} \cdot \boldsymbol{\alpha} \Bigg\} \\ - \int_{F(\mathbf{k})} d\mathbf{p}\ \mathrm{spur} \Bigg\{ \boldsymbol{\varepsilon}_{\lambda'\mathbf{k}'} \cdot \boldsymbol{\alpha} \frac{1}{H_{\mathbf{p}+\mathbf{k}} + e_{\mathbf{p}} - k} \boldsymbol{\varepsilon}_{\lambda\mathbf{k}} \cdot \boldsymbol{\alpha} \frac{e_{\mathbf{p}} - H_{\mathbf{p}}}{2e_{\mathbf{p}}} + \frac{e_{\mathbf{p}} - H_{\mathbf{p}}}{2e_{\mathbf{p}}} \boldsymbol{\varepsilon}_{\lambda\mathbf{k}} \cdot \boldsymbol{\alpha} \frac{1}{H_{\mathbf{p}+\mathbf{k}} + e_{\mathbf{p}} - k} \boldsymbol{\varepsilon}_{\lambda'\mathbf{k}'} \cdot \boldsymbol{\alpha} \Bigg\} \Bigg]. \end{aligned} \tag{18}$$

In (18) the region $E(\mathbf{k})$ is composed of those values of $\mathbf{p}$ for which the points $\mathbf{p}$ and $\mathbf{p}-\mathbf{k}$ lie in $I(\mathbf{p}, \mathbf{p}-\mathbf{k})$ for fixed $\mathbf{k}$. The $F(\mathbf{k})$ is comprised of those values of $\mathbf{p}$ for which the points $\mathbf{p}$ and $\mathbf{p}+\mathbf{k}$ lie in $I(\mathbf{p}, \mathbf{p}+\mathbf{k})$ for fixed $\mathbf{k}$. The spurs in (18) are readily evaluated and we obtain

$$\begin{aligned} H_{phs} = \frac{e^2}{8\pi^2}\Bigg[\int \frac{d\mathbf{k} d\mathbf{k}'}{k} a_{\lambda\mathbf{k}} a_{\lambda'\mathbf{k}'} \boldsymbol{\varepsilon}_{\lambda\mathbf{k}} \cdot \boldsymbol{\varepsilon}_{\lambda'\mathbf{k}'} \delta(k+k') \Bigg\{ - \int_{E(\mathbf{k})} \frac{d\mathbf{p}}{e_{\mathbf{p}}} \left(1 + \frac{2p_\lambda^2}{e_{\mathbf{p}} k + \mathbf{p} \cdot \mathbf{k}} \right) - \int_{F(\mathbf{k})} \frac{d\mathbf{p}}{e_{\mathbf{p}}} \left(1 - \frac{2p_\lambda^2}{e_{\mathbf{p}} k + \mathbf{p} \cdot \mathbf{k}} \right) \Bigg\} + \mathrm{C.C.} \Bigg] \\ + \frac{e^2}{(2\pi)^2} \int \frac{d\mathbf{k} d\mathbf{k}'}{k} a_{\lambda'\mathbf{k}'} + a_{\lambda\mathbf{k}} \boldsymbol{\varepsilon}_{\lambda\mathbf{k}} \cdot \boldsymbol{\varepsilon}_{\lambda'\mathbf{k}'} \delta(\mathbf{k}-\mathbf{k}') \Bigg\{ - \int_{E(\mathbf{k})} \frac{d\mathbf{p}}{e_{\mathbf{p}}} \left(1 + \frac{2p_\lambda^2}{e_{\mathbf{p}} k + \mathbf{p} \cdot \mathbf{k}} \right) - \int_{F(\mathbf{k})} \frac{d\mathbf{p}}{e_{\mathbf{p}}} \left(1 - \frac{2p_\lambda^2}{e_{\mathbf{p}} k + \mathbf{p} \cdot \mathbf{k}} \right) \Bigg\}. \end{aligned} \tag{19}$$

In (19), p_λ is the component of $\mathbf{p}$ in the direction of the polarization vector $\boldsymbol{\varepsilon}_{\lambda\mathbf{k}}$. The expression in (14) determining the photon self-energy is the sum of two negative quadratically diverging integrals, one positive cubically diverging integral and one negative cubically diverging integral. This combination can be made to vanish by an appropriate choice of the region $I(\mathbf{p}, \mathbf{p}')$.

Is it possible to choose the regions $I(\mathbf{p}, \mathbf{p}')$ and $II(\mathbf{p}, \mathbf{p}')$ so that both the photon and electron self-energy vanish simultaneously? This question can be answered with certainty in the affirmative provided each of the regions $I(\mathbf{p}, \mathbf{p}')$ and $II(\mathbf{p}, \mathbf{p}')$ are split into two parts which may be different depending on whether the plane of polarization of the photon lies in the plane of the two vectors, $\mathbf{p}$ and $\mathbf{p}'$, or is perpendicular to this plane. If we had made this separation of $I(\mathbf{p}, \mathbf{p}')$ and $II(\mathbf{p}, \mathbf{p}')$ then (16) would have been composed of the sum of eight integrals. The vanishing of the coefficient $A(\mathbf{p})$ of (17) depends essentially on making the two regions $I(\mathbf{p}, \mathbf{p}')$ and $II(\mathbf{p}, \mathbf{p}')$ of different total volume. The vector coefficient $\mathbf{B}(\mathbf{p})$ of (17) is shape dependent and depends essentially on the component of $\mathbf{p}'$ which is perpendicular to the polarization vectors of the photons. On the other hand, the cubically divergent terms of (19) depend on the component of $\mathbf{p}$ which is parallel to the polarization. If we had properly treated the photon self-energy, the expression for the photon self-energy would then have been the sum of eight integrals. The leading divergences in these integrals are the same as those in (19). It is this correct expression for the photon self-energy which one must make zero rather than (19). We now see that the photon and electron self-energies can both be made to vanish.

V. COMMENTS ON RELATIVISTIC INVARIANCE

The condition that a theory be relativistically invariant[1] may be based on the system of commutation relations

$$\begin{aligned}
&[P_x, P_y]=0, \text{ etc.}\\
&[H, P_x]=0, \text{ etc.}\\
&[L_x, L_y]=[M_y, M_x]=iL_z, \text{ etc.}\\
&[M_x, L_y]=[L_x, M_y]=iM_z, \text{ etc.}\\
&[L_x, M_x]=0, \text{ etc.}\\
&[L_x, P_x]=0, \text{ etc.}\\
&[L_x, H]=0, \text{ etc.}\\
&[L_x, P_y]=iP_z, \text{ etc.}\\
&[M_x, H]=iP_x, \text{ etc.}\\
&[M_x, P_x]=iH, \text{ etc.}\\
&[M_x, P_y]=0, \text{ etc.}
\end{aligned} \tag{20}$$

In these equations H is the energy of the system and P_x is the x-component of the momentum, L_z is the z-component of the angular momentum, and the M_x, M_y, M_z are the generators of infinitesimal Lorentz transformations. If we use for H the expression as given by Eq. (1) omitting the Coulomb self-energy parts, and if we use for the P_x, P_y, P_z the sum of the momenta of the photons, electrons and positrons, we may then solve equations $[M_x, P_z]=iH$, $[M_x, P_y]=0$, and $[M_x, P_x]=0$ for M_x. We can also solve for M_y and M_z. The structure of the terms M_x, M_y and M_z is similar to that of H. Simple forms for L_x, L_y and L_z are obtainable which are similar to those of P_x, P_y and P_z. One can then show that, provided certain indefinite divergent integrals are taken to be zero, all the commutation rules relating to (20) are satisfied. These integrals arise, for example, when one computes $[M_x, H]$ and must be taken to be zero if we are to have $[M_x, H]=iP_x$. This means, of course, that the limiting processes by means of which H is defined must be carried out so as to satisfy (20).

In Eq. (9) we introduced a unitary transformation to eliminate the interaction between the positron-electron current and the transverse electromagnetic field. We may look upon this transformation in a manner which is different from the way we have used it thus far. We may suppose that the Coulomb self-energy of the electron has been eliminated from (1) and that the integrals defining H_1 have been carried out in such a manner as to insure the satisfying of relations (20). S_1, a finite Hermitian operator, is then taken to eliminate those parts of H_1 contained in the regions $I(\mathbf{p}, \mathbf{p}')$, $II(\mathbf{p}, \mathbf{p}')$. Since S_1 is now a finite Hermitian operator, e^{iS_1} is, in fact, a unitary operator and $H'=e^{-iS_1}He^{iS_1}$, $M_x'=e^{-iS_1}M_xe^{iS_1}$, etc. will also satisfy relations (20). We now note that all the matrix elements of e^{iS_1} approach zero as the regions $I(\mathbf{p}, \mathbf{p}')$ and $II(\mathbf{p}, \mathbf{p}')$ become infinitely large. In view of this behavior of e^{iS_1} it is not surprising that differing limiting processes can lead to very different results for the first few terms of the expansion of H' as given by (9). We wish to note here that if this above procedure is adopted, then $i[S_1, H_1]$ is no longer the same as $-[S_1, [S_1, H_0]]$ so that (9) can no longer be reduced to (11). It suffices to say that this modification does not alter the possibility of obtaining a vanishing photon and electron self-energy to the order e^2.

[1] P. A. M. Dirac, Rev. Mod. Phys. 21, 392 (1949).

Scarcity of States of Li^7, from Magnetic Observation of $Be^9(d,\alpha)Li^7$

D. R. INGLIS*
Department of Physics, Johns Hopkins University, Baltimore, Maryland†
(Received December 9, 1949)

The alpha-spectrum of the reaction $Be^9(d,\alpha)Li^7$ is observed at a bombarding energy 600 kev. Above the well-known 480-kev excited state of Li^7 there is no further excited state, having a transition as much as 5 percent as intense as the ground-state transition, in the range of excitation energies up to 2.5 Mev and from there, where the $(d,2\alpha)$ reaction begins to obscure the observations, up to 3.6 Mev there is no sharp line more than 10 percent as intense as the ground-state line. The observations are made with a magnetic heavy-particle spectrograph giving an extended spectrum with a second-order focus on a photographic plate.

THE mirror nuclei Li^7 and Be^7 are of particular interest because they are the "simplest complex nuclei," where one expects most simply to encounter the general problems of nuclear structure, including the coupling of angular momentum vectors. The well-known 480-kev excited state[1] of Li^7 discovered by Rumbaugh and Hafstad has been suggestive of theoretical developments[2–4] and the previous indications that it had no near neighbors have seemed to favor the simple interpretation[2] that the ground state and this excited state together form a ^2P. Difficulties with this interpretation have led to a more complex interpretation[4] in which one can find no reason for a singular isolation of the 480-kev state. This situation lends interest to the extended search for further excited states here reported, which serves to emphasize the apparent isolation of the 480-kev state. The recent discovery[5] of the mirrored counterpart of the excited state at 429 kev in Be^7 (perhaps just by chance a few percent lower than in Li^7 as was to be anticipated on the basis of the original interpretation[2] of the supposed doublet splitting) heightens interest in the problem.

APPARATUS

The small horizontal statitron used to accelerate the deuterons has been described elsewhere.[6] The magnetically deflected beam passes, at a distance of about three meters from the magnet, through a slit, the insulated sides of which form pick-up electrodes which actuate the voltage regulation of the statitron. About a meter beyond this, the beam passes obliquely through the thin Be^9 target foil, covering an area roughly 3×6 mm. Of the alphas leaving the target at right angles to the beam some enter the 0.2-mm slit of the magnetic spectrograph and are bent in a plane normal to the beam to focus, at various positions according to their energy, on a photographic plate.

The spectrograph with its target chamber is shown in Fig. 1, in which the incident beam is to be imagined entering normal to the plane of the figure. The figure differs slightly from the situation in this experiment: The entrance slit has been removed from the tube near the target to be put in the path of the incident beam instead, and the photographic plate has been laid aside and replaced by a proportional counter used in a later experiment. The spectrograph is of a type[7] characterized by its second-order focus along a straight line, different positions on this "plate line" corresponding to different energies. The nature of the second-order focus may be described by considering a ray from the target varied in angle slightly about a central ray. The first-order focus, an intersection which remains steady in first order of this small angle, moves along a curve as the direction of the central ray is varied, and this curve has a cusp at that particular angle of the central ray which gives a second-order focus and is employed in the construction of the spectrograph. This angle of incidence is $\sin^{-1} 3^{-\frac{1}{2}} \approx 35°$ from the vertical, and the plate line makes an angle $\tan^{-1} 8^{-\frac{1}{2}} = 19\frac{1}{2}°$ with the horizontal flat side of the pole faces. The particles being focused enter and leave the same flat edge of the segment-shaped region ("infinite half-space") containing the magnetic field normal to the plane of the figure. The distance between the pole faces is only 0.794 cm, so the effect of fringing field is small. This cuts down the solid angle

* Now at Argonne National Laboratory, Chicago, Illinois.
† This work was aided by a contract with the U. S. AEC.
[1] L. H. Rumbaugh and L. R. Hafstad, Phys. Rev. **50**, 681 (1936); Rumbaugh, Roberts, and Hafstad, Phys. Rev. **54**, 657 (1938); E. R. Graves, Phys. Rev. **57**, 855 (1940); Buechner, Strait, Stergiopoulos, and Sperduto, Phys. Rev. **74**, 1569 (1948); Rubin, Snyder, Lauritsen, and Fowler, Phys. Rev. **74**, 1564 (1948); L. C. Elliott and R. E. Bell, Phys. Rev. **74**, 1869 (1948); Rasmussen, Lauritsen, and Lauritsen, Phys. Rev. **75**, 199 (1948); J. K. Boggild, Kgl. Danske Vid. Sels. Math.-fys. Medd. **23**, 4, 26 (1945). *Note added during publication:* Observations very similar to those here discussed, made at quite a different bombarding energy, have recently been reported by W. W. Buechner and E. N. Strait, Phys. Rev. **76**, 1547 (1949).
[2] D. R. Inglis, Phys. Rev. **50**, 783 (1936).
[3] W. H. Furry, Phys. Rev. **50**, 784 (1936); G. Breit and J. R. Stehn, Phys. Rev. **53**, 459 (1938); G. Breit and J. K. Knipp, Phys. Rev. **54**, 652 (1938).
[4] S. S. Hanna and D. R. Inglis, Phys. Rev. **75**, 1767 (1949).
[5] Brown, Chao, Fowler, and Lauritsen and T. Lauritsen and R. G. Thomas, Phys. Rev. **78**, 88 (1950).
[6] Inglis, Krone, and Hanna, Rev. Sci. Inst. **20**, 834 (1949).
[7] Information concerning this type of focus was received from Drs. E. M. Hafner and H. S. Snyder in valued discussions at Brookhaven in 1948. They have described a more general type of focus which includes this as a special case in a privately circulated report (see also an abstract with W. F. Donoghue, Phys. Rev. **75**, 331 (1949). The idea for the type of focus used in this work apparently originated with T. H. Fowler of the University of Bristol, who intends to describe it further.

in one direction, but the second-order focus helps in the other direction.

The pole faces themselves form part of the vacuum chamber. The Armco iron pole pieces, each 5 cm thick, are separated by the trapezoidal-shaped brass spacers shown, and the vacuum space is closed by a bent brass strip soldered around the curved edge of the poles and by a flat brass plate soldered to the flat edge of the poles. The flat plate had appropriate holes milled in it for the entrance and exit of the particles, the exit hole being wide enough to allow the plate holder to slide down along its axis until the photographic plate contacts the iron surface.

The plate holder accommodates two standard 2.54 ×7.62 cm plates (Ilford C-2, 50 micron), end to end, on each of its three faces. Thus, three exposures can be made on each loading (by retracting and rotating the holder through an o-ring seal), and for each exposure the 15.2 cm of plate subtends a spectrum of particle energies differing by a factor of 2.08 between the two ends of the plate. The minimum and maximum radii of curvature are 14.0 and 20.38 cm, with fringing field neglected, or 14.37 and 20.72 cm if one extends the edge of the field by half the distance between the pole faces, as a rough allowance for fringing field.

The spectrograph, including the two pole pieces, is slipped down between the poles of an electromagnet which weighs about 700 kg, constructed in 1941 in connection with a spectrograph somewhat similar to the one here described but of the more conventional 90° type. The poles may be moved horizontally, sliding on the faces of the yoke above the coils, to fit snugly around the spectrograph. The magnet is fed by an "Edison" battery sufficiently steady that the use of a regulating circuit is unnecessary. Currents up to 14 amperes at 150 volts have been used, 8.2 amperes for the exposure here reported. The field was shown to be homogeneous within about ½ percent in the significant region by exploration with a "gaussmeter" (permanent-magnet torsional torque-balance) and it was later found convenient to mount the probe of such an instrument in a hole in a wooden block to fix its position but permit its rotation in the fringing field, for comparison of fields of different exposures. Provision for such a probe in the homogeneous field while running would have been convenient.

It was thought, but has not been adequately verified, that the inhomogeneities near the flat edge would be mainly of such a nature as to alter the relation between plate position and target position from the ideal theoretical one, not to blur the focus. Preliminary observations were made with a Po alpha-sources replacing the target outside of a narrow slit, to locate the best entrance-slit position by trial. In this spectrograph the distance between the points where the plate line and central ray meet the top edge of the field is 22.8 cm, and the calculated vertical distance from the top edge to the entrance slit is 2⅓ as great, or 10.7 cm, if one neglects edge effects. The fringing field correction extends the latter distance to 11.6 cm. Experimentally, a target position 11.1 cm above the plane of the edge of the field gave a slightly sharper focus. The observed half-width of the Po alpha-line was about 2 mm on the plate, with an entrance slit 0.2 mm wide. (The Po deposit on a Ni button was 5 months old.) The sharpness of the focus did not vary significantly with the position of the line over a little more than half of the plate span, where it could be observed—a field strong enough to focus the Po alphas at the near end of the plate span was not available.

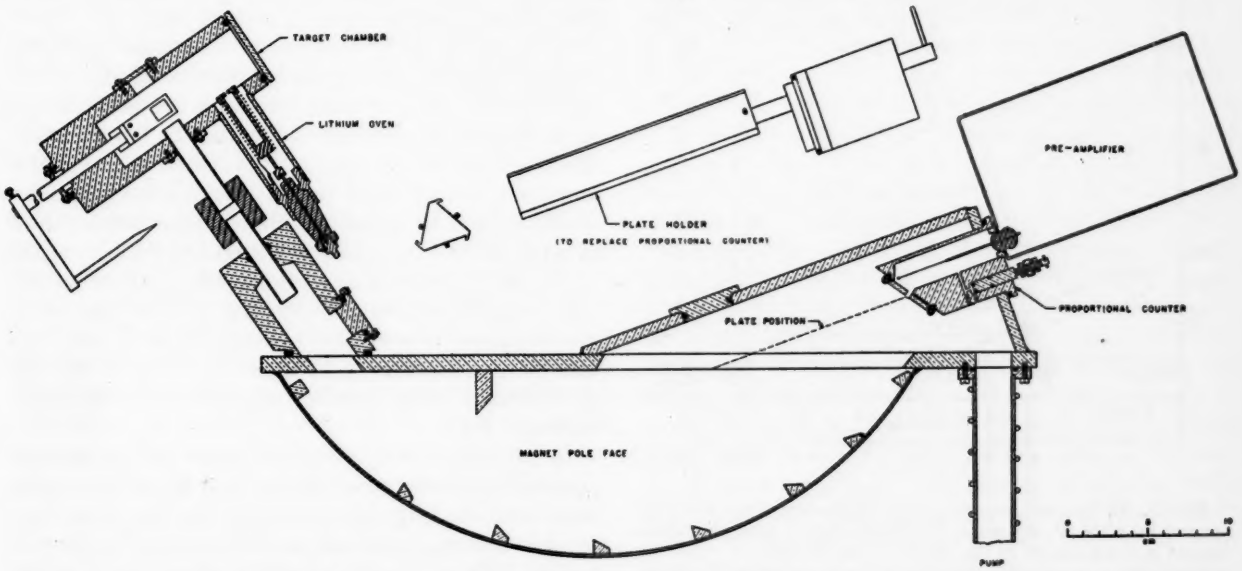

FIG. 1. Heavy-particle magnetic spectrograph. The photographic plate holder and the proportional counter are interchangeable. In the present work the photographic method is used, with the plates in position along the broken line. The proportional counter is used for reactions having low energy product particles, particularly $B^{10}(p,\alpha)Be^7$.

The principal advantage of this type of a spectrograph for this type of work is the wide range of energies covered by a single exposure. This may more than compensate the low intensity inherent in the narrow gap between the pole faces and the consequent lack of "double focusing" to bring particles back into the central plane. In other instruments double focusing is available only at one point of a spectrum, and is therefore more appropriately used with a counter than a photographic plate. This spectrograph fully exploits the advantage of the photographic plate, and is a poor instrument when used with a counter as depicted in Fig. 1. (This counter was later introduced to help with the identification of the rather low energy alphas in the reaction $B^{10}(p,\alpha)Be^7$, which, however, are also recognizable as short tracks in an emulsion. No report of that work need be made now that much more complete data on it are available elsewhere.[5]) The greater sharpness of focus resulting from the second-order focus was not fully exploited in this work, being masked in part by the target thickness used to obtain convenient intensity (see below). When not needed for sharpness, the second-order focus is still an advantage in permitting a wide entrance angle (and to this end the entrance tube should have been a little larger at the lower end, and also arranged with baffles to minimize background from wall scattering).

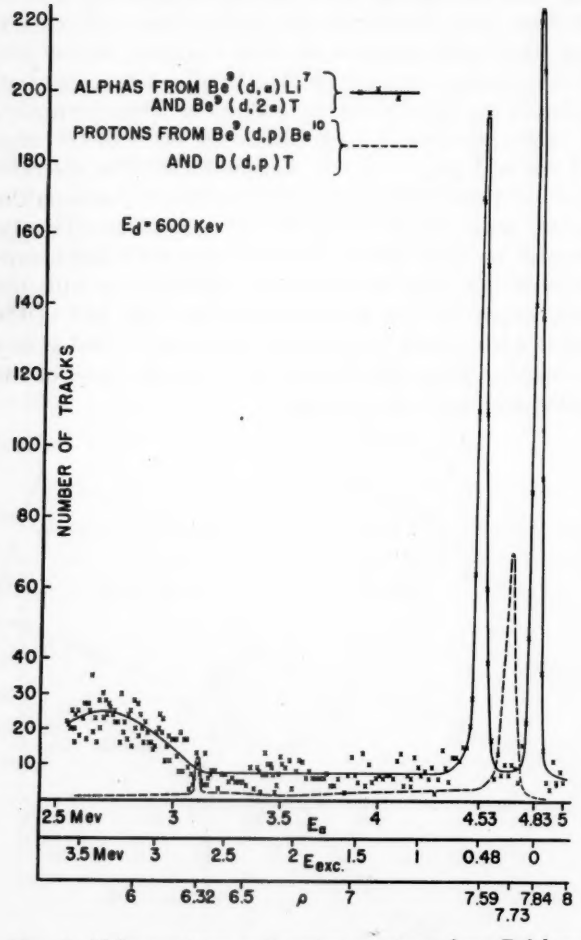

FIG. 2. Alpha-spectrum and proton spectrum from Be^9 bombarded by 600-kev deuterons. The small crosses represent alpha-counts in small swaths of the plate. In the background region the plotted points are numerous enough to be statistically significant, although the individual counts represent statistically uncertain small numbers of observed alpha-tracks. Individual proton counts are not shown.

RESULTS

The spectrum of alphas arising from the bombardment of Be^9 by 600-kev deuterons is shown in Fig. 2. The intensity of the alphas arriving at various positions along the length of the plate span is plotted against their energy, E_α, with subsidiary scales giving the corresponding excitation energy E_{exc} of the residual Li^7 nucleus, as well as radius of curvature, ρ, of the alphas arriving at each point from the entrance slit, determined from the geometry of the spectrograph. The right side of Fig. 2 corresponds to the right end, or high energy end, of the plate span in Fig. 1. The peaks corresponding to the reaction $Be^9(d,\alpha)Li^7$ going to the ground state and the well-known 480-kev state are prominent at the high alpha-energy or low excitation-energy end of the spectrum, but further to the left beyond the 0.48-Mev peak, one sees a region of low background intensity extending to beyond 2.5-Mev excitation in which the plotted points scatter by no more than would be expected of the fluctuations in such small numbers of counts. The points are sufficiently numerous to establish the absence of peaks above the background (about 3 percent of the ground-state peak) in this region. Then from about 3 Mev to the edge of the plate at 3.6-Mev excitation energy is a region of intensity about three times the background intensity, and this is attributed to the high energy alpha from the reaction $Be^9(d,2\alpha)T$, the threshold for which is expected to be at $E_{exc}=2.51$ Mev.

Each plotted point represents the number of alpha-tracks counted in a swath across the middle of the exposed strip of the plates, the swath being 4 mm long in the transverse direction of the plate by 0.3 mm wide. The tracks are distinct enough that they can be counted most conveniently with an intermediate magnification of 450 without oil immersion. Swaths have been counted at intervals of 1 mm along the length of the plates, and in the most interesting regions intermediate swaths were counted without overlapping. At the junction of the two plates a short gap in energy where the emulsion was marred, from $\rho=6.76$ to 6.9 in., is filled in with data obtained from another plate at a slightly higher magnetic field.

In the region away from the peaks the background of alphas with the proper energy (and $H\rho$) to have come from near the target is sufficiently low that some care is taken to distinguish the tracks from other background tracks. This is done by requiring that they have the right direction and length, within a reasonable spread. The acceptable range of lengths varies with position on

the plate, and is determined by observing the range of straggling of the easily recognizable alphas in the high energy peak, and then scaling this down according to the energy expected at other points on the plate, by use of the range-energy relation. In some swaths in the background region the rejected tracks are more numerous than the acceptable tracks, but most of them are unacceptable by a wide margin; so the trend of the observations is not critically affected by the criteria for acceptance, and in almost all cases the acceptability is judged at a glance without actually measuring the track.

In order to minimize the contribution of target thickness to line width the fairly thin target was supported in a frame without backing and was oriented at an appropriate angle, with the deuterons entering one face and the observed alphas leaving the other face of the target, as shown in Fig. 3. It is then, of course, in principal possible to set an ideally flat target at such an angle that the energy loss along the path *ab* of the deuteron before causing a reaction at *b* is just equal to the energy loss of an alpha along the path *ac* after a reaction at *a*, so that the two alphas emerge from the target with the same energy, apart from straggling. For this, $\tan\theta=(dE_d/ds)/(dE_\alpha/ds)$, the ratio of stopping powers of Be for deuterons and alphas. For deuterons at 600 kev or protons at 300 kev, the stopping power of Be is available[8] (394 kev/(mg/cm²)), but not of Be for alphas, so we make use of the usual assumption that the ratio of stopping powers for deuterons to alphas is the same in Al as in Be. The angular setting used in this work was 18°, and at this angle the effective thickness of the target[9] for the 600-kev deuterons passing obliquely through it is about 43 kev (obtained by using the nominal thickness, 15 micro-inches or 0.10 mg/cm², and Warshaw's value for Al, 294 kev/(mg/cm²)), and the effective thickness for the high energy group of alphas is the same. Thus, the net contribution to the line width vanishes at the right side of Fig. 2, but toward the left the energy loss of the alphas increases until at an alpha-energy of 2.5 Mev, the alpha-energy loss is about 67 kev, the difference contributing about 24 kev to the width of a hypothetical line at the left side of Fig. 2.

The broken line in Fig. 2 shows the distribution of protons observed on the same pair of plates. Their tracks were of course much longer and easily distinguishable from the alphas. The statistical scattering of the individual points is not shown in Fig. 2, but is similar to that of the alphas. The energy scale E_α in Fig. 2 applies, of course, also to proton energy E_p. The peak at $\rho=7.73$ corresponds to the reaction $Be^9(d,p)Be^{10}$ going to the ground state. The little peak at $\rho=6.62$ falls at the right position to be identified

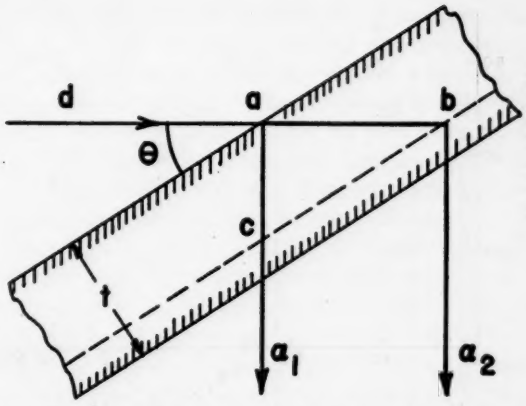

FIG. 3. Geometry of particles penetrating ideal target.

with the reaction $D(d,p)T$ associated with a deuterium contamination of the target. It is interesting to note that the small $D(d,p)$ peak is narrower than the high peaks arising from the Be in the target, only about half as wide as the $Be^9(d,p)$ proton peak, or two-thirds as wide as either of the main alpha-peaks, apparently because the deuterium contamination exists principally on the surface of the Be. That the $Be^9(d,p)$ peak is broader than the main alpha-peaks (by about 20 kev) is understandable because the target angle is set for the latter, and the protons lose less energy than the alphas in penetrating the target obliquely (by about 30 kev as estimated from target thickness).

The question arises whether a transition of appreciable intensity to a sharp higher excited state of Li^7 might be missed because of imperfections in the method which might on some parts of the plate broaden a peak to such an extent that it might be lost in the background. The sharpness of the small $D(d,p)$ peak indicates even more clearly than does the preliminary investigation with Po alphas that there is no deterioration of the focusing properties of the spectrograph itself as one goes to the left in Fig. 2. We must still inquire whether any property of the target geometry might introduce trouble. Neither the straggling in the target nor, as we have seen, deviation of the target setting from the ideal angle can account for the observed width of the main alpha peaks, which is about 75 kev. The width of these lines would then be expected to arise either from variations in the thickness of the target, which is apt to be appreciable,[8] or local variations in its orientation because of small-scale wrinkles (which the appearance of the target, mounted by allowing the surface tension of a cement to draw it fairly taught in a frame, would not preclude). Of these target defects the wrinkles would affect the energy loss of the deuterons, which enter at near-grazing incidence, much more than that of the product particles, which leave almost normal to the target. This contribution from the deuterons is the same at all energies of the product particles. The effect of variations in target thickness is proportional to the total energy loss by deuterons plus

[8] S. D. Warshaw, Phys. Rev. **76**, 1759 (1948).

[9] The evaporated Be targets used were very generously supplied by Dr. Hugh Bradner of the University of California Radiation Laboratory. The nominal thickness used is a rough value given by him for the batch. Our results are not sensitively dependent on it.

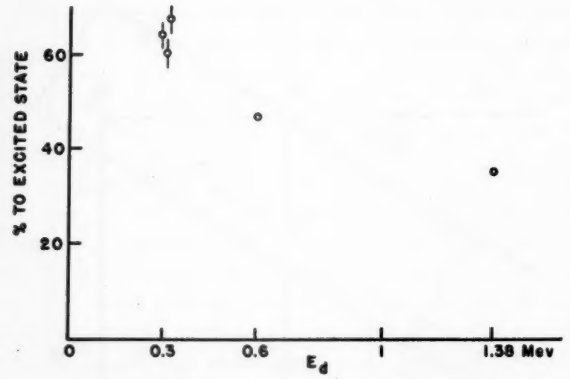

FIG. 4. Fraction of the alphas from $Be^9(d,\alpha)Li$ going to the 480-kev state. In the neighborhood of 300-kev bombarding energy, the curves given by Graves (reference 1) indicate about 64 percent to the excited state and 36 percent to the ground state. At 600 kev, the present work gives 47 percent and at 1.38 Mev the work of Buechner, Strait, Stergiopoulos, and Sperduto indicates 36 percent to the excited state.

alphas, which is greater by about 20 percent, according to the figures quoted above, at the left side of Fig. 2 than at the right. Even if this were responsible for the entire width of the main peaks, peaks arising from transitions to higher single excited states of Li^7 would thus be only very slightly wider than these. We thus conclude that no peaks have been missed because of instrumental broadening. The resolution is sufficient to have permitted detection of any transition in the empty region more intense than about 5 percent of either of the main peaks. Against the background of the continuum of alphas from the competing $(d,2\alpha)$ reaction in the neighborhood of $E_{exc}=3$ Mev a transition to a sharp state as much as 10 percent as intense as the main peaks would have been detected.

The energy scale E_α on the pair of plates represented by Fig. 2 was determined by equating the Q of the high energy peak to that determined from the similar work of Buechner, Strait, Stergiopoulos, and Sperduto,[1] since they, being primarily interested in accurate energy determinations, took care to calibrate by exposing the same plate to Po alphas under identical conditions. (In this work the Po alphas were observed on other plates under nearly identical conditions.) From the relative positions of the high energy group and the Po alphas on their Fig. 2, one finds for $Be^9(d,\alpha)Li^7$ to the ground state the energy release $Q=7.16$ Mev, which is here used. The energies of the proton peaks in our Fig. 2 are then $E=3.12$ and 4.69 Mev, corresponding to $Q=3.96$ and 4.68 Mev for the reactions $D(d,p)T$ and $Be^9(d,p)Be^{10}$, respectively.

The relative number of alphas involved in transitions to the ground state and to the 480-kev excited state is given by the ratio of the areas under the two peaks, above an estimated background level. Measurement of these areas shows that about 46.6 percent of the transitions go to the excited state at this bombarding energy, 600 kev. This is compared with the results at other bombarding energies, taken from the data of other workers, in Fig. 4. One notes an apparent decline in the relative transition probability to the excited state with increasing bombarding energy.

DISCUSSION OF RESULTS

The failure to observe peaks in the alpha-spectrum between $E_{exc}=0.48$ and 2.5 Mev does not necessarily mean that states of Li^7 do not exist in this region of excitation. It means rather that the transition probabilities to any states that might exist in this region are anomalously small, and one must judge the likelihood of encountering such weak transitions and compare with the results of other reactions before drawing a conclusion concerning the lack of states. Most of the work on the other reactions leading to the same two

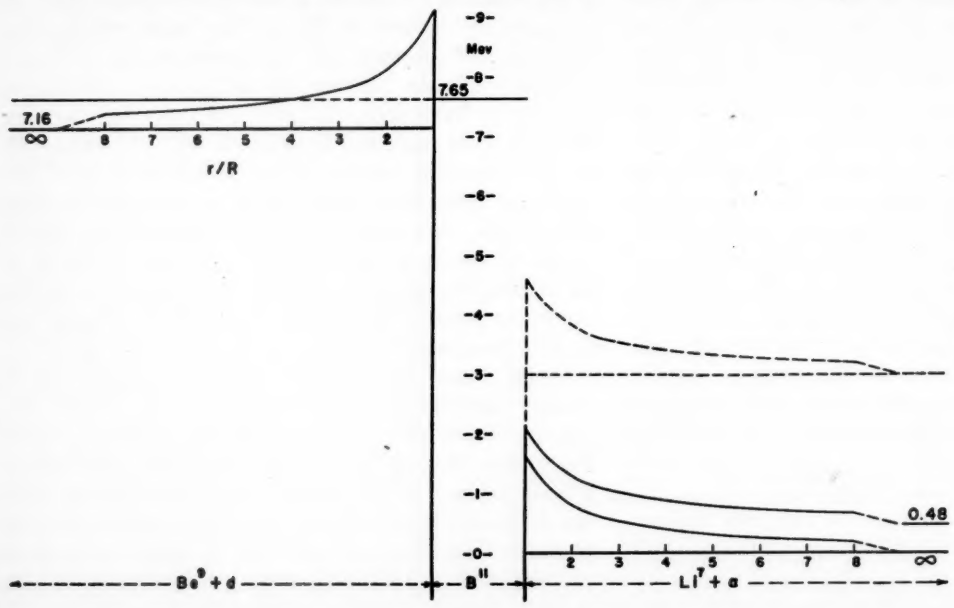

FIG. 5. Potential barriers associated with the formation and disintegration of the compound nucleus B^{11} in the reaction $Be^9(d,\alpha)Li^7$.

states of Li^7 has been carried out as investigation of the properties of transitions involving these known states, and not as exploration for unknown states. Nevertheless, the region of excitation energy up to 1 or 1.5 Mev above the ground state has been explored in a preliminary way in $Li^6(d,p)Li^7$, and more thoroughly in the gamma-spectrum from $Li^7(\alpha,\alpha')$ at $E_\alpha = 5.3$ Mev by Seigbahn and Slätis.[10] Thus there is a considerable coverage of a part of the energy region by other reactions, with no indication of any excited states of Li^7 above 480 kev.

The low probability of penetrating a Coulomb barrier associated with a high excited state of the final nucleus might in principle depress the transition probability to an excited state relative to the ground state, but the reaction here investigated is much too highly exoergic to allow this mechanism to account for our failure to observe higher excited states. The situation is indicated schematically in Fig. 5. The left side of the figure represents the energy of the system as a function of the static separation of the two constituents involved in the formation of the compound nucleus, and the right side similarly represents the subsequent disintegration. In the approximation in which the constituent particles are considered separated and without influence on one another's internal motion when beyond an idealized "nuclear radius," we may draw a Coulomb barrier for the 480-kev state which is everywhere displaced just 480 kev upward from that of the ground state. That is, the alpha is considered separated either from Li^7 or Li^{7*} from the beginning. Even up to the highest excitation energies in which we are here interested, the top of the excited Coulomb barrier falls far short of the excitation energy of the compound nucleus provided by the experimental synthesis, as is suggested by the dotted curve.

In a very rough approximation one may then conclude that there is for any excited state in the range investigated plenty of energy available and no problem of penetration at all. A more refined approach would take into account the partitions of energy among nucleons in the compound nucleus and might indeed find the barrier more of a deterrent for a hypothetical higher excited state of the final nucleus in spite of the presence of ample total energy to pass over it. This would be expected to bring in a comparatively small factor from relative volumes of momentum space, not a large factor from relative penetrabilities, so is probably not adequate to account for the blank region in the alpha-spectrum. This consideration suggests that this reaction might be significantly better than $Li^6(d,p)Li^7$, which has a smaller energy release but still gets over the excited barrier, and surely better than $B^{10}(n,\alpha)Li^7$ as a tool for searching for excited states of Li^7. Inelastic scattering, especially with very high energy particles, might be still better.

Above the threshold at 2.51-Mev excitation energy, the failure to observe excited states in Li^7 might in principle be due to the energy indeterminacy of such states arising from the possibility of disintegration of Li^7 into an alpha and a triton. Actually, this mechanism by no means precludes the existence of states of Li^7 in this region as sharp as our experimental main peaks, as is clear from the general prevalence of resonant levels in nuclei even at much higher excitation energies, and in particular in Li^7 at 7.38 Mev, as observed[11] in the reaction $Li^6(n,\alpha)T$. This mechanism, involving the disintegration of Li^7 into an alpha and a triton is, of course, to be distinguished from the effect of the competing reaction $Be^9(d,2\alpha)T$, which contributes alphas on our plates only above this threshold, but which competes with the entire spectrum of $Be^9(d,\alpha)Li^7$ indiscriminately (at a given bombarding energy) and is not expected to affect, in any systematic way depending on alpha-energy, the *relative* intensity of lines in this spectrum. Thus our failure to observe peaks seems quite as significant above the threshold as below.

I thank Drs. S. S. Hanna and I. Resnick, who were investigating other problems concurrently, for their cooperation in the statitron maintenance.

[10] K. Siegbahn and S. Slätis, Arkiv. f. Mat. Astr. o. Fys. **34A**, No. 6 (1946).

[11] Goldsmith and Ibser, quoted by Hornyak and Lauritsen, Rev. Mod. Phys. **20**, 192 (1948).

Analysis of Proton-Proton Scattering by Means of the f Function

G. BREIT AND R. D. HATCHER*
Yale University,† New Haven, Connecticut
(Received December 28, 1949)

The approximately linear relationship between the f function and the energy, E, is discussed by elementary methods. Formulas for the comparison of derivatives of f with respect to E are given for potentials of different shapes. The comparison of potentials is reduced to that of wave functions at a standard energy. A discussion of the relation between the meson mass corresponding to experiments on proton-proton scattering and the mass of the π-meson is included. The variation in the comparison owing to lack of reproduction of the curvature of the (f, E) plot is estimated and the uncertainties caused by relativistic corrections as well as modifications of the Yukawa potential at distances of the order of the Compton wave-length for the proton are considered.

I. INTRODUCTION

THE convenience of employing quantities varying approximately linearly with energy in the analysis of nucleon-nucleon scattering experiments has been emphasized recently by Blatt and Jackson[1,2] who used some unpublished calculations of Schwinger. Their starting point is an application of a variational method to the calculation of phase shifts. The phase shift is given implicitly by the requirement that a certain quantity be stationary. Such an approach can be very useful for simplifying some parts of the calculation and is doubtless the best available one for problems admitting of no explicit final formula. In the calculation of phase shifts from assumed potential energies, however, there is no difficulty in writing down an explicit expression for the final answer. The exclusive employment of power series in the energy for the representation of the answer limits the range of applicability of the results obtained by the variational method. The series used has a finite radius of convergence. Some of the expansions of the needed quantities which have been obtained by means of the differential equation are subject to the same limitation. The starting point in all such work is, however, the simple relation between phase shift and the logarithmic derivative of the wave function. In this relation one can express the wave function and its ordinary derivative by means of series having a larger circle of convergence. These series converge at all energies in many cases.

The approximately linear dependence of the quantity dealt with by the variational method has been understood as a simple consequence of properties of the quantities X, Ψ, $\cdots$ of BCP.[3] Power series in the energy for the quantity f of BCP have not been systematically worked out, however, from the latter viewpoint. The most closely related work is that of Bethe[4] who stops at a point in the development which he considers to be sufficiently accurate for comparison with existing experiments. A more methodical approach was made use of in connection with a presentation[5] of numerical values of phase shifts for the meson and Gauss error potentials from 0.2 to 40 Mev. A brief account of this arrangement of the calculation appears warranted since it is somewhat simpler than those published. By means of it one can expand f as easily around $E=E_0$, where E_0 is an arbitrary value of the energy, as about $E=0$.

II. GENERAL RELATIONS

The notation is that of BCP, BTE, BB.[3] Minor changes will be indicated, as needed. The main ones are the omission of the subscript 0 for zero angular momentum and the employment of the symbol $\mathfrak{F}$ for

---

* Now at New York University, New York, New York.
† Assisted by the Joint Program of the ONR and the AEC.
[1] J. D. Jackson and J. M. Blatt, Phys. Rev. **76**, 1296A (1949). The writers are indebted to Messrs. Jackson and Blatt for furnishing them with the manuscript of a more complete paper on the same subject.
[2] John M. Blatt and J. David Jackson, Phys. Rev. **76**, 18 (1949).
[3] G. Breit and W. G. Bouricius, Phys. Rev. **75**, 1029 (1949). This paper is referred to here as BB. It contains a list of references to older papers on proton-proton scattering. The conventions of BB for referring to papers by the authors' initials will be used here as well, the paper of Breit, Condon, and Present being designated by BCP, that of Breit, Thaxton, and Eisenbud by BTE and that of Hoisington, Share, and Breit by HSB.
Equations (7.26), (7.27) of BB were included in that paper for the purpose of obtaining a short way of calculating X and Ψ. These quantities rather than Θ are needed for the calculation of f. The series for X and Ψ can be obtained without the use of Bessel functions. Through an oversight BB failed to state that they had no proof that Eqs. (7.26) and (7.27) give Θ and $\partial\Theta/\partial x$, although the text preceding these equations contains a caution against direct calculation of Θ by means of the equations referred to; the consideration of types of terms in X and Ψ has indicated Eq. (7.26) as a short-hand way of predicting terms in X and Ψ. Helpful correspondence with Messrs. J. D. Jackson and J. M. Blatt has indicated the desirability of the statements just made. It has been known in connection with the computation of Coulomb functions at this laboratory that the Stirling expansion of the logarithmic derivative of the Γ-function in the formula for Θ agrees with the Bessel function expansion when the coefficients of η^{-2} are compared for the first few terms. For this reason as well as the contour integral argument mentioned in YWB it was believed that the expansion in Bessel functions is an asymptotic one. This belief is supported by the paper by R. Jastrow, Phys. Rev. **73**, 60 (1948).
[4] H. A. Bethe, ONR Conference, Chicago (1948); Phys. Rev. **76**, 38 (1949). Very similar considerations worked out by one of us (G.B.) were available to us at the time and were mentioned in an exchange of views at Chicago. Our work did not cover applications to the photoelectric effect of the deuteron.
[5] Hatcher, Arfken, and Breit, Phys. Rev. **75**, 1389 (1949). This paper is referred to as HAB.

the *real* function which is r times the radial function in the presence of the scattering potential. In terms of the s wave phase shift K, the regular functions F and the irregular functions G,

$$\mathfrak{F}=F\cos K+G\sin K \tag{1}$$

at points outside the range of interaction.

Inside the potential well the function $\mathfrak{F}$ is the regular solution of the appropriate radial equation in the presence of the scattering potential. This solution is supposed to be joined smoothly to the solution outside the potential well. The differential equation satisfied by $\mathfrak{F}$ is of the form

$$\mathfrak{F}''+[\kappa+\lambda\varphi(r/a_1)+\mu\psi(r/a_2)+\cdots]\mathfrak{F}=0 \tag{2}$$

where a prime indicates differentiation with respect to r. The form of Eq. (2) is the same as that of Eq. (9) of BTE[3] and Eq. (9.1) of this reference may be applied, on replacement of x by r. The logarithmic derivative at a point outside the nuclear potential is

$$y=\mathfrak{F}'/\mathfrak{F}=(G'+F'\cot K)/(G+F\cot K) \tag{2.1}$$

and is conveniently considered as a function of the variables

$$x_1=\cot K,\quad x_2=F,\quad x_3=G,\quad x_4=F',\quad x_5=G'. \tag{2.2}$$

With the usual understanding of partial differentiation for a function of more than one variable one has

$$\partial y/\partial x_1=(k\sin^2 K)/\mathfrak{F}^2,\quad k^2=\kappa \tag{2.3}$$

where k is the wave number times 2π.

For two nuclear potentials such as the meson and the square well the values of the depth parameters λ, μ, and of the range constants a_1, a_2, $\cdots$ are different, in general. A suitable adjustment of the parameters can make K and, therefore, x_1 the same at some preassigned energy E_0 which may have the value zero in a special case. Values of quantities for one of the potentials will be denoted by the superscript s (for standard) and the calculation will be arranged by referring the values of K to those of K^s. Values of quantities for $E=E_0$ will be designated by the subscript 0. One has then

$$(K-K^s)_0=0 \tag{2.4}$$

and

$$\partial y/\partial\kappa=(\partial y/\partial x_1)(\partial x_1/\partial\kappa)+\Sigma_2{}^5(\partial y/\partial x_j)(\partial x_j/\partial\kappa). \tag{2.5}$$

There is an equation corresponding to Eq. (2.5) also for y^s. Comparing the two for $E=E_0$ one sees that the sum over j from 2 to 5 has the same value for the two equations. In fact, the terms in the sum are functions of κ, x_1, x_2, $\cdots$, x_5 which are obtainable from Eq. (2.1). Of the $\partial x_j/\partial\kappa$ only that for $j=1$ depends on the choice of potential and all the $\partial y/\partial x_j$ are equal to the $\partial y^s/\partial x^s{}_j$ at the comparison energy. One has, therefore,

$$[\partial(y-y^s)/\partial\kappa]_0=[(\partial y/\partial x_1)]_0[\partial(x_1-x^s{}_1)/\partial\kappa]_0. \tag{2.6}$$

On the other hand according to BCP[3] and BTE,[3]

$$\partial y/\partial\kappa=-\mathfrak{F}^{-2}\int_0^R\mathfrak{F}^2dr,\ \partial^2y/\partial\kappa^2$$

$$=-2\mathfrak{F}^{-2}\int^R(\partial y/\partial\kappa)^2\mathfrak{F}^2dr, \tag{2.7}$$

$$\partial^3y/\partial\kappa^3=-6\mathfrak{F}^{-2}\int_0^R(\partial y/\partial\kappa)(\partial^2y/\partial\kappa^2)\mathfrak{F}^2dr$$

so that the values of the successive derivatives can be obtained by means of iterated integrals. Here R is such that for $r>R$ the field is Coulombian. For the first derivative the application of Eqs. (2.3), (2.7) to Eq. (2.6) gives

$$[\partial(kx_1-kx^s{}_1)/\partial(k^2)]_0=\left[\int_0^R(\mathfrak{F}^{(s)2}-\mathfrak{F}^2)dr/\sin^2K\right]_0. \tag{2.8}$$

This relation connects the values of the rate of change with energy of $k\cot K$ for two potentials at the reference energy for which K and K^s are the same.

If the range and depth or other parameters for two types of potentials have been adjusted so that at $E=E_0$, the phase shifts and the first derivatives of the phase shifts with respect to energy are the same, then in the present notation all the x are respectively equal to the x^s and $\partial x_1/\partial\kappa=\partial x^s{}_1/\partial\kappa$. On the other hand the $\partial x_j/\partial\kappa$ are identically the same for the two potentials. The $\partial^2y/\partial x_i\partial x_j$ are also the same at $E=E_0$ and of the $\partial^2x_i/\partial\kappa^2$ only $\partial^2x_1/\partial\kappa^2$ is different. Accordingly the relation

$$\partial^2y/\partial\kappa^2=\Sigma_{i,j}(\partial^2y/\partial x_i\partial x_j)(\partial x_i/\partial\kappa)(\partial x_j/\partial\kappa)$$
$$+\Sigma_i(\partial y/\partial x_i)(\partial^2x_i/\partial\kappa^2) \tag{2.81}$$

differs from the corresponding relation for y^s *only* on account of a difference in $\partial^2x_1/\partial\kappa^2$ and $\partial^2x^s{}_1/\partial\kappa^2$. One has then

$$[\partial^2(y-y^s)/\partial\kappa^2]_0=[\partial y/\partial x_1]_0[\partial^2(x_1-x^s{}_1)/\partial\kappa^2]_0 \tag{2.9}$$

and hence by an application of Eq. (2.7),

$$[\partial^2\Delta/\partial\kappa^2]_0$$

$$=\left[(2/\sin^2K)\int_0^R[(\mathfrak{F}^s)^{-2}(I^s{}_1)^2-\mathfrak{F}^{-2}I_1{}^2]dr\right]_0, \tag{3.0}$$

where

$$I_1(r)=\int_0^r\mathfrak{F}^2(r')dr', \tag{3.1}$$

$$\Delta=k(x_1-x^s{}_1) \tag{3.2}$$

and $I^s{}_1$ is defined in terms of $\mathfrak{F}^s$ in the same way as I_1 in terms of $\mathfrak{F}$.

If two potentials are such that $\partial\Delta/\partial\kappa$ and $\partial^2\Delta/\partial\kappa^2$ are both zero, then a simple condition for $\partial^3\Delta/\partial\kappa^3$ follows

from expressions for $\partial^3 y/\partial\kappa^3$, $\partial^3 y^s/\partial\kappa^3$. The first of these contains terms in

$$(\partial^3 y/\partial x_i\partial x_j\partial x_k)(\partial x_i/\partial\kappa)(\partial x_j/\partial\kappa)(\partial x_k/\partial\kappa),$$
$$(\partial^2 y/\partial x_i\partial x_k)(\partial^2 x_i/\partial\kappa^2)(\partial x_j/\partial\kappa),\quad (\partial y/\partial x_i)(\partial^3 x_i/\partial\kappa^3)$$

which may be referred to as terms of the first, second, and third type respectively. All of the derivatives of y with respect to the x_i are equal for the two potentials because of the equality of the phase shifts and the derivatives of the x_i occurring in terms of first and second type are also reproduced because of the assumption that $\partial^2\Delta/\partial\kappa^2=0$ which implies that $\partial^2 K/\partial\kappa^2$ is reproduced. Only terms of the third type can be different, therefore. Among these the $\partial^3 x_j/\partial\kappa^3$ are reproduced except for $j=1$. It follows, therefore, that

$$[\partial^3(y-y^s)/\partial\kappa^3]_0=[\partial y/\partial x_1]_0[\partial^3(x_1-x^s{}_1)/\partial\kappa^3]_0 \quad (4)$$

and by means of Eq. (2.7) one obtains

$$\partial^3\Delta/\partial\kappa^3=(12/\sin^2 K)\int_0^R[(\mathfrak{F}^s)^{-2}I^s{}_1I^s{}_2-\mathfrak{F}^{-2}I_1I_2]dr. \quad (4.1)$$

$$I_2(r)=\int_0^r (I_1^2/\mathfrak{F}^2)dr. \quad (4.2)$$

Relations such as Eq. (2.6) for the first derivative and Eqs. (2.9), (4) for the second and third will retain their form as the scheme proceeds. At each stage the curves of K plotted against E are made to have contact of increasingly higher order and the first non-vanishing derivative is then calculable by a simple formula.

By adjusting range and depth parameters it is not possible, in general, to make the phase shift curves agree with each other at a preassigned energy more closely than to within the value of K and $\partial K/\partial E$. For such families of potential energy curves the above plan furnishes, therefore, only a comparison of curvatures of the (f, E) plots through the application of Eq. (2.9) and without making use of Eq. (4.1). For proton-proton scattering the curvature of the (f, E) curve is still uncertain and there is no special need for the higher derivatives at this time.

The calculation of the third derivative gives about the same amount of information as the calculation of an additional phase shift and the latter is no harder to perform. The calculation of phase shifts at a few energies is in some respects the more reliable method because it amounts to the determination of K and f by interpolation and is rather independent of the influence of higher derivatives that have not been calculated. If the wave functions have to be dealt with numerically, the accuracy requirements become distributed between several numerical tables rather than concentrated into one. The plan of the work of HAB[5] was influenced by these considerations. The arrangement of the formulas here presented is such that the comparison of the $\partial^2 f/\partial E^2$ can be carried out at any energy provided the (f, E) plots are tangent at that energy. Differences in curvature appear as effects of different values of

$$\int_0^R \mathfrak{F}^{-2}(r)\left[\int_0^r \mathfrak{F}^2(r')dr'\right]^2 dr$$

for the two potentials for the same value of

$$\int_0^R \mathfrak{F}^2(r)dr$$

and of $\mathfrak{F}(R)$. The difference of curvature of the (f, E) plots can thus be expressed as an effect of a difference in the shapes of the $(\mathfrak{F}^2, r)$ curves. If desired one can calculate $\partial^2(k\cot K)/\partial\kappa^2$ directly from Eq. (2.81). The formula then becomes longer and more obscure.

III. FORMS FOR PROTON-PROTON SCATTERING

Retaining the connection between k and κ as in Eq. (2.3) and employing the original definition[3] of f one has from Eqs. (2.6), (3.0)

$$\begin{aligned}\partial(f-f^s)/\partial\kappa&=(aC_0^2/\sin^2 K)(I^s{}_1-I_1)\\ \partial^2(f-f^s)/\partial\kappa^2&=(2aC_0^2/\sin^2 K)(I^s{}_2-I_2)\end{aligned} \quad (5)$$

and a formula for the third derivative which corresponds to Eq. (4). Here $a=\hbar^2/\mu e^2$, C_0 is the usual coefficient of the lowest power of kr in F and I_1, I_2 are given by Eqs. (3.1), (4.2). At any energy one can conveniently introduce a radial function u related to $\mathfrak{F}$ by

$$u=C_0\mathfrak{F}/\sin K. \quad (5.1)$$

The function u does not vanish for $E=0$ as is clear from the fact that in the notation of YWB, BTE[3] etc.

$$u=\Psi_0+(2r/a)[\ln(2r/a)]\Phi_0+(r/a)\Phi_0 f. \quad (5.2)$$

The $\mathfrak{F}$ which occurs in I_1, I_2 combines with the factors $C_0^2/\sin^2 K$ in Eq. (5) so as to leave no quantities requiring the evaluation of 0/0 at $E=0$. Equations (5) are meant in the sense of successive adjustment to higher order tangency of the (f, E) curves similarly to Eqs. (3.0), (4.1) of the preceding section. The replacement of $\mathfrak{F}$ by u is not essential unless the comparison energy is $E=0$.

For $E=0$ substitution into the equations of BB[3] gives outside the nuclear potential

$$u=-(k^2/2)[\theta_0+(\gamma-\tfrac{1}{2})\varphi_0]+x^2\varphi_0 f/8, \quad (5.3)$$

which can also be expressed as

$$u=-x[K_1(x)+(\gamma-\tfrac{1}{2})I_1(x)]+(x/4)I_1(x)f, \quad (5.4)$$

$$x^2=8r/a \quad (5.41)$$

and as

$$u=-x[\,\mathfrak{K}_1(x)-I_1\ln(x/2)]+(x/4)I_1(x)f. \quad (5.5)$$

The function $\mathfrak{K}_1$ is related to Basset's K_1 by Eq. (7.6) of BB and a rapidly converging series for $\mathfrak{K}_1$ is listed as Eq. (7.7) in BB. If the comparison potential has a very small range then Eqs. (5.2)–(5.5) hold down to very small distances and the (f, E) curve becomes a

horizontal straight line, as has been shown by BCP. In this limit Eq. (5) gives

$$\partial f/\partial\kappa = a\int_0^R [(u^s)^2 - u^2]dr. \tag{6}$$

Here both u and u^s are given by Eq. (5.2) or the alternative forms (5.3), (5.4), (5.5) for distances greater than the nuclear radius. At smaller distances u^s is still given by the same equations but u is now the solution of the radial equation for r times the radial function in the presence of the potential well and for zero energy. Equation (6) was used in this sense by HAB.[5] Introducing

$$r_e = r mc^2/e^2, \tag{6.1}$$

this formula becomes

$$\partial f/\partial(E/mc^2) = \int_0^\infty [(u^s)^2 - u^2]dr_e. \tag{6.2}$$

This is Eq. (2.2) of HAB with u_0 replaced by u^s.

For the comparison of the curvature of the (f, E) plots of two potentials giving the same df/dE at $E=0$ one obtains in a manner similar to that which led to Eq. (3.0)

$$\partial^2(f-f^s)/\partial(E/mc^2)^2$$
$$= 2(\mu/m)\alpha^2 \int_0^{R_e} \left\{ [u^s(r_e)]^{-2} \left[\int_0^{r_e} (u^s)^2 dr_e' \right]^2 - [u(r_e)]^{-2} \left[\int_0^{r_e} u^2 dr_e' \right]^2 \right\} dr_e. \tag{6.3}$$

Here μ is the reduced mass, α the fine structure constant and the constant multiplying the integral has the approximate value 0.0977(2). If E is expressed in Mev rather than mc^2 the corresponding constant is approximately 0.186(8). By means of Eq. (6.3) one can compare the curvatures of the (f, E) plots for two potentials at $E=0$. Since for the square well the curvature can be obtained analytically, the calculation is conveniently reducible by means of Eq. (6.3) to that of a square well. It should be stated that in Eq. (6.3) the comparison is made between two potentials which give the same df/dE at $E=0$ and that u^s *in Eq. (6.3) differs, therefore, from* u^s *in Eq. (6.2).* In the latter u^s corresponds to a potential of zero range.

The relations for the quantity $k\cot K$ may be considered as a special case of those for f. In fact if one makes $e\to 0$ in f then $(e^2/\hbar)f \to v\cot K$, a quantity which differs from $k\cot K$ only by a constant factor $\mu/\hbar$.

It is also possible to neglect the Coulomb field inside the potential well in first approximation as has been done by BCP and BTE for the square well potential. Chew and Goldberger[6] have shown that one can do so successfully also for potentials with longer tails. Such calculations can be carried out by means of the expansions of the logarithmic derivative of the wave function by means of Eqs. (9), (9.1) of BTE.

[6] G. F. Chew and M. L. Goldberger, Phys. Rev. **75**, 1637 (1949).

IV. EXPERIMENTAL VALUES

A brief discussion of experimental values appears proper in view of the fact that the emphasis in HAB[5] has been on the difference in range determination which results from fitting the f curve at different values of E. The present work makes use of sixteen phase shifts up to 4.2 Mev. No use is being made of the observations by Heydenburg, Hafstad, and Tuve[7] in the energy region from 200 to 600 kev since the main object of these experiments was to establish the existence of a minimum in scattering at 45° rather than a quantitative determination of the phase shifts. The values used are: (a) Those of Herb, Kerst, Parkinson, and Plain,[8] Heydenburg, Hafstad, and Tuve[9] as analyzed by BTE; (b) the experimental values of Ragan, Kanne, and Taschek[10] with the same interpretation as in BB; (c) the experimental values of Blair, Freier, Lampi, Sleator, and Williams[11] with the interpretation of Critchfield and Dodder;[11] (d) the value at 4.2 Mev obtained by May and Powell.[12] The value at 7 Mev due to Dearnley, Oxley, and Perry[13] is not used since it is understood that a repetition of the experiments is in much better agreement with the extrapolation of the lower energy phase shifts into the region of 7 Mev.

The largest relative weight ~25 was given to the values of Herb, Kerst, Parkinson, and Plain. The experiments of Blair, Freier, Lampi, Sleator, and Williams in the interpretation of Critchfield and Dodder were used with relative weights from 11 to 8, those of Heydenburg, Hafstad, and Tuve with weights from 8 to 6. The values given by BB for $E=250$ and 300 kev from experiments by Ragan, Kanne, and Taschek had weights of 1.6 and 2.4 and those of May and Powell of 1.1 to 0.4. There is considerable uncertainty regarding the proper weighting. The nominal probable error was the criterion for the weights listed. This criterion is admittedly arbitrary, does not necessarily correspond to the relative value of the observations, and is used only for lack of something better. Fitting the experimental values by the parabola

$$f = f^{(0)} + f^{(1)}E + f^{(2)}E^2, \tag{7}$$

the following values were found by a least squares

[7] Hafstad, Heydenburg, and Tuve, Phys. Rev. **53**, 239 (1938).
[8] Herb, Kerst, Parkinson, and Plain, Phys. Rev. **55**, 998 (1939).
[9] Heydenburg, Hafstad, and Tuve, Phys. Rev. **56**, 1078 (1939).
[10] Ragan, Kanne, and Taschek, Phys. Rev. **60**, 628 (1941).
[11] Blair, Freier, Lampi, Sleator, and Williams, Phys. Rev. **74**, 553 (1948); C. L. Critchfield and D. C. Dodder, Phys. Rev. **75**, 419 (1949).
[12] A. N. May and C. F. Powell, Proc. Roy. Soc. **A190**, 170 (1947).
[13] Dearnley, Oxley, and Perry, Phys. Rev. **73**, 1290 (1948).
The writers would like to acknowledge their indebtedness to Dr. Oxley for a discussion of the above experiments and to Mr. J. Rouvina for acquainting them with the newer data.

adjustment

$$f^{(0)}=7.77,\quad f^{(1)}=0.976,\quad f^{(2)}=-0.015. \qquad (7.1)$$

The values given by Bethe do not make use of $f^{(2)}$ and correspond in the present notation to $f^{(0)}=7.77$, $f^{(1)}=0.942$. In making the comparison, allowance is made for the fact that Bethe's f is the f of BCP plus $2-2\gamma$, where γ is the Euler-Mascheroni constant. The values of $f^{(0)}$ and $f^{(1)}$ listed in Eq. (7.1) give an equivalent square well range and depth of $r=1.00e^2/mc^2$, $D=10.4(8)$ Mev. These numbers correspond to the same $f^{(0)}$, $f^{(1)}$ for both potentials and mean equivalence for representing data at $E=0$ in the sense of Eqs. (8.7), (8.8) of BB. The square well parameters are essentially the same as those in BTE. By means of Eqs. (3)–(3.5) of HAB and the values of $f^{(0)}$, $f^{(1)}$ in Eq. (7.1) in the present paper the parameters C', a' of the Yukawa potential were calculated. This yielded

$$C'=84.4,\quad a'=0.432. \qquad (7.2)$$

The units for these parameters are mc^2 for energy, e^2/mc^2 for length; C' is the coefficient of the exponential function and a' the meson potential range. The meson mass corresponding to a' is 317 electron masses which may be compared with 326 electron masses in the work of HSB.

If one omits $f^{(2)}$ in the least squares analysis of experimental values, the values of $f^{(0)}$ and $f^{(1)}$ change to 7.82, 0.916 respectively. This type of fit gives an approximately 6 percent shorter range of force and a meson mass of $\sim 337m$. The values in Eq. (7.1) cannot be taken literally. A least squares fit of the data with an adjustable $f^{(2)}$ is not significant as long as it results in a value of $f^{(2)}$ which differs by a factor of more than 2 from the value expected for the meson potential. Since the experimental data are not certain enough to give a reliable $f^{(2)}$ the "best" meson potential fitting experiment could be reasonably taken to be determinable by at least squares adjustment of $f^{(0)}$ and $f^{(1)}$ to experimental data subject to the restricting condition of a value of $f^{(2)}$ which corresponds according to scattering theory to the trial values of $f^{(0)}$ and $f^{(1)}$. This would amount to a least squares adjustment for best values of C' and a'. Such a calculation would be laborious. An approximate estimate of the change which it would produce in the meson mass can be made as follows. The value of $f^{(2)}$ which corresponds to $a'=0.42$, $C'=89.6$ is -0.0054. According to Eq. (3.6) of HAB, $f^{(2)}$ varies approximately as a'^2 and, therefore, the probable value of $f^{(2)}$ is $-0.0054\times(0.432/0.42)^2=-0.0057$. A least squares adjustment of $f^{(1)}$ is likely to give, therefore, $0.916+(0.0057/0.015)(0.976-0.916)=0.939$, a value which is somewhat accidentally very close to Bethe's estimate. The corresponding meson mass is $\sim 330m$.

Relativistic corrections are not large enough to be of real interest in making the comparison with the mass of the π-meson. Without attempting a precise evaluation their order of magnitude will be estimated. The corrections involve[14] among other terms the additions $(p^2J+Jp^2)/2Mc^2$ to the negative of the potential energy. Here p is the relative momentum. These terms are analogous to the magnetic interaction of electrodynamics. They cause an increase in depth of the potential well with energy which makes the (K_0, E) curve steeper, the (f, E) curve flatter and the range shorter. The fractional change in depth is then

$$dC'/C'dE\cong 1/2Mc^2, \qquad (8)$$

which is $\sim 1/1800$ in Mev^{-1} units. The factor 1/2 appears here because E is twice the energy of relative motion which is p^2/M. Applying Eq. (3) of HAB, one finds a change in $f^{(0)}$ which varies linearly with E and corresponds to a change of $f^{(1)}$ by the amount

$$\delta f^{(1)}=-\alpha\gamma_1(dC'/C'dE)/(2a'C'^{\frac{1}{2}}). \qquad (8.1)$$

This quantity is $\sim -274/(2\times 0.42\times 90^{\frac{1}{2}}\times 1800)=-0.02$. It corresponds to a 2 percent decrease in $f^{(1)}$ and a 2 percent decrease in meson mass. These estimates of the effect of the velocity dependence caused by relativistic effects are qualitative rather than quantitative. There are additional terms in the Hamiltonian[14] which have not been considered here.

Since the theoretical basis for the Yukawa potential may need modification at $r\sim\hbar/Mc$, calculations were made in which the meson potential curve was cut off by a straight line parallel to the r axis from $r=0$ to $r=\hbar/Mc$. Here M is the proton mass. On this basis the values of the parameters corresponding to the fit to experimental data used in Eq. (7.1) are

$$C'=87.7,\quad a'=0.428 \qquad (9)$$

in place of the values in Eq. (7.2). The range of force is about one percent smaller and the meson mass is accordingly one percent larger.

The effects considered are small in comparison with the apparent difference in the masses of the π-meson and that corresponding to proton-proton scattering. Aside from the possibility that the situation will be changed by further experiments or by a better interpretation of existing ones, the present work indicates a higher mass for the Yukawa type particle held responsible for the p-p interaction than the currently believed in mass of the π-meson.

[14] G. Breit, Phys. Rev. **51**, 248 (1937); **51**, 778 (1937); **53**, 153 (1938).

PHYSICAL REVIEW VOLUME 78, NUMBER 2 APRIL 15, 1950

Dipole Transitions in the Nuclear Photo-Effect*

J. S. LEVINGER AND H. A. BETHE
Cornell University, Ithaca, New York
(Received January 12, 1950)

In this paper we apply sum rules to calculate under certain approximations the integrated cross section and the mean energy for photon absorption by heavy nuclei. In Section II we calculate the summed oscillator strength for dipole transitions as $\Sigma_n f_{on}=(NZ/A)(1+0.8x)$ where x is the fraction of attractive exchange force for the neutron-proton potential. For $N=Z$ this gives the cross section integrated over photon energy $\int_0^\infty \sigma dW=0.015A(1+0.8x)$ Mev-barns. In Section III we calculate the mean energy $\bar{W}$ for photon absorption. The mean energy is 4/3 the average kinetic energy of a nucleon for pure ordinary forces, or about 19 Mev; and is greatly increased by attractive exchange force. The harmonic mean energy

$$W_H=\Sigma_n f_{on}/[\Sigma_n f_{on}/(E_n-E_o)]$$

is much too low using the model of uncorrelated nucleons, but is reasonable if we use the alpha-particle model of the nucleus. In Section IV we develop a sum rule for quadrupole transitions, and show that quadrupole transitions can account for only about six percent of the experimentally observed integrated cross section. In Section V we apply the sum rules for dipole transitions to the photo-disintegration of the deuteron, and compare the results from sum rules with those from direct calculations of the cross section. In Section VI we determine the asymptotic behavior of the cross section for dipole transitions at high photon energies. This is determined by the nature of the singularities in the neutron-proton potential. In the last section we discuss the G.E. experiments on the cross section for photo-disintegration, and its energy dependence, and find that our calculations explain the general features of the experiments. It is not necessary to assume the Goldhaber-Teller model of dipole vibrations by the entire nucleus.

I. INTRODUCTION

THE recent G.E. experiments[1,2] on the cross section and energy dependence of the nuclear photo-effect indicate that there are strong dipole transitions. At low excitation energy (a few Mev) it is commonly assumed that dipole and quadrupole transitions are about equally strong, the dipole transitions being greatly reduced by correlations between the motions of the nucleons.[3] Following this assumption, calculations of quadrupole transitions in the nuclear photo-effect were made some time ago by Weisskopf,[4] and others. However, correlations between the nucleons should cease to exist when very highly excited states (excitation energy more than about 20 Mev) are considered. Indeed, Goldhaber and Teller[5] have suggested that radiative transitions lead to rather sharply defined states in which there is anticorrelation between neutrons and protons, i.e., all protons move together against all neutrons.

In this paper we shall calculate dipole transitions in the nuclear photo-effect, without making Goldhaber and Teller's assumption of dipole vibrations of the whole nucleus. We wish to see which results are peculiar to their model, and which are characteristic for all dipole transitions.

Calculations of the photoelectric cross section for a nuclear transition from the ground state to a particular excited state demands knowledge of the wave functions of both the ground state and excited state. Very little is known of the wave function for the ground state of a heavy nucleus, and much less is known of the wave functions for the excited states. In this paper we shall sum over all excited states, using closure for the matrix elements, so that our results will depend only on the wave function assumed for the ground state.

In Section II we calculate $\sum_n f_{on}$ for heavy nuclei, where f_{on} is the oscillator strength for a dipole transition from ground state o to excited state n. Feenberg[6] and Siegert[7] have shown that attractive exchange forces increase the summed oscillator strength above the customary value for pure ordinary forces. We shall calculate this increase for two assumed shapes of the neutron-proton potential. From the summed oscillator strength we find $\int \sigma dW$, where W is the photon energy, and σ is the cross section for photon absorption. (σ is the sum of all the partial cross sections for the various nuclear reactions that may occur subsequent to the photon absorption: $\gamma-n$, $\gamma-p$, $\gamma-\gamma$, etc.)

In Section III we calculate $\sum_n(E_n-E_o)f_{on}$, where E_n-E_o is the energy difference between the ground and excited state. The ratio

$$\sum_n(E_n-E_o)f_{on}/(\sum_n f_{on})=\int \sigma W dW \Big/ \int \sigma dW=\bar{W},$$

the mean energy for photons absorbed in the photo-electric effect. We also discuss the harmonic mean energy $\sum_n f_{on}/[\sum_n f_{on}/(E_n-E_o)]$. In Section IV we develop a sum rule for quadrupole transitions, and show that quadrupole transitions alone are unable to account for the results of the G.E. experiments. In Section V we apply the sum rules for dipole transitions to the photoelectric cross section of the deuteron, and compare the results with those from direct calculations of the cross section. In Section VI we discuss the asymptotic form for the dipole cross section at high energies. In Section VII we discuss the G.E. experi-

* Supported in part by the ONR.
[1] J. L. Lawson and M. L. Perlman, Phys. Rev. **74**, 1190 (1948).
[2] G. C. Baldwin and G. S. Klaiber, Phys. Rev. **73**, 1156 (1948).
[3] H. A. Bethe, Rev. Mod. Phys. **9**, 71 (1937), Sections 87 to 90.
[4] V. F. Weisskopf, Phys. Rev. **59**, 318 (1941).
[5] M. Goldhaber and E. Teller, Phys. Rev. **74**, 1046 (1948).
[6] E. Feenberg, Phys. Rev. **49**, 328 (1936).
[7] A. J. F. Siegert, Phys. Rev. **52**, 787 (1937).

ments on the nuclear photo-effect, and compare the experimental results with the calculations of this paper.

We shall make several important approximations for the nuclear ground state. First, we shall use the Hartree-type approximation of one nucleon moving in the potential due to all the other nucleons; i.e., we assume that there are no correlation effects among the nucleons. We shall also neglect surface effects due to the finite size of the nucleus. Further, we are considering the case of pure central forces, and we are assuming that the forces on a nucleon in a nucleus are just the sum of the forces due to all the other nucleons. This neglects the possibility of "many-body forces."

We shall calculate the results from the dipole sum rules for both square and Yukawa wells for the neutron-proton potential; and we shall use the fraction of the neutron-proton force that is exchange as a parameter. In principle this parameter could be determined by comparison of our calculations with experimental data, but both the data and the calculations are at present too uncertain to make this practical. The nuclear radius also enters into our calculations. We shall use nuclear radius $=r_0A^{\frac{1}{3}}$, and calculate for both $r_0=1.50\times10^{-13}$ cm, and $r_0=1.37\times10^{-13}$ cm.[8]

II. SUM RULE FOR OSCILLATOR STRENGTH

The oscillator strength f_{on} for a photoelectric dipole transition between state o and state n is defined as

$$f_{on}=[2M(E_n-E_o)/\hbar^2]\left|\int \psi_o^* z\psi_n d\tau\right|^2=|z_{on}/\lambda\!\!\!^{-}_{on}|^2. \quad (1)$$

Here z is the component of the displacement along the direction of polarization of the photon; and $\lambda\!\!\!^{-}_{on}$ is the wave-length divided by 2π, for a nucleon of mass M and energy (E_n-E_o).

The photoelectric cross section for absorption of a photon of energy $W=E_n-E_o$ is proportional to the oscillator strength:

$$\sigma_{on}=(2\pi^2e^2\hbar/Mc)f_{on}, \quad (2)$$

where f_{on} is the oscillator strength per unit energy in the final state.

For the case of electrons in an atom, the Thomas-Reiche-Kuhn sum rule[9] states that the sum of the oscillator strengths equals the number of electrons:

$$\sum_n f_{on}=Z. \quad (3)$$

$\sum_n$ means sum over discrete levels and integrate over the continuum.

When we consider the displacement from the center of mass of the nucleus,[3] each proton behaves as if its charge were $e(N/A)$, where N is the number of neutrons in the nucleus; and each neutron as if its charge were $-e(Z/A)$. The summed oscillator strength becomes

$$\sum_n f_{on}=Z(N/A)^2+N(-Z/A)^2=NZ/A. \quad (4)$$

Thus, for the case $N=Z=A/2$, the summed oscillator strength is $Z/2$. The remainder goes into transitions in which the nucleus as a whole vibrates due to the electric field and this vibration does not lead to photon absorption.

Using Eqs. (2) and (4) for the case $N=Z$, we have the integrated cross section for photon absorption

$$\int \sigma dW=\frac{\pi^2e^2\hbar}{Mc}\frac{A}{2}=0.015A \text{ Mev-barn}. \quad (5)$$

This result agrees with that given by Goldhaber and Teller[5] in their theory of dipole vibrations of the entire nucleus.

Feenberg[6] and Siegert[7] have shown that the sum rules are modified for exchange forces. We want first to find $(E_n-E_o)(\sum_i z_i)_{on}$, where $\sum_i$ means summation over all protons in the nucleus. We multiply the Schrödinger equations for ψ_o^* and ψ_n by ψ_n and ψ_o^*, respectively, subtract, multiply by the coordinate $\sum_i z_i$, and integrate over-all space for all nucleon coordinates. ψ_o is the wave function of the ground state for the whole nucleus.

$$\begin{aligned}(\hbar^2/2M)\nabla^2\psi_o^*+E_o\psi_o^*-V\psi_o^*=0 \quad &|\psi_n,\\ (\hbar^2/2M)\nabla^2\psi_n+E_n\psi_n-V\psi_n=0 \quad &|\psi_o^*,\end{aligned} \quad (6)$$

$$(E_n-E_o)\psi_n\psi_o^*+(\hbar^2/2M)(\psi_o^*\nabla^2\psi_n-\psi_n\nabla^2\psi_o^*) -\psi_nV\psi_o^*+\psi_o^*V\psi_n=0, \quad (7)$$

$$(E_n-E_o)(\textstyle\sum_i z_i)_{on}=\dfrac{\hbar^2}{2M}\displaystyle\int\sum_i(\psi_n\nabla^2\psi_o^*-\psi_o^*\nabla^2\psi_n)z_i d\tau$$

$$+\int\sum_i(\psi_n z_i V\psi_o^*-\psi_o^* z_i V\psi_n)d\tau. \quad (8)$$

The first integral on the right is integrated by parts. The second integral on the right gives a contribution only for exchange forces between neutron and proton. For ordinary forces the potential and coordinate commute. Exchange between two protons does not contribute since we sum over all protons in the dipole moment. We shall consider an attractive exchange force of the same shape as the ordinary force, and of magnitude a fraction x of the entire force between neutron and proton. We then write in the second integral $V=xV(r_{ij})P_{ij}$ where r_{ij} is the distance between proton and neutron and P_{ij} is the operator for exchanging the ith the proton with the jth neutron. Using the Hermitian character of zP_{ij}, Eq. (8) becomes:

$$(E_n-E_o)(\textstyle\sum_i z_i)_{on}=\dfrac{\hbar^2}{2M}\displaystyle\int\sum_i\left(-\psi_n\frac{\partial\psi_o^*}{\partial z_i}+\psi_o^*\frac{\partial\psi_n}{\partial z_i}\right)d\tau$$

$$-\sum_i\sum_j x\int\psi_nV(r_{ij})(z_i-z_j)P_{ij}\psi_o^*d\tau. \quad (9)$$

[8] Fernbach, Serber, and Taylor, Phys. Rev. **75**, 1352 (1949).
[9] H. A. Bethe, *Handbuch der Physik* (1933), Vol. 24/1, p. 434.

We want N/A times the result summed over all protons combined with $-Z/A$ times this result summed over all neutrons. When we sum over all neutrons the roles of neutron and proton are reversed in the second integral on the right, and we have the negative of the result of Eq. (9). We find

$$\sum_n f_{on}=\sum_n\Big\{\int\Big[\frac{N}{A}\sum_i\Big(\psi_o^*\frac{\partial\psi_n}{\partial z_i}-\psi_n\frac{\partial\psi_o^*}{\partial z_i}\Big)-\frac{Z}{A}\sum_j\Big(\psi_o^*\frac{\partial\psi_n}{\partial z_j}-\psi_n\frac{\partial\psi_o^*}{\partial z_j}\Big)\Big]d\tau-\sum_i\sum_j\frac{2M}{\hbar^2}x\int\psi_n V(r_{ij})(z_i-z_j)P_{ij}\psi_o^*d\tau\Big\}\times\Big\{\int\Big(\frac{N}{A}\sum_i\psi_n z_i\psi_o^*-\frac{Z}{A}\sum_j\psi_n z_j\psi_o^*\Big)d\tau\Big\},\tag{10}$$

$$\sum_n f_{on}=NZ/A-\frac{2M}{\hbar^2}x\times\int\psi_o^*\sum_i\sum_j\Big[\tfrac{1}{2}(z_i-z_j)+(N/A-\tfrac{1}{2})(z_i+z_j)\Big]\times(z_i-z_j)V(r_{ij})P_{ij}\psi_o d\tau.$$

We have two reasons to neglect the term $(N/A-\frac{1}{2})\times(z_i^2-z_j^2)$ as small when compared with $\frac{1}{2}(z_i-z_j)^2$. One is that $(N/A-\frac{1}{2})\ll\frac{1}{2}$, and the other that protons and neutrons have similar distributions in the nucleus, so $z_i^2-z_j^2$ is small. Making this approximation we have a result in agreement[10] with Siegert's.

$$\sum_n f_{on}=NZ/A-(2M/\hbar^2)x\times\frac{1}{6}\int\psi_o^*\sum_i\sum_j r_{ij}^2V(r_{ij})P_{ij}\psi_o d\tau.\tag{11}$$

We shall compute the last term of Eq. (11) on two different assumptions as to the potential $V(r)$. For purposes of illustration, let us first ignore the exchange operator P_{ij} and evaluate Eq. (11) for the square well potential.

$$\begin{aligned}V&=-V_o \quad r<b \quad V_o=s\pi^2\hbar^2/4Mb^2,\\ V&=0 \qquad r>b\end{aligned}\tag{12}$$

where b is the intrinsic range and s is the depth parameter of Blatt and Jackson.[11] ψ_o is the wave function for all nucleons involving all their coordinates. When we consider the contribution of the ith proton and jth neutron, integration over the coordinates of all the other particles gives just unity. We shall neglect effects due to the edge of the nucleus, and use the model of a uniformly dense nucleus of radius $r_oA^{\frac{1}{3}}$.

$$|\psi_o|^2=\frac{1}{(4/3)\pi r_o^3A}.\tag{13}$$

For this wave function, each nucleon is "smeared out" over the whole nucleus; and each of the NZ neutron-proton pairs gives the same contribution. Using this potential and wave function in Eq. (11) we have

$$\begin{aligned}\sum_n f_{on}&=NZ/A-\Big(\frac{2M}{\hbar^2}\frac{1}{6}x\Big)\Big(s\frac{\pi^2}{4}\frac{\hbar^2}{Mb^2}\Big)\times\Big(\frac{4}{3}\pi r_o^3A\Big)^{-1}NZ\int_0^b r^2 4\pi r^2dr\\ &=(NZ/A)\Big[1+\frac{\pi^2}{20}s(b/r_o)^2x\Big].\end{aligned}\tag{14}$$

The exchange effect on the summed oscillator strengths is the same order of magnitude as the first term in the bracket due to ordinary forces. For three-fourths of the interactions we should use the triplet well and for one-fourth of the interactions the singlet well.

Ignoring the exchange operator in Eq. (11), as is done in reaching this result, overestimates the effect of the exchange forces since the P_{ij} term has an interference effect. In calculating the effect of the exchange operator with interference we shall follow the treatment of the mixed density for a completely degenerate Fermi gas.[12] We use plane waves for each nucleon, with wave numbers chosen in accord with the Pauli principle. This neglects surface effects at the edge of the nucleus; as well as correlation effects among nucleons. For ground state wave function we use[13]

$$\psi_o=\prod_i\prod_j\exp(i\mathbf{k}_i\cdot\mathbf{r}_i)\exp(i\mathbf{k}_j\cdot\mathbf{r}_j).\tag{15}$$

Then

$$\psi_o^*P_{ij}\psi_o=\prod_i\prod_j\exp(-i\mathbf{k}_i\cdot\mathbf{r})\exp(i\mathbf{k}_j\cdot\mathbf{r}),\tag{16}$$

where $\mathbf{r}=\mathbf{r}_i-\mathbf{r}_j$ is the vector between the ith proton and jth neutron. We now wish to sum this over all protons and neutrons, for use in Eq. (11). Take the direction of $\mathbf{r}$ as the polar axis. The $\sum_i$ over protons is replaced by an integral over their wave numbers:

$$((4/3)\pi k^3)^{-1}\int_0^k\exp(-i\mathbf{k}_i\cdot\mathbf{r}_i)k_i^2\sin\theta dk_i d\theta d\varphi=\frac{3}{(kr)^2}\Big[\frac{\sin kr}{kr}-\cos kr\Big].\tag{17}$$

Here k is the maximum wave number for protons in the

[10] Our exchange term appears at first to be twice that given by Siegert. This apparent difference arises from our different notation for summing over the nucleons.

[11] J. M. Blatt and J. D. Jackson, Phys. Rev. **76**, 18 (1949).

[12] H. A. Bethe and R. Bacher, Rev. Mod. Phys. **8**, 25 (1936).

[13] It is not necessary to write the determinantal wave function obeying the Pauli principle of antisymmetry between protons (or between neutrons) since we are concerned only with exchange between proton and neutron.

nucleus. We obtain the same result for the sum, or integration, over neutrons using k', the maximum wave number for neutrons.

To a first approximation, $Z=N$, and for this case

$$k=k'=(9\pi)^{\frac{1}{3}}/2r_o. \tag{18}$$

In evaluating Eq. (11) we use Eq. (17) for the interference effect due to the exchange operator and otherwise follow our derivation of Eq. (14).

$$\sum_n f_{on}=NZ/A-\frac{2M}{\hbar^2}\frac{1}{6}x\frac{NZ}{(4/3)\pi r_o^3 A}$$
$$\times\int_0^\infty\left[\frac{3}{(kr)^2}\left(\frac{\sin kr}{kr}-\cos kr\right)\right]^2 V(r)4\pi r^4 dr. \tag{19}$$

The integral is evaluated for both square and Yukawa wells. For the former,

$$\sum_n f_{on}=(NZ/A)\left[1+\frac{\pi^2}{20}s(b/r_o)^3 x f_1(kb)\right],$$

where

$$f_1(kb)=\frac{45}{(kb)^4}\left[\frac{1}{2}+\frac{\sin 2kb}{4kb}-\frac{\sin^2 kb}{(kb)^2}\right]. \tag{20}$$

For the Yukawa well $V=-V_o\exp(-\mu r)/r$,

$$\sum_n f_{on}=(NZ/A)\left[1+6\frac{M}{\mu\hbar^2}x\frac{V_o}{(\mu r_o)^3}f_2(kb)\right],$$

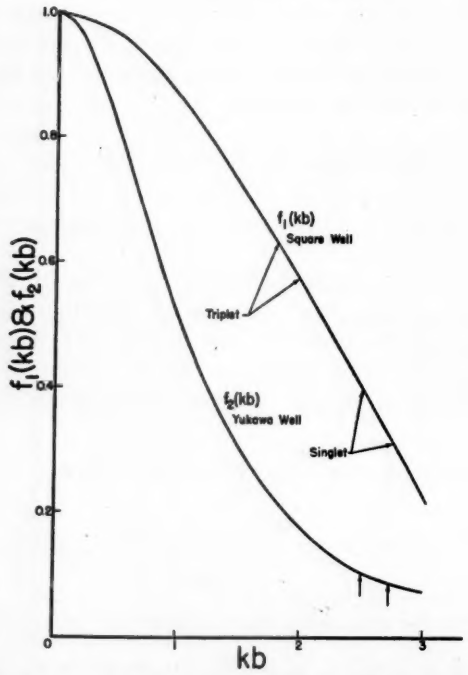

FIG. 1. Interference functions $f_1(kb)$ and $f_2(kb)$. See Eqs. (20) and (21) of the text. k is the maximum nucleon wave number, and b is the intrinsic range of the neutron-proton potential. The arrows show the values of kb used, using the nuclear constants of Eq. (22).

where

$$f_2(kb)=\frac{3}{8}\left(\frac{\mu}{k}\right)^4\left[-2+\left(1+\frac{\mu^2}{2k^2}\right)\log(1+4k^2/\mu^2)\right] \tag{21}$$

and[11] $\mu^{-1}=b/2.12$. The interference functions $f_1(kb)$ for square well and $f_2(kb)$ for Yukawa well are plotted in Fig. 1. For k small, the interference function gives unity. In these equations r_o is the parameter for nuclear radius taken as 1.50×10^{-13} cm or 1.37×10^{-13} cm, and x is the fraction of attractive exchange force.

The following were assumed for the neutron-proton potential:[11,14]

Square well:

triplet range $b=1.8\times10^{-13}$ cm,
depth $V_o=1.50(\pi^2/4)(\hbar^2/Mb^2)$,
singlet range $b=2.5\times10^{-13}$ cm,
depth $V_o=0.95(\pi^2/4)(\hbar^2/Mb^2)$. (22)

Yukawa well for both singlet and triplet:
$\mu^{-1}=1.18\times10^{-13}$ cm;
intrinsic range $b=2.12\mu^{-1}=2.5\times10^{-13}$ cm,
triplet depth $V_o=(1.45)3.56b\,\hbar^2/Mb^2$,
singlet depth $V_o=(0.95)3.56b\,\hbar^2/Mb^2$.

The numerical results for Eqs. (20) and (21) are given in Table I.

The summed oscillator strength, considering interference, is about $(NZ/A)(1+0.8x)$. That is, attractive exchange forces roughly double the summed oscillator strength.

Neglecting the interference effect, the result for the summed oscillator strengths is proportional to the assumed value of $(b/r_o)^3$. [See Eq. (14) for the square well.] Since the interference function decreases with increasing kb (and k depends on r_o), the result including interference is seen to be much less sensitive to the assumed value of b/r_o. Neglecting interference, the long tail of the Yukawa well gave a much larger contribution to the summed oscillator strength than did the square well. With interference this tail has very little effect, and the Yukawa well and square well give about the same contribution.

Corresponding to this summed oscillator strength we have the integrated cross section for photon absorption

$$\int\sigma dW=(2\pi^2e^2\hbar/Mc)\sum_n f_{on}$$
$$=(2\pi^2e^2\hbar/Mc)(NZ/A)(1+0.8x). \tag{23}$$

For the case $N=Z=A/2$ this gives the numerical result

$$\int\sigma dW=0.015A(1+0.8x)\text{ Mev barns}. \tag{24}$$

In the last section we show that this result is consistent with present experimental data.

[14] H. A. Bethe, Phys. Rev. **76**, 38 (1949).

TABLE I. Summed oscillator strength (times A/NZ).

	Square well		Yukawa well	
r_o(cm)$\times 10^{13}$	1.50	1.37	1.50	1.37
Neglecting interference	$(1+1.48x)$	$(1+1.96x)$	$(1+6.5x)$	$(1+8.5x)$
With interference	$(1+0.80x)$	$(1+0.91x)$	$(1+0.69x)$	$(1+0.71x)$

III. MEAN ENERGY FOR PHOTON ABSORPTION

In this section we shall evaluate the mean energy for photon absorption:

$$\bar{W}=\sum_n f_{on}(E_n-E_o)/(\sum_n f_{on})$$
$$=\int \sigma W dW \Big/ \int \sigma dW. \quad (25)$$

The numerator of this expression is given from Eq. (9) (integrate the first term on the right of Eq. (9) by parts).

$$\sum_n f_{on}(E_n-E_o)$$
$$=\frac{2M}{\hbar^2}\sum_n\left|(E_n-E_o)\left[\frac{N}{A}(\sum_i z_i)_{on}-\frac{Z}{A}(\sum_j z_j)_{on}\right]\right|^2$$
$$=\frac{2M}{\hbar^2}\sum_n\left|\frac{\hbar^2}{2M}\int\left(2\frac{N}{A}\sum_i\psi_o^*\frac{\partial\psi_n}{\partial z_i}-2\frac{Z}{A}\sum_j\psi_o^*\frac{\partial\psi_n}{\partial z_j}\right)d\tau\right.$$
$$\left.-\sum_i\sum_j x\int\psi_n V(z_i-z_j)P_{ij}\psi_o^*d\tau\right|^2. \quad (26)$$

The first term in the second writing of Eq. (26) occurs for any force and the second term is due only to exchange forces. When squared we will have three terms: (1) the first term squared, which we shall call the ordinary term (it is the only term for pure ordinary forces); (2) the cross-product term; and (3) the pure exchange term. We shall evaluate these separately.

The ordinary term can be written using matrix notations where P is the z component of momentum:

$$\sum_{n\ \mathrm{ord}} f_{on}(E_n-E_o)$$
$$=\frac{2M}{\hbar^2}\sum_n\frac{i\hbar}{M}\left(\frac{N}{A}(\sum_i P_i)_{on}-\frac{Z}{A}(\sum_j P_j)_{on}\right)$$
$$\times\left[-\frac{i\hbar}{M}\left(\frac{N}{A}(\sum_i P_i)_{no}-\frac{Z}{A}(\sum_j P_j)_{no}\right)\right]$$
$$=\frac{2}{M}[(N/A)^2(\sum_i P_i^2)_{oo}+(Z/A)^2(\sum_j P_j^2)_{oo}]. \quad (27)$$

In writing the last term we are neglecting correlation terms by taking only the diagonal elements in the double summation. That is, we are neglecting terms of the form $(P_iP_{i'})_{oo}$, where $i\neq i'$; and similar terms for two different neutrons, or a neutron and a proton. There will always be at least a small amount of correlation of momentum since the center of mass of the nucleus remains at rest in the ground state. If a particular proton has a momentum p_1, then the sum of the momenta of all the other nucleons is $-p_1$. If this momentum $-p_1$ is assumed to be distributed evenly among the other $A-1$ nucleons, the correlation terms can be computed to be $1/(A-1)$ of the diagonal terms that we shall calculate, and can therefore be neglected for heavy nuclei.

We can rewrite Eq. (27) using $p_i^2/2M=\frac{1}{2}T_i$ where T_i is the kinetic energy of the ith particle. (P is the z-component of momentum)

$$\sum_{n\ \mathrm{ord}} f_{on}(E_n-E_o)$$
$$=(4/3)[(N/A)^2(\sum_i T_i)_{oo}+(Z/A)^2(\sum_j T_j)_{oo}]$$
$$=(4/3)\bar{T}(NZ/A). \quad (28)$$

Here $\bar{T}$ is the expectation value of the kinetic energy for the average nucleon in the nucleus.[15] Using the uncorrelated plane-wave model of the nucleus with nucleons of wave number from 0 to $k_{\max}$ filling up phase space according to the Pauli principle,

$$\bar{T}=\frac{\hbar^2\langle k^2\rangle_{\mathrm{Av}}}{2M}$$

and

$$\langle k^2\rangle_{\mathrm{Av}}=\left(\int_0^{k_{\max}}k^2k^2dk\right)\Big/\left(\int_0^{k_{\max}}k^2dk\right)=\frac{3}{5}k_{\max}^2. \quad (29)$$

For the case of pure ordinary forces, the mean energy $\bar{W}$ for photon absorption is from Eqs. (12), (28), and (29),

$$\bar{W}=\sum_n f_{on}(E_n-E_o)/\sum_n f_{on}=(4/5)T_{\max}. \quad (30)$$

The value of $k_{\max}$ and $T_{\max}$ depend on the assumed nuclear radius. For parameter $r_o=1.37\times10^{-13}$ cm, $(4/5)T_{\max}=19$ Mev; while for $r_o=1.50\times10^{-13}$ cm, $(4/5)T_{\max}=16$ Mev. (The value of $\bar{W}$ depends on $1/r_o^2$; but is independent of A in our approximation where we neglect surface effects.)

The cross product (cp) term in $\sum_n(E_n-E_o)f_{on}$ is from Eq. (26)

$$\sum_{n\ \mathrm{cp}}(E_n-E_o)f_{on}$$
$$=-\sum_n 2\left[\int\left(-\frac{N}{A}\sum_i 2\psi_n\frac{\partial\psi_0^*}{\partial z_i}+\frac{Z}{A}\sum_j 2\psi_n\frac{\partial\psi_o^*}{\partial z_j}\right)d\tau\right]$$
$$\times\left[\sum_i\sum_j x\int\psi_n V(z_i-z_j)P_{ij}\psi_o^*d\tau\right]$$

[15] In taking the average, each proton is given weight N^2, and each neutron is given weight Z^2.

$$=4\frac{N}{A}x\int\sum_i\sum_j\frac{\partial\psi_o^*}{\partial z_i}V(z_i-z_j)P_{ij}\psi_o d\tau$$

$$-4\frac{Z}{A}x\int\sum_i\sum_j\frac{\partial\psi_o^*}{\partial z_j}V(z_i-z_j)P_{ij}\psi_o d\tau. \quad (31)$$

Using the plane-wave expression for ψ_o given in Eq. (15), we have $\partial\psi_o^*/\partial z_i=-k_{iz}\psi_o^*$ and $\partial\psi_o^*/\partial z_j=-ik_{jz}\psi_o^*$. Equation (31) becomes

$$\sum_{n\ \mathrm{cp}}(E_n-E_o)f_{on}$$

$$=4\frac{N}{A}x\int\sum_i\sum_j[-ik_{iz}\psi_o^*V(z_i-z_j)P_{ij}\psi_o$$

$$+ik_{jz}\psi_o^*V(z_i-z_j)P_{ij}\psi_o]d\tau$$

$$+4\left(-\frac{N}{A}+\frac{Z}{A}\right)x\int\sum_i\sum_j ik_{jz}\psi_o^*$$

$$\times V(z_i-z_j)P_{ij}\psi_0 d\tau. \quad (32)$$

We neglect the second term, since for actual nuclei $|Z/A-N/A|\ll N/A$; and we take $N/A=\frac{1}{2}$. Using $z_i-z_j=z$ and Eq. (16) for $\psi_o^*P_{ij}\psi_o$ the first term can be rewritten as

$$\sum_{n\ \mathrm{cp}}(E_n-E_o)f_{on}=2x\int\sum_i\sum_j\frac{\partial}{\partial z}(\psi_o^*P_{ij}\psi_o)Vz d\tau$$

$$=-2x\int\sum_i\sum_j\psi_o^*P_{ij}\psi_o\frac{\partial}{\partial z}(Vz)d\tau. \quad (33)$$

The sum over protons and neutrons is performed by integrating over their momenta, as in deriving Eq. (19). We have

$$\sum_{n\ \mathrm{cp}}(E_n-E_o)f_{on}=-\frac{NZ}{A}\frac{6}{r_0^3}x\int\left(\frac{1}{3}\frac{\partial V}{\partial r}r+V\right)$$

$$\times\left[\frac{3}{(kr)^2}\left(\frac{\sin kr}{kr}-\cos kr\right)\right]^2 r^2dr. \quad (34)$$

We shall evaluate this for both a square well and for a Yukawa well. For the square well of depth V_o and width b the integration gives

$$\sum_{n\ \mathrm{cp}}(E_n-E_o)f_{on}=(NZ/A)2V_0(b/r_0)^3xf_3(kb),$$

where

$$f_3(kb)=\frac{9}{(kb)^4}\left[-2\left(\frac{\sin kb}{kb}\right)^2+4\frac{\sin 2kb}{2kb}\right.$$

$$\left.-2+kb\,\mathrm{Si}(2kb)\right]. \quad (35)$$

where $\mathrm{Si}(x)$ is the integral sine function. For the Yukawa well, $V=-V_o\exp(-\mu r)/r$, Eq. (34) gives

$$\sum_{n\ \mathrm{cp}}(E_n-E_o)f_{on}=(NZ/A)18(V_o/\mu^2r_0^3)xf_4(kb),$$

where

$$f_4(kb)=-\tfrac{1}{4}(\mu/k)^4+\tfrac{1}{2}(\mu/k)^2-(\mu/k)^3\tan^{-1}(2k/\mu)$$

$$+\tfrac{1}{16}[(\mu/k)^6+8(\mu/k)^4]\log(1+4k^2/\mu^2) \quad (36)$$

and $\mu^{-1}=b/2\cdot 12$. The functions $f_3(kb)$ and $f_4(kb)$ are plotted in Fig. 2.

The third type of term is the exchange-exchange term which from Eq. (26) is

$$\sum_{n\ \mathrm{exch}}(E_n-E_o)f_{on}=\frac{2M}{\hbar^2}\sum_i\sum_j\tfrac{1}{3}x^2\int\psi_o^*V^2r^2\psi_o d\tau. \quad (37)$$

The square well potential gives

$$\sum_{n\ \mathrm{exch}}(E_n-E_o)f_{on}=(NZ/A)(b/r_o)^3x^2s(\pi^2/10)V_o. \quad (38)$$

For the Yukawa potential $V=-V_o\exp(-\mu r)/r$ we have

$$\sum_{n\ \mathrm{exch}}(E_n-E_o)f_{on}=\frac{NZ}{A}\frac{x^2}{4}\frac{2M}{\hbar^2}\left(\frac{b}{2.12r_o}\right)^3V_o^2. \quad (39)$$

These equations for the contribution of the cross-product and exchange-exchange terms are evaluated assuming the nuclear constants given in Eq. (22).

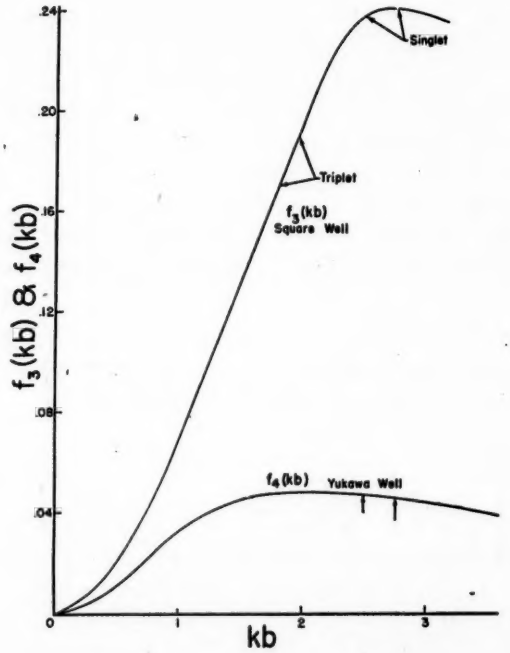

FIG. 2. Interference functions $f_3(kb)$ and $f_4(kb)$. See Eqs. (35) and (36) of the text. k is the maximum nucleon wave number; and b is the effective range of the neutron-proton potential. The arrows show the values of kb used, using the nuclear constants of Eq. (22).

Combining the ordinary, the cross-product and the exchange terms we find the mean energy for photon absorption $\bar{W}=\sum_n(E_n-E_o)f_{on}/\sum_n f_{on}$ for square well and $r_o=1.50\times10^{-13}$ cm (curve B)

$$\bar{W}=\frac{16+30x+101x^2}{1+0.80x}\text{ Mev};\qquad(40)$$

for square well and $r_o=1.37\times10^{-13}$ cm (curve A)

$$\bar{W}=\frac{19+42x+132x^2}{1+0.91x}\text{ Mev};\qquad(41)$$

for Yukawa well and $r_o=1.50\times10^{-13}$ cm (curve D)

$$\bar{W}=\frac{16+28x+36x^2}{1+0.69x}\text{ Mev};\qquad(42)$$

and for Yukawa well and $r_o=1.37\times10^{-13}$ cm (curve C)

$$\bar{W}=\frac{19+36x+48x^2}{1+0.71x}\text{ Mev}.\qquad(43)$$

These four equations are plotted in Fig. 3.

In these four equations, the denominator is the value for $\sum_n f_{on}$ given in Table I, considering interference. The first term in the numerator is the ordinary term which was evaluated as 4/3 of the expectation value of the kinetic energy of an average nucleon. This term is sensitive to the assumed value for the parameter r_o in the nuclear radius $r_oA^{\frac{1}{3}}$; and does not depend on the well shape or character of the force between the nucleons. The second term in the numerator is the contribution from the ordinary-exchange cross-product terms of Eqs. (35) or (36); and is therefore proportional to the fraction x of exchange force. The value of this term is sensitive to the ratio b/r_o, but it not sensitive to the well-shape. The third term in the numerator is the exchange-exchange term of Eqs. (38) or (39), and is therefore proportional to x^2. It is sensitive to the value of b/r_o; and also sensitive to the well-shape; being almost three times as large for the square well as for the Yukawa well. (The Gaussian and exponential wells, for the same effective range, give intermediate values between those for square and Yukawa wells.) With our model, which neglects surface effects at the boundary of the nucleus, $\bar{W}$ does not depend on A.

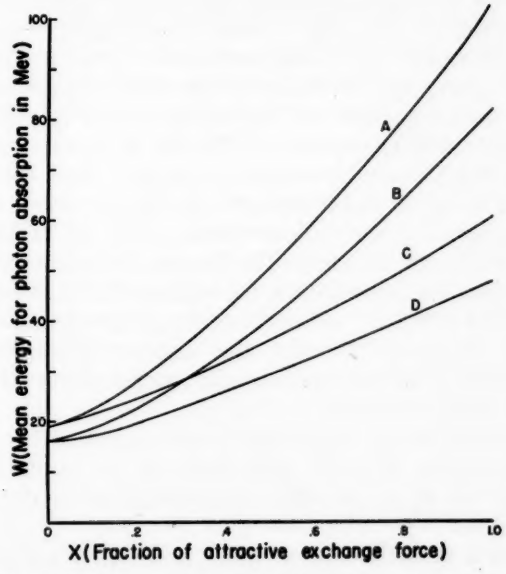

FIG. 3. Mean energy for photon absorption. The 4 curves are: A: square well, $r_o=1.37\times10^{-13}$ cm, see Eq. (41); B: square well, $r_o=1.50\times10^{-13}$ cm, see Eq. (40); C: Yukawa well, $r_o=1.37\times10^{-13}$ cm, see Eq. (43); D: Yukawa well, $r_o=1.50\times10^{-13}$ cm, see Eq. (42).

We would also like to calculate the harmonic mean energy for photon absorption

$$W_H=\sum_n f_{on}/[\sum_n f_{on}/(E_n-E_o)].$$

From Eq. (1) for the oscillator strength we have for a single proton

$$\sum_n f_{on}/(E_n-E_o)=\sum_n(2M/\hbar^2)|z_{on}|^2=(2M/\hbar^2)(z^2)_{oo}.\qquad(44)$$

If we take z_i as the component of displacement of the ith proton from the center of mass of the nucleus, and neglect all correlation terms:

$$\sum_n f_{on}/(E_n-E_o)=\frac{2M}{\hbar^2}\sum_n\left|\frac{N}{A}\sum_i(z_i)_{on}-\frac{Z}{A}\sum_j(z_j)_{on}\right|^2$$

$$=\frac{2M}{\hbar^2}\langle z^2\rangle_{oo}(NZ/A).\qquad(45)$$

Here $\langle z^2\rangle_{oo}$ is the expectation value of the squared z component of displacement for the average nucleon in the nucleus. This result is independent of whether the force between nucleons is ordinary or exchange in character. Combining this result with that of Table I for $\sum_n f_{on}$ we have

$$W_H=\sum_n f_{on}/\sum_n f_{on}/(E_n-E_o)\cong\frac{\hbar^2}{2M\langle z^2\rangle_{oo}}(1+0.8x).\qquad(46)$$

If we evaluate $\langle z^2\rangle_{oo}$ from our assumed values for the nuclear radius we find that W_H is only about 5 Mev for Cu^{63} and varies as $A^{-\frac{1}{3}}$, reaching a value of less than 1 Mev for uranium. This large nuclear absorption of comparatively low energy photons has not been observed. Let us instead determine $\langle z^2\rangle_{oo}$ from experiment.

Using Eq. (45) and the relation between oscillator strength and cross section we have

$$\int\frac{\sigma}{W}dW=\frac{2\pi^2e^2h}{Mc}\sum_n f_{on}/(E_n-E_o)$$

$$=\left(\frac{e^2}{\hbar c}\right)\frac{4\pi^2}{3}\frac{NZ}{A}\langle r^2\rangle_{oo}.\qquad(47)$$

Using the experimental measurements discussed in the last section, we have $\langle r^2\rangle_{oo}=5.8\times10^{-26}$ cm^2 for the nucleus Ge^{76}. This compares with $\frac{3}{5}(r_oA^{\frac{1}{3}})^2=20\times10^{-26}$ cm^2 or 24×10^{-26} cm^2, depending on which value for r_o we assume.

These comparisons suggest that we should have a model where the mean square displacement in the ground state $\langle r^2\rangle_{oo}$ does not vary greatly with A, and is much smaller than the value found where r is measured from the center of the nucleus. We can obtain better agreement with experiment by considering as a tentative model a nucleus made up of sub-units, such as alpha-particles. For dipole transitions in a nucleus made of alpha-particles the distance r_i for the ith proton should be measured from the center of the alpha-particle of which the ith proton is a member.[16] Then $\langle r^2\rangle_{oo}$ will not vary with A, and will be much smaller than calculated above. We might assume that the alpha-particle in a heavy nucleus is a sphere of uniform density occupying four times the volume allotted to a single nucleon. Then $\langle r^2\rangle_{oo}$ would equal $\frac{3}{5}(r_o4^{\frac{1}{3}})^2=2.9\times10^{-26}$ cm^2 or 3.5×10^{-26} cm^2, depending on which value for r_o we use. This is of the same order of magnitude as the experimental results.

One might wonder whether the alpha-particle model would give very different results for $\sum_n f_{on}$ and $\bar{W}$ from those calculated on the plane-wave model. The result $\sum_n f_{on}=NZ/A$ for ordinary forces is independent of correlation among the nucleons. The increase due to attractive exchange forces came mainly from neutron-proton distances of order $k^{-1}\cong10^{-13}$ cm, due to interference effects and the short-range potential. For these small distances the plane-wave model should not be too bad. The result $\bar{W}=(4/3)\bar{T}_{oo}$ for ordinary forces would be changed somewhat, due to the different calculation of the average kinetic energy $\bar{T}_{oo}$. The contributions to $\bar{W}$ from the cross-product and exchange terms will not be greatly changed, since again the main contributions come from small neutron-proton distances.

IV. QUADRUPOLE TRANSITIONS

The electric moment for pure ordinary forces is[3]

$$D_{on}=(e\hbar/M\omega)[\exp(i\mathbf{k}\cdot\mathbf{r})\nabla]_{on}. \tag{48}$$

For the quadrupole moment we take the second term, $i\mathbf{k}\cdot\mathbf{r}$, in the expansion of the exponential. This gives ky, where y is the component of $\mathbf{r}$ along the direction of propagation. The gradient is in the direction of polarization of the photon. Defining the oscillator strength as[3]

$$g_{on}=(2M\omega/e^2\hbar)(D_{on})^2, \tag{49}$$

we have the quadrupole oscillator strength as

$$g_{on}=(2k^2/M\hbar\omega)|(yP_z)_{on}|^2 =[2(E_n-E_o)/\hbar^2Mc^2]|(yP_z)_{on}|^2. \tag{50}$$

Then

$$\sum_n g_{on}/(E_n-E_o)=(2/\hbar^2Mc^2)\sum_n(yP_z)_{on}(P_zy)_{no} =(2/\hbar^2Mc^2)(yP_z^2y)_{oo}. \tag{51}$$

The integrated cross section for quadrupole transitions becomes, according to (2)

$$\int_0^\infty \sigma_q dW/W=4\pi^2(e^2/\hbar c)(1/Mc^2)(1/M)(yP_z^2y)_{oo}. \tag{52}$$

Assuming no correlation between y and p_z we write this as

$$\int_0^\infty \sigma_q dW/W=4\pi^2(e^2/\hbar c)(\tfrac{2}{3}T_{oo}/Mc^2)\tfrac{1}{3}\langle r^2\rangle_{oo}. \tag{53}$$

This result should be multiplied by the number of protons in the nucleus, if we assume no correlations among the protons, and the average kinetic energy $\bar{T}_{oo}$ should be used. For Ge^{76} we have the numerical result of 6 mb; or only about six percent of the experimental result for this quantity of over 100 mb as discussed in the last section. Thus quadrupole transitions represent only a small fraction of the nuclear photo-effect.

There is, however, good evidence that quadrupole transitions are as important as dipole transitions for low excitation energy. The measurements of internal conversion of gamma-radiation following beta- or alpha-decay indicate that dipole transitions, at an excitation energy of roughly 1 Mev, are very weak.[3] The small gamma-ray widths observed in most $(n-\gamma)$ reactions indicate that the oscillator strength for radiative transitions to the ground state are very small,[3] indicating that at 8 Mev excitation dipole transitions are not important. Earlier measurements[3] indicated that $(p-\gamma)$ reactions for light nuclei had gamma-ray width corresponding to quadrupole rather than dipole transitions. However recent measurements[17,18] give a much larger gamma-ray width, indicating dipole transitions. This is true, e.g., of the well-known reaction $Li^7(p,\gamma)Be^8$. The most striking, however, is the $He^3(p,\gamma)$ reaction,[18] where the gamma-ray width of about 1 kev corresponds to an oscillator strength of about one-half for the transition from the excited state of He^4 at 22 Mev down to the ground state. The sum of all dipole transitions from the ground state, for ordinary forces, is only $NZ/A=1$ for He^4, so this represents a very strong dipole transition. Further the angular distribution observed for the photons from this reaction proves that it is a dipole transition.

We have shown above that photo-nuclear reactions, which appear to occur principally at an excitation energy[2] of 20 to 30 Mev are predominantly dipole transitions.

Thus a model is needed which will suppress dipole transitions at excitation energies of, say, less than 10

[16] We can get this same result by considering the correlations among the particles in deriving Eq. (45).

[17] Fowler, Lauritsen, and Lauritsen, Rev. Mod. Phys. **20**, 236 (1948).

[18] R. F. Taschek *et al.* (private communication).

Mev, but allow them at higher energies. Strong correlation between neutrons and protons, as, for example, in the alpha-particle model, will suppress dipole transitions at low energies. In a nucleus composed entirely of alpha-particles there will be no dipole transitions[3] due to vibration of the alpha-particles in the nucleus, as in the dipole approximation all the alpha-particles experience the same electric field and vibrate together. (We should put $N=0$ in our sum rule $\sum_n f_{on}=NZ/A$, giving no dipole transitions.) But at higher photon energies the photon can disrupt a particular alpha-particle by a dipole transition, thus transferring energy to the nucleus. That is, correlations will not prevent dipole transitions for photon energies great enough to excite the first excited state of the alpha-particle, or about 20 Mev. At very high photon energies, where the value of λ for the photon is comparable to the size of the alpha-particle, higher multipole transitions will again be of importance.

We must make clear that correlations among the nucleons can never prevent dipole transitions altogether. Correlations can only prevent dipole transitions in some given energy range, but this decrease must be compensated for by stronger dipole transitions in some other energy range. The sum rule for ordinary forces $\sum_n f_{on}=NZ/A$ is not altered by correlations among the nucleons.

Thus the alpha-particle model gives qualitatively correct predictions for the integrated cross section $\int \sigma dW/W$, and for the energy dependence of ratio of quadrupole to dipole transitions. It is, of course, only a tentative model, and should not be taken too literally.

V. APPLICATION TO THE DEUTERON

Calculations of the photoelectric cross section for the deuteron for various photon energies have been performed on various assumptions as to size and shape of well, and the exchange character of the neutron-proton force. By comparison with these results we are able to check our calculations using sum rules. Also discussion of this simplest case of the photoelectric effect helps us to obtain some physical understanding of the change in the sum rule due to exchange forces.

For the deuteron, we shall use z as the component along the polarization of the displacement of the proton from the neutron, which is twice the proton displacement from the center of mass. We use the reduced mass $M/2$ for the proton; and the dipole oscillator strength is

$$f_{on}=\frac{2(M/2)}{\hbar^2}(E_n-E_o)\tfrac{1}{4}(z_{on})^2. \tag{54}$$

Using Eq. (9) for $(E_n-E_o)z_{on}$ we find the summed oscillator strength

$$\sum_n f_{on}=\tfrac{1}{4}\left[1-\tfrac{2}{3}xM\hbar^{-2}\int \psi_o^* V r^2 P_{ij}\psi_o d\tau\right]. \tag{55}$$

Pure ordinary forces ($x=0$) give $\sum f_{on}=\frac{1}{4}$ and give the integrated cross section

$$\int \sigma dW=\frac{2\pi^2e^2\hbar}{(M/2)c}\sum_n f_{on}=\pi^2e^2\hbar/Mc. \tag{56}$$

This well-known result is in agreement with the result found by integration of the Bethe-Peierls formula, which holds for zero range of nuclear forces; and is also in agreement with the result for ordinary forces given by Breit and Condon[19] for a square well of finite range.

We have evaluated the contribution to the summed oscillator strength due to exchange forces for a square well and also for a Yukawa well using the nuclear constants given in Eq. (22). For the square well using the complete wave function and the constants of Eq. (22) we have

$$\sum_n f_{on}=\tfrac{1}{4}+0.10x. \tag{57}$$

For the Yukawa well we use Hulthen's approximate wave function for the ground state[20] and obtain

$$\sum_n f_{on}=\tfrac{1}{4}+0.083x. \tag{58}$$

Thus for $x=1$ (pure attractive exchange force) there is a 40 percent increase or a 33 percent increase in the summed oscillator strength for the square and Yukawa wells, respectively.

This increase for a square well is in qualitative agreement with Breit and Condon's[19] results for exchange forces. The result for the Yukawa well can be compared with the dipole cross section found for a Yukawa potential half exchange and half ordinary in character:[20]

$$\sigma=20.4[1-\gamma^2/(29+\gamma)^2]^2(\gamma-1)^{\frac{1}{2}}\gamma^{-3}\text{ mb}. \tag{59}$$

Here γ is the ratio of photon energy to deuteron binding energy. Numerical integration gives

$$\int_0^\infty \sigma dW=35.8\text{ Mev}-\text{mb}=(\pi^2e^2\hbar/Mc)\cdot(1.2). \tag{60}$$

This 20 percent increase due to half exchange force is in fair agreement with 17 percent as found from the sum rule calculation (Eq. 58). [Both Eqs. (58) and (59) are based on an approximate wave function for the ground state of the Yukawa potential.]†

The calculation of $\sum_n(E_n-E_o)f_{on}$ and $\bar{W}$ involves three terms as for the similar calculation for heavy nuclei:

$$\sum_n(E_n-E_o)f_{on}=\tfrac{1}{3}T_{oo}+2x\int \frac{\partial\psi_o^*}{\partial z}Vz\psi_o d\tau$$

$$+(M/\hbar^2)x^2\int \psi_o^* V^2 z^2\psi_0 d\tau. \tag{61}$$

[19] G. Breit and E. U. Condon, Phys. Rev. 49, 904 (1936).
[20] J. S. Levinger, Phys. Rev. 76, 699 (1949).

† E. Guth has called to our attention similar work on sum rules for the deuteron photoelectric effect by K. Way, Phys. Rev. 51, 552 (1937). K. Way found that the summed oscillator strength was increased for complete exchange force by a relative fraction about equal to αb, for a square well, a Gaussian well, or a velocity dependent potential. The work in this section for a square well and a Yukawa well is in good agreement with her result.

This is evaluated for square and Yukawa wells with the constants of Eq. (22), and the mean energy for photon absorption is found.

$$\bar{W}=\frac{17.2+27.5x+36x^2}{1+0.40x}\text{ Mev (square well)},$$
$$\bar{W}=\frac{16.4+21.6x+12.6x^2}{1+0.33x}\text{ Mev (Yukawa well)}. \tag{62}$$

Equation (62) for the Yukawa well with $x=\frac{1}{2}$ gives a mean absorption energy of 26 Mev, in approximate agreement with $\bar{W}=29.7$ Mev found by numerical integration of Eq. (59).

The harmonic mean energy W_H is calculated from Eq. (46). This gives $W_H=6\epsilon=13.2$ Mev for zero range of nuclear forces; $3.90\epsilon(1+0.40x)$ for the square well chosen; and $3.57\epsilon(1+0.33x)$ for the Yukawa well chosen. The first number agrees with the result from integration of the Bethe-Peierls formula; while the third result using $x=\frac{1}{2}$ agrees with that found from integration of Eq. (59).

We have found that the summed oscillator strength is increased by an attractive exchange force; and the mean energy for photon absorption is greatly increased by such a force. This can be understood qualitatively since an attractive exchange force for the ground (S) state means a repulsive exchange force for the final (P) state. This repulsive exchange force decreases the P wave function at small distances and thus the matrix element for small E_n. For large E_n, it shifts the first node of the radial wave function to larger values of r which reduces destructive interference and thus increases the matrix element. Since $\sum_n f_{on}/(E_n-E_o)$ is independent of whether the force is ordinary or exchange, $\sum_n f_{on}$ will be increased by an attractive exchange force, and higher moments will be increased even more.

This reference to S and P states is just a special case for the general case of parity change due to dipole photoelectric transitions in any nuclei; the same interpretation holds for the more general case. This physical argument implies that the presence of exchange forces will not affect cross sections for quadrupole transitions.

VI. ASYMPTOTIC EXPRESSION FOR PHOTOELECTRIC CROSS SECTION

For the deuteron we are able to calculate still higher moments such as $\sum_n f_{on}(E_n-E_o)^2$. This is of interest in finding the asymptotic behavior of the dipole term in the photoelectric cross section for high photon energies. If for a particular potential we find that $\sum_n f_{on}(E_n-E_o)^s$ is finite, but that $\sum_n f_{on}(E_n-E_o)^{s+1}$ is infinite, this shows that the asymptotic form of the dipole term in the photoelectric cross section decreases as W^{-t}, where W is the photon energy and $s+1<t\leqq s+2$. We shall calculate the higher moments for the deuteron photoelectric cross section for the case of a pure ordinary force, and for several well shapes.

The first moment $\sum_n f_{on}(E_n-E_o)=\frac{1}{3}T_{oo}$ is finite for wells of finite size. The mean kinetic energy for a square well is approximately

$$T_{oo}=-\frac{\hbar^2}{M}\int\psi_o^*\nabla^2\psi_o d\tau$$
$$=\frac{\hbar^2}{M}\frac{2\alpha}{1+\alpha b}\left[\int_0^b k^2\sin^2krdr-\int_b^\infty\alpha^2e^{-2\alpha r}dr\right]. \tag{63}$$

For negligible range of nuclear forces $kb\cong\pi/2$, and the average of $\sin^2kr\cong\frac{1}{2}$ so the first integral in the bracket gives a result proportional to $1/b$. Since the first moment diverges for zero range of nuclear forces, the exponent t for the asymptotic form for this case has the limits $1<t\leqq2$. This agrees with $t=\frac{3}{2}$ given for this potential by the Bethe-Peierls formula.

We shall use the matrix relations:[9]

$$\begin{aligned}&(E_n-E_o)z_{on}\sim i\hbar(\dot{z})_{on}\sim(i\hbar/M)(p_z)_{on},\\&(E_n-E_o)(p_z)_{on}\sim i\hbar(\dot{p}_z)_{on}\sim i\hbar(\partial V/\partial z)_{on}\end{aligned} \tag{64}$$

in determining the higher moments. The second moment gives:

$$\sum_n f_{on}(E_n-E_o)^2=\frac{2M}{\hbar^2}\sum_n(E_n-E_o)^3(z_{on})^2$$
$$\sim\sum_n(E_n-E_o)|(P_z)_{on}|^2\sim\sum_n(P_z)_{on}\left(\frac{\partial V}{\partial z}\right)_{no}$$
$$\sim\left(P_z\frac{\partial V}{\partial z}\right)_{oo}\sim\left(\frac{\partial^2V}{\partial z^2}\right)_{oo}\sim(\nabla^2V)_{oo}. \tag{65}$$

For the Yukawa potential we have

$$\nabla^2V=4\pi\rho+\mu^2V. \tag{66}$$

Here ρ is the density of the source of the meson field, and will be taken as a δ-function around the origin. Both terms on the right of Eq. (66) give finite results in Eq. (65) for the second moment.

For the square well potential of depth V_o and range b

$$\nabla^2V=V_o\delta'(r-b)+(2/r)V_o\delta(r-b). \tag{67}$$

Both terms on the right of this equation give finite results in Eq. (65).

The third moment:

$$\sum_n f_{on}(E_n-E_o)^3\sim\sum_n[(E_n-E_o)(p_z)_{on}]^2$$
$$\sim\sum_n[(\partial V/\partial z)_{on}]^2\sim[(\partial V/\partial r)^2]_{oo}. \tag{68}$$

For the Yukawa potential, the leading term in the third moment calculation is $(1/r^4)_{oo}$ which diverges at the origin. Then the asymptotic form for the Yukawa potential is W^{-t} where $3<t\leqq4$. This agrees with the calculation for the Yukawa potential (half exchange and half ordinary)[20] which gives $t=7/2$.

For the square well potential, the third moment is proportional to $[\delta(r-b)\delta(r-b)]_{oo}$ which diverges at $r=b$. The square well, also, has an asymptotic form with $3<t\leqq 4$. However, this divergence is caused by the artificial singularity of the infinitely steep walls of the well. If the walls are made to have a high but not infinite slope the third moment converges.

Equation (68) shows that the third moment converges for any potential that has a finite derivative at each point. A smooth potential, such as the Gaussian, will have a smooth wave function, with very small high Fourier components, and will therefore have very small probability of dipole transitions with photons of very short wave-length.

It is of interest to note that the electronic photo-electric effect has just the same $W^{-7/2}$ asymptotic dependence as that for the nuclear photo-effect for the Yukawa potential. The asymptotic dependence is set by the singularities in the potential, and the Yukawa singularity at the origin of $\exp(-\mu r)/r$ is the same as $1/r$ for the Coulomb potential.*

In general the asymptotic dependence of the cross section at high energies depends just on the nature of the singularities of the nuclear potential. The results for singularities at the origin apply to heavy nuclei as well as to the deuteron: it is only necessary that there be a finite probability for two nucleons to come very close, then $[(\partial V/\partial r)^2]_{oo}$ will be infinite whenever V has a singularity as $r^{-\frac{1}{2}}$ or stronger at small distances.

For comparison with experimental results, we must know in what region, if any, the asymptotic form for dipole transitions holds. The photon energy must be large enough that the de Broglie wave-length $\lambda\!\!\!^{-}$ of the emitted nucleon is small compared to the effective range of the potential. But if the photon wave-length becomes comparable to the size of the nuclear system, the dipole transition cross section will not correspond to the experimentally determined photoelectric cross section: we must consider retardation effects, quadrupole and higher moments, and perhaps mesonic effects. If the effective range of nuclear forces and the size of the nuclear system are about the same (as for the alpha-particle) there is a region of photon energies satisfying these criteria, since the depth of the nuclear potential well is much less than Mc^2.

For the deuteron case, the range of the neutron-proton potential is much less than the size of the deuteron ($\alpha b<1$). For wave-lengths of the emitted proton $\lambda\!\!\!^{-}_p \gg b$, Eq. (59) for dipole transitions for a Yukawa well gives results in approximate agreement with the Bethe-Peierls formula, which takes range $b=0$. (In this energy region nearly all the contribution is from the region outside the potential.) For $\lambda\!\!\!^{-}_p \ll b$, the interference term in Eq. (59) changes the $W^{-3/2}$ energy dependence of the Bethe-Peierls formula to a $W^{-7/2}$ dependence. The inequality $\lambda\!\!\!^{-}_p \ll b$ gives $\hbar^2/2ME \ll b^2$, where E is the proton energy; or proton energy $E \gg \hbar^2/2Mb^2 \cong V_o$, the depth of the neutron-proton potential for a square well. Dipole transitions are the principal term in the deuteron photo-disintegration provided $\lambda\!\!\!^{-}_\gamma \alpha \gg 1$, or $(\hbar c/W)(M\epsilon)^{\frac{1}{2}}/\hbar \gg 1$, where W is the photon energy and we have used the definition of α. This relation gives $W \ll (\epsilon Mc^2)^{\frac{1}{2}} = 45$ Mev. Since the depth of the neutron-proton potential is comparable to 45 Mev, we find that for the deuteron there is actually no range of photon energies where the total cross section for photo-disintegration follows the asymptotic $W^{-7/2}$ form.[21]

* *Note added in proof:* Similar conclusions have been reached by L. I. Schiff, Bull. Am. Phys. Soc. **25**, No. 1, Abstract E2 (1950).

VII. EXPERIMENTAL DATA

The G.E. experiments provide information concerning the integrated cross section for photo-nuclear reactions, the energy dependence of the photo-nuclear cross section, and set an upper limit on elastic nuclear scattering of photons.

Lawson and Perlman[1] measured the C^{11} activity produced by the $C^{12}(\gamma,n)$ reaction. The photons were produced as bremsstrahlung in the betatron, and the photon intensity measured by reference to a pair spectrometer. They expressed the photon intensity as number of quanta/Mev-min., at a photon energy of 30 Mev. The ratio of (γ,n) processes/min.-atom, to the number of quanta/Mev. min., is given as 1.5×10^{-25} Mev-cm^2 $\pm$20 percent. This result was obtained both with electron energy of 100 Mev and 50 Mev.

Lawson and Perlman interpret their result assuming a sharply peaked curve of cross section *vs.* photon energy. We shall here express their result in a more general manner. Let $\gamma(W)$ be the photon spectrum from the betatron, normalized to 1 photon/Mev at $W=30$ Mev. Then their result can be written

$$\int_0^{W_{\max}} \sigma_{(\gamma,n)}(W)\gamma(W)dW = 0.15 \text{ Mev-barn} \pm 20 \text{ percent} \quad (69)$$

for $W_{\max}=100$ Mev, or 50 Mev. A rough approximation to $\gamma(W)$ is the normalized bremsstrahlung spectrum $\gamma(W)=30/W$. The upper limit for the integral can be infinity, since Lawson and Perlman found no difference for upper limit 50 or 100 Mev. Then the integrated (γ,n) cross section for C^{12} can be rewritten as

$$\int_0^{\infty} \sigma_{(\gamma,n)}dW/W = 0.005 \text{ barn} \pm 20 \text{ percent}. \quad (70)$$

Measurements of the relative yields of many photo-nuclear reactions, using the method of induced activities, were made with the same photon spectrum by Perlman and Friedlander.[22] Combining their relative

[21] We should also note that Eq. (59) holds exactly only for the special case of half ordinary and half exchange forces, with wells of the same shape. Further, Siegert's theorem, reference 7, has been extrapolated to high photon energies, where it may not hold.

[22] M. L. Perlman and G. Friedlander, Phys. Rev. **74**, 442 (1948) and Phys. Rev. **75**, 988 (1949).

yields with the absolute determination by Lawson and Perlman, we now have experimental data for $\int\sigma_p dW/W$ for many different nuclei, where σ_p refers to the partial cross sections for specific nuclear disintegrations studied by the method of induced activities. There are always some nuclear reactions that are missed by this method since they result in stable isotopes. To obtain information on $\int\sigma dW/W$ we therefore look for the nucleus which gives the largest experimental result for $(1/A)\int\sigma_p dW/W$, since for that nucleus the partial cross section σ_p is probably most nearly equal to the photon absorption cross section σ.[23] This integrated cross section is largest for $Ge^{76}(\gamma,n)$, for which $\int\sigma_p dW/W=0.126$ barn. This result is used in Section III in estimating the mean square displacement $\langle r^2\rangle_{oo}$, and in Section IV to show that quadrupole transitions can account for only a small fraction of the experimentally determined cross section.

We want to obtain an experimental value for $\int\sigma dW$, since our sum rules for that quantity are not greatly affected by the nuclear model used. $\int\sigma dW=W_H\int\sigma dW/W$, where W_H is the harmonic mean energy for photon absorption. W_H can be obtained from Baldwin and Klaiber's measurements[2] of the energy dependence of the $Cu^{63}(\gamma,n)$ cross section. Using their value $W_H=21$ Mev, the relative yield $Cu^{63}(\gamma,n)/C^{12}(\gamma,n)$ and Lawson and Perlman's measurements on $C^{12}(\gamma,n)$ we have for Cu^{63}

$$\int\sigma_{(\gamma,n)}dW=(33/2.3)(21)0.005=1.5 \text{ Mev-barns}$$
$$\pm 30 \text{ percent.} \quad (71)$$

This result should be increased by 10 percent, since the $Cu^{63}(\gamma,2n)$ and $Cu^{63}(\gamma,2p)$ yields together represent 10 percent of the $Cu^{63}(\gamma,n)$ yield.[22] Further, the $Cu^{63}(\gamma,p)$ and $Cu^{63}(\gamma,np)$ reactions that lead to stable isotopes are probably appreciable.[24]

We conclude that for Cu^{63}, $\int\sigma dW\geqq 1.5$ Mev-barns ± 30 percent. This result agrees with that given by Lawson and Perlman, and is derived in detail here only to show that we did not need any assumption as to the shape of the $\sigma(W)$ curve, but only the harmonic mean energy W_H. Since W_H for photon absorption is not known reliably for any other nuclei (see below) this is at present the only experimental result for $\int\sigma dW$.

This experimental result is in good agreement with our Eq. (24) for dipole transitions. For Cu^{63} our calculation gives $\int\sigma dW=0.95(1+0.8x)$ Mev-barn. For no exchange forces we have 0.95 Mev-barn, which is the same result as given by Goldhaber and Teller,[5] and is not too far outside the experimental error. Solving for the fraction of exchange force we have $x=0.8\pm 0.7$. The value $x=0.55\pm 0.05$ from the Berkeley neutron-proton scattering experiments[25] gives a result well within the experimental error. We conclude that the experimental value of $\int\sigma dW$ for Cu^{63} is strong evidence for dipole transitions, and weak evidence for exchange forces.

The energy dependence of photonuclear reactions has been measured by Baldwin and Klaiber[2] for $C^{12}(\gamma,n)$, $Cu^{63}(\gamma,n)$ and photo-fission, and by McElhinney and others[26] for $Cu^{63}(\gamma,n)$ and $Ta^{182}(\gamma,n)$. These measurements were made by differentiating the curve of yield of induced activity *vs.* maximum energy of the bremsstrahlung spectrum. Bothe and Gentner[27] have measured the relative yields for several (γ,n) reactions at 11- and 17-Mev photon energies.

All these measurements have large uncertainties in the curve of $\sigma_{(\gamma,n)}$ *vs.* photon energy. (For example, the two measurements on Cu^{63} disagree.) Further, the curve $\sigma_{(\gamma,n)}$ *vs.* W gives an accurate picture of the curve of photon absorption cross section σ *vs.* W only if the (γ,n) reaction is the predominant photonuclear reaction. We can determine this by comparing the experimental value of $\int\sigma_{(\gamma,n)}dW$ with the value $\int\sigma dW$ given by our sum rules. The comparison for $Cu^{63}(\gamma,n)$ given shows that for this nucleus the (γ,n) reaction is predominant. For $C^{12}(\gamma,n)$ and $Ta^{182}(\gamma,n)$ the integrated (γ,n) cross section is only about one-third of the expected value of $\int\sigma dW$, and, as shown by Goldhaber and Teller, the photo-fission cross section is much less than this fraction.

Evidence for the difference between measurements of the (γ,n) cross section and other measurements of nuclear photon absorption was found in recent preliminary results by McDaniel and Walker.[28] They measured the yield of neutrons from photo-disintegration of various nuclei for photons of 17.5 Mev, and obtained a smooth curve for relative neutron yield *vs.* A. In contrast, Wäffler *et al.*[29] found that the relative yield for induced activity produced by the (γ,n) reaction at this photon energy showed large deviations from a smooth curve. We believe that neutron production is a better measure of nuclear photon absorption than is the production of radioactivity in some particular photo-nuclear reaction because at least one neutron is emitted in *any* absorption process, except (γ,p), $(\gamma,2p)$ etc. reactions which are probably relatively rare. Measurements of integrated cross sections, and of cross sections *vs.* photon energy, by this method of measuring neutron production would be of great interest.

Thus, to date, only the measurements on $Cu^{63}(\gamma,n)$ reaction give a value of mean energy for photon ab-

[23] We divide by A since from the theory of this paper the integrated cross section is roughly proportional to A.

[24] However use of the better approximation $\gamma(W)=(4/3)\times(1-W/W_{max})/W$ to the bremsstrahlung spectrum reduces by about 10 percent the integrated cross sections given in Eqs. (70) and (71).

[25] Hadley, Kelly, Leith, Segrè, Wiegand, and York, Phys. Rev. **75**, 351 (1949); and R. Serber (private communication).

[26] McElhinney, Hanson, Becker, Duffield, and Diven, Phys. Rev. **75**, 542 (1949).

[27] W. Bothe and Gentner, Zeits. f. Physik **112**, 45 (1939).

[28] McDaniel and Walker (private communication).

[29] Huber, Lienhard, Scherrer, and Wäffler, Helv. Phys. Acta **17**, 195 (1945) and **16**, 33 (1943).

sorption which can be compared with our calculations of Section III. Baldwin and Klaiber[2] give $\bar{W}=22$ Mev for the (γ,n) reaction. Since other photo-nuclear reactions of Cu^{63} generally occur at higher photon energies than does the (γ,n), we can write $\bar{W}\geqq 22$ Mev. Our calculated value for $\bar{W}$ is sensitive to the value of x, to the shape of the neutron-proton potential, and to the nuclear density. Figure 3 shows that 22 Mev corresponds to values of the fraction of exchange force varying from 0.1 to 0.3 depending on the shape of well and nuclear density assumed. The value $x=0.55\pm 0.05$ gives a very high value of $\bar{W}$ for a square well, but not too unreasonable a value for a Yukawa well; 38 Mev for a dense nucleus ($r_0=1.37\times 10^{-13}$ cm), and 31 Mev for a less dense nucleus ($r_0=1.50\times 10^{-13}$ cm). In principle better experimental measurements of $\bar{W}$ and less approximate calculations would provide good evidence on some combination of well shape, nuclear density, and the fraction of exchange force.

Similarly only the $Cu^{63}(\gamma,n)$ measurements give evidence as to the shape of the curve of the cross section for photon absorption *vs.* photon energy; and even in this case it has not been proved that competition between the (γ,n) and other photo-nuclear reactions is not appreciable. The sharply peaked curve of $\sigma_{(\gamma,n)}(W)$ found by Baldwin and Klaiber for this reaction can be taken as evidence for the Goldhaber-Teller theory[5] of dipole vibration of the entire nucleus. Goldhaber and Teller assume that only one excited nuclear level is of importance (the first excited level for the simple harmonic dipole vibration of the entire nucleus) so the width of the $\sigma(W)$ curve would be due entirely to the energy-spread of that excited level due to its short life. Goldhaber and Teller believe that the gamma-ray width of this level should be appreciable compared to the neutron width, so that there should be appreciable elastic scattering of gamma-rays in this narrow energy band. Gaertner and Yeater[30] have recently looked for gamma-rays of the resonance energy scattered at 90° from C^{12} or Cu^{63}. They set the upper limit for elastic nuclear scattering of photons as one percent of the (γ,n) cross section for C^{12}, and three percent for Cu^{63}.

The ratio of elastically scattered photons to nuclear disintegrations is $\Gamma_\gamma/(\Gamma_n+\Gamma_\gamma)\cong\Gamma_\gamma/\Gamma_n$, where Γ_γ is the gamma-ray width, and Γ_n the neutron width. Γ_γ can be found from the oscillator strength.[3] Assuming that there is a single level having the summed oscillator strength of $(NZ/A)(1+0.8x)=20$ for Cu^{63}, and that the resonance energy is about 22 Mev, then $\Gamma_\gamma=50$ kev. Gaertner and Yeater's upper limit for scattered photons then gives $\Gamma_n>1.7$ Mev for the neutron width for Cu^{63}. This neutron width is not inconsistent with the measurements of Baldwin and Klaiber, which give a "resonance width" the order of magnitude of 3 Mev. However, we could rule out the assumption that Baldwin and Klaiber's width is mostly instrumental.

[30] E. R. Gaertner and M. L. Yeater, Phys. Rev. **76**, 363 (1949).

A many-level picture of photon absorption, which is consistent with our calculations in this paper, would not give very different results from those on the Goldhaber-Teller single level theory.[31] Consider L levels, with average spacing D, so that $LD=$ the width of the $\sigma(W)$ curve observed by Baldwin and Klaiber. At high neutron energies the neutron width from state n to the ground state, $\Gamma_{no}\cong D\xi/2\pi\cong D/2\pi$, since sticking probability $\xi\cong 1$ at high neutron energies. The total neutron width from a level excited by photon absorption is

$$\Gamma_n=\sum_r \Gamma_{nr}\cong\Gamma_{no}N_n(W-B)\cong(D/2\pi)N_n(W-B). \quad (72)$$

The summation goes over neutron energies between zero and $(W-B)$, where B is the neutron binding energy, and W is the photon energy. $N_n(W-B)$ is the number of levels of the nucleus in this energy range that can be reached by neutron emission.

The gamma-width $\Gamma_{\gamma o}$ for photon emission to the ground state from a single level is about $1/L$ that for the gamma-width Γ_γ for a single level theory. The excited state can decay by photon emission to many levels above the ground state, and if the final level is less than, say, 5 Mev above ground then the emitted photon will be hard to distinguish experimentally from a photon of the resonance energy. The effective gamma-width

$$\Gamma_{\gamma\,eff}=\sum_{r=0}^{5\text{ Mev}}\Gamma_{\gamma r}\cong\Gamma_{\gamma o}N_\gamma(5\text{ Mev})\cong(\Gamma_\gamma/L)N_\gamma(5\text{ Mev}). \quad (73)$$

The ratio of scattered photons to neutron emission is

$$\frac{\sigma_{(\gamma,\gamma)}}{\sigma_{(\gamma,n)}}\cong\frac{(\Gamma_\gamma/L)N_\gamma(5\text{ Mev})}{(D/2\pi)N_n(W-B)}=\frac{\Gamma_\gamma}{\Gamma}2\pi\frac{N_\gamma(5\text{ Mev})}{N_n(W-B)}, \quad (74)$$

where we have used the relation $LD=\Gamma=$ observed width of "resonance curve." The ratio Γ_γ/Γ is the ratio used for the Goldhaber-Teller theory. For Cu^{63} the energy $W-B\cong 22-11=11$ Mev; so the ratio of levels reached by photon emission to those reached by neutron emission $N_\gamma(5\text{ Mev})/N_n(W-B)$ will be less than unity, and perhaps of order of magnitude 0.01; so this calculation gives a result that the ratio (scattered photons/emitted neutrons) would be roughly one-tenth that predicted from the Goldhaber-Teller theory.

Several reports have appeared very recently which confirm the experimental work discussed in this section. Strauch[32] has measured the transition curves in lead for photons from the Berkeley synchrotron causing the (γ,n) reaction in C^{12} or Cu^{63}. He finds the mean energy for photons causing these reactions to be 30 and 20 Mev, respectively, in agreement with Baldwin and Klaiber's measurements by a different method. Helmholz and

[31] This calculation of (photon emission/neutron emission) was done by H. A. Bethe and H. Hurwitz, of the Knolls Atomic Power Laboratory, General Electric Company, Schenectady, New York.

[32] K. Strauch, Phys. Rev. **78**, 84 (1950).

Strauch[33] have measured the yields for several photonuclear reactions with the Berkeley synchrotron, and find a preliminary value of 1 Mev-barn for the integrated $Cu^{63}(\gamma,n)$ cross section, in agreement with the work of Lawson and Perlman. Dressel, Goldhaber, and Hanson,[34] have measured resonance scattering of photons, using the 22-Mev Illinois betatron. They used the activation of Pr^{141} by the (γ,n) reaction to detect scattered photons of high energy. The cross section for resonance scattering of photons for lead nuclei is roughly 1 mb per steradian, and is considerably less than this for copper and antimony nuclei. Their upper limit for scattering by copper nuclei is about one-tenth that found by Gaertner and Yeater. The result for lead is consistent with the Goldhaber-Teller theory for a resonance width of 4 Mev, and is also consistent with the theory of this paper.*

Our calculations from sum rules do not give a definite prediction as to the shape of the $\sigma(W)$ curve; but only the integrated cross section and the mean energy for photon absorption. The curve could be broad, or could have a sharp resonance. If we take the alpha-particle model of the nucleus as a first approximation, we might expect a strong resonance at a photon energy of roughly 20 Mev, as photons of this energy are emitted with a high probability in the $T^3(p,\gamma)He^4$ reaction.[18] However, "alpha-particles" in the nucleus will certainly behave differently from free alpha-particles, and the resonance might be greatly broadened.

The alpha-particle model gives qualitatively satisfactory results concerning the ratio $\sigma_{(\gamma,p)}/\sigma_{(\gamma,n)}$ for heavy nuclei. Hirzel and Wäffler[35] found this ratio for a photon energy of 17 Mev to be many times greater than that predicted by the statistical theory of nuclei. Perlman and Friedlander[22] find even larger (γ,p) yields [roughly 10 percent of (γ,n) yields] using the G.E. betatron at 100 Mev, or 50 Mev electron energy. The only two isotopes which were measured by both groups are Si^{30} and Mo^{98}. The (γ,p) yield, relative to $Cu^{63}(\gamma,n)$ was increased 14 times for the former, and three times for the latter, by use of the higher energy photons from the betatron rather than the 17-Mev gammas.

Courant[36] assumed a surface photoelectric effect for the whole nucleus for proton emission and found too low a proton yield to account for Hirzel and Wäffler's results. Schiff[37] assumed that only nuclear levels of special properties could be excited by photons, and obtained rough agreement with Hirzel and Wäffler's results. However neither author found that the (γ,p) yield should increase rapidly with increasing photon energy.

We propose the following tentative picture which is similar to that suggested in a letter by Courant: The main process of nuclear absorption is by absorption of energy by a single proton in a nuclear alpha-particle. Usually this proton interacts with other nucleons before getting out of the nucleus; the excitation energy then becomes shared among many nucleons, and a neutron of energy corresponding to the nuclear temperature will in general be emitted, in accord with the statistical theory. Occasionally the proton escapes without making any collisions. (This will occur for a proton emitted from a surface alpha-particle in the right direction.) Since the mean free path for protons in a nucleus increases with increasing proton energy, the probability of proton escape increases with proton energy.

We want to make clear that these calculations from the alpha-particle model are tentative, and of a preliminary nature only.

In conclusion, we have shown by sum rules that there *are* dipole transitions, and that quadrupole transitions can account for only a small fraction of the observed integrated photonuclear cross sections. Goldhaber and Teller assume a specific model for dipole transitions; i.e., that there is a dipole vibration of the entire nucleus. From this model they obtain the integrated cross section, predict a sharp resonance curve for photon absorption, estimate the resonance energy and predict elastic nuclear scattering of photons. Making no *ad hoc* assumption of dipole vibration of the entire nucleus, we have found an integrated cross section somewhat larger than that of Goldhaber and Teller, due to exchange forces. Either integrated cross section agrees with present experiments. We find a reasonable mean energy for photon absorption, if a Yukawa well is used with not too high a fraction of exchange force. Experimental evidence on the shape of the $\sigma(W)$ curve is not yet decisive; we could obtain qualitative agreement with a resonance peak by consideration of the alpha-particle model. We predict a somewhat lower elastic scattering of photons than do Goldhaber and Teller. Either result is in agreement with present experiments. We can qualitatively understand the ratio of proton to neutron emission, using the alpha-

[33] A. C. Helmholz and K. Strauch, Phys. Rev. **78**, 86 (1950).
[34] Dressel, Goldhaber, and Hanson, Phys. Rev. **77**, 754 (1950).
* *Note added in proof:* Gaerttner and Yeater, Phys. Rev. **77**, 714 (1950) have recently measured the cross sections for photo-nuclear reactions in nitrogen and oxygen. Cloud-chamber observations of reactions produced by x-rays from the G.E. betatron showed "flags," singles, and stars. The flags are interpreted as (γ, pn) reactions, and the singles as (γ, n) processes. Gaerttner and Yeater found that flag production was the predominant process, for both oxygen and nitrogen. They calculate the total integrated photo-nuclear cross section as about 0.6 Mev-barn, for both nuclei. These measurements confirm the increase of the integrated photo-nuclear cross section due to exchange forces. Using this data, together with our Eq. (24), we find that the fraction of exchange force $x=2\pm1$, where we have assumed a 30 percent uncertainty in their experimental result. (Equation (24) was calculated for heavy nuclei; surface effects might change the numbers for light nuclei such as oxygen and nitrogen.) Gaerttner and Yeater's measurements also show the importance of competition among different photo-nuclear reactions.
[35] Hirzel and Wäffler, Helv. Phys. Acta **20**, 373 (1947).
[36] E. D. Courant, Phys. Rev. **74**, 1226(A) (1948) and private communication.
[37] L. I. Schiff, Phys. Rev. **73**, 1311 (1948).

particle model, while Goldhaber and Teller's theory does not consider this question. We believe that many of the features of the nuclear photo-effect can be understood merely from the fact that there are dipole transitions, without a special model.

ACKNOWLEDGMENT

We wish to thank P. Morrison and H. Hurwitz for interesting discussions on these problems.

One of us (J. S. Levinger) was employed under an ONR contract during part of this research.

PHYSICAL REVIEW VOLUME 78, NUMBER 2 APRIL 15, 1950

The Fission Yield of Xe^{133} and Fine Structure in the Mass Yield Curve

J. MACNAMARA, C. B. COLLINS, AND H. G. THODE
McMaster University, Hamilton, Ontario, Canada

(Received December 27, 1949)

A mass spectrometer investigation of the xenon isotopes formed from U^{235} fission has been made and the fission yield and half-life of Xe^{133} determined. The fission gases were extracted, purified, and the mass spectrometer abundance data obtained within two weeks of the end of the irradiation period. The fission yield of Xe^{133} was found to be 6.29 ± 0.01 percent, which is 20 percent higher than that expected from the mass yield curve. This is further evidence of fine structure in the mass fission yield curve. The half-life value of Xe^{133} was found to be 5.270 ± 0.002 days.

THODE and Graham[1] first determined mass spectrometrically the relative abundances of stable isotopes of Xe and Kr resulting from the decay of fission product chains in U^{235} fission. In this way the relative fission yields of eight mass chains—83, 84, 85, 86, 131, 132, 134 and 136, were determined with considerable accuracy. When these yields are normalized to the mass-yield curve at a value of 2.8 percent for mass 131, the values fit the curve nicely with the exception of Xe^{134} which is about 35 percent above the normal fission yield curve. Glendenin[2] has pointed out that the value obtained by Thode and Graham[1] of Kr^{84} is also above the experimental mass yield curve by about 35 percent. These results indicated for the first time "fine structures" in the mass yield curve. Recently, Inghram, Hess, and Reynolds[3] reported isotope abundance data for fission product cesium, which also indicate anomalies in the mass yield curve.

If it is assumed that the yields should fall on a smooth curve, then the abnormal yields of Xe^{134} and Kr^{84} might be explained by delayed or prompt neutron emission. If this fission chain branching does occur, then the fission yield of adjacent chains will be affected. It seemed important, therefore, to determine accurately the fission yields of the 133 and 135 mass chains. In the original mass spectrometer investigations of the fission gases, Xe^{133} and Xe^{135} did not occur because of their short half-lives, and because it was not possible to get samples immediately after irradiation. However, with the Chalk River facilities of the National Research Council available, it has now been possible to extract Xe gas from irradiated uranium disks without a long "cooling" period and thus permit the investigation of 5.3-day Xe^{133}. In order to calculate the fission yield of Xe^{133} from abundance data, (after a definite irradiation and cooling time), it is necessary to know its half-life with considerable accuracy. Since the previous values obtained by radio-chemical methods,[4–12] were only good to 1 or 2 percent, a new and more accurate value was determined mass spectrometrically. This determination of the half-life of Xe^{133} and the determination of the fission yield for the 133 mass chain are reported in this paper.

THEORY

Half-Life Determination

By comparing the abundance of a radio-active isotope with that of a stable one with a mass spectrometer over a period of time, it is possible to follow its decay rate and thereby determine its half-life. By this method, very accurate half-life determinations are possible for isotopes with half-lives ranging from about one day to ten years. The fundamental decay equation is

$$n/n_0 = e^{-\lambda t} = \exp(-0.6932t/t_{\frac{1}{2}}),$$

where n is the concentration at time t and n_0 is the concentration at zero time.

By substituting for example the 133/131+132 ratio obtained with the mass spectrometer at different time

[1] H. G. Thode and R. L. Graham, Can. J. Research, **A25**, 1–14 (1947). Technical Report No. 35.
[2] G. L. Glendenin, Ph.D. thesis, Department of Chemistry, M.I.T. (August 1949).
[3] Inghram, Hess, and Reynolds, Phys. Rev. **76**, 1717 (1949).
[4] A. Langsdorf, Jr., Phys. Rev. **56**, 205 (1939).
[5] R. W. Dodson and R. D. Fowler, Phys. Rev. **57**, 967 (1940).
[6] E. P. Clancy, Phys. Rev. **60**, 87 (1941).
[7] Chien-Shiung Wu and E. Segrè, Phys. Rev. **67**, 142 (1945).
[8] W. Riezler, Naturwiss. **31**, 326 (1943).
[9] W. Seelmann-Eggebert, Naturwiss. **31**, 491 (1943).
[10] H. J. Born and W. Seelmann-Eggebert, Naturwiss. **31**, 201 (1943).
[11] H. Slatis, Arkiv f. Mat., Astr. o. Fys. **A32**, No. 16, 12 (1946).
[12] D. W. Engelkemeir and N. Sugarman, Plutonium Project Report (1946).

intervals for n/n_0 the half-life, $t_{\frac{1}{2}}$, of Xe^{133} can be determined.

Fission Yield Determination

The fission yield of the 133-mass chain for U^{235} fission is calculated from the mass spectrometer abundance ratio of Xe^{133} to Xe^{134} obtained after an irradiation time t, a "cooling" time to t_1 and at a time t_2 after extraction of the fission gases.

The two mass chains being compared are as follows:

$$Sb^{133} \xrightarrow{10\text{ min.}} Te^{133} \xrightarrow{60\text{ min.}} I^{133} \xrightarrow{22\text{ hr.}} Xe^{133} \xrightarrow{5.270\text{ day}} Cs^{13}$$

$$Sb^{134} \xrightarrow{10\text{ min.}} Te^{134} \xrightarrow{43\text{ min.}} I^{134} \xrightarrow{54\text{ min.}} Xe^{134}\text{ stable}$$

For purposes of calculating the yield of the 133-mass chain, the following assumptions can be made when cooling times of 5 to 10 days are considered:

1. That the primary fission yield of Xe^{133} is negligible (from point of view of calculations) and that Xe^{133} produced comes from the decay of I^{133}.
2. That the fission yield of I^{133} can be taken as the yield of the whole chain in view of the short half-lives of its precursors.
3. That the 134 chain will have completely decayed to Xe^{134} at the time of extraction of the fission gases.
4. That the fission yield of the 134-mass chain is 7.4 percent as taken from previous mass spectrometer work.

With these assumptions a formula can be derived for the yield of the 133-mass chain in terms of the mass spectrometer ratio of Xe^{133} to Xe^{134}.

The number of atoms of I^{133} of fission yield Y_{133} and disintegration constant λ_1 produced at constant neutron flux f for a period of irradiation time t is:

$$n=\frac{fY_{I^{133}}}{\lambda_1}[1-\exp(-\lambda_1 t)]. \qquad (1)$$

Now since we have assumed that all the Xe^{133} produced comes from the decay of I^{133}, the number of atoms of Xe^{133} of disintegration constant λ_2 produced during the irradiation period t will be:

$$n_1=\frac{fY_{I^{133}}}{\lambda_2}\left[1-\frac{\lambda_1\exp(\lambda_2 t)-\lambda_2\exp(-\lambda_1 t)}{\lambda_1-\lambda_2}\right]. \qquad (2)$$

During the "cooling" period t_1, the time elapsed from the end of the irradiation until the xenon is extracted from the uranium metal, the number of Xe^{133} atoms produced will be:

$$n_2=\frac{n\lambda_1}{\lambda_2-\lambda_1}[\exp(-\lambda_1 t_1)-\exp(-\lambda_2 t_1)]. \qquad (3)$$

The total number of atoms of Xe^{133} available at the time of dissolution is given by the sum of Eq. (2) multiplied by the decay factor $\exp(-\lambda_2 t_1)$ plus Eq. (3) with n taken from Eq. (1).

Therefore, the total number of atoms of Xe^{133} at the time of analysis is given by

$$N=[n_1\exp(-\lambda_2 t_1)+n_2]\exp(-\lambda_2 t_2), \qquad (4)$$

where t_2 is the time elapsed from the time of dissolution of the uranium until the time of analysis with the mass spectrometer.

On substituting the expressions for n_1 and n_2 in Eq. (4) the total number of atoms of Xe^{133} at the time of analysis is then given by:

$$N_{Xe^{133}}=\exp(-\lambda_2 t_2)Y_{I^{133}}\left\{\frac{1-\exp(-\lambda_1 t)}{\lambda_2-\lambda_1}\times[\exp(-\lambda_1 t_1)-\exp(-\lambda_2 t_1)]+\frac{\exp(-\lambda_2 t_1)}{\lambda_2}\times\left[1-\frac{\lambda_2\exp(-\lambda_1 t)-\lambda_1\exp(-\lambda_2 t)}{\lambda_2-\lambda_1}\right]\right\}. \qquad (5)$$

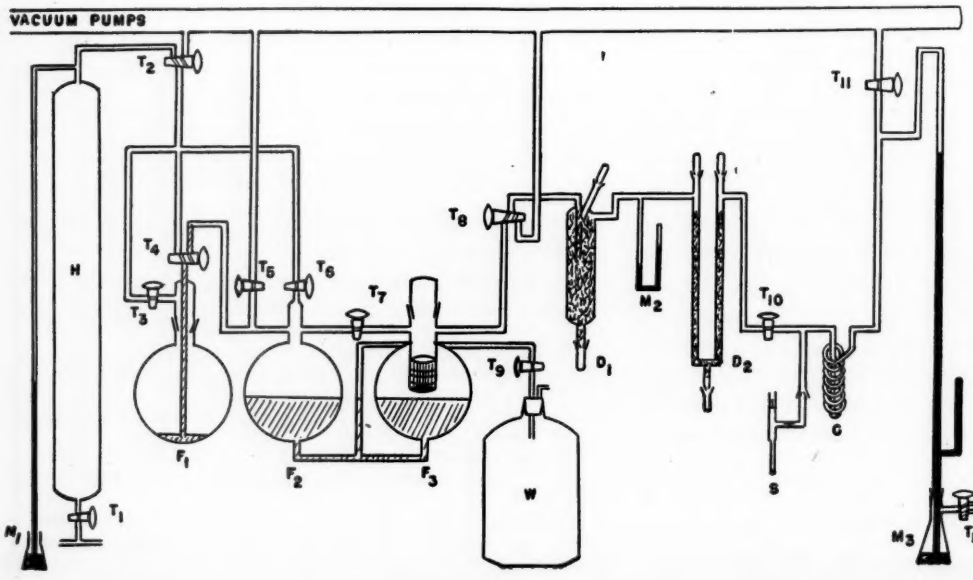

FIG. 1. Apparatus for extraction of fission product xenon and krypton from irradiated uranium.

TABLE I. Xe^{133} half-life from mass spectrometer abundance data.

Ratio of Xe mass ion currents ×100	Time after first analysis (hr.)			Xe^{133} half-life calculated (days)
	0	45.83	92.91	
133(131+132)	34.60±0.005	26.91±0.006	20.79±0.015	5.265
				5.275
				5.270
133/(131+132+134+136)		7.022±0.01	5.430±0.02	5.275
			Average	5.270±0.002

As the period of "cooling" is long compared to the half-lives of the Xe^{134} precursors, the total 134-mass chain will decay to Xe^{134}. Therefore, the total number of Xe^{134} atoms at the time of analysis is given by:

$$N_{Xe^{134}}=fY_{134}t, \tag{6}$$

where Y_{134} is the yield of the 134-mass chain. The ratio of the total number of Xe^{133} atoms to total number of Xe^{134} atoms at the time of analysis is therefore given by the equation:

$$\frac{N_{Xe^{133}}\text{ at }t_2}{N_{Xe^{134}}}=\frac{\exp(-\lambda_2 t_2)}{YXe^{134}t}Y_{133}\left\{\frac{1-\exp(-\lambda_1 t)}{\lambda_2-\lambda_1}\right.$$

$$\times[\exp(-\lambda_1 t_1)-\exp(-\lambda_2 t_1)]+\frac{\exp(-\lambda_2 t_1)}{\lambda_2}$$

$$\left.\times\left[1-\frac{\lambda_2\exp(-\lambda_1 t)-\lambda_1\exp(-\lambda_2 t)}{\lambda_2-\lambda_1}\right]\right\}. \tag{7}$$

The left-hand side of this equation is equal to the ratio of Xe^{133} to Xe^{134} at the time of analysis and is therefore given by the mass spectrometer ratio. Equation (7) was used to calculate the yield of the 133-mass chain.

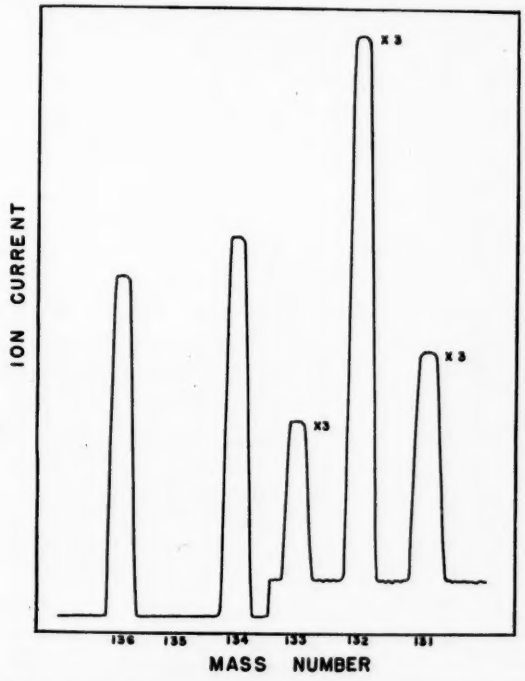

FIG. 2. Stable isotopes of fission product xenon, also Xe^{133}.

TABLE II. Fission yield of Xe^{133}. Yield of Xe^{134} taken as 7.4 percent. Thode and Graham results normalized to mass yield curve at 2.8 percent for Xe^{131}.

Sample No.	Time of irradiation hr. (t)	Time of cooling up to dissolution hr. (t_1)	Time after extraction before analysis hr. (t_2)	$\frac{Xe^{133}}{Xe^{134}}$	Yield of Xe^{133}
1	32.42	244.0	73.42	0.1644	6.285
2	25.88	211.90	51.42	0.2258	6.290
				Average	6.290±0.01
3*	68.45	193.67	50.83	0.2335	6.55

* Preliminary experiment, this result is probably high because of interruptions in the irradiation period.

EXPERIMENTAL

Preparation of Samples

Small uranium disks of about 20 g each, were irradiated with neutrons at as nearly a constant flux as possible in the pile at Chalk River. The uranium was irradiated for a sufficient period so as to produce approximately 10^{-3} cc at N.T.P. of fission product xenon and krypton. After "cooling" for ten days the uranium disks were dissolved in a saturated solution of cupric potassium chloride and the rare gases extracted by a method similar to that used by Arrol, Chackett, and Epstein.[13]

The extraction apparatus described by Arrol, Chackett, and Epstein required certain modifications to dissolve the more active disks (see Fig. 1). The apparatus was shielded with four inches of lead and stopcocks T_5, T_6 and T_7 were manipulated by remote control methods. About 800 cc of cupric potassium chloride solution in F_1 was flushed with dry hydrogen from the reservoir H to eliminate the air dissolved in the solution. The hydrogen was dried and purified by passing it through activated charcoal in a trap at liquid nitrogen temperatures. The uranium disk was placed in a platinum basket in F_3, and the reaction vessels F_2 and F_3 evacuated through T_5. The dissolving solution was then siphoned from F_1 into the reaction vessels through T_4. The rate of dissolution of the uranium disk was controlled by raising and lowering the solution in F_2 and F_3. The solution was raised and lowered by varying the pressure in F_2. Dry hydrogen was used when it was necessary to increase the pressure above the solution in F_2. The rate of dissolution was observed by the pressure readings on the manometers M_2 and M_3. M_3 was maintained at approximately 3 cm during the dissolution. The drying traps, D_1 and D_2 to eliminate HCl (gas) and water vapor, contained potassium hydroxide pellets and magnesium perchlorate, respectively. These traps were fitted with ground glass joints in order to change the drying agents during successive

[13] Arrol, Chackett, and Epstein, Can. J. Research, 27, 757 (1949).

TABLE III. Fission yields from mass spectrometer determinations and yield-curve data compared mass chains (131–138).

Mass chain	Mass yield curve	Mass spectrometer fission yield
131	2.8	2.8
132	4.2	4.2
133	5.0	6.3
134	5.5	7.4
135	5.9	—
136	6.1	6.1
137	6.2	—
138	6.2	—

dissolutions. This prevented further glass blowing once the line was contaminated. The fission gases and impurities were swept through the drying traps by the hydrogen gas produced during the dissolution of the uranium metal and absorbed on the charcoal in trap C at liquid nitrogen temperatures. Following the dissolution of the uranium, the remaining traces of Xe and Kr were flushed out with dry hydrogen from H and the system evacuated through T_{11}. The gas sample was then purified in a calcium furnace,[13] and the abundance of the xenon isotopes measured with the mass spectrometer.

The fission product solution was transferred automatically by evacuating the glass jar W and siphoning the solution from F_2 and F_3 into W.

Mass Spectrometer

The mass spectrometer used was a 180 degree direction focusing instrument.[14] The ion current measurements were made with a linear inverse feedback amplifier coupled to a Leeds and Northrup Speedomax recorder.[15] The relative abundance data reported in this paper are good to 0.1 percent or better.

RESULTS

Figure 2 shows a typical mass spectrogram for fission product xenon. Previous spectrograms[1] show no Xe^{133} because the uranium disks were allowed to cool for a number of months after irradiation to permit the various fission product chains to decay to the stable Xe^{131}, Xe^{132}, Xe^{134} and Xe^{136} isotopes. However, by analyzing the xenon produced in fission, within two weeks of the end of the irradiation period, it was possible to measure both the yield and the half-life of Xe^{133}.

Half-Life of Xe^{133}

The average value of the half-life of Xe^{133} from four determinations is 5.270 ± 0.002 days. This mass spectrometer method of determining half-lives, completely eliminates the difficulties from contamination with other radioactive isotopes which interfere with counting methods. It provides a most accurate means for determining half-lives in the range of several days to several years. Whereas the half-live values obtained by radiochemical methods are good to only 1 or 2 percent, the values obtained from mass spectrometer abundance data are good to 0.1 percent. Table I gives the results of the mass spectrometer analyses.

Fission Yield of Xe^{133}

The mass spectrometer abundance data for Xe^{133} and Xe^{134} was taken from spectrograms similar to Fig. 2. The results for three separate experiments are given in Table II. In columns 2, 3, and 4 are given the irradiation time of the uranium sample t, the cooling time t_1, and the analysis time after extraction of xenon gas t_2. Column 5 gives the abundance ratio Xe^{133}/Xe^{134} obtained with a precision of 0.1 percent and a probable accuracy of 0.5 percent and finally, column 6 gives the fission yield of the 133-mass chain, calculated by means of Eq. (7) where the half-lives of I^{133} and Xe^{133} were taken as 22 hours and 5.270 days respectively. It can be seen that the results for the two experiments check well within the limits of our precision. The results indicate that the fission yield for the 133 mass chain is also abnormal (see Fig. 3).

DISCUSSION

Table III summarizes the fission yield data which has been determined with considerable accuracy by mass spectrometer methods. These yields which include the yield of Xe^{133} reported in this paper are compared with

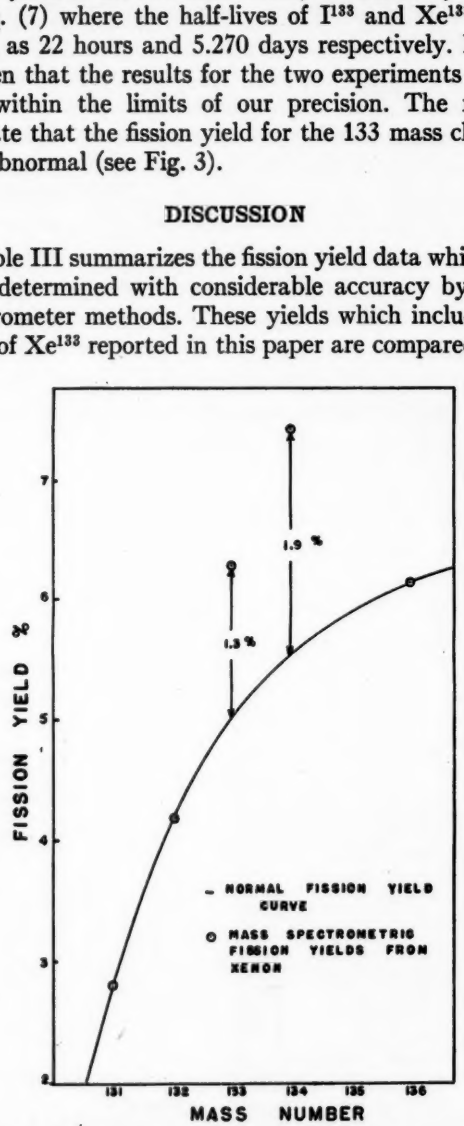

FIG. 3. Mass fission yield curve showing fine structure.

[14] Thode, Graham, and Zeigler, Can. J. Research **B23**, 40 (1945).
[15] Lossing, Shields, and Thode, Can. J. Research **B25**, 397 (1947).

corresponding values taken from the smooth mass yield curve.

It is seen that the mass spectrometric values fit nicely on the mass yield curve with the exception of Xe^{133}, Xe^{134}, and possibly Kr^{84} which are 20, 35, and 35 percent too high respectively (see Fig. 3).

Recently, C. W. Stanley and S. Katcoff[16] published a most interesting paper on the properties of 86-second I^{136}. According to their results the accumulative yield of I^{136} from U^{235} fission is 3.1 percent or about one-half the value predicted by the mass yield curve for the 136 chain. Furthermore, the yield of Xe^{136} determined mass spectrometrically is 6.1 percent. Stanley and Katcoff suggest several possible explanations for the low I^{136} yield. First, an independent isomer of I^{136} with a half-life less than 30 seconds would not have been observed in their experiments. Second, the daughter produced namely Xe^{136} might have a high primary fission yield, thereby accounting for the missing fraction of the total chain yield. This latter explanation seems very unlikely in view of the low yield found for Cs^{136} and in view of the low primary yields predicted for Xe^{136} by the theories of charge distribution. The known delayed neutron emissions from I^{137} through Xe^{137} must, of course, be taken into account.

It recently occurred to G. L. Glendenin[17] that the anomalous yields might be explained at least qualitatively on the basis of the extra stability for the nuclear closed shells of 50 and 82 neutrons which occur in fission products in the regions of mass numbers 85 and 135 (krypton and xenon ranges). There is very convincing evidence that special numbers of neutrons or protons in the nucleus form a particular stable configuration. M. G. Mayer[18] has recently summarized the experimental facts which indicate a particular stability of shells of 50, 82, and 126 neutrons.

Glendenin postulates that a primary fission product (which has already emitted the usual number of prompt neutrons) containing one neutron in excess of the closed shells (51 and 83) will often emit this more loosely bound neutron immediately rather than emit β-particles or γ-rays as in the ordinary case. This process could then account for abnormal fission yields in the neighborhood of nucleids with 50 and 82 neutrons.

Table IV illustrates the chain branching in the region of 82 neutrons as proposed by Glendenin. This scheme would explain qualitatively the abnormal yields of Xe^{134}, I^{136} and the abnormal yield of Xe^{133} reported in this paper. For example, the yield of the 134 chain is increased by the reaction

$$Te^{135}(83 \text{ neutrons}) \longrightarrow Te^{134}(82 \text{ neutrons}) + n \quad (3)$$

and is decreased by the reaction

$$Sb^{134}(83 \text{ neutrons}) \longrightarrow Sb^{133}(82 \text{ neutrons}) + n. \quad (2)$$

If Te^{135} has a higher primary yield than Sb^{134} then the 134 chain will gain more than it loses by this mechanism and its yield will be high.

TABLE IV. Branching.

Sn^{131}	Sb^{131}	Te^{131}	I^{131}	Xe^{131} Stable		
Sn^{132}	Sb^{132}	Te^{132}	I^{132}	Xe^{132} Stable		
$1\uparrow n$ Sn^{133}	Sb^{133}	Te^{133}	I^{133}	Xe^{133}	Cs^{133} Stable	
	$2\uparrow n$ Sb^{134}	Te^{134}	I^{134}	Xe^{134} Stable		
	Sb^{135}	$3\uparrow n$ Te^{135}	I^{135}	Xe^{135}	Cs^{135}	Ba^{135} Stable
	Sb^{136}	Te^{136}	$4\uparrow n$ I^{136}	Xe^{136} Stable		
		Te^{137}	I^{137}	$5\uparrow n$ Xe^{137}	Cs^{137}	Ba^{137} Stable
		Te^{138}	I^{138}	Xe^{138}	$6\uparrow n$ Cs^{138}	Ba^{138} Stable

Table IV shows the side reactions of this type numbered from 1 to 6. If it is assumed that the fine structure in the mass yield curve is due to these side reactions, then the extent of some of these reactions can be established from the experimental results so far obtained. For example, the mass spectrometric yield data for Xe^{131} and Xe^{132} are in accord with the mass yield curve, the primary yield of Sn^{133} must therefore be small and the extent of reaction (1) approximately zero. Reaction (2) on the other hand must amount to 1.3 percent of total fission since the Xe^{133} yield is found to be high by this amount. In the same way the extent of reaction (3) can be established. Since Xe^{134} yield is high by 1.9 percent (see Table V), the reaction (3) must amount to 1.9+1.3 or 3.2 percent of total fission to account for it.

Coryell, Glendenin, and Edwards[19] have proposed a theory for the distribution of charge based on equal charge displacement. The predicted primary fission yields of Sn^{133}, Sb^{134} and Te^{135} taken from their charge distribution curve are 0.6, 1.7, and 2.8 percent respectively. If we assume that the probability of emission of the extra neutron in excess of a closed shell is practically 100 percent, the extent of reactions (1), (2) and (3) are 0.6, 1.7 and 2.8 percent of total fission respectively. Similarly taking Present's theory[20] of charge distribution and again assuming 100 percent probability of emission of the extra neutron, these values are 0, 0.4 and 1.6, respectively. These results are compared in Table V.

The proposed mechanism of chain branching in the neighborhood of closed neutron shells does serve to

[16] E. W. Stanley and S. Katcoff, J. Chem. Phys. 17, 653 (1949).
[17] G. L. Glendenin, Phys. Rev. 75, 337 (1949).
[18] M. G. Mayer, Phys. Rev. 74, 235 (1948).
[19] Coryell, Glendenin, and Edwards, Memo CL-LEG-I (July 25, 1946); Phys. Rev. 75, 337 (1949).
[20] R. D. Present, Phys. Rev. 72, 7 (1947).

TABLE V. Extent of reactions. (1–4 of Table IV).

Reaction	Determined from mass spectrometer yield data	From Coryell Glendenin theory*	From Present's theory*
(1) ($Sn^{132} \rightarrow Sn^{132} + n$)	0	0.6	0
(2) ($Sb^{134} \rightarrow Sb^{133} + n$)	1.3	1.7	0.4
(3) ($Te^{135} \rightarrow Te^{134} + n$)	3.2	2.8	1.6
(4) ($I^{136} \rightarrow I^{135} + n$)	<3.0**	2.7	2.5

* Assuming probability of emission of extra neutron is 100 percent when nucleid formed as primary product.
** Yield determined by radio-chemical methods (Katcoff and Stanley).

explain at least qualitatively the anomalous fission yields reported above. However, the relative isotope abundance data for fission product Cs reported recently by Inghram, Hess, and Reynolds,[3] is not consistent with the above yield data if we accept the Glendenin mechanism. If their relative abundance data for Cs^{133}, Cs^{135}, and Cs^{137} are normalized to our value of 6.3 percent for the yield of the 133 chain, then the yields of these chains become 6.3, 7.8, and 6.1 percent, respectively. An abnormally high yield is, therefore, indicated for Cs^{135}. The extent of reactions (3) and (4) indicated in Table V, however, would predict a low yield for Cs^{135}.

Further yield data is necessary to verify the Glendenin explanation of fine structure in the mass yield curve. Work is in progress to determine directly by mass spectrometer methods the yields of Xe^{135}, Ba^{138}, and to re-determine the yields of Cs^{133}, Cs^{135}, Cs^{137} and Xe^{133}.

A study of the yields of the Xe and Kr isotopes in the fission of U^{233} will also be of considerable interest. With the mass yield curve shifted by 2 mass units the fine structure, if related to closed neutron shells, will appear at the same mass numbers but at different yield values. For example, the yields of the Kr isotopes will be considerably greater and any fine structure in the neighborhood of the 50-neutron shell will be more readily established. This investigation is now in progress.

ACKNOWLEDGMENTS

The authors wish to thank the National Research Council of Canada for financial assistance and to acknowledge the use of the facilities of the Chalk River laboratories, particularly those of the Chemistry Department. We also wish to thank Mr. T. G. Church, Dr. W. E. Grummitt, and Dr. L. G. Cook for their aid and helpful discussions.

On the Charge Independence of Nuclear Forces

JULIAN SCHWINGER
Harvard University, Cambridge, Massachusetts
(Received January 5, 1950)

It is shown that the small difference between the neutron-proton and proton-proton interactions in the ^1S state can be accounted for by magnetic forces, provided the nuclear interaction is described by the Yukawa potential. A variational principle is used to facilitate the comparison of the interactions, and for the determination of the effect of magnetic forces. A short discussion of variational principles is presented in the Appendix.

IT has long been known that the nuclear potentials operating in the ^1S state between a pair of protons, and a neutron and proton, are of approximately equal depth if range and shape are assumed identical.[1] There exists, however, a small but real difference, the neutron-proton potential depth exceeding that of two protons by several percent.[2] It will be shown in this note that magnetic interaction between nucleons adequately accounts for this difference, if the nuclear potential resembles that of Yukawa. The evidence in favor of the fundamental charge independence of nuclear forces is thereby greatly strengthened.

The comparison between neutron-proton and proton-proton interactions inferred from scattering data, as well as the determination of the effect of magnetic forces, is facilitated by a formulation of the scattering problem in terms of a variational principle.[3] A useful variational expression for the ^1S phase shift δ, which characterizes the effect of non-Coulomb forces between protons, is the following,

$$\operatorname*{Lim}_{\substack{R\to\infty\\ \epsilon\to 0}}\Big\{\int_0^R[(du/dr)^2-(M/\hbar^2)(E-(e^2/r)-V_{pp})u^2]dr - \int_\epsilon^R[(dv/dr)^2-(M/\hbar^2)(E-(e^2/r))v^2]dr - (1/b_0)\log(\gamma^2(\epsilon/b_0))v^2(0)\Big\} = \Big[k\cot\delta\frac{2\pi\eta}{e^{2\pi\eta}-1}+\frac{1}{b_0}\Big(Re\frac{\Gamma'(i\eta)}{\Gamma(i\eta)}-\log\eta\Big)\Big]v^2(0), \tag{1}$$

where $\log\gamma=C=0.5772$, $b_0=\hbar^2/Me^2$, $\eta=1/(2kb_0)$, and the other symbols have their standard significance. This expression for $\cot\delta$ has the property that it is stationary with respect to independent variations of $u(r)$ and $v(r)$, subject only to the restrictions

$$u(0)=0, \quad u(r)-v(r)\to 0, \quad r\to\infty. \tag{2}$$

The stationary value is attained for functions that satisfy the differential equations

$$[(d^2/dr^2)+(M/\hbar^2)(E-(e^2/r)-V_{pp})]u=0, \quad [(d^2/dr^2)+(M/\hbar^2)(E-(e^2/r))]v=0, \tag{3}$$

in addition to (2). Furthermore, this stationary value yields the correct nuclear phase shift. The verification of these assertions will be performed in the Appendix.

The advantage of this formula for the phase shift is that it involves the behavior of the wave function u only within the region of nuclear interaction, since $u\to v$ as $V_{pp}\to 0$, according to (2) and (3). In addition, the replacement of u and v within this region by slightly different functions will produce only a small error in the calculated value of $\cot\delta$, in virtue of the stationary property. A convenient set of functions for this purpose is provided by the solutions of the equations

$$((d^2/dr^2)-(M/\hbar^2)V_{pp})u_0=0; \quad (d^2/dr^2)v_0=0, \quad u_0(0)=0; \quad u_0-v_0\to 0, \quad r\to\infty, \tag{4}$$

that is, (2) and (3) with $E=0$, and $e=0$. We are thus going to employ trial functions which describe the zero energy scattering of two protons arising from non-Coulomb interactions alone. That this is a useful approximation stems from the large magnitude of the nuclear potential within the range of nuclear forces, in comparison with the Coulomb potential and the energy of relative motion, provided the latter is suitably restricted. From the comparison of the resulting phase shift formula with the empirical data, we shall be able to infer the hypothetical scattering properties of two protons interacting by non-Coulomb forces, which can be contrasted with the corresponding observed properties of a neutron and proton, thus affording a direct comparison of the two non-Coulomb interactions. We shall, finally, be able to compute the effect of a magnetic interaction addition to the nuclear potential by simply altering that potential as it appears explicitly in the variational expression for the phase shift. The implied alteration in the wave function has no first-order effect, in view of the stationary property.

On inserting the approximate functions u_0 and v_0 in (1), we obtain

$$\frac{\pi}{e^{2\pi\eta}-1}\cot\delta+Re\frac{\Gamma'(i\eta)}{\Gamma(i\eta)}-\log\eta=b_0\Big[\frac{1}{a}+\frac{1}{2}k^2r_s\Big], \tag{5}$$

[1] Breit, Condon, and Present, Phys. Rev. **50**, 825 (1936).
[2] Breit, Hoisington, Share, and Thaxton, Phys. Rev. **55**, 1103 (1939).
[3] J. Schwinger, Lectures on nuclear physics, Harvard, 1947; Phys. Rev. **72**, 724 (1947). J. M. Blatt, Phys. Rev. **74**, 92 (1948); J. M. Blatt and J. D. Jackson, Phys. Rev. **76**, 18 (1949).

where

$$r_e=\frac{2}{v_0^2(0)}\int_0^\infty (v_0^2-u_0^2)dr, \tag{6}$$

and

$$\frac{1}{a}=\frac{1}{a_{pp}}-\frac{1}{b_0}\left[\frac{1}{v_0^2(0)}\int_\epsilon^\infty \frac{v_0^2-u_0^2}{r}dr+\log\left(\gamma^2\frac{\epsilon}{b_0}\right)\right]_{\epsilon\to 0}$$
$$=\frac{1}{a_{pp}}+\frac{1}{b_0}\int_0^\infty \log\left(\gamma^2\frac{r}{b_0}\right)\frac{d}{dr}\left(\frac{v_0^2-u_0^2}{v_0^2(0)}\right)dr. \tag{7}$$

Here a_{pp} is the amplitude for the zero energy scattering of two protons by non-Coulomb forces, which replaces the phase shift in the form assumed by (1) with e and E equal to zero:

$$\operatorname*{Lim}_{R\to\infty}\left\{\int_0^R\left[\left(\frac{du_0}{dr}\right)^2+\frac{M}{\hbar^2}V_{pp}u_0^2\right]dr - \int_0^R\left(\frac{dv_0}{dr}\right)^2 dr\right\}=\frac{1}{a_{pp}}-v_0^2(0). \tag{8}$$

Equation (5) represents an expression for the phase shift in terms of two parameters, a and r_e, which completely characterize the effect of short range non-Coulomb interactions within a restricted energy domain. That the experimental data permits such a representation is demonstrated by plotting the left side of (5) as a function of proton kinetic energy and observing that the ensuing points form an accurate straight line.[3,4] The result of such a treatment of the data obtained with Van de Graaff generators[5] is expressed by

$$r_e=(2.65\pm 0.07)10^{-13}\text{ cm},\quad b_0/a=3.755\pm 0.024. \tag{9}$$

Although the constant a is obtained directly from experiment, the determination of the scattering amplitude a_{pp} requires some assumption concerning the nuclear potential. This is indicated by the formula

$$1/a_{pp}=1/a-1/b_0[\log(b_0/\bar{r})-2C], \tag{10}$$

since the average distance $\bar{r}$, defined by

$$\int_0^\infty \log\frac{r}{\bar{r}}\frac{d}{dr}(v_0^2-u_0^2)dr=0, \tag{11}$$

involves the detailed behavior of the wave functions. A good initial approximation to $\bar{r}$ is provided by the wave functions associated with $1/a_{pp}=0$, that is, a state of zero binding energy. We shall consider two potentials, a rectangular well and a Yukawa potential. For the rectangular well, of range r_0, the functions u_0 and v_0 are

$$u_0=\sin(\pi/2)r/r_0,\quad r<r_0;\quad u_0=1,\quad r>r_0, \tag{12}$$
$$v_0=1,$$

whence

$$\log\frac{r_e}{\bar{r}}=\int_0^1\frac{\sin^2(\pi/2)x}{x}dx=0.8241, \tag{13}$$

in which we have replaced r_0 by r_e, since the two are identical, according to (6) and (12). The approximate but accurate function

$$u_0=1-e^{-\beta r},\quad v_0=1, \tag{14}$$

will be used for the Yukawa potential, in which β is related to the measured r_e by

$$1/\beta=\tfrac{1}{3}r_e. \tag{15}$$

On performing the integrations in (11), we find

$$\log(r_e/\bar{r})=\log\tfrac{3}{2}+C=0.9827. \tag{16}$$

From these approximate evaluations of $\bar{r}$ we obtain, for the rectangular and Yukawa potentials, respectively,

$$b_0/a_{pp}=3.755-\log(b_0/r_e)+0.330 =1.699, \tag{17}$$

and

$$b_0/a_{pp}=3.755-\log(b_0/r_e)+0.172 =1.541. \tag{18}$$

Having computed these approximate values of b_0/a_{pp}, we may return to the evaluation of $\bar{r}$, according to (11), and insert wave functions appropriate to a finite scattering amplitude. This is easily done for the rectangular potential, and the result, correct to first order in r_e/a_{pp}, is

$$\log\frac{r_e}{\bar{r}}=\left(1+2\frac{r_e}{a_{pp}}\right)\int_0^1\frac{\sin^2(\pi/2)x}{x}dx-2\frac{r_e}{a_{pp}} =0.7692. \tag{19}$$

For the Yukawa potential, we employ the approximate wave function

$$u_0=1+(r/a_{pp})-e^{-\beta r},\quad v_0=1+(r/a_{pp}), \tag{20}$$

and obtain

$$\log(r_e/\bar{r})=\log\tfrac{3}{2}+C-(2/9)(r_e/a_{pp})=0.9512. \tag{21}$$

We may now compute corrected values of b_0/a_{pp}:

$$b_0/a_{pp}=1.754\pm 0.035\text{ (rectangular potential)} =1.573\pm 0.035\text{ (Yukawa potential).} \tag{22}$$

The probable error is that associated with the inaccuracy of $1/a$ and r_e. Our results[6] are, finally, to be compared with the ^1S neutron-proton zero energy scattering amplitude which, in these units ($b_0=2.881\times 10^{-12}$

[4] L. Landau and J. Smorodinsky, J. Phys. U.S.S.R. 8, 154 (1944).
[5] J. D. Jackson, thesis, M.I.T., 1949.

[6] The numerical values for $1/a_{pp}$ differ slightly from those obtained by H. A. Bethe, Phys. Rev. 76, 38 (1949).

cm), is given by[7]

$$b_0/a_{np}=1.217\pm0.003. \tag{23}$$

The discrepancy between (22) and (23) appears to be real and indicates that the neutron-proton interaction is somewhat stronger than the non-Coulomb proton-proton interaction.

We shall now show that the magnetic interaction between nucleons produces just such a difference, thereby implying that specifically nuclear forces are accurately charge independent. A suitable basis for such a discussion is the following approximate Dirac Hamiltonian for two nucleons with charges e_1, e_2 and anomalous magnetic moments μ_1', μ_2',

$$\begin{aligned}H=&c\boldsymbol{\alpha}_1\cdot\mathbf{p}_1+\beta_1Mc^2+c\boldsymbol{\alpha}_2\cdot\mathbf{p}_2+\beta_2Mc^2+V\\&+\frac{e_1e_2}{r}\left(1-\frac{1}{2}\boldsymbol{\alpha}_1\cdot\boldsymbol{\alpha}_2-\frac{1}{2}\frac{(\boldsymbol{\alpha}_1\mathbf{r})(\boldsymbol{\alpha}_2\cdot\mathbf{r})}{r^2}\right)\\&-e_1\boldsymbol{\alpha}_1\cdot\frac{\mu_2'\beta_2\boldsymbol{\sigma}_2\times\mathbf{r}}{r^3}-e_2\boldsymbol{\alpha}_2\cdot\frac{\mu_1'\beta_1\boldsymbol{\sigma}_1\times(-\mathbf{r})}{r^3}\\&-\frac{\mu_1'\mu_2'}{r^3}\left(3\frac{\beta_1\boldsymbol{\sigma}_1\cdot\mathbf{r}\beta_2\boldsymbol{\sigma}_2\cdot\mathbf{r}}{r^2}-\beta_1\boldsymbol{\sigma}_1\cdot\beta_2\boldsymbol{\sigma}_2\right)\\&-\frac{8\pi}{3}\mu_1'\mu_2'\beta_1\boldsymbol{\sigma}_1\cdot\beta_2\boldsymbol{\sigma}_2\delta(\mathbf{r})+i\mu_1'\beta_1\boldsymbol{\alpha}_1\cdot e_2\frac{\mathbf{r}}{r^3}\\&+i\mu_2'\beta_2\boldsymbol{\alpha}_2\cdot e_1\frac{(-\mathbf{r})}{r^3}.\end{aligned} \tag{24}$$

Here $\mathbf{r}=\mathbf{r}_1-\mathbf{r}_2$, and the successive terms following the sum of the free particle Hamiltonians describe the nuclear force interaction energy; the mutual energy of the charges, correct to order $(v/c)^2$; the energy of each charge in the magnetic field produced by the anomalous magnetic moment of the other particle; the mutual potential energy of the additional magnetic moments, separated into a tensor and a spherically symmetrical interaction; and finally the energy which the electric dipole of each particle, associated with the anomalous magnetic moment, possesses in the electric field of the other particles.

By eliminating the small components of the Dirac wave function, the Dirac Hamiltonian can be replaced by a Pauli-type Hamiltonian, in which the Coulomb and nuclear potentials are supplemented by a magnetic interaction energy. The latter can be written

$$\begin{aligned}V^{(\mathrm{mag})}=&\frac{e_1e_2}{M^2c^2}\mathbf{p}\cdot\frac{1}{r}\mathbf{p}-4\pi\frac{e_1\hbar}{2Mc}\frac{e_2\hbar}{2Mc}\delta(\mathbf{r})\\&-4\pi\left(\mu_1'\frac{e_2\hbar}{2Mc}+\mu_2'\frac{e_1\hbar}{2Mc}\right)\delta(\mathbf{r})-\frac{8\pi}{3}\mu_1\mu_2\boldsymbol{\sigma}_1\cdot\boldsymbol{\sigma}_2\delta(\mathbf{r}),\end{aligned} \tag{25}$$

in which various terms, ineffective in S states, have been discarded. The successive contributions to $V^{(\mathrm{mag})}$ have the following significance. The first term represents the magnetic interaction between the convection currents associated with the charges, as specialized to the center of gravity system ($\mathbf{p}_1=-\mathbf{p}_2=\mathbf{p}$); the second term contains the sum of the energies which the electric dipole moment of each particle, accompanying the Dirac magnetic moment, possesses in the electric field of the other particle; the third term is the analogous electric energy attributable to the anomalous magnetic moments, differing fundamentally from the preceding term by the absence of the Thomas factor; and finally we have the interaction energy of the total spin magnetic moments, $\mu=\mu'+e\hbar/2Mc$. We are actually interested in the ^1S neutron-proton and proton-proton magnetic interaction energies. These can be written

$$V_{np}^{(\mathrm{mag})}=8\pi\mu_n(\mu_p-\tfrac{1}{2})\mu_0^2\delta(\mathbf{r}), \tag{26}$$

and

$$V_{pp}^{(\mathrm{mag})}=8\pi(\mu_p^2-\mu_p+\tfrac{1}{2})\mu_0^2\delta(\mathbf{r})+4\mu_0^2\frac{1}{\hbar^2}\mathbf{p}\cdot\frac{1}{r}\mathbf{p}, \tag{27}$$

in which $\mu_n=-1.913$, and $\mu_p=2.793$ are the magnetic moments of neutron and proton in units of $\mu_0=e\hbar/2Mc$ the nuclear magneton. It will be noted that the neutron-proton magnetic interaction is attractive, while that for two protons is repulsive.

The magnetic part of the neutron-proton interaction produces a contribution to $1/a_{np}$ which, according to the analog of (8), is given by

$$\begin{aligned}\delta\left(\frac{1}{a_{np}}\right)=&\frac{M}{\hbar^2}\frac{1}{v_0^2(0)}\int_0^\infty V_{np}^{(\mathrm{mag})}u_0^2dr\\=&\tfrac{1}{2}\mu_n(\mu_p-\tfrac{1}{2})\frac{e^2}{Mc^2}\left[\frac{u_0'(0)}{v_0(0)}\right]^2,\end{aligned} \tag{28}$$

since $\delta(\mathbf{r})=\delta(r)/4\pi r^2$. The ratio $u_0'(0)/v_0(0)$ can be computed rigorously for the rectangular well, and with reasonable accuracy from the wave function (20) for the Yukawa potential. The results, including first-order corrections in r_e/a_{np}, are

$$\begin{aligned}\frac{u_0'(0)}{v_0(0)}=&\frac{\pi}{2r_e}\left(1+\frac{r_e}{a_{np}}\right)\quad\text{(rectangular potential)}\\=&\frac{3}{r_e}\left(1+\frac{7}{9}\frac{r_e}{a_{np}}\right)\quad\text{(Yukawa potential)},\end{aligned} \tag{29}$$

from which we obtain

$$\begin{aligned}\delta\left(\frac{b_0}{a_{np}}\right)=&\frac{\pi^2}{8}\mu_n(\mu_p-\tfrac{1}{2})\left(1+2\frac{r_e}{a_{np}}\right)\left(\frac{\hbar/Mc}{r_e}\right)^2\\=&-(0.042\pm0.002),\end{aligned} \tag{30}$$

[7] This value is obtained from the free proton cross-section measurement of E. Melkonian, Phys. Rev. 76, 1744 (1949), and the recent determination of the coherent scattering amplitude by Hughes, Burgy and Ringo, Phys. Rev. 77, 291 (1950).

and

$$\delta\left(\frac{b_0}{a_{np}}\right)=\frac{9}{2}\mu_n(\mu_p-\tfrac{1}{2})\left(1+\frac{14}{9}\frac{r_e}{a_{np}}\right)\left(\frac{\hbar/Mc}{r_e}\right)^2 \quad (31)$$
$$=-(0.145\pm0.007),$$

for the rectangular and Yukawa potentials, respectively. The numerical values are obtained by the assumption that r_e is charge independent, which is consistent with the present inaccurate determinations of the neutron-proton r_e in the ^1S state. We may now compute the hypothetical scattering amplitude a_{np}',

$$\frac{b_0}{a_{np}'}=\frac{b_0}{a_{np}}-\delta\left(\frac{b_0}{a_{np}}\right) \quad (32)$$
$$=1.259\pm0.004 \text{ (rect.)}$$
$$=1.362\pm0.008 \text{ (Yukawa)},$$

which describes the neutron-proton scattering that would be produced by specifically nuclear forces alone.

The magnetic contribution to $1/a_{pp}$ is similarly given by

$$\delta\left(\frac{1}{a_{pp}}\right)=\tfrac{1}{2}(\mu_p^2-\mu_p+\tfrac{1}{2})\frac{e^2}{Mc^2}\left[\frac{u_0'(0)}{v_0(0)}\right]^2 + \frac{e^2}{Mc^2}\frac{1}{v_0^2(0)}\int_0^\infty\left(u_0'-\frac{u_0}{r}\right)^2\frac{dr}{r}. \quad (33)$$

The integral in this formula can be transformed to

$$-\int_0^\infty u_0u_0''\frac{dr}{r}=-\frac{1}{2}(u_0'(0))^2+\frac{1}{2a_{pp}^2}v_0^2(0), \quad (34)$$

which can be evaluated, with sufficient precision, as

$$\left(\int_0^1\frac{\sin^2(\pi/2)x}{x}dx-\frac{1}{2}\right)(u_0'(0))^2=0.324(u_0'(0))^2, \quad (35)$$

and

$$(\log 2-\tfrac{1}{2})(u_0'(0))^2=0.193(u_0'(0))^2, \quad (36)$$

for the two potentials. Hence

$$\delta\left(\frac{b_0}{a_{pp}}\right)=\frac{\pi^2}{8}(\mu_p^2-\mu_p+1.15)\left(1+2\frac{r_e}{a_{pp}}\right)\left(\frac{\hbar/Mc}{r_e}\right)^2 \quad (37)$$
$$=0.056\pm0.003 \text{ (rect.)}$$

and

$$\delta\left(\frac{b_0}{a_{pp}}\right)=\frac{9}{2}(\mu_p^2-\mu_p+0.886)\left(1+\frac{14}{9}\frac{r_e}{a_{pp}}\right)\left(\frac{\hbar/Mc}{r_e}\right)^2 \quad (38)$$
$$=0.195\pm0.010 \text{ (Yukawa)}.$$

The scattering amplitude a_{pp}',

$$\frac{b_0}{a_{pp}'}=\frac{b_0}{a_{pp}}-\delta\left(\frac{b_0}{a_{pp}}\right), \quad (39)$$

which describes zero energy proton-proton scattering by specifically nuclear forces, is now obtained as

$$\frac{b_0}{a_{pp}'}=1.698\pm0.035, \quad (40)$$

for the rectangular potential, and

$$\frac{b_0}{a_{pp}'}=1.378\pm0.040, \quad (41)$$

for the Yukawa potential.

We finally observed that a_{np}' and a_{pp}' are in definite disagreement for the rectangular potential, and in very satisfactory agreement for the Yukawa potential; the hypothesis of charge independent nuclear forces is accurately confirmed by experiment, provided the Yukawa potential is also assumed. It should be noted that a small difference between the neutron-proton and proton-proton nuclear interactions is to be anticipated theoretically, as a consequence of electrical perturbations of the mesons responsible for nuclear forces. Independent evidence concerning the shape of the nuclear potential, as well as a more accurate evaluation of the magnetic interaction, will be required to reveal this effect.

Note added in proof.—A more precise calculation for the Yukawa potential has been performed by Mr. B. R. Mottelson. The wave function employed in the text actually corresponds to a potential of the form $e^{-\beta r}/(1-e^{-\beta r})$, which possesses the singularity of the Yukawa potential, but differs at large distances. A corrected wave function leads to a slightly smaller value of $\bar{r}$, and increases somewhat the effect of the magnetic interaction. The results are $b_0/a_{np}'=1.396\pm0.01$, $b_0/a_{pp}'=1.302\pm0.04$. This comparison is not unsatisfactory, particularly in view of the expected, but uncertain, decrease in magnetic interaction produced by the finite spatial extension of the nucleon magnetization.

APPENDIX

The discussion of the variational principle (1) in the text will be preceded by a treatment of the simpler variational principle appropriate to neutron-proton S scattering:

$$\lim_{R\to\infty}\left\{\int_0^R\left[\left(\frac{du}{dr}\right)^2-\frac{M}{\hbar^2}(E-V_{np})u^2\right]dr - \int_0^R\left[\left(\frac{dv}{dr}\right)^2-\frac{ME}{\hbar^2}v^2\right]dr\right\}=k\cot\delta v^2(0). \quad (A1)$$

We shall demonstrate that the quantity called $k\cot\delta$ is stationary[8] with respect to independent variations of u and v, subject only to the restriction

$$u(0)=0, \quad u(r)-v(r)\to0, \quad r\to\infty. \quad (A2)$$

[8] L. Hulthèn has independently remarked on the stationary property of the phase shift. However, he has not introduced an explicit stationary expression for the phase shift, but rather an implicit characterization. See Mott and Massey, *The Theory of Atomic Collisions* (Clarendon Press, Oxford, 1949), second edition, p. 128, and W. Kohn, Phys. Rev. 74, 1763 (1948).

The stationary value is attained for functions that satisfy

$$\left[\frac{d^2}{dr^2}+\frac{M}{\hbar^2}(E-V_{np})\right]u=0, \tag{A3a}$$

$$\left[\frac{d^2}{dr^2}+\frac{ME}{\hbar^2}\right]v=0, \tag{A3b}$$

and the stationary value of δ is the rigorous phase shift. On introducing such a variation in (A1), we obtain

$$u'\delta u-v'\delta v\Big]_0^R-\int_0^R\left[\frac{d^2u}{dr^2}+\frac{M}{\hbar^2}(E-V_{np})u\right]\delta u dr$$

$$+\int_0^R\left[\frac{d^2v}{dr^2}+\frac{ME}{\hbar^2}v\right]\delta v dr=(k\ \cot\delta)v(0)\delta v(0)+\delta(k\ \cot\delta)\tfrac{1}{2}v^2(0). \tag{A4}$$

Now

$$u'\delta u-v'\delta v\Big]_0^R=v'(0)\delta v(0), \tag{A5}$$

in consequence of the restrictions (A2). Hence the conditions that $k\cot\delta$ be stationary with respect to otherwise unrestricted variations are expressed by the differential Eqs. (A3), and by

$$\frac{v'(0)}{v(0)}=k\cot\delta. \tag{A6}$$

Now the solution of (A3b) consistent with (A6) has the form

$$v(r)/v(0)=\sin(kr+\delta)/\sin\delta, \tag{A7}$$

which is indeed the asymptotic form of u, thereby identifying the stationary value of δ with the correct phase shift.

Among the advantages of a variational principle is the ease with which one infers the dependence of the stationary quantity on various parameters, such as kinetic energy and depth of potential well in (A1). In considering a small change of the energy, for example, no corresponding alteration in the wave function need be introduced, in virtue of the stationary property. Thus, we have the rigorous result

$$\frac{d}{dk^2}(k\cot\delta)=\frac{1}{v^2(0)}\int_0^\infty(v^2-u^2)dr. \tag{A8}$$

The integral in this formula involves the wave functions u and v associated with the energy E, and the effective domain of integration is the region of nuclear force. With a short range interaction, however, u and v are only slightly energy dependent, for kinetic energies that are small in comparison with the average nuclear potential. It is therefore useful to introduce an energy expansion for the wave functions within the interaction region,

$$u=u_0+k^2u_1+\cdots,\quad v=v_0+k^2v_1+\cdots, \tag{A9}$$

subject to the convenient normalization, $v(0)=1$, and obtain

$$d/(dk^2)(k\cot\delta)=\tfrac{1}{2}r_s+2pk^2r_s^3+\cdots. \tag{A10}$$

Here

$$\tfrac{1}{2}r_s=\int_0^\infty(v_0^2-u_0^2)dr,\quad v_0(0)=1, \tag{A11}$$

and

$$pr_s^3=\int_0^\infty(v_0v_1-u_0u_1)dr,\quad v_1(0)=0, \tag{A12}$$

define two energy independent parameters; the length r_s, called the effective range, and the numerical coefficient p. The resulting expansion[9] for $k\cot\delta$ is

$$k\cot\delta=\frac{1}{a}+\frac{1}{2}k^2r_s+pk^4r_s^3+\cdots, \tag{A13}$$

in which the length a describes the amplitude of the scattered wave for zero energy.

The determination of the conditions that $\cot\delta$ in (1) be stationary proceeds in the same manner. One easily obtains the differential Eqs. (3) and the requirement

$$\operatorname*{Lim}_{\epsilon\to\infty}\left[\frac{v'(\epsilon)}{v(0)}-\frac{1}{b_0}\log\left(\gamma^2\frac{\epsilon}{b_0}\right)\right]=k\cot\delta-\frac{2\pi\eta}{e^{2\pi\eta}-1}$$

$$+\frac{1}{b_0}\left(Re\frac{\Gamma'(i\eta)}{\Gamma(i\eta)}-\log\eta\right). \tag{A14}$$

Now the solution of the differential equation for v has the form

$$v(r)=f(r)\cos\delta+g(r)\sin\delta, \tag{A15}$$

where δ is the desired phase shift, and f, g are the regular and irregular Coulomb wave functions, identified by the asymptotic formulas

$$f\sim\sin\varphi,\quad g\sim\cos\varphi,\quad \varphi=kr-\eta\log 2kr+\arg\Gamma(1+i\eta). \tag{A16}$$

To compute the left side of (A14) from (A15),

$$\operatorname*{Lim}_{\epsilon\to0}\left[\frac{v'(\epsilon)}{v(0)}-\frac{1}{b_0}\log\left(\gamma^2\frac{\epsilon}{b_0}\right)\right]=\frac{f'(0)}{g(0)}\cot\delta$$

$$+\operatorname*{Lim}_{\epsilon\to0}\left[\frac{g'(\epsilon)}{g(0)}-\frac{1}{b_0}\log\left(\gamma^2\frac{\epsilon}{b_0}\right)\right], \tag{A17}$$

we require the functions f and g in the vicinity of the origin. These are known[10] to be given by

$$f(r)\sim C_0kr,\quad C_0^2=\frac{2\pi\eta}{e^{2\pi\eta}-1}, \tag{A18}$$

$$g(r)\sim\frac{1}{C_0}\left\{1+\frac{r}{b_0}\left[\log\left(\gamma^2\frac{r}{b_0}\right)-1+Re\frac{\Gamma'(i\eta)}{\Gamma(i\eta)}-\log\eta\right]\right\}.$$

Hence

$$\frac{f'(0)}{g(0)}=k\frac{2\pi\eta}{e^{2\pi\eta}-1}, \tag{A19}$$

and

$$\frac{g'(\epsilon)}{g(0)}=\frac{1}{b_0}\left[\log\left(\gamma^2\frac{\epsilon}{b_0}\right)+Re\frac{\Gamma'(i\eta)}{\Gamma(i\eta)}-\log\eta\right], \tag{A20}$$

which, inserted in (A17), yields (A14) thereby demonstrating that the stationary value of δ is the correct phase shift.

---

[9] Since the original construction of this expansion by somewhat different variational methods (reference 3), a number of derivations have been published in which the stationary property of the phase shift is not explicitly employed: F. C. Barker and R. E. Peierls, Phys. Rev. 75, 312 (1949); Hatcher, Arfken, and Breit, Phys. Rev. 75, 1389 (1949); G. F. Chew and M. L. Goldberger, Phys. Rev. 75, 1637 (1949); H. A. Bethe, Phys. Rev. 76, 38 (1949).

[10] Yost, Wheeler, and Breit, Phys. Rev. 49, 174 (1936).

Microwave Spectroscopy in the Region from Two to Three Millimeters*

O. R. GILLIAM, CHARLES M. JOHNSON, AND WALTER GORDY
Department of Physics, Duke University, Durham, North Carolina
(Received January 10, 1950)

A completely electronic sweep spectroscope of high resolution has been developed for the wave-length region from 2 to 3 millimeters (150,000 mc/sec. to 100,000 mc/sec.). The radiation source is a silicon crystal harmonic generator driven by Ratheon klystrons. Silicon crystals are used also as detectors. Radiation of wave-length 1.96 mm (154,000 mc/sec.) has been generated and detected with strength more than ten times the noise level. Some lines in the hyperfine structure of the $J=19\rightarrow20$ rotational transition of ICN at 2.32 mm have been observed. The $J=1\rightarrow2$ transition of CH_3F has been observed at 2.93, and the separation of the $K=1$ and $K=0$ lines has been determined as 1.8 mc. Precision measurements on the first rotational line ($J=0\rightarrow1$) of $C^{12}O^{16}$ and $C^{13}O^{16}$ in the 2.6-mm region have been made with an electronic frequency standard monitored by the 10 mc/sec. signal of station WWV. The following molecular constants were determined: for $C^{12}O^{16}$, $B_0=1.92262_5$ cm^{-1}, $B_e=1.93136_7$ cm^{-1}, $I_0=14.5553_1\times10^{-40}$ g cm^2, $I_e=14.4894_3\times10^{-40}$ g cm^2, $r_0=1.13078_9$A, $r_e=1.12822_7$A; for $C^{13}O^{16}$ $B_0=1.83806_9$ cm^{-1}, $I_0=15.2248_9\times10^{-40}$ g cm^2, $r_0=1.13072_5$A. The last three digits quoted for r and I have relative significance only, because of possible error in Planck's constant.

1. INTRODUCTION

IT is well known that for many years the gap in the electromagnetic spectrum between the optical and radio regions has been closed.[1] That is, energy has been detected throughout this region. However, the earlier methods of generating and detecting the radiation have not proved effective for spectroscopic measurements. Consequently, much of this spectral region is still relatively unexplored.

For the past three years a program has been underway in this laboratory for extending to higher frequencies the region in which spectroscopic measurements can be made with essentially electronic or radiofrequency instruments and techniques. A survey of the progress up to August 1948 has been given by one of us.[2] Measurements in the region from 3- to 5-mm wave-length have been reported by Smith, Gordy, Simmons, and Smith.[3] Their observations were made with a sweep spectrograph capable of high resolution, but measurements of the line frequencies were made with a cavity wave meter accurate to only a few megacycles. Since that time, Simmons, Anderson, and Gordy[4] have made spectrum line measurements in the latter region to an accuracy of 3 parts in 10^6. They used an electronic frequency standard monitored by Station WWV.

The present work extends the range of precision electronic frequency measurements above 100,000 mc. The $C^{12}O^{16}$ absorption line frequency was measured as 115,270.56±0.25 mc—a frequency over 11,000 times the WWV frequency used a a monitoring standard.

The millimeter wave components employed in the present work are similar to those referred to above for the 3- to 5-mm wave region. A silicon crystal multiplier driven by Raytheon klystrons is again used as a source. The klystron source frequency is here tripled rather than doubled, as was done in the previous work. Though it has not yet been used to measure spectral lines, a frequency quadrupler similarly designed and energized by a QK142 Raytheon klystron has been found to give usable power at wave-lengths slightly below 2 mm.

Obviously, because of their much greater output, magnetrons would be more powerful sources for millimeter wave harmonic energy. But, because of the greater difficulty in tuning them and because of their more impure (less monochromatic) spectrum as compared to that of the klystron, we have not used them. Recently, however, energy of magnetron harmonics has been detected in the region from 1.5- to 2-mm wavelength by Loubser and Townes.[5] They used an infra-red type detector (Golay cell). With this combination they were able to detect absorption of DI and NH_3 at high pressures, but to our knowledge no resonant absorption peaks have been measured with accuracy by this method.

2. MILLIMETER WAVE BANDS AND COMPONENTS

Several different sizes of wave guide are required for the millimeter wave region. The diagram given in an earlier report,[6] which shows the wave guide sizes and the band designations as employed in this laboratory, has been extended (see Fig. 1) to include the G band (2 to 3 mm) covered in the present report and the projected F band (1.3 to 2 mm), for which wave guide components are now being developed. The dimensions of the H band guide have been changed slightly from those previously used so that more effective overlapping

* The research reported in this document has been made possible through support and sponsorship extended by the Geophysical Research Directorate of the Air Force Cambridge Research Laboratories under Contract No. W(19-122)ac-35. It is published for technical information only and does not represent recommendations or conclusions of the sponsoring agency.

[1] E. F. Nichols and J. D. Tear, Annual Report of the Smithsonian Institution, pp. 175–185 (1923).
[2] W. Gordy, Rev. Mod. Phys. **20**, 668 (1948).
[3] Smith, Gordy, Simmons, and Smith, Phys. Rev. **75**, 260 (1949).
[4] Simmons, Anderson, and Gordy, Phys. Rev. **77**, 77 (1950).
[5] J. H. N. Loubser and C. H. Townes, Phys. Rev. **76**, 178 (1949).
[6] W. Gordy, reference 2, p. 670.

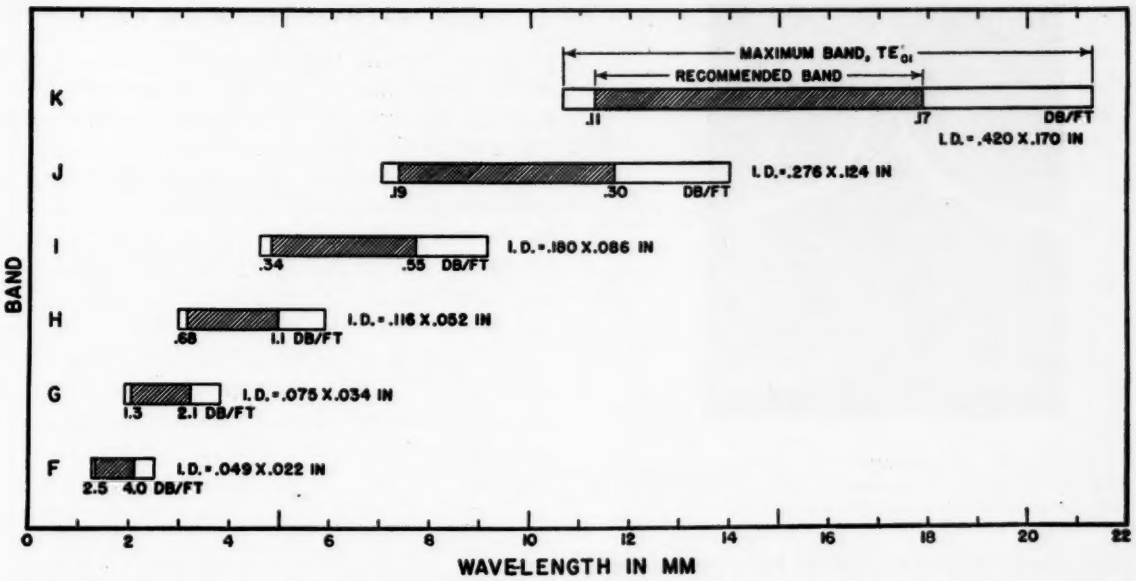

FIG. 1. Dimensions and losses for coin silver wave guide covering the region from 1.3 mm to 18 mm. The designation *F*, *G*, *H*, *I*, *J* is that adopted at this laboratory for the sub-*K* bands as indicated.

of the *I* band is obtained. The *I* and *J* band sizes here shown do not correspond exactly to the output sizes of the present Raytheon tubes. Hence, slightly tapered connectors are used. It will be noted that wave guide of six different sizes is required for making the usual wave guide components—attenuators, multipliers, crystal mounts, etc.—for the region from 1.3 mm to 18 mm. For absorption cells oversized wave guide can be used. When the third, fourth, or higher harmonics are used, additional wave guide sizes are needed for filtering the lower harmonics.

Figure 2 represents a photograph of the essential wave guide components with the exception of the absorption cell and the mixer for the frequency standard. The crystal multiplier and detector previously described[3] are reduced in size to conform to the shorter wave-lengths. For the present work the absorption cell was made of *K* band rather than of *S* band guide, as previously used. The *K* band guide was found to be more satisfactory, probably because of smaller losses in the transition sections. The cell length was 7 feet. A mica window (0.001-in. thickness) and a lead gasket (0.003 in.) pressed tightly between coupling flanges were used to seal each end of the absorption cell. This type of vacuum seal permitted the cell to be cooled to liquid air temperature. To energize the frequency tripler, Raytheon klystrons QK142 and QK226 were used. Approximately 10 milliwatts is available from the QK142 and 5 milliwatts from the QK226. No attempts were made to measure the power output from the tripler, but it was probably of the order of a microwatt. Selected Sylvania 1N26 crystals were employed both for the multiplier and detector, and for the mixer and detector of the frequency standard.

3. DETECTING METHODS

Video

As has been previously shown,[2] the simple "video" receiver compares favorably with the more awkward superheterodyne one for the detection of absorption lines whenever the available power is so small (the order of a microwatt) that the low frequency noise generated in the crystal by the microwave power is

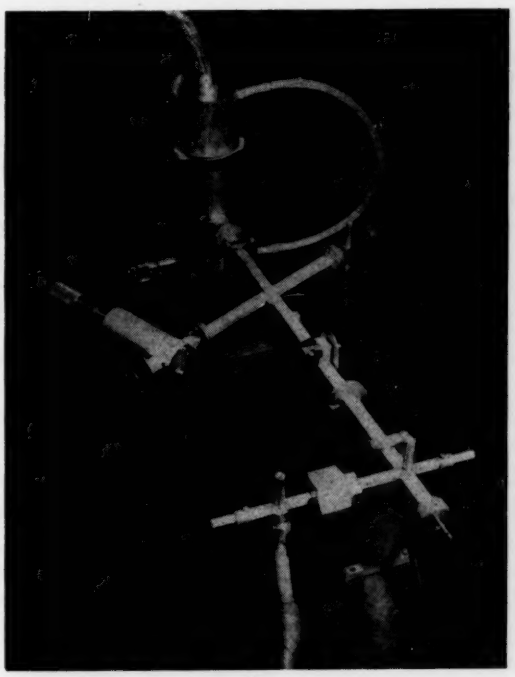

FIG. 2. Microwave components (less absorption cell and mixer for frequency standard) showing a frequency tripler and detector in the *G* band region, and associated *J* band components.

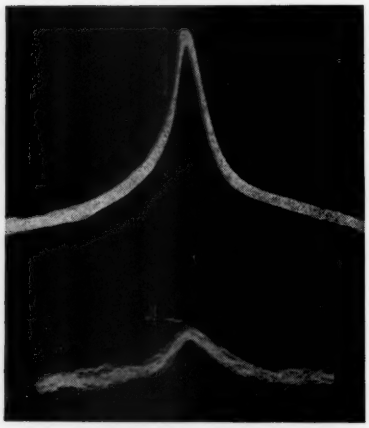

FIG. 3. Oscillograms of the lowest rotational transition of $C^{12}O^{16}$ at 115,270 mc. The upper curve was taken at the temperature of liquid air, the lower at the temperature of dry ice.

negligible. For most of the work we have used a single crystal detector followed by an amplifier with a band width of approximately 500 c.p.s. The lower frequency "cut-off" occurs at about 60 c.p.s. and is fairly sharp so that by proper adjustment of the rate of oscillator sweep the mode contour and variations caused by r-f reflections can be "filtered."[7] Figure 3 shows the $J=0\rightarrow1$ rotational line of $C^{12}O^{16}$ at 2.60-mm wave-length, and Fig. 4 shows a section of the $J=19\rightarrow20$ rotational transition of ICN at 2.32-mm wave-length, both detected by this method.

Phase-Sensitive Amplifier with Source Modulation

A second method, which was found to be more sensitive and only slightly more complicated than the method just described, employs a narrow-band phase-sensitive detector with the reference signal applied to the reflector of the oscillator so as to frequency modulate the oscillator at the reference frequency. Figure 5 shows a block diagram of this system. The principle of operation is similar to the modulation method already described by Gordy and Kessler[8] except that the phase-sensitive amplifier is used instead of the ordinary A.M. receiver. For the present work a 4000 c.p.s. receiver was used. Figure 6 shows the same ICN lines as those in Fig. 4, detected by this method and displayed on an Esterline-Angus automatic recorder. Stark modulation instead of source modulation would offer some advantages if a Stark cell of sufficiently low loss can be made for these high frequencies. The present method, however, has the advantage that the power can be detected when no absorption line is being observed. This is very desirable in this region where frequently the power drops below that necessary for satisfactory operation.

[7] W. Gordy and M. Kessler, Phys. Rev. **71**, 640 (1947).
[8] W. Gordy and M. Kessler, Phys. Rev. **72**, 644 (1947).

Superheterodyne

One of the difficulties in employing energy of harmonics higher than the third is the stringent requirement on the wave guide filters. Dr. Robert Carter has suggested to us a heterodyne detecting method which discriminates between the different harmonics. Two harmonic generators driven by separate klystrons are required for operation of the system. The outputs from the two sources are mixed, and the difference frequency is amplified by an I.F. amplifier. One of the oscillators has a fixed frequency (or its frequency is varied very slowly), and the other has a frequency sweep synchronized with the C.R.O. sweep used to display the output signal. This is equivalent to viewing the output of the fixed frequency source with a spectrum analyzer. However, the signal resulting from the beating of any two harmonics appears at a place on the scope-trace different from that of any other two. This useful result follows simply from the fact that the difference frequency of the different harmonic pairs is not the same. Thus, to obtain the same beat frequency with different harmonic combinations, the difference frequency of the fundamental sources must be changed. We have found this method useful for selecting crystals, for tuning multipliers, and for estimating the relative energies in the different harmonics. It could be used for observing absorption lines, but it would be slower than the other methods described. By mixing fourth harmonic power we have obtained signals more than ten times the noise level at a frequency of 154,000 mc (1.96-mm wave-length).

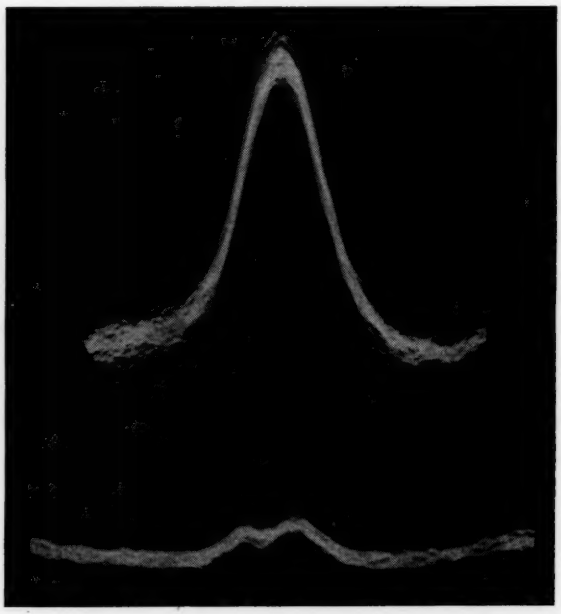

FIG. 4. Upper curve shows the unresolved $J=19\rightarrow20$, $\Delta F=+1$ transitions of ICN at $\lambda=2.32$ mm. Lower curve shows the same transition partially resolved.

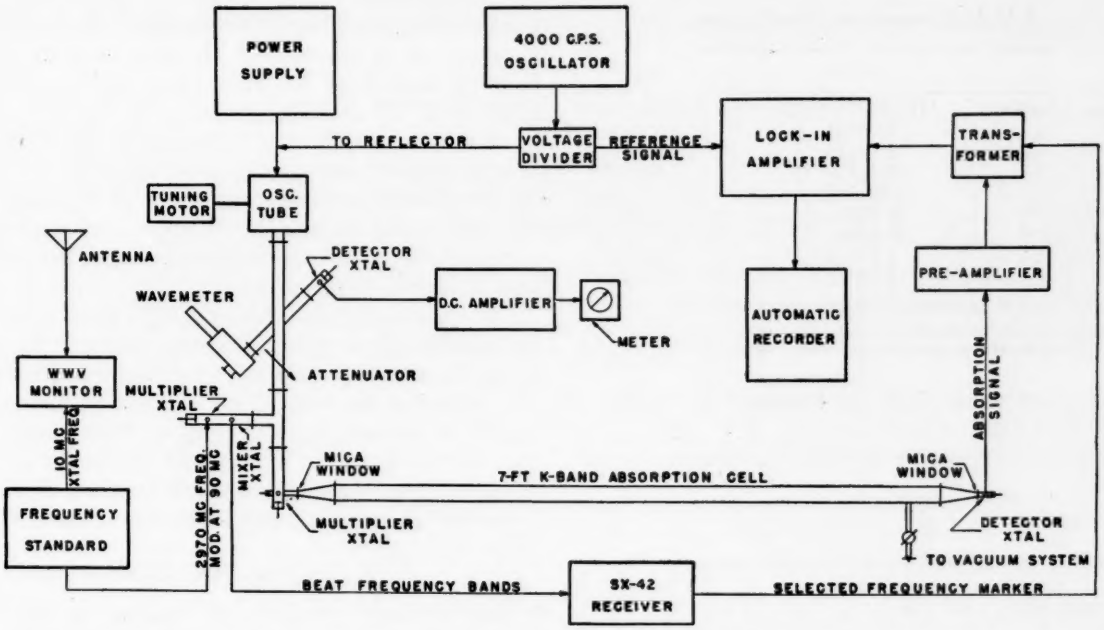

FIG. 5. Block diagram of the 2- to 3-millimeter wave spectrometer employing a phase-sensitive amplifier with source modulation and automatic recording.

4. MICROWAVE SPECTRUM AND MOLECULAR CONSTANTS OF CARBON MONOXIDE

The first rotational lines of $C^{12}O^{16}$ and $C^{13}O^{16}$† have been measured for the ground vibrational state. From these measurements precise values of the molecular constants were calculated (see Table I). Since microwave data could not be obtained on excited vibrational states, equilibrium values B_e, I_e, and r_e are not completely determined from the present work. Nevertheless, the present work improves the accuracy in these values by a factor of 10 or more because the error introduced by the anharmonicity corrections is an order of magnitude smaller than the total error in the previously determined B values. The frequency of the first rotational line is altered slightly by centrifugal stretching. Fortunately, this does not limit the accuracy of the final results since the small stretching constant can be estimated with sufficient accuracy from B and from the known vibrational frequency.

The rotational frequencies of a diatomic molecule are:

$$\nu = 2B_v(J+1) - 4D_v(J+1)^3,$$

where

$$J = 0, 1, 2, \cdots$$
$$B_v = B_e - \alpha_e(v+1/2),$$
$$B_e = h/(8\pi^2 c I_e),$$

and

$$D_v = 4B_v^3/\omega^2.$$

For the first rotational line ($J=0\rightarrow1$) and the ground vibrational state ($v=0$),

$$\nu(\text{cm}^{-1}) = 2B_0 - 4D_0,$$

where

$$B_e = B_0 + \tfrac{1}{2}\alpha_e, \quad D_0 = 4B_e^3/\omega_e^2.\ddagger$$

For $C^{12}O^{16}$ we use $\alpha_e = 0.017485 \pm 0.000015$ cm^{-1} and $D_0 = 6.4_5 \times 10^{-6}$ cm^{-1}, as determined by Herzberg and Rao.[9] For $C^{13}O^{16}$ we calculate $D_0 = 5.8_9 \times 10^{-6}$ cm^{-1}, with the easily derived formula,

$$D_0' = (\mu/\mu')^2 D_0,$$

where the prime indicates the constants for $C^{13}O^{16}$. The value of α_e listed in Table I for $C^{13}O^{16}$ is obtained from our measurements by assuming r_e for $C^{13}O^{16}$ to be the same as that for $C^{12}O^{16}$. For Planck's constant we

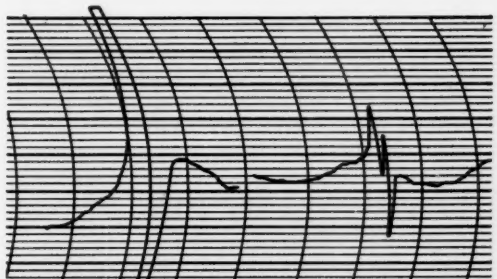

FIG. 6. Automatic recording tracings of $J=19\rightarrow20$, $\Delta F=+1$ transitions of ICN at $\lambda=2.32$ mm obtained by use of phase sensitive amplifier with source modulation. Left curve shows unresolved line. Right curve is partially resolved. The presentation represents the first derivative of the absorption curve.

† The C^{13} was concentrated to 14 percent.

‡ Here we neglect the second-order term $\frac{1}{2}\beta_e$.

[9] G. Herzberg and K. N. Rao, J. Chem. Phys. 17, 1099 (1949).

TABLE I. Molecular constants of carbon monoxide.

	$C^{12}O^{16}$	$C^{13}O^{16}$
ν_0 mc/sec. ($J=0\rightarrow1$)	115,270.56±0.25	110,201.1±0.4
B_0 cm^{-1}	1.92262_5	1.83806_9
B_e cm^{-1}	1.93136_7	1.84621_5
D_0 cm^{-1}	$(6.4_8\times10^{-6})$	$5.8_9\times10^{-6}$
α_e cm^{-1}	(0.01748_8)	0.01629_2
*I_0 g cm$^2\times10^{40}$	14.5553_1	15.2248_9
*I_e g cm$^2\times10^{40}$	14.4894_3	15.1577_1
*r_0 10^{-8} cm	1.13078_9	1.13072_5
*r_e 10^{-8} cm	1.12822_7	(1.12822_7)

* The last three digits quoted for r and I have relative significance only, because of possible error in the value of Planck's constant.

use the latest value given by DuMond and Cohen,[10] $h=6.62373\pm0.0011\times10^{-27}$ erg sec. With the value[11] $c=2.99776\pm0.00004\times10^{10}$ cm/sec. this gives

$$I=27.98440\times10^{-40}/B \text{ g cm}^2$$

and

$$r=5.290028\times10^{-20}/(\mu B)^{\frac{1}{2}} \text{ cm}.$$

Other constants used are:

$$\left.\begin{aligned} 1 \text{ A.M.U.} &= 1.65972\times10^{-24} \text{ g}^{12} \\ M_C12 &= 12.00386 \text{ A.M.U.} \\ M_C13 &= 13.00761 \text{ A.M.U.} \end{aligned}\right\}^{11}$$

With the above constants and equations we have calculated the molecular parameters listed in Table I. The values thus obtained are in remarkably good agreement with those recently obtained by Herzberg and Rao, who made observations with a 21-foot grating in the region of 1.2 microns on the third overtone of the CO vibrational band. Our B_0 values are apparently more precise than those of Herzberg and Rao by a factor of more than 10. They quote their error limits in B_0 for $C^{12}O^{16}$ as 1.5×10^{-4} cm^{-1}. We believe ours to be accurate to 7×10^{-6} cm^{-1}. The results obtained from the ultraviolet[13] are also in good agreement but are considered less accurate than those of Herzberg and Rao. The values obtained in the longer infra-red region[14] on the CO fundamental vibration-rotation band are in poor agreement with our results.

The rotational constants of $C^{12}O^{16}$ have now been measured in three widely different regions of the spectrum: the ultraviolet, the infra-red, and the microwave. This allows a checking of the calibration methods of one region against those of another. For example, one may now calibrate an infra-red or ultraviolet spectroscope indirectly with station WWV by using the carbon monoxide lines as secondary frequency standards.

5. METHYL FLUORIDE

The $J=1\rightarrow2$ transition of methyl fluoride was observed at 2.93-mm wave-length. The separation of the $K=0$ and $K=1$ lines was found to be 1.8 mc. This gives the centrifugal stretching constant $D_{JK}=0.45$ mc. The molecular structure of methyl fluoride has already been determined from measurements on the $J=0\rightarrow1$ transition.[15]

We wish to thank W. V. Smith, R. L. Carter, and R. S. Anderson for their suggestions and assistance with the electronic problems, and R. Trambarulo for preparing the sample of carbon monoxide with concentrated C^{13}.

[10] J. W. M. DuMond and E. R. Cohen, Rev. Mod. Phys. 21, 651 (1949).
[11] R. T. Birge, Rev. Mod. Phys. 13, 233 (1941).
[12] This was obtained from the value of Avogrado's number given by DuMond and Cohen, reference 10.
[13] Gerö, Herzberg, and Schmid, Phys. Rev. 52, 467 (1937).
[14] Lagemann, Nielsen, and Dickey, Phys. Rev. 72, 284 (1947).
[15] Gilliam, Edwards, and Gordy, Phys. Rev. 75, 1014 (1949).

Molecular Dipole Moments and Stark Effects. III. Dipole Moment Determinations*

R. G. SHULMAN** AND B. P. DAILEY
Chemistry Department, Columbia University, New York, New York

AND

C. H. TOWNES
Physics Department, Columbia University, New York, New York

(Received December 30, 1948)

Dipole moments of eight molecules were determined by the Stark splittings of the rotational transitions in the microwave region. The molecules and their moments in Debye units are: AsF_3, 2.815±0.025; CH_3I, 1.647±0.014; CH_3Cl, 1.869±0.010; CH_3Br, 1.797±0.015; CH_3CF_3, 2.321±0.034; PF_3, 1.025±0.009; N_2O, 0.166±0.002; and ClCN, 2.802±0.020. In all cases Stark effects followed very closely theoretical expectations.

INTRODUCTION

THE determination of molecular electric dipole moments from a study, in the microwave region, of the splitting of rotational energy levels by an electric field has a number of advantages over older methods. First of all, the moment is determined for a certain vibrational and rotational state and is not the average over all states as found by the previous methods. The variation of charge distribution and molecular shape with vibrational and centrifugal distortion may therefore be studied. The chemical purity of the sample is no longer an important requirement. Actually, since the sample is examined as a dilute gas and the rotational transition of different substances are quite easily resolved, "impurities" may be more abundant than the sample and the molecule of interest may be decomposing at a fairly rapid rate without seriously inconveniencing the microwave measurements. Microwave measurements are made at a gas pressure of approximately 0.01 mm of Hg and many substances may be studied in the vapor state which by other methods would have to be examined in solution, with the consequent complication of solvent effects. The microwave method has especial advantages for molecules having small dipole moments, since in these cases the fractional accuracy remains the same, i.e., one percent or less. As is well known, when the dipole moment is measured from the temperature dependence of the dielectric constant, large uncertainties arise when small dipole moments are measured. In this investigation the dipole moments of eight different molecules were determined by the Stark splitting of their rotational transitions observed in the microwave region. This splitting is a function of the applied field and the permanent electric moment of the molecule. The molecules considered can be divided in two groups, those without and those with hyperfine structure caused by nuclear quadrupole interaction. The former and simpler cases were the molecules CH_3CF_3, PF_3 and in the approximation used also $N^{15}N^{14}O^{16}$ and $Cl^{36}C^{12}N^{14}$. The molecules with appreciable quadrupole coupling were CH_3Cl, CH_3Br, CH_3I and AsF_3.

EXPERIMENTAL METHOD

The detailed experimental method was described in Part II of this series.[1] In that paper the dipole moment of the linear molecule OCS was determined by measuring the splitting as a function of applied voltage in three different wave guides whose internal dimensions had been measured. The average value of the OCS dipole was used to calibrate the spacings and corrections in all three guides. From this calibration the corrected values of dipole moments quoted below are derived. Thus the dipole moments reported here are all measured relative to the OCS dipole moment (assumed to be 0.7085±0.004) rather than being dependent on any particular measurements of wave guide dimensions. This procedure should allow good comparison with results of other workers if they are standardized in a similar way.

MOLECULES WITH QUADRUPOLE COUPLING

The CH_3Cl^{35} and CH_3Br^{79} transitions observed were $J=0\rightarrow1$ and $K=0\rightarrow0$. These lines exhibit only second-order Stark effects and since the nuclear spins of Cl^{35} and Br^{79} are 3/2, the theoretical treatments are similar. The CH_3I and AsF_3 transitions observed were $J=1+2$ and $K=1\rightarrow1$. These lines show first-order Stark effects and are treated similarly.

Since line widths limited the accuracy of frequency measurement, large splittings were measured in order to obtain good fractional accuracy. In order to evaluate the dipole moment the measured frequency splittings were compared with those calculated from known molecular parameters and various values of the parameter μE, the product of molecular dipole moment and electric field strength E. For these calculations the methods of Low and Townes[2] (I of this series) and of Fano[3] were used. For all four molecules of this group the electric fields were in the intermediate region where

* Work supported jointly by the Signal Corps and ONR.
** Present address: Chemistry Dept., Calif. Inst. of Tech., Pasadena, California.

[1] R. G. Shulman and C. H. Townes, Phys. Rev. 77, 500 (1950).
[2] W. Low and C. H. Townes, Phys. Rev. 76, 1295 (1949).
[3] U. Fano, J. Research Nat. Bur. of Stand. 40, 215 (1948).

TABLE I. Dipole moment of AsF_3. $\Delta\nu$ is the Stark displacement of the $J=1\rightarrow2$, $F=5/2\rightarrow7/2$, $K=1$, $M=5/2$ transition.

$\Delta\nu$(mc)	E(e.s.u./cm)	μ(Debye)
15.7	0.1394	2.737
18.1	0.1658	2.669
21.3	0.1897	2.707
51.2	0.4043	2.865
60.5	0.4730	2.863
93.5	0.7317	2.787
110.0	0.8644	2.774
59.3	0.4532	2.934
67.5	0.5127	2.927
80.6	0.6145	2.886
98.2	0.7562	2.828
Average 2.815±0.025 debye		

the molecular couplings to the field and to the nuclear quadrupole moment are comparable in magnitude.

Arsenic Trifluoride

The intermediate field solution[2] of the AsF_3 $J=1\rightarrow2$, $K=1\rightarrow1$, $F=5/2\rightarrow7/2$, $M=5/2\rightarrow5/2$ is

$$\Delta\nu=-14.70+\mu E/4+[(6.29+\mu E/4)^2+2.800\mu E+(\mu E)^2/18+176.0]^{\frac{1}{2}}, \quad (1)$$

where μE is the product of dipole moment and electric field in megacycles/sec. and $\Delta\nu$ is the displacement in megacycles/sec. from the unperturbed frequency of this transition at 23,532.1 mc.[4] A theoretical plot of $\Delta\nu$ *vs.* μE yields values of μE for the observed $\Delta\nu$. Since E had been measured, μ was found to be 2.815±0.025 Debye units (see Table I).

Methyl Iodide

The methyl iodide moment was determined from the splitting of the $J=1\rightarrow2$, $K=1\rightarrow1$, $F=7/2\rightarrow9/2$, $M=7/2\rightarrow7/2$ transition at 30,123.64 mc.[5] The calculations are identical with those for AsF_3 except that the coefficients and molecular parameters have different numerical values. They are, in the notation of Low and Townes[2]

$$\begin{gathered} a_1=(5)^{\frac{1}{2}}/3, \quad a_2=2/3, \\ \langle\psi_1|H_E|\psi_1\rangle=-(7/27)\mu E, \\ \langle\psi_2|H_E|\psi_2\rangle=(-13/54)\mu E, \\ \langle\psi_1|H_E|\psi_2\rangle=-[(5)^{\frac{1}{2}}/27]\mu E, \\ eqQ=-1934 \text{ mc}. \end{gathered} \quad (2)$$

Substituting these values

$$\Delta\nu=-93.51+0.2500\mu E+[8743.43-1.729\mu E+69.45\times10^{-4}(\mu E)^2]^{\frac{1}{2}}, \quad (3)$$

where $\Delta\nu$ is the displacement from 30, 123.64 mc. The value of μ is 1.647±0.014 Debye units (see Table II).

[4] Dailey, Rusinow, Shulman, and Townes, Phys. Rev. **74** 2451, (1948).

[5] Gordy, Simmons, and Smith, Phys. Rev. **74**, 243 (1948).

TABLE II. Dipole moment of CH_3I. $\Delta\nu$ is the Stark displacement of the $J=1\rightarrow2$, $F=7/2\rightarrow9/2$, $K=1$, $M=7/2$ transition.

$\Delta\nu$(mc)	E(e.s.u./cm)	μ(Debye)
28.82	0.4651	1.677
30.02	0.4841	1.676
35.18	0.5644	1.676
63.10	1.0565	1.581
65.70	1.0849	1.601
77.67	1.2458	1.638
84.03	1.3084	1.682
Average 1.647±0.014 debye		

Methyl Chloride

Since some deviations from theory had been indicated by earlier measurements[6] of Stark effects in this molecule, all Stark components of each of the three lines of the $J=0\rightarrow1$ transition were measured and compared with theoretical expectations over a wide range of field strengths (see Fig. 1). The general procedure in calculating Stark effects in this molecule is similar to that for the first-order case. Choosing particular values for F and M, wave functions are constructed and the energy matrix diagonalized. The allowed values of F and hence the order of the secular equation depend upon the value of M. When $|M|=J+I-1$, F can only have the two values, $J+I$ and $J+I-1$. In CH_3Cl[3] when $J=1$, $I=3/2$ and $|M|=3/2$, F can be 3/2 or 5/2. However when $|M|=1/2$, F can be 1/2, 3/2 or 5/2 and the secular equation is of the third order. The splittings for the two possible $|M|=3/2$ components are

$$\Delta\nu=\pm9.39+0.3286(\mu E)^2\mp1.878[25-0.1369(\mu E)^2+46.87\times10^{-4}(\mu E)^4]^{\frac{1}{2}} \text{ mc}, \quad (4)$$

where the upper sign refers to the splitting of the $|M|=3/2$ component of the $F=3/2\rightarrow3/2$, $J=0\rightarrow1$ transition from 25,570.77 mc[5] and the lower sign to the difference between the $|M|=3/2$ component of the $F=3/2\rightarrow5/2$, $J=0\rightarrow1$ transition and 26,589.49 mc. The expressions can be checked against the weak field case.[2,3] For μE sufficiently small, they reduce to

$$\Delta\nu_{F=3/2\rightarrow5/2}=0.3029(\mu E)^2$$

and

$$\Delta\nu_{F=3/2\rightarrow3/2}=0.3543(\mu E)^2 \quad (5)$$

which are identical with the weak field expressions. The third-order equation for $|M|=1/2$ was solved* and Fig.

[6] R. Karplus and A. H. Sharbaugh, Phys. Rev. **75**, 889, 1449 (1949).

* Fano, reference 3, solves in detail the case where $J=1$. He expresses the energy as

$$\Delta W=eqQy/4(2J-1)(2J+3)I(2I-1),$$

where y is the solution of a secular equation. However, his expressions (14b) and (15) for y contained typographical errors. The corrected expressions, which Dr. Fano has very kindly

1 is a plot of experimental results *vs.* the theoretical splitting assuming $\mu=1.869$ Debye units. This compares well with Karplus and Sharbaugh's value[6] of 1.86 ± 0.01, also found by microwave methods. In addition there seem to be no significant differences between the theoretical curves and experimental points.

Methyl Bromide

It is difficult to predict in advance which components will be most widely split for a particular value of the field. However by using the observed intensity ratios and the theoretical values of intensities in the limiting cases the components are readily identified. [For weak field and $\Delta F=+1$, the intensities are proportional to (F^2-M^2) and for strong fields when $\Delta J=+1$ intensities are proportional to $(J^2-M_J^2)$]. The CH_3Br^{79} transition measured was $J=0\rightarrow1$, $F=3/2\rightarrow5/2$ and $|M|=1/2$ at 19,107 mc. Table III shows that $\mu=1.797\pm0.015$ Debye units.

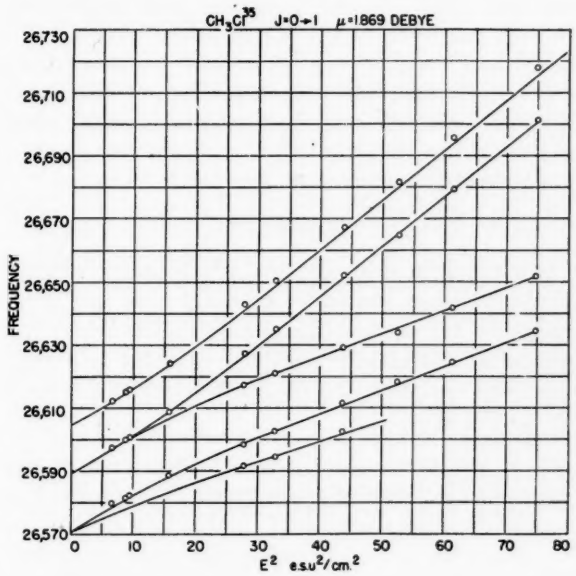

FIG. 1. Frequency of all components of CH_3Cl^{35} $J=0\rightarrow1$ transition as a function of electric field strength. Curves are computed using $\mu=1.869$ Debye.

checked, are

$$y=-\tfrac{1}{2}([I+3][2I-1]+x \pm3\{[(I-1)(2I-1)+x]^2+4I[2I-1]^2\}^{\frac{1}{2}}) \text{ for } |M|=I.$$

For $|M|<I$,

$$y=K_1+2K_2^{\frac{1}{2}}\cos[\alpha+2\rho\pi/3],$$

where $\rho=0, 1, 2$

$$\cos\alpha=(-K_3/K_2^{\frac{3}{2}})$$

and

$$K_1=2,$$
$$K_2=4I^2(I+1)^2+I(I+1)+1+2[3M^2-I(I+1)+1]x+x^2,$$
$$K_3=8I^2(I+1)^2-24I^2(I+1)^2+\tfrac{3}{2}I(I+1)+1 +3\{3M^2[2I(I+1)-7/2]-\tfrac{1}{2}I(I+1)[4I(I+1)+1]+1\}x +3[3M^2-I(I+1)+1]x^2+x^3.$$

TABLE III. Dipole moment of CH_3Br. $\Delta\nu$ is the Stark displacement of the $J=0\rightarrow1$, $F=3/2\rightarrow5/2$, $|M|=1/2$ transition.

$\Delta\nu$(mc)	E(e.s.u./cm)	μ(debye)
31.21	19.073	1.803
39.29	24.004	1.794
43.52	26.420	1.797
58.80	35.761	1.795
71.61	43.270	1.796

Average 1.797 ± 0.015 debye

TABLE IV. Dipole moment of CH_3CF_3. $\Delta\nu$ is the Stark displacement of the $J=1\rightarrow2$, $K=0$, $|M|=1$ transition.

$\Delta\nu$(mc)	E^2(e.s.u./cm)^2	μ(debye)
8.13	5.430	2.341
11.31	7.813	2.302
16.13	11.001	2.317
17.37	11.651	2.336
32.66	21.862	2.338
41.21	28.230	2.311
41.28	28.174	2.316
55.03	37.270	2.324
57.68	39.475	2.312
70.88	48.322	2.317

Average 2.321 ± 0.034 debye

MOLECULES WITHOUT QUADRUPOLE COUPLING

Methyl Fluoroform

The $J=1\rightarrow2$ transition of the symmetric top molecule CH_3CF_3 has been reported [7,8] at 20,741 mc. Since every nucleus in this molecule has zero quadrupole moment, the spectrum shows no hyperfine structure. Although both first- and second-order Stark effects are observed, only the second-order effects were measured, giving the displacement $\Delta\nu$ of the component $K=0$, $|M|=1$ from its undisturbed position. From this the dipole moment can be simply calculated as 2.321 ± 0.034 Debye units (see Table IV).

Phosphorous Trifluoride

Measurements on the displacement of the $J=1\rightarrow2$, $K=0$, $|M|=1$ transition of PF_3 from 31,279.60 mc[9] determine its dipole moment as 1.025 ± 0.005 Debye (see Table V).

Nitrous Oxide

Three quadrupole components of the $J=0\rightarrow1$ transition of the linear molecule $N^{15}N^{14}O^{16}$ have been reported.[10] They are

$F=1\rightarrow1$ 24,274.53 mc
$F=1\rightarrow2$ 24,274.61 mc
$F=1\rightarrow0$ 24,274.73 mc.

Since the lines were not resolved on our apparatus, this

[7] W. F. Edgell and A. Roberts, J. Chem. Phys. **16**, 1002 (1948).
[8] Dailey, Minden, and Shulman, Phys. Rev. **75**, 1319(A) (1949).
[9] Gilliam, Edwards, and Gordy, Phys. Rev. **75**, 1014 (1949).
[10] Coles, Elyash, and Gorman, Phys. Rev. **72**, 973 (1947).

TABLE V. Dipole moment of PF_3. $\Delta\nu$ is the Stark displacement of the $K=0$, $|M|=1$ component of the $J=1\rightarrow2$ transition.

$\Delta\nu$(mc)	E^2(e.s.u./cm)^2	μ(debye)
22.15	115.97	1.028
29.95	157.95	1.024
36.95	195.85	1.022
Average 1.025±0.009 Debye		

TABLE VI. Dipole moment of $N^{15}N^{14}O^{16}$. $\Delta\nu$ is the Stark displacement of the $J=0\rightarrow1$ transition.

$\Delta\nu$(mc)	E^2(e.s.u./cm)^2	μ(debye)
0.86	55.175	0.176
0.97	66.048	0.171
1.62	119.75	0.164
1.66	101.53	0.180
2.33	161.32	0.170
2.38	154.70	0.162
2.55	199.85	0.159
3.03	225.21	0.164
3.71	287.40	0.161
4.28	315.63	0.164
4.58	350.10	0.161
5.89	440.92	0.163
7.51	565.30	0.163
Average 0.166±0.002 debye		

was an example of the strong field case and the Stark splitting was considered independent of the quadrupole coupling. Table VI shows that the dipole moment is 0.166±0.002 Debye units. This molecule affords a good example of a small dipole moment which was not accurately determinable by other methods. Previous methods had given values ranging from 0 to 0.25 Debye.

Cyanogen Cloride

The Cl^{36} nucleus has been shown[11] to have a rather small quadrupole coupling constant of −19 mc in the molecule ClCN. Since hyperfine structure in the $J=1\rightarrow2$ transition of ClCN due to Cl^{36} and N^{14} is no wider than 5 mc, it may be ignored if wide lines and large Stark splittings are measured. Treating the $Cl^{36}C^{12}N^{14}$ molecule as a linear molecule in the strong field approximation, the dipole moment was found to be 2.802±0.014 debye units (see Table VII).

[11] C. H. Townes and L. G. Aamodt, Phys. Rev. **76**, 691 (1949).

TABLE VII. Dipole moment of ClCN. $\Delta\nu$ is the separation between the $M=0$ and $|M|=1$ components of the $J=1\rightarrow2$ transitions.

$\Delta\nu$(mc)	E^2(e.s.u./cm)^2	μ(debye)
39.03	9.318	2.804
72.6	17.486	2.792
81.8	19.467	2.809
Average 2.802±0.020 Debye		

TABLE VIII. Comparison of present result and previous measurements of dipole moments.

Molecule	Present result, debye units	Previous values
AsF_3	2.815±0.025	2.65[12]
CH_3I	1.647±0.014	1.62[12]
CH_3Cl^{35}	1.869±0.010	1.86[12,5]
CH_3Br^{79}	1.797±0.015	1.79[12]
CH_3CF_3	2.321±0.034	
PF_3	1.025±0.009	
N_2O	0.166±0.002	0.0[12]
ClCN	2.802±0.020	2.66[13]

SUMMARY

Measurement of dipole moments by Stark effects in a wide variety of molecules appear to give satisfactory results. In the cases of the methyl halides which have been rather accurately measured by other techniques, agreement with previous results is very good, as shown by Table VIII.

[12] T. G. Wesson, "Tables of electric dipole moments," Technical Report No. 11, Laboratory for Insulation Research, M.I.T.
[13] Townes, Holden, and Merritt, Phys. Rev. **74**, 1113 (1948).

PHYSICAL REVIEW VOLUME 78, NUMBER 2 APRIL 15, 1950

On the Role of the Subsidiary Condition in Quantum Electrodynamics

F. COESTER AND J. M. JAUCH
Department of Physics, State University of Iowa, Iowa City, Iowa
(Received January 9, 1950)

The S-matrix in quantum electrodynamics may be calculated alternatively from the Hamiltonian density $-j^\mu(x)A_\mu(x)$ and a Hamiltonian in which the Coulomb interaction of the charges and the interaction of the currents with the transverse field are separated. Both procedures are equivalent. Care must be taken, however, to define correctly the initial states, in particular the vacuum state. The definition of the vacuum state in both representations is discussed and the equivalence of the corresponding S-matrices is proven.

I. INTRODUCTION

THE elimination of divergencies in quantum electrodynamics by the so-called renormalization procedures makes it especially desirable to formulate the theory in a completely relativistically covariant way.[1,2] Since the treatment which has usually been adopted in the past is unsymmetrical in the space and time coordinates, the correct identification of the renormalization terms is exceedingly difficult for the higher approximations.[3] On the other hand in a relativistic theory the infinities which merely affect the normalization of mass and charge of the electron can be easily identified by their invariance property. For this reason it is highly desirable to have a consistent formalism which is covariant through all stages of the calculation. In order to achieve this end the so-called supermultiple time formalism was introduced.[4] This is a straightforward generalization of the similar formalism of Dirac, Fock, and Podolsky.[5] In this theory the part played by the hypersurfaces of simultaneity in conventional quantum electrodynamics is taken over by a one-parametric set of arbitrary space-like hypersurfaces. The theory acquires thereby a covariant outlook but this in itself does not assure us that the theory satisfies the requirements of the relativity principle, i.e., that the S-matrix is independent of the particular set of hypersurfaces chosen. The independence of the S-matrix of the orientation of the hypersurfaces was proven by Dyson[6] under the assumption that the Hamiltonian density in the interaction representation is invariant and independent of the orientation of the hypersurfaces. If the time-like and the longitudinal part of the vector potential are eliminated in the conventional way with the help of the subsidiary condition the interaction Hamiltonian is no longer independent of the orientation of the hypersurfaces. If alternatively the time-like and the longitudinal part of the vector potential are not eliminated, the definition of the vacuum state requires special attention. A difficulty in this respect does not arise when we are dealing with a vector field with a finite although arbitrarily small mass. The vector field with zero rest mass such as the photon field cannot be regarded in a straightforward manner as the limiting case of a field with finite mass, since the commutation rules of the latter become singular as the rest mass tends to zero.

II. THE SUBSIDIARY CONDITION

We choose for the fundamental units h, c, and cm. In the interaction representation the photon field variables are a set of four space and time dependent Hermitian operators $A_\mu(x)$ transforming like a four vector and satisfying the differential equation

$$\Box A_\mu(x)=0. \tag{1}$$

They satisfy further the commutation rules[7]

$$[A_\mu(x), A_\nu(x')]=-ig_{\mu\nu}D(x-x'). \tag{2}$$

The state functional $\Psi(\tau)$ is considered a function of an invariant parameter τ which takes the role of the time. With each value of τ there is associated a space-like hyperplane $\sigma(\tau)$ given by an equation of the form

$$n^\mu x_\mu+\tau=0, \tag{3}$$

where n^μ is a constant time-like four vector of magnitude one.

$$n^\mu n_\mu=-1. \tag{4}$$

The Schrödinger equation for the state vector $\Psi(\tau)$ may be written in the form

$$i(\partial\Psi/\partial\tau)=H(\tau)\Psi, \tag{5}$$

with

$$H(\tau)=-\int_{\sigma(\tau)} d\sigma j^\mu(x)A_\mu(x), \tag{6}$$

where $j(x)$ represents the current density and $d\sigma$ is the

[1] Koba, Tati, and Tomonaga, Prog. Theor. Phys. **1**, 40 (1946); **2**, 101 (1947); **2**, 198 (1947).
[2] J. Schwinger, Phys. Rev. **74**, 1439 (1948); **75**, 651 (1949); **76**, 790 (1949), quoted as S I, S II, S III, respectively.
[3] The first calculations of the self-energy of a bound electron were made with this conventional formulation of quantum electrodynamics by H. A. Bethe, Phys. Rev. **72**, 339 (1947); N. M. Kroll and W. E. Lamb, Phys. Rev. **75**, 388 (1949); J. B. French and V. F. Weisskopf, Phys. Rev. **75**, 1240 (1949).
[4] S. Tomonaga, Prog. Theor. Phys. **1**, 27 (1946).
[5] Dirac, Fock, and Podolsky, Physik Zeits. Sowjetunion **2**, 468 (1932).
[6] F. J. Dyson, Phys. Rev. **75**, 492 (1949).
[7] For the definition of the D-function see, for instance, W. Pauli, Rev. Mod. Phys. **13**, 211 (1941), Eq. (22). Also S II Appendix. The sign of the D-function as defined by Schwinger is opposite to that used by Pauli which we follow here.

invariant volume element of the hyperplane characterized by n^μ and τ.[8]

In order that the field strengths formed with the expectation values of the potentials

$$\langle A_\mu(x)\rangle=(\Psi(\tau), A_\mu(x)\Psi(\tau)), x\epsilon\sigma(\tau), \tag{7}$$

satisfy Maxwell's equation, we must restrict $\Psi(\tau)$ by the subsidiary condition

$$\partial^\mu A_\mu(x)\Psi(\tau)=0 \quad \text{for all} \quad x\epsilon\sigma(\tau) \tag{8}$$

which must hold identically in τ. The symbol ∂^μ stands for $\partial/(\partial x_\mu)$. It can be shown that the subsidiary condition (8) is equivalent to two initial conditions

$$\partial^\mu A_\mu(x)\Psi(\tau_0)=0, \quad \text{for all} \quad x\epsilon\sigma(\tau) \tag{9a}$$

$$d\partial^\mu A_\mu(x)\Psi(\tau_0)=0, \tag{9b}$$

holding for one particular $\tau=\tau_0$. The symbol d denotes the total derivative in the direction n defined by the relations

$$d=n^\nu d_\nu, \quad d_\nu F=\partial_\nu F-i[H, F]n_\nu \tag{10}$$

for any quantity F. The symbol d_ν is defined in accordance with the relation

$$\langle d_\nu F\rangle=\partial\langle F\rangle/\partial x^\nu, \tag{11}$$

where the expectation values may be taken for any state vector $\Psi(\tau)$ which is a solution of (5). Since by (2) and (6)

$$[H(\tau), \partial^\mu A_\mu(x)]=in^\mu j_\mu(x) \quad \text{for} \quad x\epsilon\sigma(\tau), \tag{12}$$

(9b) may be written as

$$\{\partial\partial^\nu A_\nu(x)-n^\nu j_\nu(x)\}\Psi(\tau_0)=0, \quad x\epsilon\sigma(\tau_0), \tag{9b'}$$

where $\partial=n^\nu\partial_\nu$. In order to prove the equivalence of (8) and (9) we show first that (8) implies (9). Differentiating (8) with respect to x^ν we find

$$\begin{aligned}\frac{\partial(\partial^\mu A_\mu\Psi(\tau))}{\partial x^\nu}&=\partial_\nu\partial^\mu A_\mu\Psi(\tau)-\eta_\nu\partial^\mu A_\mu(x)(-iH(\tau))\Psi(\tau)\\&=\partial_\nu\partial^\mu A_\mu\Psi(\tau)-in_\nu[H, \partial^\mu A_\mu]\Psi(\tau)\\&=d_\nu\partial^\mu A_\mu(x)\Psi(\tau)=0.\end{aligned} \tag{13}$$

From the last equation one finds by contraction with n^ν

$$d\partial^\mu A_\mu\Psi(\tau)=0$$

which is (9b) for $\tau=\tau_0$. In order to show that (8) follows from (9) we use the following formula (see S I Eq. (2.22))

$$\partial^\mu A_\mu(x)=\int_{\sigma'} d\sigma'(D(x-x')\partial'\partial_\mu' A^\mu(x')-\partial_\mu' A^\mu(x')\partial' D(x-x')) \tag{14}$$

which holds for arbitrary σ'. We choose $\sigma'=\sigma(\tau_0)$ and x arbitrary, apply (14) on the state vector $\Psi(\tau_0)$ and substitute on the right-hand side (9) and (12). The result is

$$\partial^\mu A_\mu(x)\Psi(\tau_0)=\int_{\sigma'} d\sigma' n^\nu j_\nu(x')D(x-x')\Psi(\tau_0), \tag{15}$$

or

$$\Omega(x, \tau)\Psi(\tau)=0 \quad \text{for} \quad \tau=\tau_0 \tag{16}$$

with

$$\Omega(x, \tau)=\partial^\mu A_\mu-\int_{\sigma'} d\sigma' n^\nu j_\nu(x')D(x-x').$$

Equation (16) holds for arbitrary x and fixed $\tau=\tau_0$. In order to show that it holds also for arbitrary τ, we consider the left-hand side of (16) as a function of τ for fixed x and show that its derivatives of all orders are zero. Since

$$\frac{d}{d\tau}(\Omega(x, \tau)\Psi(\tau))=\frac{d\Omega(x, \tau)}{d\tau}\Psi(\tau)-i\Omega(x, \tau)H(\tau)\Psi(\tau),$$

or working out the right-hand side

$$\frac{d}{d\tau}(\Omega(x, \tau)\Psi(\tau))=-iH(\tau)\Omega(x, \tau)\Psi(\tau),$$

we obtain by induction for all higher order derivatives

$$\left(\frac{d^n}{d\tau^n}\Omega(x, \tau)\Psi(\tau)\right)_{\tau=\tau_0}=0, \quad (n=0, 1, 2\cdots).$$

Hence

$$\Omega(x, \tau)\Psi(\tau)=0 \quad \text{for all } x \text{ and all } \tau. \tag{17}$$

From (17) follows (8) for $x=x'$.

III. THE COULOMB INTERACTION ENERGY

We shall now study the effect of a τ-dependent canonical transformation on the Schrödinger Eq. (5). Let a new state vector $\Phi(\tau)$ be defined by

$$\Psi(\tau)=e^{i\Sigma(\tau)}\Phi(\tau), \tag{18}$$

where Σ is a hermitian operator. Substituting (18) into (5) we find for $\Phi(\tau)$ the transformed Schrödinger equation

$$i(d\Phi/d\tau)=G(\tau)\Phi \tag{19}$$

with $G(\tau)$ given by

$$G(\tau)=e^{-i\Sigma(\tau)}H(\tau)e^{i\Sigma(\tau)}-ie^{-i\Sigma}\frac{d}{d\tau}e^{i\Sigma}.$$

[8] For the relativistic covariance of the theory it is not necessary to use the supermultiple time formalizm. The reason is that a plane in the Minkowski space is a relativistically invariant concept. It is therefore sufficient to define the state functional on hyperplanes only. Moreover all the physical results calculated with the super-multiple time formalism can also be obtained in the simpler formulation adopted here.

By developing the exponentials in a power series we may write

$$e^{-i\Sigma}He^{i\Sigma}=H+\frac{i}{1!}[H,\Sigma]+\frac{i^2}{2!}[[H,\Sigma],\Sigma]+\cdots$$

and

$$-ie^{-i\Sigma}\frac{d}{d\tau}e^{i\Sigma}=\dot{\Sigma}+\frac{i}{2!}[\dot{\Sigma},\Sigma]+\cdots. \tag{22}$$

Substituting these expressions into (20) we obtain

$$G=H+\left(\frac{i}{1!}[H,\Sigma]+\dot{\Sigma}\right)+\left(\frac{i^2}{2!}[[H,\Sigma]\Sigma]+\frac{i}{2!}[\dot{\Sigma},\Sigma]\right)+\cdots. \tag{23}$$

Here we have bracketed the expressions together which are of the same order in Σ.

For Σ we choose now the expression

$$\Sigma(\tau)=\int_\sigma d\sigma j^\mu(x)n_\mu B(x)$$

with

$$B(x)=-\partial^{-1}n^\nu A_\nu(x). \tag{25}$$

Here ∂^{-1} stands for the inverse of the operator $\partial=n^\nu\partial_\nu$. In order to fix the still arbitrary integration constant in this operator we stipulate that $\partial^{-1}F(x)$ shall mean the multiplication of each Fourier component of $F(x)$ with $(ik_\nu n^\nu)^{-1}$. This procedure defines ∂^{-1} uniquely as long as thereby no poles are introduced at the origin of the k-space.

With (24) we obtain

$$[H,\Sigma]=-\int_\sigma d\sigma\int_\sigma d\sigma'[j^\nu(x)A_\nu(x),j^\mu(x')n_\mu B(x')], \tag{26}$$

$$\dot{\Sigma}=\frac{d}{d\tau}\int d\sigma j^\mu(x)n_\mu B(x)=-\int d\sigma j^\mu(x)\partial_\mu B(x) \tag{27}$$

and

$$[\dot{\Sigma},\Sigma]=-\int_\sigma d\sigma\int_\sigma d\sigma'[j^\mu(x)\partial_\mu B(x),j^\nu(x')n_\nu B(x')]. \tag{28}$$

The second equality in (27) was obtained by a combined application of Gauss' theorem and the continuity equation, $\partial_\mu j^\mu(x)=0$, for the current density.[9]

We shall now make use of the fact that the currents on a space-like surface commute. Thus we obtain with (25) using the commutation rules (2)

$$[H,\Sigma]=i\int_\sigma d\sigma\int_\sigma d\sigma' j^\nu(x)j^\mu(x')n_\nu n_\mu\partial^{-1}D(x-x') \tag{29}$$

and

$$[\dot{\Sigma},\Sigma]=i\int_\sigma d\sigma\int_\sigma d\sigma' j^\nu(x)j^\mu(x')n_\mu\partial_\nu\partial^{-2}D(x-x'). \tag{30}$$

It is seen from these expressions that all the higher commutators in (23) vanish since the currents commute and the remaining terms in (29) and (30) are c-numbers with respect to the photon variables. Collecting terms we find thus

$$G(\tau)=-\int_\sigma d\sigma j^\mu(x)\mathfrak{A}_\mu(x)-\int_\sigma d\sigma\int_\sigma d\sigma' j^\nu(x)j^\mu(x')\times(n_\mu n_\nu\partial^{-1}+\tfrac{1}{2}n_\mu\partial_\nu\partial^{-2})D(x-x') \tag{31}$$

with

$$\mathfrak{A}_\mu(x)=A_\mu(x)+\partial_\mu B(x); \tag{32}$$

or since

$$(\partial_\mu+n_\mu\partial)\partial^{-2}D(x-x')=0, \tag{33}$$

if x and x' are on the same hyperplane,

$$G(\tau)=-\int d\sigma j^\mu(x)A_\mu(x)-\tfrac{1}{2}\int_\sigma d\sigma\int_\sigma d\sigma' j^\nu(x)j^\mu(x')n_\mu n_\nu\partial^{-1}D(x-x'). \tag{34}$$

The second term on the right is the covariant expression for the Coulomb interaction.

Equation (33) is derived without use of the subsidiary condition (8) or (17). On the state vector $\Phi(\tau)$ of a Maxwell field we must impose the subsidiary condition following from (17) by (18), that is

$$e^{-i\Sigma(\tau)}\Omega(x,\tau)e^{i\Sigma(\tau)}\Phi(\tau)=0. \tag{35}$$

By (24), (25), and (2)

$$e^{-i\Sigma(\tau)}A_\mu(x)e^{i\Sigma(\tau)}=A_\mu(x)+i[A_\mu(x),\Sigma(\tau)]=A_\mu(x)+n_\mu\partial^{-1}\int_\sigma d\sigma' j^\nu(x')n_\nu D(x-x'). \tag{36}$$

The new condition is, therefore,

$$\partial^\mu A_\mu(x)\Phi(\tau)=0 \tag{37}$$

identically in x and τ. Since by (32), (25), and (1)

$$\partial^\mu A_\mu=\partial^\mu\mathfrak{A}_\mu,$$

this may also be written

$$\partial^\mu\mathfrak{A}_\mu(x)\Phi(\tau)=0. \tag{38}$$

[9] Gauss' theorem when applied for two infinitesimally close parallel hyperplanes yields for any vector F_μ

$$\frac{d}{d\tau}\int_{\sigma(\tau)}d\sigma F_\mu n^\mu=-\int_\sigma d\sigma\partial^\lambda F_\lambda.$$

The minus sign here comes from our definition of the normal vector with the invariant scalar product $n^\lambda n_\lambda=-1$.

The current dependent term in (17) is just canceled by the second term on the right-hand side of (36).

We want to add two remarks concerning the canonical transformation (18). It was pointed out that (33) was obtained without use of the subsidiary condition (8). It is therefore possible to carry out the same transformation for a vector field with rest mass leading to a Yukawa interaction term. The Coulomb interaction term has thus nothing whatsoever to do with the subsidiary condition. The previous treatments have not made this point sufficiently clear.

The second remark refers to the fact that the condition of obtaining a Coulomb potential in the transformed Hamiltonian does not determine the transformation (18) uniquely. There exists actually a one-parameter family of such transformations. In order to verify this we define Σ again (24) but replace (25) by

$$B=N^\nu A_\nu(x) \tag{39}$$

with

$$N_\mu=\frac{2-\alpha}{4}\partial_\mu\partial^{-2}-\frac{\alpha}{2}n_\mu\partial^{-1} \tag{40}$$

where α is an arbitrary real number. Thus choice for Σ leads to the transformed Hamiltonian

$$G(\tau)=-\int_\sigma d\sigma j^\mu(x)A_\mu(x)$$
$$+i\int_\sigma d\sigma\int_\sigma d\sigma' j^\nu(x)j^\mu(x')n_\mu S_\nu(x-x') \tag{41}$$

with

$$S_\nu(x-x')=-\frac{i}{2}((1-\alpha)\partial_\nu\partial^{-2}-\alpha n_\nu\partial^{-1})D(x-x'). \tag{42}$$

Or by (33)

$$S_\nu(x-x')=\frac{i}{2}n_\nu\partial^{-1}D(x-x') \tag{43}$$

if x and x' are on the same hyperplane. Inserting (43) into (41) we have again (34).

The transformed subsidiary condition in this case reads

$$e^{-i\Sigma(\tau)}\Omega e^{i\Sigma(\tau)}\Phi(\tau)=\left\{\partial^\mu A_\mu-\left(1-\frac{\alpha}{2}\right)\right.$$
$$\left.\times\int_\sigma d\sigma' j^\nu(x')n_\nu D(x-x')\right\}\Phi(\tau)=0. \tag{44}$$

The transformed potentials are

$$e^{-i\Sigma(\tau)}A_\mu(x)e^{i\Sigma(\tau)}$$
$$=A_\mu(x)-\frac{\alpha+2}{4}n_\mu\partial^{-1}\int_\sigma d\sigma' j^\nu(x')n_\nu D(x-x'), \tag{45}$$

the definition (25) is contained in (39) with (40) as the special case $\alpha=2$. It is seen that this case is distinguished by the greatest simplicity since the subsidiary condition takes the simple form (37). Moreover only for $\alpha=2$ can our canonical transformation serve to eliminate the time-like and longitudinal component of the vector potential from the Hamiltonian. For let $\mathfrak{A}_\mu(x)$ be the transverse field defined by

$$\mathfrak{A}_\mu(x)=A_\mu-\{\partial^{-1}\partial_\mu n^\nu A_\nu+\partial^{-1}(n_\mu+\partial^{-1}\partial_\mu)\partial^\nu A_\nu\} \tag{46}$$

satisfying

$$\partial^\mu\mathfrak{A}_\mu=0 \quad \text{and} \quad n^\mu\mathfrak{A}_\mu=0 \tag{47}$$

as identities. Then

$$(A_\mu(x)-\mathfrak{A}_\mu(x))\Phi(\tau)=\left\{\partial^{-1}\left(n_\mu+\frac{6-\alpha}{4}\partial^{-1}\partial_\mu\right)\partial^\nu A_\nu\right.$$
$$\left.+\frac{\alpha-2}{4}\partial^{-1}\partial_\mu n^\nu A_\nu\right\}\Phi(\tau). \tag{48}$$

The right-hand side vanishes only if Φ satisfies the subsidiary condition and $\alpha=2$. We may therefore replace $\mathfrak{A}_\mu$ by the transverse field $\mathfrak{A}_\mu$ in this case.

IV. DEFINITION OF THE VACUUM

We shall now discuss the main problem of this note, the correct definition of the vacuum. Since the electron field does not present any difficulties in this respect we shall pay no attention to the electron variables. We refer instead to S II where this part of the problem is fully discussed.

All state vectors which represent a physical situation in a quantum mechanical system should be solutions of the Schrödinger equation. This holds true in particular for the vacuum state. It is, however, a well-known fact that the Schrödinger Eq. (5) has no solution, at least not in the ordinary sense of the word. Thus to define the vacuum state as a solution of (5) is, to put it mildly, not very convenient. In this sense the definition of the vacuum presents a difficulty which contains the essential features of the difficulties common to all problems in quantum electrodynamics. The existing theory is inadequate in this respect.

Considerable progress has been made recently by showing that it is possible to remove the undesirable consequences of the incorrect theory by superimposing on the theory a number of Lorentz- and gauge invariant rules.[10] All observable consequences of the theory may be obtained from the S-matrix, that is the unitary transformation which connects an initial state at $\tau_0=-\infty$ to a final state at $\tau_f=+\infty$. From S calculated as a consequence of (5) the divergencies are eliminated by appropriate renormalization procedures, which leave S-Lorentz invariant, independent of n_μ and unitary. Actually S is obtained from (5) by perturbation

[10] S II, III, F. J. Dyson, Phys. Rev. **75**, 486 (1949); **75**, 1736 (1949); R. P. Feynmann, Phys. Rev. **76**, 769 (1949); **74**, 1430 (1948); W. Pauli and F. Villars, Rev. Mod. Phys. **21**, 434 (1949).

theory in which the initial state $\Psi(\tau_0)$ is the zero-order approximation to $\Psi^{(0)}(\tau)$ for all τ, $\Psi(\tau_0)=\Psi^{(0)}(\tau)$. Consequently it is in the spirit of this approach to define the vacuum as an initial state at $\tau=\tau_0$ ($\tau_0\to-\infty$).

The photon field presents a characteristic difficulty which arises from the fact that free photons are always the eigenstates of transverse modes of vibration only and thus a definition of the vacuum should not make any explicit reference to longitudinal or time-like photons. On the other hand a vacuum state defined in terms of the transverse photons only is not obviously independent of the normal vector n. Its actual independence of n requires a special proof.

With the help of the transverse field $\mathfrak{A}_\mu(x)$ introduced in (46) and the decomposition into positive and negative frequency parts

$$F=F^{(+)}+F^{(-)} \tag{49}$$

defined for any field operator in S II Eqs. (1.19) and (1.16) we define the vacuum state Φ_0 in the representation in which the Schrödinger equation has the form (19) by requiring

$$\partial^\mu A_\mu(x)\Phi_0=0 \tag{50}$$

and

$$\mathfrak{A}_\mu^{(+)}(x)\Phi_0=0 \tag{51}$$

identically in x.[11] Equation (50) is the subsidiary condition in the form (37); (51) states the absence of transverse photons.

We shall show first that the conditions (50), (51) are independent of the vector n although this vector enters explicitly in (51) through (46). More precisely we shall prove the following theorem: Let Φ_0 be any state vector satisfying (50) and (51) and $\bar{n}^\mu=a_\nu{}^\mu n^\nu$ a transformed time-like unit vector connected with the original vector n by a proper Lorentz transformation. Denote further by $\bar{\mathfrak{A}}_\mu$ the transverse field defined by the equation

$$\bar{\mathfrak{A}}_\mu=A_\mu-\{\bar\partial^{-1}\partial_\mu\bar n^\nu A_\nu+\bar\partial^{-1}(\bar n_\mu+\bar\partial^{-1}\partial_\mu)\partial^\nu A_\nu\}. \tag{46'}$$

We state that under these assumptions we have[12]

$$\bar{\mathfrak{A}}_\mu^{(+)}\Phi_0=0. \tag{51'}$$

Since any proper Lorentz transformation can be generated by the infinitesimal transformations, it is sufficient to prove this theorem for the infinitesimal transformations

$$\bar n^\mu=n^\mu+\omega_\nu{}^\mu n^\nu \tag{52}$$

$$\omega_{\mu\nu}+\omega_{\nu\mu}=0. \tag{53}$$

The $\omega_{\mu\nu}$ are to be considered as infinitesimals of the first order. Up to this order we obtain by development in power series

$$\bar{\mathfrak{A}}_\mu=\mathfrak{A}_\mu+\partial^{-2}\partial_\lambda\omega_\rho{}^\lambda n^\rho\partial_\mu n^\nu A_\nu-\partial^{-1}\partial_\mu A_\nu\omega_\rho{}^\nu n^\rho +(\partial^{-2}\partial_\lambda\omega_\rho{}^\lambda n^\rho n_\mu+2\partial^{-3}\partial_\lambda\omega_\rho{}^\lambda n^\rho\partial_\mu)\partial^\nu A_\nu, \tag{54}$$

or on account of (50) and (51)

$$\mathfrak{A}_\mu^{(+)}(x)\Phi_0=\omega_\rho{}^\lambda\partial_\mu(\partial^{-2}\partial_\lambda n^\rho n^\nu A_\nu^{(+)}-\partial^{-1}A_\lambda^{(+)}n^\rho)\Phi_0. \tag{55}$$

Equation (46) yields in conjunction with (50) and (51)

$$A_\mu^{(+)}\Phi_0=\partial^{-1}\partial_\mu n^\nu A_\nu^{(+)}\Phi_0 \tag{56}$$

Substitution of (56) into (55) finally gives

$$\bar{\mathfrak{A}}_\mu^{(+)}\Phi_0=0 \quad \text{q.e.d.} \tag{57}$$

Turning now to the representation of the state vectors Ψ satisfying (5) with (6) we see that a vector Ψ_0 which corresponds to Ψ_0 is given by

$$\Psi_0=e^{i\Sigma_0}\Phi_0, \tag{58}$$

where

$$\Sigma_0=-\int_{\sigma_0}d\sigma j^\mu(x)n_\mu\partial^{-1}n^\nu A_\nu \tag{59}$$

and $\sigma_0=\sigma(\tau_0)$. If Φ_0 is the vacuum state defined by (50) and (51) then Ψ_0 given by (58) satisfies

$$e^{i\Sigma_0}\partial^\mu A_\mu(x)e^{-i\Sigma_0}\Psi_0$$

$$=\left\{\partial^\mu A_\mu-\int_{\sigma_0}d\sigma' j^\nu(x')n_\nu D(x-x')\right\}\Psi_0=0, \tag{60}$$

and

$$e^{i\Sigma_0}\mathfrak{A}_\mu^{(+)}e^{-i\Sigma_0}\Psi_0=\mathfrak{A}_\mu^{(+)}\Psi_0=0 \tag{61}$$

or substituting for $\mathfrak{A}_\mu$ its definition (46) and using (60)

$$\left\{A_\mu^{(+)}-\partial^{-1}\partial_\mu n^\nu A_\nu^{(+)}+(n_\mu\partial^{-1}+\partial_\mu\partial^{-2})\right.$$

$$\left.\times\int_{\sigma_0}d\sigma' j^\nu(x')n_\nu D^{(+)}(x-x')\right\}\Psi_0=0. \tag{62}$$

At this point the fact that the initial state in the S-matrix theory is at $\tau_0=-\infty$ becomes essential. For we shall prove that the current dependent terms in (60) and (62) vanish in the limit $\tau_0\to-\infty$.

$$\Lambda_0\equiv\int_{\sigma_0}d\sigma' j^\nu(x')n_\nu D(x-x')=\int_{\sigma_0}^{\sigma}dx' j^\nu(x')\partial_\nu D(x-x')$$

$$\text{for } x\epsilon\sigma \tag{63}$$

by Gauss' theorem since $D(x-x')=0$ if $x\epsilon\sigma$ and $x'\epsilon\sigma$.

[11] Strictly speaking a complete discussion of the vacuum problem requires both a proof that such a state exists and that it is uniquely determined by (50) and (51). These questions were discussed in various earlier papers, for instance, F. J. Belinfante, Phys. Rev. **76**, 226 (1949); Physica **12**, 17 (1946); V. A. Fock and B. Podolsky, Physik Zeits. Sowjetunion **1**, 801 (1932); **2**, 275 (1932); S. T. Ma, Phys. Rev. **75**, 535 (1949). From these discussions it is obvious that Eqs. (50) and (51) imply that Φ_0 is not a vector in Hilbert space since it cannot be normalized even in a bounded system. The exact mathematical specifications to define the needed extension are not known. This state of affairs is intimately connected with the ambiguity for the self-energy of the electron discovered by Belinfante (Phys. Rev. **76**, 226 (1949)). These questions invite further study. Since they go beyond the purpose of this paper, we shall content ourselves with this remark.

[12] This theorem was also stated and proven by F. J. Belinfante, Phys. Rev. **76**, 228 (1949). As far as the essential content is concerned the proof given here is little more than Belinfante's proof written covariantly in x space.

By a simple adjustment of the origin we may choose τ without loss in generality in such a way that $\sigma=\sigma(0)$. Since Λ_0 is invariant under Lorentz transformations we may evaluate it in the coordinate system in which $n^\mu=(1,0\,0\,0)$. Substituting the Fourier series

$$D(x-x')=\frac{i}{(2\pi)^3}\int dk\epsilon(k)\delta(k^\mu k_\mu)e^{ik(x-x')}, \quad (64)$$

where

$$\epsilon(k)=\begin{cases}+1 & \text{if} \quad n^\mu k_\mu<0\\ -1 & \text{if} \quad n^\mu k_\mu>0,\end{cases} \quad (65)$$

and

$$j^\nu(x')=\frac{1}{(2\pi)^2}\int dl j^\nu(l)e^{il x'}, \quad (66)$$

we find

$$\Lambda_0=\frac{i}{(2\pi)^6}\int_{\tau_0}^{0}dx'^0\int d^3x'\int dk\int dl\epsilon(k)$$
$$\times\delta(k^\mu k_\mu)ik_\nu j^\nu(l)e^{i(l-k)x'+ikx}.$$

In this expression the three-dimensional integral over x' can be carried out giving a three-dimensional δ-function $\delta(l-k)$. We are left with

$$\lim_{\tau_0\to-\infty}\Lambda_0=-\frac{1}{(2\pi)^3}\int_{-\infty}^{0}dx'^0\int dl^0\int dk\epsilon(k)\delta(k^\mu k_\mu)$$
$$k_\nu j^\nu(k,l^0)\exp[-i(l^0-k^0)x'^0+\mathbf{ik}\cdot\mathbf{x}]. \quad (67)$$

The integration over x'^0 gives

$$\int_{-\infty}^{0}dx'^0\exp[-i(l^0-k^0)x'^0]=\pi\delta(l^0-k^0)+\frac{i}{l^0-k^0}.$$

If this is substituted into (67) the first term with $\delta(l^0-k^0)$ gives zero since its effect is simply to replace the current term by $k_\nu j^\nu(k)=0$ on account of the continuity equation. The pole in the second term can be removed if we substitute

$$k_\nu j^\nu(k,l^0)=-(l^0-k^0)j_0(k,l^0)$$

which again follows from the continuity equation. We are then left with an expression of the form

$$\lim_{\tau_0\to-\infty}\Lambda_0=\frac{i}{(2\pi)^3}\int dl^0\int dk j_0(k,l^0)\epsilon(k)\delta(k^\mu k_\mu)e^{i\mathbf{k}\cdot\mathbf{x}}. \quad (68)$$

This term vanishes also since the integration over k^0 involves the integral

$$\int dk\,\epsilon(k)\delta(k^\mu k_\mu)=\frac{1}{2\omega}(\epsilon(k,\omega)+\epsilon(k,-\omega))=0$$

$\omega=+(k^2)^{\frac{1}{2}}$. We have therefore proven

$$\lim_{\tau_0\to-\infty}\int_{\sigma(\tau_0)}d\sigma' j^\nu(x')n_\nu D(x-x')=0 \quad (69)$$

identically in x. Thus (60) and (62) reduce for $\tau_0\to-\infty$ to

$$\partial^\mu A_\mu(x)\Psi_0=0, \quad (70)$$

and

$$(A_\mu^{(+)}(x)-\partial_\mu\partial^{-1}n^\nu A_\nu^{(+)})\Psi_0=0. \quad (71)$$

The correct definition of the initial vacuum state at $\tau_0=-\infty$ is therefore given by (70) and (71) (or (70) and (61)). We see that for a hypersurface at infinity the definition of the vacuum is identical for the state vectors Ψ and Φ.[13] It should be emphasized that this simple result, which is essential for the discussions of the following section, does not hold for a finite initial time. Any initial state in which photons are present will satisfy (70) but not (71).

IV. EVALUATION OF THE S-MATRIX

According to Dyson[14] the nth order term in the S-matrix calculated from (5) may be written in the form

$$S^{(n)}=\frac{(i)^n}{n!}\int dx_n\int dx_{n-1}\cdots\int dx_1 P(j^{\mu_n}(x_n)\cdots j^{\mu_1}(x_1))$$
$$\times P(A_{\mu_n}(x_n)\cdots A_{\mu_1}(x_1)) \quad (72)$$

where P stands for the permutation operator which orders the factors for every set of n points $x_1\cdots x_n$ in such a way that the factors occur from right to left in the same order in which $x_1\cdots x_n$ occur in time. $S^{(n)}$ shall be decomposed into a number of terms, each of which contains a definite number of virtual photon exchanges, by shifting in (72) the $A_\mu^{(-)}$ to the left of the $A_\mu^{(+)}$. We denote by $(A_{\mu_n}(x_n)\cdots A_{\mu_1}(x_1))_{\text{ord}}$ the arrangement where all negative frequency parts stand to the left of all positive frequency parts.[15] Since this definition determines the "ordered product" uniquely we have

$$\{P(A_{\mu_n}(x_n)\cdots A_{\mu_1}(x_1)\}_{\text{ord}}=(A_{\mu_n}(x_n)\cdots A_{\mu_1}(x_1))_{\text{ord}}. \quad (73)$$

From the commutation rules (2) follows

$$[A_\mu^{(+)}(x),A_\nu^{(-)}(x')]\theta(x-x')$$
$$+[A_\nu^{(+)}(x'),A_\mu^{(-)}(x)]\theta(x'-x)=\tfrac{1}{2}g_{\mu\nu}D_F(x-x'), \quad (74)$$

[13] Equation (69) is the reason why it is justifiable to speak in some cases as if the currents were zero at infinity. This remark has often occurred in the literature in connection with radiation problems. It is in general hardly justified, however. The current density as an operator is never zero anywhere. This would contradict the commutation rules and the continuity equation. The vanishing of surface integrals at infinity requires a special proof of the sort given here for (69).

In a recent paper (Phys. Rev. 76, 391 (1949)) N. Hu has made an attempt to prove the equivalence of the two methods of treating radiation problems. We feel that in this paper both the surface integrals at infinity and the definition of the vacuum are inadequately treated.

[14] F. J. Dyson, Phys. Rev. 75, 492, 1737 (1949).

[15] This notation has been introduced by A. Houriet and A. Kind, Helv. Phys. Acta 22, 321 (1949). For instance

$$(A_\mu(x)A_\nu(x')_{\text{ord}}=A_\nu^{(-)}(x')A_\mu^{(+)}(x)+A_\mu^{(-)}A_\nu^{(+)}(x')$$
$$+A_\mu^{(-)}(x)A_\nu^{(-)}(x')+A_\mu^{(+)}(x)A_\nu^{(+)}(x').$$

where

$$\theta(x)=\begin{cases}1 & \text{for } n^\mu x_\mu<0\\ 0 & \text{for } n^\mu x_\mu>0,\end{cases} \tag{75}$$

and[16]

$$D_F(x)=D^{(1)}(x)-i\epsilon(x)D(x). \tag{76}$$

With the help of these definitions and relations $P(A_{\mu_n}(x_n)\cdots A_{\mu_1}(x_1))$ can be replaced under the integral (72) by

$$\begin{aligned}&[(n-1)/2]g_{\mu_1\mu_2}D_F(x_1-x_2)P(A_{\mu_n}(x_n)\cdots A_{\mu_3}(x_3))\\&\quad+A_{\mu_n}{}^{(-)}(x_n)P(A_{\mu_{n-1}}(x_{n-1})\cdots A_{\mu_1}(x_1))\\&\quad+P(A_{\mu_{n-1}}(x_{n-1})\cdots A_{\mu_1}(x_1))A_{\mu_n}{}^{(+)}(x_n)).\end{aligned} \tag{77}$$

Here we use the fact that the integration variables may be conveniently relabeled in each term. From (77) it follows that we can replace $P(A_{\mu_n}(x_n)\cdots A_{\mu_1}(x_1))$ by

$$\begin{aligned}&\sum_{k=0}^{m}f(n,k)D_F(x_1-x_2)\cdots D_F(x_{2k-1}-x_{2k})\\&\qquad\times(A_{\mu_{2k+1}}(x_{2k+1})\cdots A_{\mu_n}(x_n))_{\text{ord}},\end{aligned} \tag{78}$$

where $m=n/2$ for even n and $m=(n-1)/2$ for odd n. The coefficients $f(n,k)$ are determined by the recursion formula

$$f(n,k)=f(n-1,k)+[(n-1)/2]f(n-2,k-1), \tag{79}$$

in which $f(n,k)=0$ by definition for $k>m$ or $k<0$. Indeed, assuming that the substitution (78) is valid for $n-1$, its validity for n follows from (77) and (79). Equation (78) can be easily verified directly for $n=2$ and one finds that $f(2,0)=1$, $f(2,1)=\frac{1}{2}$.

$$f(n,k)=\frac{n!}{2^{2k}k!(n-2k)!}. \tag{80}$$

We claim that in (78) $A_\mu(x)$ can be replaced by the transverse field $\mathfrak{A}_\mu(x)$ if $S^{(n)}$ operates on an initial state $\Psi^{(0)}$ satisfying (70). According to (46) and (68)

$$A_\mu{}^{(\pm)}(x)\Psi^{(0)}=(\mathfrak{A}_\mu{}^{(\pm)}+\partial_\mu\partial^{-1}n^\nu A_\nu{}^{(\pm)})\Psi^{(0)}. \tag{81}$$

The second term gives no contribution in the S-matrix since we shall show that

$$\begin{aligned}&\int dx_\nu P(j^{\mu_n}(x_n)\cdots j^{\mu_r}(x_r)\cdots j^{\mu_1}(x_1))\\&\qquad\times\partial_{\mu_r}\partial^{-1}n^\nu A_\nu{}^{(\pm)}(x_r)=0.\end{aligned} \tag{82}$$

For (82) is of the general form

$$\int dx J^\mu(x)\partial_\mu F(x).$$

With the help of the Fourier transformation

$$J^\mu(x)=\frac{1}{(2\pi)^2}\int dk J^\mu(k)e^{ikx},$$

$$F(x)=\frac{1}{(2\pi)^2}\int dl F(l)e^{ilx},$$

we get

$$\int dx J^\mu(x)\partial_\mu F(x)=-\int dk k_\mu J^\mu(k)F(-k).$$

This vanishes if $\partial_\mu J^\mu(x)=0$ and therefore $k_\mu J^\mu(k)=0$. In order to prove (82) it is therefore only necessary to show that

$$\partial_{\mu_r}P(j^{\mu_n}\cdots j^{\mu_1})=0. \tag{83}$$

This is obviously a consequence of the continuity equation as long as $\tau_r=\tau(x_r)$ is different from any other τ_s. If τ_r approaches τ_s, we may write in the neighborhood of τ_s

$$\begin{aligned}P(j^{\mu_s}(x_r)j^{\mu_s}(x_s))&=j^{\mu_s}(x_r)j^{\mu_s}(x_s)\\&\quad-\tfrac{1}{2}\theta(x_s-x_r)[j^{\mu_r}(x_r),j^{\mu_s}(x_s)].\end{aligned}$$

Therefore

$$\partial_{\mu_r}P(j^{\mu_r}(x_r)j^{\mu_s}(x_s))=-\tfrac{1}{2}[j^{\mu_r}(x_r),j^{\mu_s}(x_s)]\partial_{\mu_r}\theta(x_s-x_r).$$

Since θ is constant except for $\tau_r=\tau_s$ where it jumps by 1 the derivative introduces a δ-type singularity multiplying the commutator of the currents which vanishes for $\tau_r=\tau_s$. Thus (83) holds for all x and consequently (82) is established.

This argument can be applied successively to all factors $A_\mu{}^{(\pm)}$ in the "ordered products," since $\mathfrak{A}_\mu{}^{(\pm)}$ commutes with $\partial^\nu A_\nu{}^{(\pm)}$ and $n^\nu A_\nu{}^{(\pm)}$. Thus after the transformation (77) A_μ can be replaced in $S^{(n)}$ by the transverse field $\mathfrak{A}_\mu$. The S-matrix commutes therefore with $\partial^\mu A_\mu$ and the final state at $\tau=+\infty$ satisfies (70) as well as the initial state.

If, in particular, there are no photons present either in the initial or in the final state, then only the $S^{(n)}$ with even n are different from zero and in these only the term with $k=n/2$ on the right-hand side of (77) contributes anything to $S^{(n)}$. Schwinger and Dyson achieved this result by assuming the vacuum definition

$$A_\mu{}^{(+)}\Psi_0=0. \tag{84}$$

Such a definition of the vacuum is not acceptable, however, as was pointed out by Belinfante.[17] We mention here only the fact that the sign of the commutation rules for the 0-components $A_0(x)$ implies that $A_0{}^{(+)}$ is an emission operator. Consequently $A_0{}^{(+)}\Psi_0=0$ implies that $\Psi_0=0$.

Alternatively the S-matrix might also be calculated from (19) with (34). Since (19) and (5) are equivalent

[16] For a definition of $D^{(1)}(x)$ see, for instance, W. Pauli, Rev. Mod. Phys. 13, 212 (1941), Eq. (22').

[17] F. J. Belinfante, Phys. Rev. 76, 228 (1949).

Schrödinger equations and $\Phi^{(0)}=\Psi^{(0)}$, the result must be the same. The effects of virtual photon exchange and Coulomb interaction are combined in the expression $\frac{1}{2}g_{\mu\nu}D_F(x-x')$. If S is calculated from (19), they appear separately.

We have thus proven that the two S-matrices calculated from (5) and (19) are identical. This result rests essentially on the equivalence of the two Hamiltonians (6) and (34) and on the identity of the subsidiary conditions (70) and (50) for the initial states. It should be borne in mind that it holds therefore only for the S-matrix connecting states at $\tau=-\infty$ and $\tau=+\infty$ but not for a unitary operator connecting states at finite times.

The identity of the two S-matrices can also easily be verified by direct computation using the relation

$$\frac{1}{2}g_{\mu\nu}D_F(x-x')=\langle P(\mathfrak{A}_\mu(x)\mathfrak{A}_\nu(x'))_0 + \frac{1}{2}\{(n_\mu\partial_\nu+n_\nu\partial_\mu)\partial^{-1}+\partial^{-2}\partial_\mu\partial_\nu\}D_F(x-x'). \quad (85)$$

If the right-hand side of (85) is substituted into (72) after transformation according to (77), $S^{(n)}$ acquires the form obtained directly from (19) with (34). The second term on the right-hand side reduces to the contribution from the Coulomb interaction.

PHYSICAL REVIEW VOLUME 78, NUMBER 2 APRIL 15, 1950

On the Forces Producing the Ultrasonic Wind

FRANCIS E. FOX AND KARL F. HERZFELD
Department of Physics, Catholic University of America, Washington, D. C.

(Received December 30, 1949)

The ultrasonic wind has been erroneously ascribed to a pumping action of the quartz oscillator. Eckart has investigated it starting from the hydrodynamical equations. Without adding anything essentially new to his calculations, it is shown here that the cause of the wind is the linear momentum of the wave motion taken up by the liquid through sound absorption.

THE "ultrasonic wind"—the macroscopic flow of a gas or liquid due to the passage of ultrasonic waves—is a well-known phenomena which complicates the measurement of radiation pressures.[1] It has been ascribed[2] previously to a "pumping action" of the vibrating quartz. On the other hand Eckart[3] has recently published a detailed investigation in which the hydrodynamic equations are considered from the viewpoint of successive approximations, and he ascribes it to forces acting directly on the liquid. From this viewpoint the subject is directly related to the problem of stresses in the liquid which has been investigated frequently and includes, of course, the problem of radiation pressure.[4] It is our intention to show that it is possible to give a very simple physical picture of the forces which produce the ultrasonic wind, and confirm this by a simple calculation which has been made for other purposes by Bopp.[5] Similar but less detailed considerations have been presented by Cady.[6]

The physical picture is as follows:

In a plane electromagnetic wave of intensity I in vacuum, there exists a flow of linear momentum in the direction of wave propagation equal to

$$I/c=\bar{U}$$

per unit time and area. Here $\bar{U}$ is the time-averaged energy density of the wave.

Similarly in a plane progressive sound wave of intensity I and sound velocity V, there is transported, per second, through a centimeter square normal to the direction of propagation, the linear momentum

$$I/V=\bar{U}. \quad (1)$$

If this sound wave is propagated through a medium which (partially) adsorbs it, the linear momentum due to the adsorbed energy is taken out of the wave and transferred to the medium, i.e. if 2α is the absorption coefficient for intensity, then there is exerted on a volume element $d\tau$ the volume force

$$(2\alpha I d\tau/V). \quad (2)$$

According to this view, no force is exerted if there is no absorption; on the other hand, if the beam is totally absorbed, the total force exerted is equal to the whole energy entering the liquid per second, divided by V.

The details of the hydrodynamic flow set up are then a problem in classical hydrodynamics, namely to calculate the macroscopic flow due to the volume force given above. Since the absorption coefficient α depends

[1] See e.g. F. E. Fox and G. D. Rock, Phys. Rev. **54**, 223 (1938); J. Acous. Soc. Am. **12**, 505 (1941).
[2] See e.g. L. Bergmann, *Der Ultraschall* (Edwards Brothers, Berlin, 1942; reprint, 1944), third edition, p. 79.
[3] C. Eckart, Phys. Rev. **75**, 68 (1948).
[4] Lord Rayleigh, Phil. Mag. **3**, 338 (1902); **2**, 364 (1905). P. Langevin, Rev. d'acoustique, **1**, 93 (1932); **2**; 315 (1933). L. Brillouin, *Les Tenseurs en Mécanique et en Elasticité* (Dover Publications, New York, 1938, 1946). R. T. Beyer, Am. J. Phys. **18**, 25 (1950).
For other literature, see Bergman, reference 2, pp. 72, 73. See also a forthcoming paper of J. S. Mendousee of Catholic University.
[5] F. Bopp, Ann. d. Physik **38**, 495 (1940).
[6] W. G. Cady, Final Report, Subcontract D.I.C. 178 188, Rad. Lab. OEM-Sr-262, pp. 33, 50.

also on a "volume viscosity" while the subsequent hydrodynamic flow depends only on the usual shear viscosity, this agrees with Eckart's statement that the acoustic wind should permit a determination of volume viscosity. According to the preceding argument, this is true however only insofar as the acoustic wind provides another method of measuring the absorption coefficient α.

The mathematical proof of the preceding argument in its simplest form follows, and is an application to the forces acting on a liquid with sound absorption of that given by Bopp.[5]

Consider a plane sound wave progressing in the x direction. The equations of continuity and of motion are

$$\frac{\partial \rho}{\partial t}+\frac{\partial}{\partial x}(\rho u)=0, \tag{3}$$

$$\rho\frac{\partial u}{\partial t}+\rho u\frac{\partial u}{\partial x}=-\frac{\partial P}{\partial x}. \tag{4}$$

Here P is not the hydrostatic pressure, but the negative of the xx component of the general stress tensor, the other components being zero for reasons of symmetry. Multiply (3) with u and add to (4). One gets

$$\frac{\partial}{\partial t}(\rho u)+\frac{\partial}{\partial x}(\rho u^2)=-\frac{\partial P}{\partial x}. \tag{5}$$

Equation (5) is exact.

Taking now time averages over sufficiently long times after the establishment of a stationary state, one has

$$\frac{\partial}{\partial x}\langle \rho u^2\rangle_{Av}=-\frac{\partial \bar{P}}{\partial x}. \tag{6}$$

Equation (6) is, of course, a form of Bernoulli's principle. The term $\langle \rho u^2\rangle_{Av}$ is twice the average kinetic energy, $2\bar{T}$; in the case of a progressive wave, it is equal to I/V. Integrating (6) between two places A and B, one finds

$$2(\bar{T}_B-\bar{T}_A)=\bar{P}_A-\bar{P}_B. \tag{6'}$$

Equation (6') may be interpreted as follows: Consider a thin sheet of liquid normal to the direction of wave propagation, bounded by very thin, non-absorbing and non-reflecting plastic films. Then the force acting on unit area of the sheet is equal P_A-P_B, and this is equal to the flow of linear momentum absorbed per second.[7,8]

If the beam is completely absorbed, the total force acting on the liquid is independent of the absorption coefficient and is given by (1).

In a strictly one-dimensional system, like the one treated above, the volume forces produced by sound absorption do not result in flow, but are compensated by elastic stresses, as pointed out by Eckart. This is so in fact in all cases in which volume forces can be deduced from a scalar potential. On the other hand, in the general case of complicated three-dimensional wave patterns, a simple calculation like the above one cannot be made, since one cannot easily define the energy flow and the momentum carried by it (similar difficulties would occur in electromagnetic theory if one tries in such a case to express the Poynting vector by the energy density). Accordingly the preceding mathematical treatment is applicable to the production of flow only in cases where the wave pattern can be approximated locally by plane waves, but the over-all geometry is such (as in Eckart's example) as to produce volume forces not deducible from a scalar potential.

While Eqs. (3) to (6') are exact, this is not so for the next argument in which, after calculating the volume forces due to sound absorption, with the time average of the velocity zero, one then uses these forces as if they were conservative external forces, to calculate the flow. This neglects mixed non-linear terms containing the product of the density and of the particle velocity in the sound wave and in the flow, the time average of which does not vanish exactly. Therefore this consideration is only valid to the extent that the linearized hydrodynamical equations can be used for the flow (not for the sound).

We wish to express our thanks to Dr. C. Eckart for illuminating discussions.

---

[7] This statement is of course in agreement with Eckart's developments. Divergence or diffraction of the beam would not produce a resultant force, only absorption does so. His suggestion of deducing the "volume viscosity" from the flow amounts to a proposal of using as a new method of measuring the absorption coefficient.

[8] Mendousse has kindly pointed out to us that (6') applies to a fixed position of A and B while the above interpretation is Lagrangian, i.e., considers definite parts of the liquid. This difference can, however, be made negligible.

Average Thermionic Constants of Polycrystalline Tungsten Wires

M. H. NICHOLS* †
Palmer Physical Laboratory, Princeton University, Princeton, New Jersey
(Received January 6, 1950)

Because of its property of producing large crystals, the "doped" variety of tungsten wire is used in the study of the thermionic properties of single crystal surfaces of tungsten. In order to determine the effect of the impurities added to produce this property, the average high field thermionic constants of polycrystalline doped tungsten wire and undoped tungsten wire were measured. The thermionic constants from the doped wire are somewhat lower than those from the undoped wire which agree well with previously published values. Chemical and spectroscopic analyses before and after heat treatment are included. It is concluded that the differences in thermionic properties between the two types of wire are probably due to different distributions of the types of crystal surfaces exposed.

I. INTRODUCTION

IN order to study experimentally the thermionic properties of the different crystal surfaces of tungsten, it has been found convenient to make use of the crystal growth properties of "non-sag" or "doped" tungsten wire.[1,2] With the proper heat treatment, it is possible to grow large crystals in this type of wire which occupy the entire cross section of the wire and are several cm long.[3,4]‡ As a result of the working given the wire during the drawing process, the crystals are generally oriented with a face diagonal parallel to the wire axis. The crystal growth properties of this type of wire result from about 1 percent of "dope" consisting of Na_2O, K_2O, $CaCl_2$, Al_2O_3 and SiO_2 added before the sintering process.[3] Because of the addition of these impurities, there is some question as to whether the thermionic properties of such wire are characteristic of clean tungsten. Because of the importance of past and future experimental results using single crystals grown in doped tungsten wire, it was decided to measure the average high field thermionic constants of doped and undoped polycrystalline tungsten wire in order to permit a direct comparison. The definition and physical meaning of the average high field thermionic constants, φ^{**} and A^{**} of polycrystalline surfaces are discussed by Herring and Nichols.[5]

The doped tungsten wire used for the measurements presented in this paper was Callite Corporation # 200H (this wire is similar in properties to General Electric Company Type 218). The undoped tungsten wire was from General Electric lot exp. 8983 dated 1/13/38. This lot was supposed to be very pure.

II. EXPERIMENTALLY DETERMINED AVERAGE EMISSION CONSTANTS OF DOPED POLYCRYSTALLINE TUNGSTEN WIRE

Two specimens were measured; one was polished smooth to remove the die marks[6] and the other was unpolished. These were mounted one at a time in a tube using suitable guard rings and arranged to measure the total thermionic emission current from the wire over a 2-cm length. The tube was pumped, outgased, gettered, and sealed off by methods already described.[7] The temperatures were determined by the Forsythe and Watson[8] temperature scale using the function $A/d^{\frac{1}{2}}$ according to the Jones-Langmuir notation.[9] The wire diameters were determined before and after the experiment (in order to correct for evaporation effects during heat treatment) by weighing a measured length.[9] In the case of polished wire, the diameter was checked to the nearest fringe of mercury green light by a wedge interferometer method. All heating of the wires was accomplished by use of alternating current in order to eliminate direct current etch effects.[10,11]

The average high field thermionic constants φ^{**} and A^{**} were determined as follows. A Schottky plot was made at a temperature of 1700°K over a voltage range 600 to 3000. The points plotted a straight line to within experimental error over this range. The slope of the straight line drawn through the points agreed with the corresponding theoretical value based on the mirror image theory to better than 5 percent for the polished specimens. The experimentally determined slope was about 10 percent larger than the theoretical slope, based on a smooth surface, in the case of the die marked specimens. Richardson plots of the emission current over a temperature range 1350 to 2200°K were made at

* Research done in 1939–40 while the author was a National Research Fellow.

† Now at the California Institute of Technology, Pasadena, California.

[1] R. P. Johnson and W. Shockley, Phys. Rev. **49**, 436 (1936).

[2] M. H. Nichols, Phys. Rev. **57**, 297 (1940).

[3] C. J. Smithells, *Tungsten* (D. Van Nostrand Company, Inc., New York, 1936), second edition.

[4] C. S. Robinson, J. App. Phys. **13**, 647 (1942).

‡ The author has been informed by Mr. George Moore, of the Bell Telephone Laboratories, that there is a difference in the properties of prewar "non-sag" type of tungsten wire and the corresponding postwar production in that it is very difficult to produce large crystals in the latter. This may be due to different impurities occurring in the ores or manufacturing processes.

[5] C. Herring and M. H. Nichols, Rev. Mod. Phys. **21**, 185 (1949).

[6] Johnson, White, and Nelson, Rev. Sci. Inst. **9**, 253 (1938).

[7] W. B. Nottingham, J. App. Phys. **8**, 762 (1937).

[8] W. E. Forsythe and E. M. Watson, J. Opt. Soc. Am. **24**, 114 (1934).

[9] H. A. Jones and I. Langmuir, Gen. Elec. Rev. **30**, 310 (1927).

[10] R. P. Johnson, Phys. Rev. **54**, 459 (1938).

[11] R. W. Schmidt, Zeits. f. Physik **120**, 69 (1942).

TABLE I. Average emission constants of doped wire.

Type of wire	φ^{**}	A^{**}	Heat treatment
Doped (Callite #200H) polished smooth	4.464	42	Temperature raised steadily from 1000°K to 2600°K over a period of twenty hours. Then 2.5 min. at 2700°K.
	4.455	36	Above plus 125 min. at 2850°K and 105 min. at 2900°K. (Wire diameter reduced about 3 percent by evaporation.)
Doped (Callite #200H) unpolished	4.449	40	10 min. at 2700°K, 8 min. at 2850°K, 3 min. at 2900°K, 40 hr. at 2300°K.

TABLE II. Average emission constants of undoped wire.

Type of wire	φ^{**}	A^{**}	Heat treatment
Undoped (G.E. lot exp. #8983) polished smooth	4.557	55	Temperature raised steadily from 1000°K to 2600°K over a period of 6½ hours. Then 1.5 min. at 2700°K, 0.7 min. at 2900°K, 63 hours at 2200°K.
	4.519	49	Above plus 22 min. at 2900°K, and 36 hr. at 2200°K.
Undoped (G.E. lot exp. #8983) unpolished	4.529	53	17 min. at 2875°K, 1 min. at 2950°K, 78 hr. at 2200°K.

a collecting voltage of 1100. The average thermionic constants φ_v^{**} and A^{**} were determined from these Richardson plots by fitting a least squares straight line to the data assigning the error to the $1/T$ coordinate. In all cases in this section and in Section III, the probable error in φ_v^{**} was less than 0.013 volt and in A^{**} less than 5 amp/cm² deg² as determined from the deviations from the least squares straight line. The "zero field" value φ^{**} is given by $\varphi_v^{**}+kSV^{\frac{1}{2}}/e$ where S is the slope of the experimental Schottky plot ($\ln i_v$ *versus* $V^{\frac{1}{2}}/T$) and V is the collecting voltage at which the thermionic currents for the Richardson plots were measured.[5] The results are summarized in Table I.

These results are not in good agreement with previously accepted values of about 4.52 volts and 60 amp/cm² deg² for clean polycrystalline tungsten.[12–18]

III. EXPERIMENTALLY DETERMINED AVERAGE EMISSION CONSTANTS OF UNDOPED POLYCRYSTALLINE TUNGSTEN WIRE

In order to compare the above results with those from undoped tungsten wire, two specimens were cut from G.E. lot exp. #8983 dated 1/13/38; one specimen was polished and the other was used unpolished. The results are summarized in Table II. The heat treatment consisted of short flashes at the high temperatures separated by long periods of heating at 2200°K.[19] These results are in better agreement with the previously accepted values.[12–18]

IV. PURITY OF SPECIMENS

The following data on purity of tungsten wire as it comes from the mill—i.e., after sintering, swaging, and drawing—were supplied by Mr. P. Dorticos.[20]

TABLE III. Data on purity of the specimens.

Type of wire	NVR	MO	Fe
"Doped" (GE 218 non-sag)	0.004 percent	0.002	0.011
Undoped	0.001	0.16	0.007

TABLE IV. Results of spectroscopic analysis of specimens.

Element	Doped	Undoped
Mo	5	100
Ni	10	1
Fe	5	5
Ca	40	30
Al	20	5
Si	3	3
Cu	1	1
Mg	5	2

Table III gives the results in percent from "wet analysis" on G.E. Type 218 doped wire and undoped tungsten. NVR is non-volatile residue determined by passage of CCl_4 and air over a boat containing tungsten wire in an electrically heated furnace. The tungsten passes over as tungsten oxychloride. The NVR is made up of SiO_2, Na_2O, K_2O, $CaCl_2$, and Al_2O_3. It is to be noted that the impurities in the undoped wire are very small with the exception of the Mo. Dorticos comments that the undoped sample shows unusually high Mo content. It is not clear whether the undoped sample is the same as G.E. lot # exp 8983 used for Table II. According to the results of Freitag and Krüger,[17] this concentration of molybdenum would have a negligible effect on the work function. It should be noticed that with the exception of the Mo, the impurity content is about the same in both samples. Since about 1 percent NVR was originally added to the doped variety to control crystal growth, most of the NVR has been eliminated during the sintering and swaging processes.

A spectroscopic analysis[20] is given in Table IV. This table should be read horizontally—i.e., the numbers given are relative and apply only to the same elements. This table agrees with Table III and, with the exception of Mo, shows about the same order of magnitude of impurities in each case.

For his work on tungsten in 1923–1924, Dushman used a variety of wire known as General Electric K

[12] C. Davisson and L. H. Germer, Phys. Rev. **20**, 300 (1922).
[13] Dushman, Rowe, Ewald, and Kidner, Phys. Rev. **25** (1925).
[14] C. Zwikker, Proc. Amst. Acad. Sci. **29**, 792 (1926).
[15] H. B. Wahlin and L. V. Whitney, Phys. Rev. **50**, 735 (1936).
[16] A. L. Reimann, Phil. Mag. **25**, 834 (1938), supplement.
[17] H. Freitag and F. Krüger, Ann. d. Physik **21**, 697 (1934).
[18] W. B. Nottingham, Phys. Rev. **47**, 806 (A) (1935).
[19] E. A. Coomes, Phys. Rev. **55**, 519 (1939).
[20] Letter from Mr. P. Dorticos, Lamp Department, General Electric Company, Cleveland Wire Works (May 19, 1941).

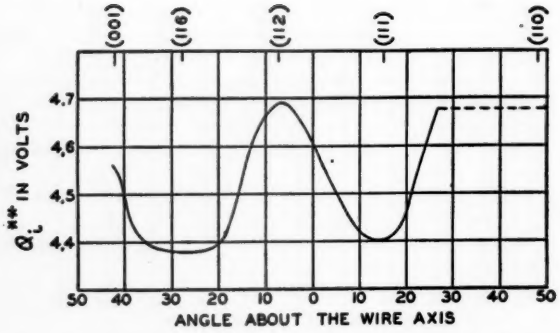

FIG. 1. Approximate values of φ^{**} from a single crystal tungsten wire (see reference 2) plotted as a function of the angle about the wire axis. The Miller indices of the various crystal directions are indicated.

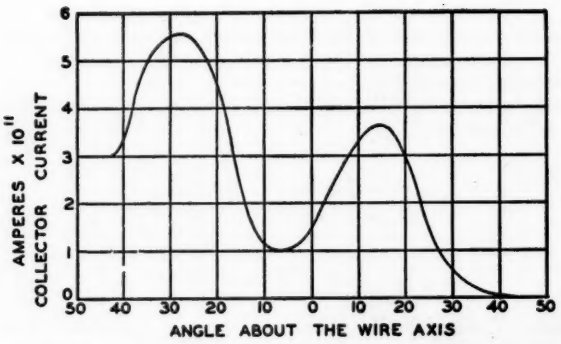

FIG. 2. Emission current from the single crystal wire of Fig. 1 at a temperature of 1465°K plotted as a function of the angle about the wire axis.

wire.[21] For further information, at the request of the writer, Dorticos[22] performed the following experiment on *K* wire and the G.E. 218 doped variety. A $\frac{1}{8}$-in. diameter rod of each material was heated in hydrogen, by passage of current, through six cycles of one hour at 2900°K followed by twelve hours at 2000°K. Then after this heat treatment a spectroscopic analysis yielded the results in Table V. The letter *p* means that the element indicated is present in average amounts; the sign + means a little more than average; ++ means in excess of that; and − means less than average, etc.; *A* means absent. These results show no substantial differences between K tungsten and 218 tungsten after such severe heat treatment. No analyses were made prior to heat treatment.

At the request of the writer, Smoluchowski[23] made a spectroscopic comparison between a raw Callite 200H wire (0.312 mm in diameter) and another section of the same wire which was recrystallized in very pure hydrogen and was severely heat treated in vaccum. The main observed difference was that the Cu and the Mo lines were very much weaker in the heat treated sample. Due to low dispersion and small samples, some other lines could not be well identified.

V. DISCUSSION

The heat treatment given all specimens was sufficient to result in stable emission throughout all temperature cycles. Therefore the difference must be caused by some permanent effect brought about by the differences in the impurities originally present. Now the chemical analyses in Section IV show that the amount of impurities present after heat treatment is very small so that the effect cannot be attributed to a difference in the resistivity which would effect the temperature scale (about 5 percent difference in resistivity would be required) or to a volume effect on the work function. Since after sufficient heat treatment the thermionic emission was stable for all temperature cycles, impurities in the surface double layer seem doubtful. Although the doped tungsten wire after heat treatment shows about the same relative impurity content as does the undoped wire, the doping strongly effects the crystal growth properties.[3] *It therefore seems likely that the difference in work function between the doped and undoped specimens is caused by a different distribution of the types of crystal surfaces exposed.* In this connection crude calculations, using the patch theory, indicate that tungsten wire having perfectly random crystal orientation would display a somewhat larger work function than would the type of preferred orientation which the doped wire displays.[5] Unfortunately the literature on the final crystal orientation in the undoped type of wire does not seem conclusive.[5]

It might also be mentioned that about a 5 percent difference in the average emissivity of the surface would be required to explain the difference in the observed work function of the two types of wire on the basis of its effect on the temperature. Since it appears that the fractional amounts of the surface exposed in the two cases are not much different[5] (though apparently different enough to explain the effect on the basis of work function differences) it seems unlikely that the effect can be attributed to different emissivities of the various crystal surfaces exposed.

It is of some interest to compare the results of Table I with the data represented by Fig. 5 of reference 2# which were taken from a single crystal grown in doped (G.E. Type 218) tungsten wire. From these data it is possible to compute approximately the value of the apparent work function φ^{**} of the tungsten single crystal wire as a function of the angle taken about the wire axis. These values are plotted in Fig. 1. It can be shown that the apparent high field work function, φ^{**},

[21] Letter from Dr. S. Dushman, General Electric Research Laboratory (November 17, 1941).
[22] Letter from Mr. P. Dorticos, Lamp Department, General Electric Company, Cleveland Wire Works (April 13, 1942).
[23] Letter from Dr. R. Smoluchowski while at the General Electric Research Laboratory (May 25, 1942).

Because of a numerical error, the values of φ^{**} (φ_0 in the notation in this reference) in Table I of this reference are 0.03 volt too low. It should also be pointed out that in Fig. 5 of this reference the temperatures should be 1890°K and 1465°K.

averaged over the wire surface is given by [5,24]

$$\varphi^{**}=\sum_i w_i\varphi_i^{**}, \quad (1)$$

where w_i is the fraction of the total emission which comes from the ith type of crystal surface whose apparent work function is φ_i^{**}. The corresponding value of the emission constant A^{**} is given by

$$\log A^{**}=\log j_0/T^2+e\varphi^{**}/2.303kT, \quad (2)$$

where j_0 is the average current per unit area extrapolated to zero field. Figure 2 is a plot of the current measured as a function of the angle about the wire axis corresponding to a temperature of 1465°K. Using Eq. (1) in connection with Figs. 1 and 2, graphical integration yields a value of 4.45 volts for φ^{**} and a corresponding value of 41 amp/cm² deg² for A^{**}. These approximate results are in agreement with those of Table I.

These results further emphasize[2,5] the fact that the average thermionic constants from polycrystalline emitters depend upon the types and relative amounts of the various crystal surfaces exposed and are generally not characteristic of a uniform surface.

[24] C. Herring, Phys. Rev. **59**, 889 (1941).

TABLE V. Results of spectroscopic analysis of specimens after heat treatment.

Element	K Tungsten	218 Tungsten
Ca	p^{++}	p^+
Fe	p^+	p^+
Mo	p	p^+
Ti	p^+	p^+
Cr	p^{--}	p^{--}
Ni	p	p
Al	p^-	p^-
Mg	p^+	p
Si	A?	p^-
Na and K — no difference		

VI. ACKNOWLEDGMENT

The author is indebted to Mr. P. Dorticos and to Dr. R. Smoluchowski of the General Electric Company for carrying out the chemical analyses reported in Section V. The author is also indebted to Professor W. B. Nottingham of the Massachusetts Institute of Technology for reading and critizing the manuscript.

PHYSICAL REVIEW VOLUME 78, NUMBER 2 APRIL 15, 1950

The Radiative Collisions of Positrons and Electrons*

J. KATZENSTEIN
Lyman Laboratory of Physics, Harvard University, Cambridge, Massachusetts

(Received November 25, 1949)

The general matrix elements for the collision of two electrons (e-e case) or a positron and an electron (p-e case) accompanied by the emission of a quantum of radiation are formulated. It is expected that the two cross sections will differ considerably both because of the existence of a dipole for the p-e case, and because of the essentially different nature of the exchange phenomenon in the p-e case arising there from the possibility of virtual pair creation or annihilation rather than the indistinguishability of the particles. Two cases are calculated in detail; the non-relativistic limit and the extreme relativistic limit in which the quantum energy is restricted to $\leqq E^1$ in the laboratory system. In the former case the cross section for the e-e case is found to vanish if the momentum of the quantum is neglected, while the p-e cross section is comparable to that for the "bremsstrahlung" process. In the latter case the cross sections of the two cases are of the same order of magnitude the e-e cross section being greater because of the exchange terms, the exchange terms of the p-e case being negligible in all of the cases considered.

I. INTRODUCTION

THE elastic scattering of electrons by electrons has been treated by Møller,[1] Breit,[2] and Bethe and Fermi,[3] using both correspondence principle methods and the quantum electrodynamics. The results of Møller have been adapted by Bhabha[4] to the case when one of the colliding particles is a positron.

The scattering of two charged particles by each other with the emission of a quantum of radiation has been treated by Møller[5] for particles of arbitrary masses. This author only carries out the complete calculation of the collision cross section for the limiting case that the mass of one of the particles becomes infinite, and thus obtains an expression identical to that obtained by Bethe and Heitler[6] for the "bremsstrahlung" process. The process is generalized in a paper by Havas[7] for the case that any number of quanta are emitted.

* Summary of a thesis presented in partial fulfillment of the requirements for the degree of Doctor of Philosophy at Harvard University.

[1] C. Møller, Ann. d. Physik **126**, 259 (1930).
[2] G. Breit, Phys. Rev. **34**, 553 (1929).
[3] H. Bethe and E. Fermi, Zeits. f. Physik **77**, 296 (1932).
[4] H. J. Bhabha, Proc. Roy. Soc. **A154**, 195 (1936).
[5] C. Møller, Proc. Roy. Soc. **A152**, 481 (1935).
[6] H. Bethe and W. Heitler, Proc. Roy. Soc. **A146**, 83 (1934).
[7] P. Havas, Phys. Rev. **68**, 214 (1945).

The present investigation treats the radiative collisions for the case that both of the particles are electrons (*e-e* case) and the case that one of the particles is an electron and the other a positron (*p-e* case). Classical considerations lead one to expect a higher probability for the latter process as a classically-defined dipole moment can exist which is absent for the case that both particles possess the same sign of charge. Also the exchange phenomenon attending the collision of identical particles is likewise present for the collision of particles and anti-particles as is pointed out by Bhabha.[4] The exchange phenomenon in the latter case, however, is of an essentially different nature than that arising in the collision of identical particles since it rises from the virtual annihilation and creation of a pair. It is these two points, the existence of a classically defined dipole moment and an essentially different type of exchange effect, that lead one to the expectation that the cross sections for the two processes should differ considerably.

We shall use so-called "natural units" throughout the calculation. Such units take as the unit of mass the electronic mass m, the unit of length the Compton wave-length, h/mc, and the unit of velocity the velocity of light in vacuum, c. In such units the units of momentum and energy are mc and mc^2, respectively.

As a general solution of the problem is extremely laborious, we shall confine outselves to two limiting approximations; first, the non-relativistic limit, and second, the extreme relativistic limit, with the restriction that the energy of the emitted quantum in the center-of-gravity system is of the order of magnitude of the proper electron energy.

II. FORMULATION OF THE MATRIX ELEMENT FOR THE ELECTRON-ELECTRON COLLISION

The matrix element for the electron-electron collision with the emission of a quantum of energy k according to Møller[5] is:

$$\left(\frac{32\pi^3\alpha^3}{L^3k}\right)^{\frac{1}{2}}\sum_{''}\frac{(u_2'^*\boldsymbol{\alpha}\cdot\mathbf{f}u_2'')}{E_1+E_2-E_2''-E_1'}\left\{-\frac{(u_2''^*u_2)(u_1'^*u_1)-(u_2''^*\boldsymbol{\alpha}u_2)\cdot(u_1'^*\boldsymbol{\alpha}u_1)}{(E_1-E_1')^2-q_1^2}\right\}$$
$$+\sum_{'''}\left\{-\frac{(u_2'^*u_2''')(u_1'^*u_1)-(u_2'^*\boldsymbol{\alpha}u_2''')\cdot(u_1'\boldsymbol{\alpha}u_1)}{(E_1-E_1')^2-q_1^2}\right\}\frac{(u_2'''^*\boldsymbol{\alpha}\cdot\mathbf{f}u_2)}{E_2'+E_1'-E_1-E_2'''}$$
$$+(\text{term with 1 and 2 interchanged})-(\text{exchange terms}). \quad (1)$$

The subscripts 1 and 2 refer to quantities belonging to one or the other of the particles while the presence or absence of a prime refers to the final or initial state. The double or triple primes refer to the intermediate state. α is the fine-structure constant while L is the edge length of the normalization cube. The summations $\sum''$ and $\sum'''$ refer to sums over those intermediate states for which momentum is conserved. The term written explicitly refers to the emission of the quantum by the particle labeled 2. There will be a similar term for the particle labeled 1 which is identical except for an interchange of subscripts. From these "direct" terms there can be obtained the two exchange terms by changing the subscripts of all quantities referring to the final state (primed quantities). This procedure corresponds to the use of anti-symmetric wave functions to describe the electrons as required by the exclusion principle.

The sum over intermediate states is carried out with the aid of the so-called "selection operators."[9] These are operators which give vanishing results when applied to a Dirac amplitude which refers to a state of positive (negative) energy and zero when applied to a Dirac amplitude referring to a state of negative (positive) energy. We obtain for the sum over the intermediate state of the first term in (1) the following expression:

$$\sum_{''}\frac{(u_2'^*\boldsymbol{\alpha}\cdot\mathbf{f}u_2'')(u_2''^*u_2)(u_1'^*u_1)}{(E_1+E_2-E_2''-E_1')[(E_1-E_1')^2-q_1^2]}=\frac{(u_2'^*\boldsymbol{\alpha}\cdot\mathbf{f}}{(E_1-E_1')^2-q_1^2}\left\{\frac{|E_2''|-\boldsymbol{\alpha}\cdot\mathbf{p}_2''-\beta}{2|E_2''|}\frac{1}{E_1+E_2-|E_2''|-E_1'}\right.$$
$$\left.+\frac{|E_2''|+\boldsymbol{\alpha}\cdot\mathbf{p}_2''+\beta}{2|E_2''|}\frac{1}{E_1+E_2+|E_2''|-E_1'}\right\}u_2'')(u_2''^*u_2)(u_1'^*u_1). \quad (2)$$

By use of the momentum conservation equation $\mathbf{p}_2''=\mathbf{p}_2'+\mathbf{k}$ this expression may be simplified to the following:

$$\frac{(u_2'^*\{I_2\}u_2)(u_1'^*u_1)}{(E_1-E_1')^2-q_1^2};\quad \{I_2\}=\left\{\frac{k(\boldsymbol{\alpha}\cdot\mathbf{f})+ik(\boldsymbol{\sigma}\cdot\mathbf{f}')-2(\mathbf{f}\cdot\mathbf{p}_2')}{2(E_2'k-\mathbf{p}_2'\mathbf{k})}\right\};\quad \mathbf{f}\times\mathbf{f}'=\frac{\mathbf{k}}{|k|}=\mathbf{n}. \quad (3)$$

If one carries out this summation for all the terms in (1), one obtains the following expression for the matrix element for the collision of two electrons accompanied by the emission of a quantum of energy k. $\boldsymbol{\alpha}$, $\boldsymbol{\beta}$, and $\boldsymbol{\sigma}$

[8] C. Møller, Proc. Roy. Soc. A152, 481 (1935).
[9] H. Casimir, Helv. Phys. Acta 6, 287 (1933).

are the usual Dirac matrices.

$$H_{e-e}=\left(\frac{32\pi^3\alpha^3}{L^3k}\right)^{\frac{1}{2}}\Bigg(-\frac{1}{(E_1-E_1')^2-q_1^2}[(u_2'^*\{I_2\}u_2)(u_1'^*u_1)-(u_2'^*\{I_2\}\alpha u_2)\cdot(u_1'^*\alpha u_1)$$
$$+(u_2'^*\{II_2\}u_2)(u_1'^*u_1)-(u_2'^*\alpha\{II_2\}u_2)\cdot(u_1'^*\alpha u_1)]\Bigg)+(1\text{ and }2\text{ interchanged})-(\text{exchange terms}) \quad (4)$$

$$\{II_2\}=\left\{\frac{k(\alpha\cdot\mathbf{f})-i(\sigma\cdot\mathbf{f}')+2(\mathbf{f}\cdot\mathbf{p}_2)}{2(E_2k-\mathbf{p}_2\cdot\mathbf{k})}\right\}. \quad (5)$$

III. FORMULATION OF THE MATRIX ELEMENT FOR THE POSITRON-ELECTRON COLLISION

We shall describe the transitions of a positron in terms of a negative-energy energy electron which carries out the positron transition in the opposite sense. Thus the transition of the positron from a certain initial state to a certain final state is viewed as the transition of a negative-energy electron from the final state of the positron, evacuating a "hole" there in the infinite sea of negative-energies, and filling the "hole" corresponding to the positron initially present. We shall denote the Dirac amplitudes, energies and momenta referring to this negative energy electron by the subscript 1, while the corresponding quantities for a positive energy electron remain unsubscripted. We shall denote the energies and momenta of the positron by the subscript $+$. The following well-known relations connect the energies and momenta of the positron to those of the corresponding negative-energy electron.

$$|E_1|=E_+ \quad \mathbf{p}_1=-\mathbf{p}_+. \quad (6)$$

Further we shall denote by the absence or presence of a prime the initial and final states respectively of the *positron* which are just reverse from those of the negative-energy electron.

The direct matrix element for the case that the positron emits the quantum becomes:

$$H_{p-e}=\left(\frac{32\pi^3\alpha^3}{L^3k}\right)^{\frac{1}{2}}\Bigg\{\sum_{''}\frac{(u_1^*\alpha\cdot\mathbf{f}u_1'')}{E-E'-|E_1'|-E_1''}\left[\frac{(u_1''^*u_1')(u'^*u)-(u_1''^*\alpha u_1')\cdot(u'^*\alpha u)}{(E-E')^2-q^2}\right]$$
$$+\sum_{'''}\left[-\frac{(u_1^*u_1''')(u'^*u)-(u_1^*\alpha u_1''')\cdot(u'^*\alpha u)}{(E-E')^2-q^2}\right]\frac{(u_1'''^*\alpha\cdot\mathbf{f}u_1')}{E'-E-|E_1|-E_1'''}\Bigg\}. \quad (7)$$

The above expression is similar to (1) except for the interchange of denominators between terms, the interchange of primes on the Dirac amplitudes, and the sign of the energies of the intermediate states. The first two differences are due to the description of the process in terms of a particle making the reverse transition. The change in the sign of the intermediate state energy stems from the fact that a positive-energy intermediary state of the positron corresponds to a negative-energy state of the corresponding electron, while a negative-energy intermediary state of the positron corresponds to a positive-energy state for the electron.

The sum over the intermediate energy states is carried out with the help of the selection operators exactly as in the case cf the electron. After carrying out the summation one obtains for this term:

$$H_{p-e}=-\left(\frac{32\pi^3\alpha^3}{L^3k}\right)^{\frac{1}{2}}\frac{1}{(E-E')^2-q^2}$$
$$\times\{(u_1^*[I_1]u_1')(u'^*u)-(u_1^*\alpha[I_1]u_1')\cdot(u'^*\alpha u)$$
$$+(u_1^*[II_1]u_1')(u'^*u)-(u_1^*[II_1]\alpha u_1')\cdot(u'^*\alpha u)\} \quad (8)$$

$$[I_1]=\left[\frac{-k(\alpha\cdot\mathbf{f})-ik(\sigma\cdot\mathbf{f}')+2(\mathbf{f}\cdot\mathbf{p}_1')}{2(|E_1'|k+\mathbf{p}_1'\cdot\mathbf{k})}\right]$$

$$[II_1]=\left[\frac{-k(\alpha\cdot\mathbf{f})+ik(\sigma\cdot\mathbf{f}')-2(\mathbf{f}\cdot\mathbf{p}_1)}{2(|E_1|k+\mathbf{p}_1\cdot\mathbf{k})}\right].$$

If we insert the values for the energy and momentum of the positron as given by (6) we obtain the following relations between the operators for the emission by a positron (9) and the operators for emission by an electron (3) and (5).

$$[I_+]=\left[-\frac{k(\alpha\cdot\mathbf{f})-ik(\sigma\cdot\mathbf{f}')-2(\mathbf{f}\cdot\mathbf{p}_+')}{2(E_+'k-\mathbf{p}_+'\cdot\mathbf{k})}\right]=-\{I_+\}^*$$
$$[II_+]=\left[-\frac{k(\alpha\cdot\mathbf{f})+ik(\sigma\cdot\mathbf{f}')+2(\mathbf{f}\cdot\mathbf{p}_+)}{2(E_+k-\mathbf{p}_+\cdot\mathbf{k})}\right]=-\{II_+\}^*. \quad (10)$$

The matrix element for the emission of the quantum by the electron can be written down at once:

$$H_{p-e}=-\left(\frac{32\pi^3\alpha^3}{L^3k}\right)^{\frac{1}{2}}\frac{1}{(E_+-E_+')^2-q_+^2}$$
$$\times[(u'^*\{I\}u)(u_1^*u_1')-(u'^*\{I\}\alpha u)\cdot(u_1^*\alpha u_1')$$
$$+(u'^*\{II\}u)(u_1^*u_1')-(u'^*\alpha\{II\}u)\cdot(u_1^*\alpha u_1')]. \quad (11)$$

It is seen to be virtually identical to the first term in (5).

If one compares the terms (8) and (11) noting the relation (10) it is seen that the two terms are negative Hermitian conjugates of each other. Hence the square of their sum will be the same as the square of the sum of the first two terms of (5) except for the sign of the

cross-product term. For the *e-e* case this cross-product term is positive while for the *p-e* case it is negative because of (10). This is just what one would expect from the algebraic signs of the charges, but we have obtained it without introducing the explicit sign of charge.

We now must consider the exchange terms for the *p-e* case. Unlike the case of two electrons where the exchange terms correspond to the non-identifiability of the two electrons, the exchange terms for the *p-e* case correspond to the annihilation or creation of a pair. These exchange terms are found to be:

$$\left[\frac{(u'^*\{I\}u_1')(u_1^*u)-(u'^*\{I\}\alpha u_1')\cdot(u_1^*\alpha u)}{(E+E_+)^2-(\mathbf{p}+\mathbf{p}_+)^2}\right]$$
$$+\left[\frac{(u_1^*\{II\}u)(u'^*u_1')-(u_1^*\alpha\{II\}u)\cdot(u'^*\alpha u_1')}{(E'+E_+')^2-(\mathbf{p}'+\mathbf{p}_+')^2}\right]$$
$$+\left[\frac{(u'^*[I_+]u_1')(u_1^*u)-(u'^*\alpha[I_+]u_1')\cdot(u_1^*\alpha u)}{(E+E_+)^2-(\mathbf{p}+\mathbf{p}_+)^2}\right]$$
$$+\left[\frac{(u_1^*[II_+]u)(u'^*u_1')-(u_1^*[II_+]\alpha u)\cdot(u'^*\alpha u_1')}{(E'+E_+')^2-(\mathbf{p}'+\mathbf{p}_+')^2}\right]. \tag{12}$$

The denominators of these terms are seen to differ from the *e-e* case in that they contain energies and momenta referring solely to the initial or final states and not to both, and that the corresponding quantities are added. This difference arises from the fact that the intermediate state may contain all four particles or none at all. This means that the energy denominators will be quite large and the probability for such virtual pair creation or annihilation very small. We shall see that the exchange terms are negligible compared to the direct terms in the (*p-e*) collision for the cases considered.

IV. THE NON-RELATIVISTIC LIMIT

The first of the two limiting cases for which we shall carry out explicit calculations is the non-relativistic approximation. We shall obtain the cross section for radiative collisions when the velocities of the particles are small compared to the velocity of light. In natural units such as we are using, this means that all energies are approximately equal to unity and all momenta are numbers small compared to unity.

In (1) and (7) we note that each term consists of two parts

$$(u_2''^*u_2)(u_1'^*u_1)-(u_2''^*\alpha u_2)\cdot(u_1'^*\alpha u_1). \tag{13}$$

The first term gives the Coulomb or longitudinal interaction and the second the interaction by means of a virtual quantum or transverse interaction. This latter term corresponds to the retardation. The expectation value of the operator α is v/c so the transverse interaction is of the order v^2/c^2 compared to the longitudinal interaction and hence may be neglected in the non-relativistic approximation.

If we examine the invariant energy-momentum denominators (which we shall hereafter refer to as the Møller denominators) we note that the exchange terms in the *p-e* case become negligible for this approximation though not in the *e-e* case. As:

	Exchange		Direct	
e-e case	$\dfrac{1}{(E_1-E_2')^2-(\mathbf{p}_1-\mathbf{p}_2')^2}$	$\to\dfrac{1}{(\mathbf{p}_1-\mathbf{p}_2')^2}$	$\dfrac{1}{(E_2-E_2')^2-(\mathbf{p}_2-\mathbf{p}_2')^2}$	$\to\dfrac{1}{(\mathbf{p}_2-\mathbf{p}_2')^2}$
p-e case	$\dfrac{1}{(E+E_+)^2-(\mathbf{p}+\mathbf{p}_+)^2}$	$\to\dfrac{1}{4}$	$\dfrac{1}{(E-E')^2-(\mathbf{p}-\mathbf{p}')^2}$	$\to\dfrac{1}{4}$.

(14)

Since all momenta are numbers small compared to unity, we are justified in neglecting the exchange terms in the (*p-e*) case as small compared to the direct terms.

This result leads to the conclusion that the positron and electron behave like independent particles in all collisions where the energies involved are small compared to the proper energy of the particles; i.e., the non-relativistic limit. This is exactly what one would expect as the connection between the particles and their anti-particles is given by the Dirac "hole" theory which is an essentially relativistic theory, and such a connection should be expected to disappear in the non-relativistic limit.

We shall carry out the calculation initially for the center-of-gravity system, i.e. that reference system such that $\mathbf{p}_2=-\mathbf{p}_1$. The conservation equation then reads:

$$\frac{p_2^2}{2}+\frac{p_1^2}{2}=\frac{p_2'^2}{2}+\frac{p_1'^2}{2}+k \quad k=p_2^2-\frac{p_2'^2}{2}-\frac{p_1'^2}{2}. \tag{15}$$

These equations show that $k\sim p^2$. Since $p\ll 1$ we are justified in neglecting the momentum of the light quantum as compared to that of the particles. Hence $\mathbf{p}_2'\approx\mathbf{p}_1'$. This approximation simplifies the calculations considerably. Though we neglect the momentum of emitted quantum, we do not neglect its energy, i.e. $|\mathbf{p}_1|\neq|\mathbf{p}_1'|$; $|\mathbf{p}_2|\neq|\mathbf{p}_2'|$.

Since $\mathbf{p}_1=-\mathbf{p}_2$, $\mathbf{p}_1'=-\mathbf{p}_2'$ the matrix element referring to particle 2 is related to that referring to particle 1 by

the following relationship:

$$(u_1'^*\{I_1\}u_1)(u_2'^*u_2)=R[(u_2'^*\{I_2\}u_2)(u_1'^*u_1)]. \quad (16)$$

R is the operator which inverts the space coordinates of the electron alone leaving the coordinates of the light quantum propagation vector unaltered. The matrix element for the e-e collision can be then written as:

$$H_{e-e}=\left(\frac{32\pi^3\alpha^3}{L^9k}\right)^{\frac{1}{2}}\left[\frac{1}{(\mathbf{p}_1-\mathbf{p}_1')^2}-\frac{1}{(\mathbf{p}_1+\mathbf{p}_1')}\right](1+R)$$

$$\times[(u_1'^*\{I_1\}u_1)(u_2'^*u_2)+(u_1'^*\{II_1\}u_1)(u_2'^*u_2)]. \quad (17)$$

The corresponding matrix element for the p-e collision can be written, using the identities (10) as:

$$H_{p-e}=\left(\frac{32\pi^3\alpha^3}{L^9k}\right)^{\frac{1}{2}}\left[\frac{1}{(\mathbf{p}-\mathbf{p}')^2}\right](1-R)$$

$$\times[(u'^*\{I\}u)(u_1^*u_1')+(u'^*\{II\}u)(u_1^*u_1')].$$

As is well known the operator R has the eigenvalue $+1$ when applied to the components of an axial vector or a scalar, while it has the eigenvalue -1 when applied to the components of a polar vector. The operators $\{I\}$ and $\{II\}$ are sums of the operators $(\boldsymbol{\alpha}\cdot\mathbf{f})$, $(\mathbf{p}\cdot\mathbf{f})$, $(\mathbf{p}'\cdot\mathbf{f})$ and $(\boldsymbol{\sigma}\cdot\mathbf{f}')$. All except the last are components of polar vectors referring to the electrons and change sign under application of the Operator R. The components of $\mathbf{f}$ and $\mathbf{f}'$ are unchanged as the operator R does not invert the coordinates of the quantum propagation vector. The operator $(\sigma\cdot\mathbf{f}')$ will cancel between the terms $\{I\}$ and $\{II\}$ as it occurs with opposite signs in them. Hence we see that (17) is identically zero. The transition probability for the radiative collision for the electrons is zero in the non-relativistic limit if the momentum of the emitted quantum is neglected.

This result is entirely in accord with the classical radiation theory. For, in the limit of wave-lengths large compared to the dimensions of the radiating system, the radiated intensity is calculated by coherent superposition of the radiation emitted by each of the accelerated particles. In the e-e collision the acceleration of the particles is always equal and opposite when the momentum of the emitted quantum is neglected. Hence the waves will destructively interfere and the net intensity radiated is negligible. If, however, one of the particles is positively charged, the two waves will constructively interfere and the net intensity radiated will be considerable.

The matrix element for the p-e collision is:

$$H_{p-e}=\left(\frac{32\pi^3\alpha^3}{L^9k}\right)^{\frac{1}{2}}\left[\frac{2}{(\mathbf{p}-\mathbf{p}')^2}\right]$$

$$\times[(u'^*\{2(\boldsymbol{\alpha}\cdot\mathbf{f})+2(\mathbf{p}-\mathbf{p}'\cdot\mathbf{f})\}u)(u_1^*u_1')]. \quad (18)$$

The transition probability is given by the well-known expression[10] which in natural units is

$$w=2\pi|H|^2\rho_F. \quad (19)$$

Dividing by an electron flux of one electron per volume L^3 moving with the velocity $v=p$ we get for the differential cross section

$$d\phi=\frac{2\pi L^3}{p}|H|^2\rho_F. \quad (20)$$

ρ_F is the density of final states into which the scattered electron can go and into which the quantum can be emitted. For the non-relativistic approximation and neglecting k compared with p' we have for ρ_F:

$$\rho_F=\frac{L^3p'k^2d\Omega_{p'}d\Omega_k}{2(2\pi)^6}. \quad (21)$$

Inserting this expression and integrating over the solid angle of p' and k we obtain for the total cross section:

$$\Phi=\frac{128}{3}\frac{1}{p^2}\phi_0\log\frac{(p+p')}{(p-p')}\frac{dk}{k} \quad (22)$$

$$\Phi_0=\text{natural cross section}=(\hbar/mc)^2\alpha^3.$$

We introduce the variable $\epsilon=k/p^2$ which gives the fraction of the kinetic energy which is radiated. The cross section now becomes:

$$\Phi=\frac{128}{3}\frac{1}{k}\Phi_0\log\left[\frac{1+(1-\epsilon)^{\frac{1}{2}}}{1-(1-\epsilon)^{\frac{1}{2}}}\right]d\epsilon. \quad (23)$$

Transforming this cross section to the laboratory system (in which we denote quantities with a star) this expression becomes:

$$\Phi^*=\frac{256}{3}\frac{1}{k}\Phi_0\log\frac{1+(1-2\epsilon^*)^{\frac{1}{2}}}{1-(1-2\epsilon^*)^{\frac{1}{2}}}d\epsilon^*. \quad (24)$$

It is easily seen that ϵ^* can only range from 0 to $\frac{1}{2}$ as compared to 0 to 1 for ϵ. In the center-of-gravity system the positron and electron can effectively come to rest giving all of their kinetic energy up as radiation. Conservation of momentum forbids this in the laboratory system. The maximum energy which can be radiated is then half the initial total energy.

The expression (24) is the same except for the numerical factor of 32 as that given by Heitler[11] for the non-relativistic "brehmsstrahlung." Since both particles radiate the square of the matrix element will thus contribute a factor of 4. Further, another factor of 4 comes from the reduced mass of the positron and electron. Finally a factor of 2 is introduced in passing from the center-of-gravity to the laboratory system.

[10] W. Heitler, *Quantum Theory of Radiation* (Clarendon Press, Oxford, 1944), second edition, p. 90.
[11] W. Heitler, reference 10, p. 166.

The cross section vanishes in the limit $\epsilon=1$ or $\epsilon^*=\frac{1}{2}$. This is due to the failure of the Born approximation (plane wave functions) in the limit of low velocities. The criterion for the validity of the Born approximation is $e^2/\hbar v=\alpha/(v/c)\ll 1$. The Born approximation is valid far into the non-relativistic region because of the smallness of α. However it fails for those collisions in which the colliding particles slow down to the velocities of the order of $(1/137)c$. In this region the exact theory of Sommerfeld[12] gives a non-vanishing cross section for $\epsilon=1$. This result is well known and we will not discuss it further.

In the limit $\epsilon\rightarrow 0$ we see that the cross section diverges logarithmically (in addition to the well-known infra-red catastrophe due to the factor $1/k$; it being convenient to isolate this latter effect by discussing instead of the cross section Φ, the radiated intensity $k\Phi$).

This logarithmic divergence of the radiated intensity $k\Phi$ in the limit of very soft quanta is a Rutherford-type of infinity which arises from the implicit assumption that the Coulomb field extends to infinity. Although the interaction potential falls off directly with the impact parameter, the density of final states increases with the square of the impact parameter leading to a very large probability for collisions in which a very soft quantum is emitted. In the theory of the "brehmsstrahlung"[6] the screening of the nuclear field by the atomic electrons restricts the effective range of the Coulomb potential to a finite value and thus eliminates this form of divergence. In our problem the idea of screening is replaced when considering the passage of positrons through matter by the restriction that the positrons interact only with the nearest electron, thus restricting the impact parameter to the order of magnitude of the mean distance between electrons.

This idea may be illustrated by introducing instead of the Coulomb potential, the modified potential $e^{-r/a}/r$. Such a potential behaves like the Coulomb potential for $r<a$ and drops rapidly to zero for $r>a$. a is then the effective range of the screened Coulomb field. We obtain for the cross section in the center-of-gravity system:

$$\Phi=\frac{128}{3}\Phi_0\left\{\frac{1}{2p^2}\log\left(\frac{\left[1+(1-\epsilon)^{\frac{1}{2}}\right]^2+\dfrac{1}{a^2p^2}}{\left[1-(1-\epsilon)^{\frac{1}{2}}\right]^2+\dfrac{1}{a^2p^2}}\right)-\frac{2}{a^2p^2\left[(1+(1-\epsilon)^{\frac{1}{2}})^2+\dfrac{1}{a^2p^2}\right]\left[(1-(1-\epsilon)^{\frac{1}{2}})^2+\dfrac{1}{a^2p^2}\right]}\right\}. \tag{25}$$

The parameter $1/a^2p^2=\lambda^2/a^2$ where λ is the deBroglie wave-length of the incident particle. So long as the effective range of the Coulomb field is large compared to the deBroglie wave-length of the particles we may discard the second term as well as the term $1/a^2p^2$ in the numerator of the logarithm. Equation (25) then becomes

$$\Phi=\frac{64}{3}\Phi_0\log\left[\frac{\left[1+(1-\epsilon)^{\frac{1}{2}}\right]^2}{\left[1-(1-\epsilon)^{\frac{1}{2}}\right]^2+(1/a^2p^2)}\right]\frac{d\epsilon}{k}. \tag{26}$$

This expression is the same as (23) except in the limit $\epsilon\rightarrow 0$ it converges to the value $(128/3)\log(2ap)$.

V. THE EXTREME RELATIVISTIC LIMIT

We turn now to the second of the two limiting cases which we shall treat, the extreme relativistic limit. Since in natural units $p\gg 1$ in this limit and $E=(1+p^2)^{\frac{1}{2}}$ we shall be able in most parts of the calculation to take $p\cong E$. As a further simplification we shall assume that the maximum energy of the emitted quantum $k\sim 1$ so that k can be considered small compared to all energy and momentum quantities. The simplification that this assumption introduces is obvious when we examine the numerator of expressions (3) and (5), the radiation operators. The first two terms are of order k while the third is of order p. By restricting the magnitude of k in the center-of-gravity system to values ≤ 1 these first two terms are negligible compared to the third term. This restriction is not as narrow as would first appear since in going over to the laboratory system by means of a Lorentz transformation a forward emitted quantum is hardened by the Doppler effect so that its energy $k\sim E^{\frac{1}{2}}$. As virtually the total emission takes place in a narrow cone about the axis of initial velocities this result will give the emitted spectrum up to energies of the order of the square root of the energy of the incident particle.

In this approximation the expressions (3) and (5) now have the matrix dependence of the unit matrix and can be factored out of the Dirac amplitudes. Since the energy and momentum of the emitted quantum is small we can make the further approximation $E_2'=E_1'$; $\mathbf{p}_2'=-\mathbf{p}_1'$. As we are working in the center-of-gravity reference system we have $E_2=E_1$; $\mathbf{p}_2=-\mathbf{p}_1$. Thus we may drop the subscripts on the energy and momentum quantities. The matrix element for the e-e collision is then

$$H_{e\leftarrow e}=-\left(\frac{32\pi^3\alpha^3}{L^9k^3}\right)^{\frac{1}{2}}\left[(\mathbf{p}\cdot\mathbf{f})\left(\frac{1}{E-\mathbf{p}\cdot\mathbf{n}}-\frac{1}{E+\mathbf{p}\cdot\mathbf{n}}\right)-(\mathbf{p}\cdot\mathbf{f})\left(\frac{1}{E'-\mathbf{p}'\cdot\mathbf{n}}-\frac{1}{E'+\mathbf{p}'\cdot\mathbf{n}}\right)\right]\times\left\{\frac{(u_2'^*u_2)(u_1'^*u_1)-(u_2'^*\alpha u_2)\cdot(u_1'^*\alpha u_1)}{(E-E')^2-(\mathbf{p}-\mathbf{p}')^2}-\frac{(u_2'^*u_1)(u_1'^*u_2)-(u_2'^*\alpha u_1)\cdot(u_1'^*\alpha u_2)}{(E-E')^2-(\mathbf{p}+\mathbf{p}')^2}\right\}. \tag{27}$$

[12] A. Sommerfeld, Ann. d. Physik **11**, 251 (1931).

We note that the curly-bracketed quantity is, except for a constant factor just the elastic scattering cross section for electrons as formed by Møller.[13] Our approximation is then seen to correspond to the procedure employed in classical radiation theory; to calculate the orbits of the particles under the assumption that energy is conserved, and, using the accelerations so obtained to calculate the intensity of the emitted radiation. Such a procedure is justified so long as the energy radiated is only a small fraction of the total energy of the system.

The expression (27) must be squared and summed over the spin directions of the particles and the polarization directions of the quantum. We then obtain

$$\sum_f \sum_{\sigma_1,\sigma_1',\sigma_2,\sigma_2'} |H_{e\to e}|^2 = \frac{128\pi^3\alpha^3}{L^9 k}\left[\frac{p^4\cos^2\delta\sin^2\delta}{[1+p^2\sin^2\delta]^2}+\frac{p'^4\cos^2\gamma\sin^2\gamma}{[1+p'^2\sin^2\gamma]^2}-\frac{p^2p'^2[\cos\theta-\cos\delta\cos\gamma]\cos\delta\cos\gamma}{[1+p^2\sin^2\delta][1+p'^2\sin^2\gamma]}\right]$$
$$\times\left[\frac{8+2(1+\cos\theta)^2}{[(E-E')^2-(p^2+p'^2-2pp'\cos\theta]^2}+\frac{8+2(1-\cos\theta)^2}{[(E-E')^2-(p^2+p'^2+2pp'\cos\theta]^2}\right.$$
$$\left.-\frac{16}{[(E-E')^2-(p^2+p'^2-2pp'\cos\theta)][(E-E')^2-(p^2+p'^2+2pp'\cos\theta)]}\right] \quad (28)$$

where θ is the angle between $\mathbf{p}$ and $\mathbf{p}'$ (the scattering angle), and δ and γ the angle between $\mathbf{k}$ and $\mathbf{p}$ and $\mathbf{p}'$ respectively.

Before attempting to integrate the expression over all angles we shall try to get some idea of its general behavior. Since $k \ll E$ we can equate primed and unprimed quantities except in the Møller denominators. If this is done for the denominators it is seen that they vanish for $\theta=0$ or $\theta=\pi$. To avoid this infinity (which corresponds to a complete miss) we shall expand these denominators in powers of k/E and retain only the lowest power that is necessary to prevent them from vanishing in the limit $\theta\to 0$ or $\theta\to\pi$. Introducing the parameters

$$w=1-\cos\theta, \quad y=1-\cos\gamma, \quad z=1-\cos\delta, \quad (29)$$

we then obtain for the expression (28):

$$\sum_f \sum_{\sigma_1,\sigma_1',\sigma_2,\sigma_2'} |H_{e\to e}|^2 = \frac{128\pi^3\alpha^3}{L^9 k^3}\left[\frac{y(2-y)(1-y)^2}{[1+p^2y(1-y)]^2}+\frac{z(2-z)(1-z)^2}{[1+p^2z(1-z)]^2}-\frac{[y+z-yz-w](1-y)(1-z)}{[1+p^2y(1-y)][1+p^2z(1-z)]}\right]$$
$$\times\left(\frac{8+2(2-w)^2}{\left[\frac{ky}{2E^3}+2w\right]^2}+\frac{8+2w^2}{\left[\frac{ky}{2E^3}+2(2-w)\right]^2}-\frac{16}{\left[\frac{ky}{2E^3}+2w\right]\left[\frac{ky}{2E^3}+2(2-w)\right]}\right). \quad (30)$$

As far as the w-dependence is concerned the function will have large maxima for $w=0$ and $w=2$. Physically this corresponds to the fact that the cross section is appreciable only for very small scattering angles. The y and z dependence gives zero for y and $z=0$ or 2. However, there are steep maxima for values of y or z which are very close to 0 or 2, namely, y or $z=(1/2p^2)$ or $2-(1/2p^2)$. The behavior of these terms corresponds physically to the fact that there must be a component of momentum transverse to the propagation vector of the quantum if there is to be emission which one expects from classical radiation theory. However the Doppler denominators $(E-\mathbf{p}\cdot\mathbf{n})$, $(E+\mathbf{p}\cdot\mathbf{n})$ reduce the probability for the emission of a quantum whose propagation vector makes an angle greater than $1/(2p^2)$ with the momentum vector virtually to zero. So while there must be a transverse component of momentum if a quantum is to be emitted at all it must be very small.

The combination of the Doppler and Møller denominators makes it evident that the quantum will be emitted almost directly forward or backward and the emergent particles will come off at a very small angle with the incident particles. Although the Møller denominators give a maximum for zero scattering angle, there can be no emission, for conservation of momentum then demands that the light quantum propagation vector be parallel to the momentum vectors. There is then no transverse component of momentum, and hence there can be no emission of the light quantum.

This "hollow-peak" behavior of the radiative cross section leads one to question the original approximation. For should the neglected terms in the curly-bracketed expression give a finite probability for radiation when the scattering angle is zero, then it is not correct to discard them. Even if their contribution is of a smaller order of magnitude then the term considered, the steep maxima of Møller denominators for the scattering angles 0 and π will make their contribution to the total cross section considerable. A brief calculation, however, shows these neglected terms to give no contribution to the cross section for scattering angles of 0 or π.

[13] C. Møller, Ann. d. Physik **126**, 259 (1930).

Integrating over the angle variables we obtain for the cross section of the e-e collision in the limit $E \gg k$:

$$\Phi/\Phi_0 = (512/k^2)Edk, \tag{31}$$

where Φ_0 is the natural cross section as defined in (22).

We note that the emitted intensity $k\Phi$ diverges like $1/k$ in the limit that the energy of the emitted quantum goes to zero. This again is a Rutherford-type infinity corresponding to an infinite probability for a "complete miss." Such an infinity may be excluded as in the non-relativistic limit by restricting the value that the impact parameter may assume. The divergence in part arises from the retardation terms which correspond to the emission by one particle of a virtual quantum and the absorption of the virtual quantum by the other particle. The momentum of the virtual quantum k' is just equal to q, the momentum transfer between the interacting particles. If the quantum is to be a virtual quantum it must be indetectable from the vacuum fluctuations of the radiation field. Thus utilizing the uncertainty relation between energy and time measurements a relation can be established between the energy of the virtual quantum and the distance between the interacting particles. For the uncertainty in time must be r/c the "time of flight" of the virtual quantum. In ordinary units we have

$$(\Delta E)(\Delta t) = k'(r/c) \geq \hbar, \quad k' > ch/r. \tag{32}$$

If r be restricted to be less than some maximum value, then $k' = q$ must always be greater than some minimum value hence likewise the Møller denominator $(E-E')^2 - q^2$ must remain finite. Thus the restriction upon the impact parameter has the same effect upon the terms arising from the retarded interaction as upon the Coulomb terms that was shown in Part IV, although it is more difficult to display this behavior explicitly. Thus the divergence of the cross section in the limit of soft quanta may be eliminated by restricting the value of the impact parameter to the order of the mean distance between electrons.

We turn now to the p-e collision. We see at once that the exchange terms will be small compared to the direct terms except for the case that the emergent particles come off almost parallel to each other. This corresponds to the emission of a very energetic quantum; the opposite situation to the one considered.

The matrix element for the p-e collision, omitting the exchange terms becomes:

$$H_{p-e} = -\left(\frac{32\pi^3\alpha^3}{L^9 k}\right)^{\frac{1}{2}}\left[(\mathbf{p}\cdot\mathbf{f})\left(\frac{1}{E-\mathbf{p}\cdot\mathbf{n}}+\frac{1}{E+\mathbf{p}\cdot\mathbf{n}}\right)\right.$$
$$\left.-(\mathbf{p}'\cdot\mathbf{f})\left(\frac{1}{E'-\mathbf{p}'\cdot\mathbf{n}}+\frac{1}{E'+\mathbf{p}'\cdot\mathbf{n}}\right)\right]$$
$$\times\left[\frac{(u'^*u)(u_1^*u_1')-(u'^*\boldsymbol{\alpha}u)\cdot(u_1^*\boldsymbol{\alpha}u_1')}{(E-E')^2-(\mathbf{p}-\mathbf{p}')^2}\right]. \tag{33}$$

It is seen to differ from the matrix element (27) for the e-e collision only in the omission of the exchange term and in the addition, instead of subtraction, of the Doppler factors. This latter difference is unimportant in the extreme relativistic limit as $[1/(E-\mathbf{p}\cdot\mathbf{n})] \gg [1/(E+\mathbf{p}\cdot\mathbf{n})]$ and the sum of these two terms will differ little from their difference. One sees thus that coherence effects are no longer important in the extreme relativistic limit. Such coherent superposition of the radiation emitted by each particle is permissible only if the wave-length of the emitted radiation is large compared with the physical dimensions of the radiating system. Such is not the case in the limit considered. The typical dimension of our radiating system is the impact parameter. The minimum value which the impact parameter can assume is $\hbar/mc$; smaller values are beyond the limit of measureability. This is of the order of magnitude of the wave-length of the quanta considered. The Møller denominators give an appreciable probability for the process only for very small scattering angles. Since we are considering the collision to be quasi-elastic ($k \ll E$) the impact parameter varies inversely with the scattering angle. So for a very small scattering we should expect a large impact parameter ($b > \hbar/mc = \lambda$). Also if the energy of the emitted quantum decreases (and the wave-length increases) the maxima of the Møller denominators become steeper, and the scattering angle for an appreciable probability of radiation gets smaller corresponding to a still larger impact parameter. So $b > \lambda$ for all but a negligible fraction of the emitted radiation. Hence the radiation from the two particles will be incoherent, and the charge of the emitting particle is inconsequential.

After integrating over-all angles we obtain finally for the positron cross section:

$$\Phi/\Phi_0 = (96/k^2)Edk. \tag{34}$$

We now want to transfer the cross section over into the laboratory system of reference. In the center-of-gravity system half the radiation is emitted in a narrow cone about the direction of the initial velocities in the forward direction and half is emitted in a similar cone in the backward direction. The half-angle of the cone is of the order of $1/2p^2$. Upon transferring to the laboratory system the backward scattered radiation is softened by a factor $1/(2E^*)^{\frac{1}{2}}$ and is nearly isotropic. The forward scattered radiation is hardened by a factor $(2E^*)^{\frac{1}{2}}$ and is emitted into a still narrower cone of half-angle of the order of $1/E^*$. Only the forward scattered radiation will be significant. The cross section for the forward-scattered radiation in the laboratory system is for the e-e case:

$$\frac{\Phi^*}{\Phi_0} = \frac{256}{k^{*2}}\left[\frac{E^*}{2}\left(1+\frac{p^*}{E^*}\right)\right]dk^* \tag{35}$$

and for the p-e case

$$\frac{\phi^*}{\phi_0}=\frac{48}{k^{*2}}\left[\frac{E^*}{2}\left(1+\frac{p^*}{E^*}\right)\right]dk^*. \tag{36}$$

These expressions are valid for $k\leq(E^*)^{\frac{1}{2}}$.

VI. CONCLUSIONS

The two cases calculated in detail do not, unfortunately, include the most important experimental situations. We may, however, draw certain conclusions regarding the general behavior of the cross section. The constructive interference of the radiation from oppositely charged particles and the corresponding annulment of radiation from particles of the same charge has been verified for the cases that the radiation from the two particles is coherent. Also the exchange effects were found to be negligible in the p-e case except in the extreme relativistic limit when a very energetic quantum is emitted.

The cross section for the e-e collisions was found to be negligible in the non-relativistic limit. For p-e collisions in this limit it is seen to agree with the expression for the "bremsstrahlung" from impacts of electrons on protons ($Z=1$), except for a numerical factor. We note further that the natural cross section for the "bremsstrahlung" is $\Phi_0=(\hbar/mc)^2\alpha^3Z^2$, that is Z^2 times the natural cross section for the p-e collision. It is then apparent that for light atoms the radiative collisions of positrons with orbital electrons will be of the same importance for energy loss as radiative collisions with the nucleus. The former process depends on the number of electrons per atom hence is proportional to Z while the latter is proportional to Z^2. For heavy atoms radiative impacts with the nucleus will predominate. Since the energy loss of electrons from radiative collisions with orbital electrons is zero we would expect the stopping of positrons of moderate energies in absorbers of low atomic weight to be greater than that of electrons even when the annihilations of the positrons in matter are not taken into account.

It is recognized that we have treated the electron in the collision as free so when the positron energy is of the same order as the ionization energy of the atom, the treatment breaks down. In such low energy regions, however, the most important cause of energy loss comes from exciting and ionizing impacts rather than radiative collisions.[14]

We can only infer a limited amount of information about the collisions in the extreme relativistic limit. All we can assert is that the cross sections for the emission of comparatively low energy quanta $k\leq E^{\frac{1}{2}}$ is of the same order of magnitude for both p-e and e-e collisions, the latter being larger by virtue of the exchange phenomenon. The quanta are emitted in the forward direction in a very narrow cone about the direction of the incident particle. The cross section increases with the energy instead of the logarithm of the energy as in the case of the "bremsstrahlung" cross section.

I wish to thank Professor W. H. Furry for having suggested this problem and for the considerable assistance and encouragement afforded me in carrying out the calculation.

[14] W. Heitler, reference 10, p. 217.

Letters to the Editor

PUBLICATION of brief reports of important discoveries in physics may be secured by addressing them to this department. The closing date for this department is five weeks prior to the date of issue. No proof will be sent to the authors. The Board of Editors does not hold itself responsible for the opinions expressed by the correspondents. Communications should not exceed 600 words in length.

On Polarization of Radiation by Interstellar Medium

W. A. HILTNER
Yerkes and McDonald Observatories, Universities of Chicago and Texas, Williams Bay, Wisconsin and Fort Davis, Texas
February 20, 1950

IT has been suggested by several authors that the polarization of the radiation from distant stars[1] is a consequence of elongated interstellar particles with axes pointing in a common direction.[2-4] It has been assumed that these particles were aligned by interstellar magnetic fields which are believed to exist[5] and which have been successfully employed by Fermi[6] in theoretical investigations on the origin of cosmic rays.

If the mechanism assumed above for the origin of interstellar polarization is correct then it must satisfy the observed characteristics of this polarization. The most stringent requirement is that the mechanism must predict the observed amount of polarization as a function of wave-length. If interstellar polarization is produced by the same particles as those that are responsible for interstellar absorption then it follows that interstellar polarization should show the same wave-length dependency as interstellar absorption which is known to be $1/\lambda$. The original observations of July, 1948, indicated that the amount of polarization is approximately independent of wave-length, in sharp contrast to interstellar absorption. It is important, therefore, that the spectral region be extended to more extreme wave-lengths than those originally employed.

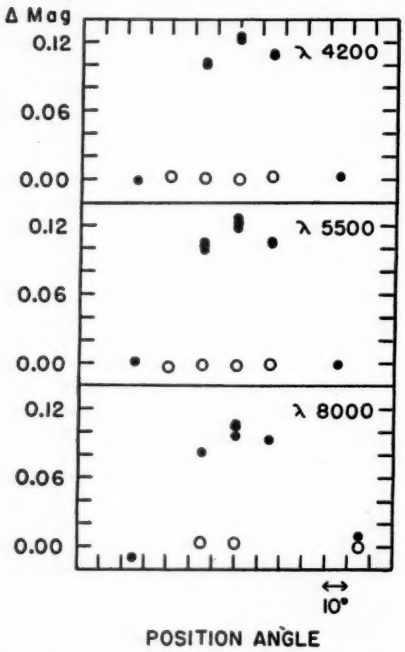

FIG. 1. Interstellar polarization of BD+62°643, closed circles, as a function of wave-length. Open circles refer to BD+40°500. The ordinates represent the change in intensity (expressed in magnitudes) when the Polaroid was rotated through 90°. See Astrophys. J. 109, 471 (1949) regarding the observational procedure.

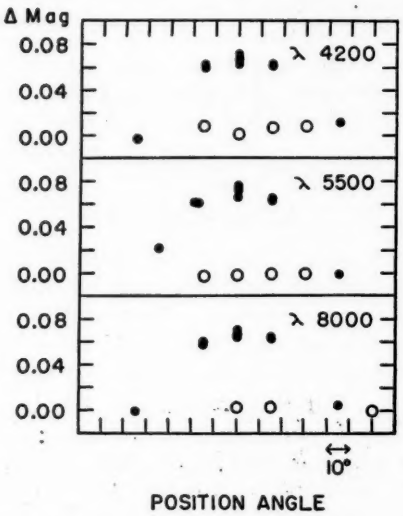

FIG. 2. Interstellar polarization of BD+58°607, closed circles, as a function of wave-length. Open circles refer to BD+40°500.

In December, 1949 observations were extended to the infra-red. A [Ag]−Cs_2O photo-cell (Ce−25) was used in conjunction with H_D in a.c. Polaroid. The estimated effective wave-length is 8000A. Two stars were observed, BD+62°643 and BD+58°607, with BD+40°500 serving as a check star with an assumed zero polarization. The results of these observations are shown in Figs. 1 and 2. The observations at effective wave-lengths 4200A and 5500A were made with a 1P21 multiplier photo-cell with Corning filters No. 5850 and 3385 respectively.

It is obvious that interstellar polarization does not show the same wave-length dependency as interstellar absorption, that is, as $1/\lambda$, but, to a first approximation, is independent of wave-length. Since electron scattering is independent of wave-length, the question arises as to whether or not an orientation of electrons by an interaction of their spins on the assumed magnetic fields may be responsible for the observed polarization.

A lower limit for the number of free electrons N_e per cm³ in interstellar space can be easily computed on the assumption that the electrons are uniformly distributed in space and that their spins are oriented in such a manner that the cross section, σ, for scattering of radiation has the value zero for one component and Thomson's value, $\sigma=8\pi e^4/3m^2c^4$ for the other. This assumption is an extreme one but it will provide a most favorable test for the idea. For the cluster h and χ Persei it has been observed that $\delta=0.075$. The accepted distance of this cluster is 1920 parsecs.[7] Consequently the minimum number of electrons necessary to produce the observed polarization is $N_e\sim17$. This must be contrasted with the estimated $N_e\sim3$ from other considerations.[8] While the latter estimate is uncertain, it is unlikely that it is in error by a large factor; indeed considerations relating to the dynamics of the galaxy would appear to rule out a value of $N_e\gg3$.

Although the new material presented here is limited, it is difficult to ignore the somewhat smaller polarization of BD+62°643 at 8000A than at the shorter wave-lengths and the remarkable constancy of polarization with wave-length in the case of BD +58°607. If further observational material confirms the suggestion that the wave-length dependency of polarization is not entirely uniform from star to star then this may give a clue to the origin of the observed polarization. Van de Hulst[9] has shown that the law of interstellar reddening can be predicted by the proper size distribution and refractive index of the interstellar particles. It seems likely that the same procedure may be applicable to the

prediction of the observed polarization as a function of wavelength.

It is a pleasure to thank Dr. Öhman for emphasizing the importance of extending the observations to more extreme wavelengths, and Drs. S. Chandrasekhar and O. Struve, for valuable discussions.

[1] W. A. Hiltner, Astrophys. J. 109, 471 (1949).
[2] Lyman Spitzer, Jr. and John W. Tukey, Science 109, 461 (1949).
[3] Leverett Davis, Jr. and Jesse L. Greenstein, Phys. Rev. 75, 1605 (1949).
[4] W. A. Hiltner, reference 1.
[5] H. Alfvén, Ark. f. mot. astr. och fysik 29B, No. 2 (1943).
[6] E. Fermi, Phys. Rev. 75, 1169 (1949).
[7] W. P. Bidelman, Astrophys. J. 98, 78 (1943).
[8] B. Stromgren, Astrophys. J. 108, 242 (1948).
[9] H. C. van de Hulst, Rech. Astr. del 'Obs. d'Utrecht, XI, Part 2 (1949).

Measurements of the Influence on the Fountain Effect of He^3 Dissolved in He^4

K. W. Taconis, J. J. M. Beenakker, and Z. Dokoupil
Kamerlingh Onnes Laboratory, University, Leyden, Holland
February 27, 1950

HELIUM gas containing 0.23 percent He^3 was condensed in a vessel of approximately 1 cm^3 capacity, which was connected to a second vessel by means of a narrow slit above the liquid level. The slit was almost gas-tight but open to the helium film. The pressure inside either of the two vessels, which were surrounded by a helium bath, could be measured against the vapor pressure of the bath by means of two differential oil manometers. In the second vessel there was a heating coil.

It is well known that in pure He^4 a fountain pressure (Δp) occurs between two vessels when a temperature difference (ΔT) is established, the contact being by way of the helium film. When ΔT is a few hundredths of a degree, Δp corresponds already to about 1 meter of liquid helium, hence the colder vessel in our arrangement will be emptied completely. With this apparatus, which is like that used by Daunt *et al.*,[1] in similar experiments, we found that the normal fountain effect can be compensated by dissolving He^3 in the colder vessel. Preliminary investigations at 1.38°K show that the "reduction" of the fountain pressure is approximately ρRTX, in which X is the He^3 concentration in the liquid in the colder vessel, the warmer vessel containing no He^3. The quantity ρRTX is the value of the osmotic pressure (P) for a dilute He^3 solution according to Van't Hoff's law. The same reduction, P, in the fountain pressure may be expected to a first approximation from the two-fluid model, if one assumes that the He^3 dissolves in the normal fluid only. According to the formulas given by De Boer and Gorter[2] (case A) the gradient of X gives rise to a gradient in x, the concentration of the normal fluid. In this picture the normal fountain effect is due to a gradient of x and this gradient is decreased by the gradient in He^3 concentration.

The values of X were derived from the measured values of the excess vapor pressure in the colder vessel due to the presence of He^3 in the vapor. This excess gives the concentration in the vapor; by measuring the height of the liquid level to obtain the volumes of liquid and vapor, we could then calculate X, the concentration in the liquid. The second column of Table I gives the values of the fountain pressure derived from the measured ΔT values using dates from Meyer and Mellink,[3] (the difference of the levels in the two vessels and the difference in vapor pressure above the two liquids can be neglected in first approximation in comparison with the fountain pressures).

Columns 4 and 5 of Table I give the calculated relative concentration c_V and c_L of He^3 in He^4 in the vapor and liquid respectively. The ratio c_V/c_L should be 300 at this temperature according to earlier measurements,[3] however, in these experiments we did not prevent the film creep circulation and did not stir the liquid as formerly, so that we are not surprised by these lower values.[4]

TABLE I. Measurements on the fountain effect.

ρRTX (mm Hg)	P (mm Hg)	v_{liq} (mm^3)	$c_V \cdot 10^3$	$c_L \cdot 10^3$	c_V/c_L
3.3	3.2	54	11	1.1	100
4.2	4.1	52	9	1.4	64
4.6	5.6	28	13	1.6	81
5.4	5.8	33	9.5	1.8	53
~8	8.5	~5	16	2.2	73

We thank Professor Gorter for very useful discussions.

Results at other temperatures will be published in Physica 's-Grav., when the accuracy of the measurements has been improved by a slight modification of the apparatus.

[1] Daunt, Probst, and Johnston, Phys. Rev. 73, 638 (1948).
[2] C. J. Gorter and J. de Boer, Phys. Rev. 77, 569 (1950); Commun. Kamerlingh Onnes Lab. Leyden, Suppl. No. 101a.
[3] L. Meyer and J. H. Mellink, Physica 's-Grav. 13, 197 (1947); Commun. Kamerlingh Onnes Lab. Leyden No. 272b.
[4] Taconis, Beenakker, Nier, and Aldrich, Physica 's-Grav. 15, 733 (1949); Commun. Kamerlingh Onnes Lab. Leyden No. 279a.

On the Determination of the Relative Positron Activity of Cu^{64} in a Source of Cu^{61}

C. Sharp Cook and Chia-hua Chang
Department of Physics, Washington University, St. Louis, Missouri
March 1, 1950

PREVIOUS studies[1,2] of the positron spectrum of Cu^{61} have been reported under the assumption that any other activity in the source is of negligible proportions. This has been borne out through the fact that half-life measurements made at different parts of the spectrum have indicated, within experimental error, a single value of 3.33 hours, corresponding to the half-life for Cu^{61}. However, since these sources were prepared by deuteron bombardment of nickel it is quite possible that a certain amount of Cu^{64} was produced from the 1.16 percent abundant Ni^{64} isotope by a $(d,2n)$ reaction. The purpose of this discussion is to set an upper limit on the amount of positron activity which could have been attributed to Cu^{64}.

In order to determine the amount of Cu^{64} present in a given sample the decay of the Auger electrons[2] was observed by means of a lens-type magnetic spectrometer over a period of more than 24 hours following the removal of the nickel target from the cyclotron. Copper was separated by means of the electrochemical process previously described.[1]

The concentration of Auger electron energies into a small interval is advantageous for this experiment. One does not need a source of very high intensity in order to have an appreciable counting rate above background even for the very weak Cu^{64} activity. In addition the relative activity of Cu^{64} to Cu^{61} as measured by the K-capture process is larger than the corresponding ratio of positron activities. The lower intensity activity can thus be more easily observed.

If only the 3.33 hour Cu^{61} activity were present, correction of the experimentally observed data to an initial time should always lead to an Auger line whose intensity is constant. Correction of the data during the initial stages of the decay gave this result. However, as time progressed, it was found that the 3.33 hour half-life correction gave ever increasing intensities for the Auger line at the initially chosen time. The assumption of the existence of a small amount of a second activity having a half-life of 12.8 hours could however account for the decay of the sample as observed.

When corrected to the end of the 2½ hour period of cyclotron bombardment the Auger line was found to have consisted of 99.23 percent of the 3.33 hour Cu^{61} and 0.77 percent of the 12.8 hour Cu^{64}.

In order to calculate the relative positron activities the experimentally determined[4] ratio $(K_{64}/\beta_{64}^+)/(K_{61}/\beta_{61}^+)=5.5$ was used. This gives a value of $\beta_{64}^+/\beta_{61}^+=0.00141$ from our observed value $K_{64}/K_{61}=0.00775$.

The longest period of cyclotron bombardment which has been used for production of Cu^{61} has been 4 hours. On the basis of the ratio of activities after 2½ hours of bombardment time one finds that after 4 hours of bombardment time the relative positron activities $\beta_{64}^+/\beta_{61}^+$ would be 0.00157. No positron source has been studied for a period lasting more than three half-lives of Cu^{61} following the removal of the nickel target from the cyclotron. Using the data above one finds that even after three half-lives the sample which was bombarded for four hours would have a positron activity ratio $\beta_{64}^+/\beta_{61}^+=0.00733$. Quite a bit less than one percent of the activity can thus be attributed to Cu^{64}.

This study verifies the fact that only negligible quantities of the Cu^{64} positron activity existed in the samples which have been studied to determine the shape of the positron spectrum of Cu^{61}.

This work has been supported by the joint program of the ONR and AEC.

[1] C. S. Cook and L. M. Langer, Phys. Rev. **74**, 227 (1948).
[2] G. E. Owen and C. S. Cook, Phys. Rev. **76**, 1536 (1949).
[3] The Auger electrons were assumed for this experiment to represent a ratio of intensities for the K-capture processes in the two isotopes under consideration. In reality a small amount of the intensity of the Auger line for Cu^{61} would be caused by the internal conversion electrons. However, their intensity is much less than the K-capture intensity and could not cause a detectable change in the experimentally observed value. [See Boehm, Blaser, Marmier, and Preiswerk, Phys. Rev. **77**, 295 (1950) and Owen, Cook, and Owen (article to be submitted to Phys. Rev.).]
[4] Bradt, Gugelot, Huber, Medicus, Preiswerk, and Scherrer, Helv. Phys. Acta **18**, 252 (1945).

The Latitude and Longitude Effects in Cosmic Rays Over the United States and Canada at 30,000 Feet*

A. T. Biehl and H. V. Neher
California Institute of Technology, Pasadena, California
March 2, 1950

THE change with geomagnetic latitude of the ionizing particles at 310 g/cm^{-2} atmospheric pressure (30,000 ft.) that could penetrate various thicknesses of absorber was measured by Biehl, Neher, and Roesch[1] over a range of latitude of 64° geomagnetic north to the geomagnetic equator along longitude 80°W. These flights show that most of the latitude effect is over at 50° as one proceeds north and this was independent of the absorber used or of whether the total radiation at that altitude was measured or only that near the vertical. On the other hand Swann, Morris and Seymour[2] find a 10 percent increase for a 10° increase in geomagnetic latitude at 30,000 feet even beyond the "knee" of the curve. Although no mention of an absorber was made, presumably their measurements were made with a lead absorber.

A number of flights having a further bearing on this point have recently been made, covering the latitude range particularly from 40° to 64° geomagnetic north with counter telescopes and ionization chambers, the latter both unshielded and shielded with 10 cm of lead.

In Fig. 1 the measurements made with two of our ionization chambers,[3] which were sealed off 12 years ago, are shown, the one with no lead shield, the other with a 10 cm lead shield. Curve A is that taken[1] in June 1948 along longitude 80° W while B was taken in October, 1949 along 115° W using the same instrument as for A. Curve C was taken with a companion instrument along 115° W but surrounded with 10 cm of lead. B is the result of 3 flights made within a period of five days. Where these flights overlapped they differed by ±2.0 percent, which was well outside the experimental errors and are hence assumed to represent real changes in the primary radiation during this period. Curve B is therefore drawn to represent the mean of these flights.

In Fig. 2 are shown the corresponding results with counter telescopes over the same range of latitudes at the same two longitudes, namely 80° and 115° W. Curve A′ and C′ have been published previously[1] but are here given in greater detail. Curve B′ was taken in October, 1949. In addition curve D′ is given which represents the mean of six flights made during the summer of 1948 along longitude 117° W and at 33,000 ft. pressure altitude.

Comparing corresponding curves in Figs. 1 and 2 the following conclusions are evident: (a) There is a small increase both with counter telescopes and ionization chambers of 2.5 to 3 percent from latitude 50° to 64° N and is approximately the same with or without a 10 cm lead absorber. (b) In going south with latitude 50° N the curves taken along longitude 80° W fall off more slowly than along longitude 115° W.

Table I gives a summary of the experimental situation. (Numbers given in the table are in percent change of radiation per degree change in geomagnetic latitude.)

In seeking an explanation for why the curves along 80° W longitude fall off at a different rate from along 115° W, we measured the film taken with the unshielded ionization chamber along a constant geomagnetic latitude line on a flight at 30,000 ft. from California to Florida on August 1, 1949. The route varied less than 0.5° from geomagnetic latitude 40.8° N and a slight correction taken from Figs. 1 and 2 of approximately 1 percent per degree

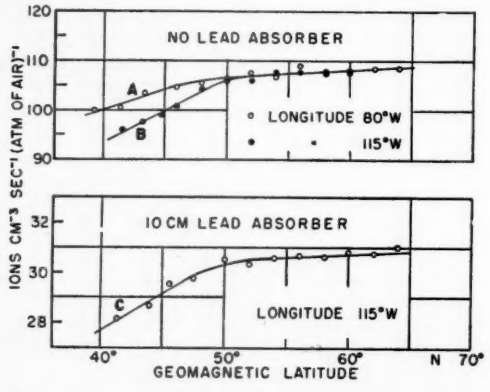

FIG. 1. These curves show the ionization as a function of latitude at two different longitudes at an altitude corresponding to 310 g/cm^{-2} air pressure. The probable errors in the points, as determined by the scatter of the individual discharges on the film, are given approximately by the diameter of the points.

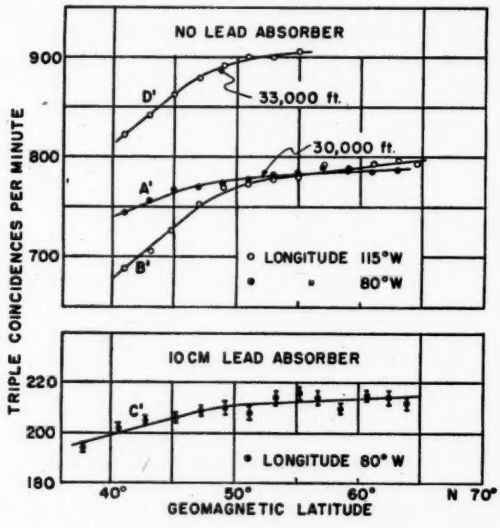

FIG. 2. Similar curves to those in Fig. 1 but taken with counter telescopes pointing vertically.

TABLE I. Percentage increase per degree change in latitude.

λ_{mag}	No added absorber: Total ionization	No added absorber: Vertical radiation	10 cm lead: Total ionization	10 cm lead: Vertical radiation
A. Along longitude 80° W				
45°N	1.3	1.3	1.9	—
50°–64°N	0.16	0.18	0.25	—
B. Along longitude 115° W				
45°N	0.7	0.6	—	0.6
50°–64°N	0.2	0.1	—	0.18

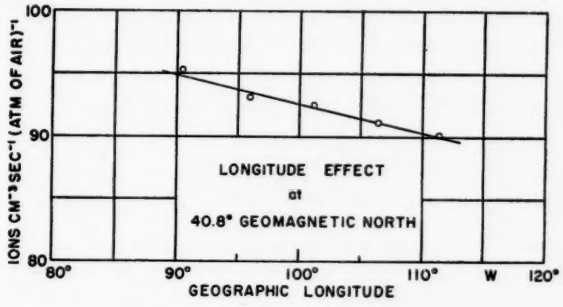

FIG. 3. The longitude effect at 310 g/cm^{-2} air pressure as determined with the unshielded ionization chamber.

was applied when necessary. The result is plotted in Fig. 3. It is seen that there is in fact a longitude effect amounting to -0.24 percent per degree change in longitude. Extrapolated to 80° W and 115° W this curve would indicate on 8.2 percent decrease in going from 80° W to 115° W at this geomagnetic latitude and altitude. From Figs. 1 and 2 we find a corresponding difference of 6.2 percent for the ionization chamber and 8.2 percent for the counter telescope, each unshielded.

With the help of the theory of the behavior of charged particles in the magnetic field of a dipole as worked out by Vallarta *et al.* we have made an estimate of the longitude effect to be expected at this latitude due only to the eccentricity of the equivalent magnetic dipole of the earth. Thus one can calculate approximately the change in minimum momentum of the incident particles for a given change in longitude in terms of the corresponding change in latitude. Using the experimental data for the latitude effect as given in Fig. 1 the calculated value of the longitude effect at 40.8° geomagnetic north and 100° geographic west is -0.29, a value consistent with the measured value of -0.24 percent per degree change in longitude.

We wish to express our gratitude to the ONR and the United States Air Forces for making these flights possible. We also wish to thank Major W. A. Gustafson, Captain Z. Shawhan, Captain George Freyer and other members of the crew of the B-29 for their cooperation and expert handling of the plane.

* Supported in part by the joint program of the ONR and AEC.

[1] A. T. Biehl, H. V. Neher, and W. C. Roesch, Phys. Rev. **76**, 914 (1949).
[2] Swann, Morris and Seymour, Phys. Rev. **75**, 1317A (1949).
[3] R. A. Millikan and H. V. Neher, Phys. Rev. **50**, 15 (1936).

Energy Band Structures in Semiconductors

W. SHOCKLEY
Bell Telephone Laboratories, Murray Hill, New Jersey
March 6, 1950

A METHOD of attack is proposed which for semiconductors has the potentiality of actually determining the shapes of the energy surfaces in the Brillouin zone in detail by proper comparison with experiment. The essential feature is that the most complicated family of energy surfaces arising from a degenerate energy band in a cubic crystal can be described by three parameters. Similar results for the restricted case of tight binding have been discussed by Sommerfeld and Bethe.[1] We shall illustrate the more general case in terms of the wave functions near the bottom of an energy band which has its lowest energy H_0 at the center of the Brillouin zone and is triply degenerate with p-type wave functions,[2] type δ, which have the periodicity of the lattice. These are denoted by

$$\psi_x = xu_x(x^2, y^2, z^2) = xu_x(x^2, z^2, y^2), \quad \text{etc.}$$

A wave function near the lowest energy of the band may be written as

$$\Phi = [a_x\psi_x + a_y\psi_y + a_z\psi_z + \Sigma_{\alpha i} b_{\alpha i}\varphi_{\alpha i}] \exp(i\mathbf{P}\cdot\mathbf{r}/\hbar),$$

where the $\varphi_{\alpha i}$ are also periodic and satisfy $H\varphi_{\alpha i} = H_\alpha\varphi_{\alpha i}$. In order to solve the eigenvalue problem $(H-W)\Phi = 0$, a set of equations for the coefficients is found by multiplying by $\exp(-i\mathbf{P}\cdot\mathbf{r}/\hbar)\psi_x^*$, etc. and the resulting system treated by a method similar to that of Van Vleck[3] so as to eliminate the b's. This gives

$$[AP_x^2 + B(P_y^2 + P_z^2) - K]a_x + C[P_xP_ya_y + P_xP_za_z] = 0, \quad (1)$$

and similar equations with permuted indices (x, y, z), where $K = W - H_0$ is essentially the kinetic energy of motion and

$$A - \tfrac{1}{2}m = \Sigma_{\alpha i}(x|p_x|\alpha i)(\alpha i|p_x|x)/m^2(H_0 - H_\alpha),$$
$$B - \tfrac{1}{2}m = \Sigma_{\alpha i}(x|p_y|\alpha i)(\alpha i|p_y|x)/m^2(H_0 - H_\alpha),$$
$$C = \Sigma_{\alpha i}[(x|p_x|\alpha i)(\alpha i|p_y|y) + (x|p_y|\alpha i)(\alpha i|p_x|y)]/m^2(H_0 - H_\alpha).$$

These equations are formally identical with equations for the frequency and polarization of an acoustical wave of displacement

$$\delta\mathbf{r} = \mathbf{G}\exp i(\mathbf{k}\cdot\mathbf{r} + \omega t)$$

which gives

$$[c_{11}k_x^2 + c_{44}(k_y^2 + k_z^2) - \rho\omega^2]G_x + (c_{12} + c_{44})(k_xk_yG_y + k_xk_zG_z) = 0.$$

The secular equations for both the quantum and the mechanical cases give surfaces of three sheets in $\mathbf{k}$ space for a given eigenvalue, the "polarization vector" (a_x, a_y, a_z) of the wave function being analogous to $\mathbf{G}$. The present treatment was suggested by the analogy of the surfaces Fig. 1 computed[4] for the $3p$ band in NaCl to acoustical surfaces. The symmetry of (1) follows directly, of course, from the fact that it is quadratic in P and that the crystal is cubic.

A similar procedure for wave functions of the form[2] $x^2 - y^2$, $y^2 - z^2$ (type γ) leads to secular equation of two constants:

$$K^2 + 2FK + GP^4 + 3(F^2 - L(P_x^4 + P_y^4 + P_z^4) = 0,$$

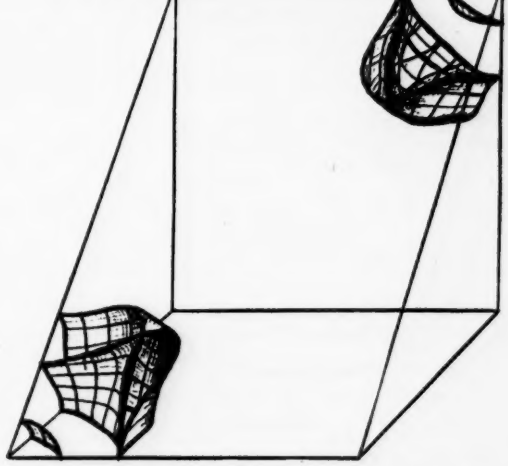

FIG. 1. Energy surface for degenerate band for $\mathbf{k} \approx 0$.

where F and G are similar to A, B, C. This formula can also be obtained directly from the condition that for $\mathbf{P}\|[111]$ the degeneracy of $x^2+\omega y^2+\omega^2 z^2$ and $x^2+\omega^2 y^2+\omega z^2$ ($\omega^3=1$) is not removed.

In the event that the minimum energy occurs at a lower symmetry point in the Brillouin zone, similar procedures can be adopted; however, more parameters may be involved.

Experimental results of G. L. Pearson[5] and H. Suhl[6] of the magneto-resistance of germanium indicate strongly that isotropic scattering and spherical energy surfaces cannot explain the data. It is to be hoped that the method of "deformation potentials"[7] can be extended to the case of degenerate energy bands so as to give a not more than three parameter (A, B, C) theory which may be compared with experiment to determine the band shapes.

I am indebted to J. Bardeen, C. Herring, and F. Seitz for helpful discussions of group-theoretical aspects of this problem, and to P. M. Morse for suitable perspective.

[1] A. Sommerfeld and H. Bethe, *Handbuch. der Physik* 24/2 (Julius Springer, Berlin, 1933).
[2] For a classification of Kubic Harmonics see F. C. Von der Lage and H. A. Bethe, Phys. Rev. 71, 612 (1947).
[3] J. H. Van Vleck, Phys. Rev. 33, 467 (1929); see L. I. Schiff, *Quantum Mechanics* (McGraw-Hill Book Company, Inc., New York, 1949), p. 155.
[4] W. Shockley, Phys. Rev. 50, 754 (1936).
[5] G. L. Pearson, Bull. Am. Phys. Soc. 25, No. 2, I13 (1950).
[6] H. Suhl, Bull. Am. Phys. Soc. 25, No. 2, I14 (1950).
[7] W. Shockley and J. Bardeen, Phys. Rev. 77, 407 (1950).

Microwave Measurements on the Stable Selenium Isotopes in OCSe*

S. Geschwind, H. Minden, and C. H. Townes
Columbia University, New York, New York
February 27, 1950

From a re-examination of the $J=2\rightarrow3$ transition in OCSe (previously studied by Strandberg[1]), the relative masses of the stable Se isotopes have been determined, and an upper limit of 0.002×10^{-24} cm^2 assigned to the quadrupole moments.

A balanced bridge superheterodyne spectrometer[2] was used to obtain OCSe rotational lines (which occur near 24,000 Mc) as narrow as 60 kc. This high resolution allowed very accurate frequency measurements to be made by the usual comparison with harmonics of a quartz crystal. The differences between isotopic lines and their statistical errors resulting from approximately seven measurements of each are given in Table I. Allowing for possible systematic errors, these separations are probably accurate to 0.015 Mc. They differ appreciably—in one case as much as 0.5 Mc—from an earlier measurement,[1] and hence modify considerably the isotopic masses previously obtained.

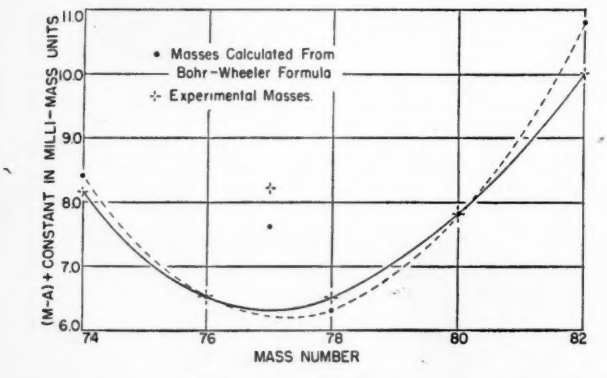

FIG. 1. Variation of masses of the stable Se isotopes as a function of mass number. The experimental masses are determined after assuming Se^{76} and Se^{80} are correctly given by the semi-empirical Bohr-Wheeler formula.

TABLE I. Observed frequency differences between the $O^{16}C^{12}Se$ lines.

	$\Delta\nu$(Mc/sec.)
$O^{16}C^{12}Se^{78}\rightarrow OCSe^{74}$	320.43 ±0.013
$O^{16}C^{12}Se^{78}\rightarrow OCSe^{76}$	156.15 ±0.006
$O^{16}C^{12}Se^{78}\rightarrow OCSe^{77}$	76.95 ±0.008
$O^{16}C^{12}Se^{78}\rightarrow OCSe^{80}$	148.58 ±0.008
$O^{16}C^{12}Se^{78}\rightarrow OCSe^{82}$	290.10 ±0.004
$O^{16}C^{13}S^{32}\rightarrow OCSe^{77}$*	5.458 ±0.007

* The absolute frequency of the $OCSe^{77}$ line is 29,331.38 assuming the $O^{16}C^{12}S^{32}$ frequency as previously measured to be 24,325.92.

TABLE II. Experimentally determined masses of stable Se isotopes compared with masses calculated from semi-empirical mass formula.

A (mass number)	Experimental masses	Masses calculated from Bohr-Wheeler mass formula
74	73.9481 ±0.0006	73.9484
76	75.9465*	75.9465
77	76.9482 ±0.0004	76.9476
78	77.9465 ±0.0004	77.9463
80	79.9478*	79.9478
82	81.9500 ±0.0006	81.9508

* These masses are assumed to be given exactly by the Bohr-Wheeler formula.

If zero-point vibrations were not present, the rotational frequencies of OCSe and a known mass of one Se isotope would give the other five Se masses to an accuracy limited only by the errors of measurement. The 0.015 Mc frequency uncertainty would then correspond to an error of 0.00018 mass unit. Zero-point vibrations are of course unavoidable, but if two isotopic Se masses are taken to be known, the errors due to zero-point vibrations can be largely eliminated and the other four Se masses determined with rather good accuracy.[2,3] Table II lists the masses and the maximum errors expected due to a combination of experimental uncertainty and the residual errors due to zero-point vibrations. These latter will be discussed more fully in a subsequent paper.

The experimental masses (assuming values of Se^{76} and Se^{80} given by the Bohr-Wheeler formula) are plotted in Fig. 1 and compared with predictions of the Bohr-Wheeler formula.[4] It may be seen that agreement between the curvature of the mass defect and the odd-even mass difference is rather good, although there are some discrepancies larger than the errors allowed in Table II. This method of mass measurement is especially good for determination of the odd-even mass difference since the distance which the odd isotope, Se^{77}, lies off the curve of the even masses is unaffected by errors in the assumed Se^{76} and Se^{80} masses or by uncertainties due to zero-point vibrations. The odd-even mass difference is found to be 0.0018 mass units, rather than $\delta=0.036/A^{\frac{1}{2}}=0.0014$ from the Bohr-Wheeler formula.

Although the OCSe lines were obtained as narrow as 60 kc, no noticeable asymmetry or splitting suggestive of hyperfine structure was observed in Se^{77} or in any other Se isotopes. In addition, the Se^{77} line-width was measured to be the same, within 5 kc, as that of Se^{76}. This agrees with previous observations,[1] and is a rather strong indication that the spins of the even isotopes are zero, and that of Se^{77} one-half, since then no quadrupole hyperfine structure could be observed. If the Se^{77} spin is not $\frac{1}{2}$, examination of the theoretical quadrupole coupling patterns for various spins gives an upper limit of 1 Mc to the quadrupole coupling constant $eQ\partial^2V/\partial z^2$. In comparison, S^{33} shows a coupling constant of -28.5 Mc in the very similar molecule OCS. Estimating $\partial^2v/\partial z^2$ for Se in OCSe by the same method[5] as was used for OCS, an upper limit of 0.002×10^{-24} cm^2 may be assigned to the Se^{77} quadrupole moment. Such a small quadrupole moment is puzzling in view of measurements on the optical hyperfine structure which indicate a spin for Se^{77} of 5/2 or greater.[6] It may be connected, however, with closure of a proton shell[7] at Se^{77}.

Since the Se^{79} is still unknown, Mr. William Low searched for a line due to $OCSe^{79}$, using a recording Stark modulation spectrometer and with the OCSe gas at dry ice temperatures. If the Se^{79} occurred naturally, it should produce a line very near that due to the $OCSe^{80}$, $v_2=2$, $l=0$ transition. No absorption attributable to Se^{79} was found, however, and since the nearby OCSe, $v_2=2$, $l=0$ line strength was about seven times noise background (at $-78°$C), an upper limit of one part in 10,000 may be set on the natural abundance of Se^{79}.

The design of the heterodyne spectrometer has benefited from the advice of Professor Yardley Beers. In addition, the authors appreciate the considerable help of Mr. R. H. Ellis, Jr. in construction of the spectrometer, and the interest of Mr. Paul Kisliuk who some time ago initiated work on these measurements but was not able to carry them through with the equipment then available.

* Work supported jointly by the Signal Corps and ONR.
[1] Strandberg, Wentink, and Hill, Phys. Rev. 75, 827 (1949).
[2] Columbia Radiation Laboratory Quarterly Report (June 30, 1949).
[3] Townes, Holden, and Merritt, Phys. Rev. 74, 113 (1948).
[4] Quoted by M. G. Mayer and E. Teller, Phys. Rev. 76, 1227 (1949).
[5] C. H. Townes and B. P. Dailey, J. Chem. Phys. 17, 796 (1949).
[6] J. E. Mack and O. V. Arroe, Phys. Rev. 76, 173 (1949), and private communication.
[7] Townes, Foley, and Low, Phys. Rev. 76, 1415 (1949).

Resonance and Thermal Neutron Scattering in V^{51}

M. Hamermesh and C. O. Muehlhause
Argonne National Laboratory, Chicago, Illinois
February 27, 1950

A LITERAL application of the Breit-Wigner scattering theory enables one to correlate the experimental values of the resonance and thermal cross sections of V^{51}

Harris, Hibdon, and Muehlhause[1] have reported a prominent neutron scattering resonance ($\Gamma_n \gg \Gamma_\gamma$) in V^{51} at $\sim$2700 ev with a scattering resonance integral, Σ_s, of 192b. This quantity yields the coherent thermal scattering amplitude, a, via the following relations:

$$a=g(\lambda\!\!\!^{-}_0\Gamma_n/2E_0), \quad \Sigma_s=\tfrac{1}{2}\pi g\sigma_0\Gamma_n/E_0,$$

and

$$\sigma_0=4\pi\lambda\!\!\!^{-}_0{}^2=2.60\times10^6/E_0,$$

where $\lambda\!\!\!^{-}_0$=neutron wave-length at the resonance energy, Γ_n=neutron width, E_0=resonance energy, and $g=\frac{1}{2}(1\pm1/2i+1)$ is the statistical weight factor ($i=7/2$, spin of V^{51}). These relations yield the formula

$$a=\lambda\!\!\!^{-}_0\Sigma_s/\pi\sigma_0=0.555b^{\frac{1}{2}} \text{ (units of } 10^{-12} \text{ cm)}.$$

Shull and Wollan[2] have reported the coherent thermal scattering cross section, σ_{coh}, to be less than 0.1b (units of 10^{-24} cm^2). This quantity, according to the one-level Breit-Wigner formula, is given by:

$$\sigma_{coh}=4\pi|R-(g\lambda\!\!\!^{-}_0\Gamma_n/2E_0)|^2=4\pi|R-a|^2;$$

where $R=0.137A^{\frac{1}{3}}$ is the nuclear radius. For V^{51} we have $R=0.508b^{\frac{1}{2}}$ and therefore:

$$\sigma_{coh}=4\pi|0.508-0.555|^2\simeq0.03b \text{ (negative phase)}.$$

The resonance data are also in good agreement with the total thermal scattering cross section, σ_s, given by Hibdon[3] as 5.02b. This quantity can be used to determine the total angular momentum, J, of the compound state at 2700 ev. Again the one-level Breit-Wigner expression for σ_s yields:

$$\sigma_s=4\pi g|R-(a/g)|^2+4\pi(1-g)R^2,$$

from which

$$\sigma_s=5.02b \ (g=7/16 \text{ for } J=3),$$

or

$$\sigma_s=3.04b \ (g=9/16 \text{ for } J=4).$$

Preference is therefore indicated for $J=3$. One may also conclude that

$$\sigma_{max}\simeq420b \quad \text{and} \quad \Gamma\simeq780 \text{ ev}.$$

Since one resonance level determines the thermal scattering cross section so completely it appears that the next closest level, ϵ_2, from zero energy is such that $|\epsilon_2|\gg2700$ ev. Other cases of light odd-Z, even-n, isotopes which display this same level pattern are:[4-6] Na, Cl, Co, and Mn.

[1] Harris, Hibdon, and Muehlhause (unpublished work).
[2] C. G. Shull and E. O. Wollan, Naturwiss. 10, 291 (1949).
[3] C. T. Hibdon (unpublished work).
[4] Hibdon, Muehlhause, Selove, and Woolf, Phys. Rev. 77, 730 (1950).
[5] C. T. Hibdon and C. O. Muehlhause, Phys. Rev. 76, 188 (A) (1949); S. Harris and C. O. Muehlhause, Phys. Rev. 76, 189 (A) (1949).
[6] Harris, Hibdon, and Muehlhause (unpublished work).

Observations of the Rapid Withdrawal of Stored Holes from Germanium Transistors and Varistors

L. A. Meacham and S. E. Michaels
Bell Telephone Laboratories, Murray Hill, New Jersey
March 6, 1950

IN the course of a study of transistor response to square pulses of applied voltage and current, the behavior illustrated in Fig. 1 was found to be typical of units employing N-type germanium. The collector current I_c is there shown as a function of time for different pulsed values of I_e (emitter current) and V_c (collector voltage), applied as independent parameters. For each of the curves except the ones marked "steady state," V_c was pulsed from zero to 10 volts in the "reverse" direction (for which the point contact normally has a high resistance) for a period of one microsecond.

The bursts of collector current provoked by preceding emitter current appeared to be explainable most reasonably on the basis of a rapid gathering-in of holes[1] produced by the forward emitter current and existing within the germanium at the time of application of collector potential. This explanation suggested that the same electrode might be used first to inject holes as an emitter and then to withdraw them as a collector. When this was tried, bursts of reverse current exceeding 24 milliamperes and overloading the pulser were obtained for the same voltage pulses, which interrupted a normal forward current of only 1 milliampere. With the forward current reduced to zero, the reverse current pulses became square and only a fraction of a milliampere in height.

Using a more powerful pulse generator for examining conventional germanium varistors (diodes) of various types, we found that the response curves could be classified into several dis-

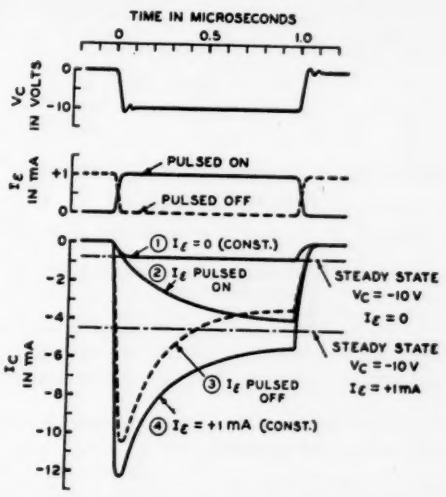

FIG. 1. Pulse study of transistors—typical wave forms.

tinctive types, this classification apparently having little or no relation to the steady-state characteristics. Typical response curves are shown in Fig. 2. In each case the forward current between pulses was 40 milliamperes and the potential V was carried from a small positive value to -50 volts with a rise time of approximately 0.03 microsecond. Curve A represents a large class of varistors showing no appreciable effect of hole withdrawal. Curve B shows a small or moderate burst, having an exponential decay with a time constant of the order of 0.1 microsecond. In curve C, the reverse current first rises roughly in proportion to the voltage, then drops very abruptly and once more rises, after which

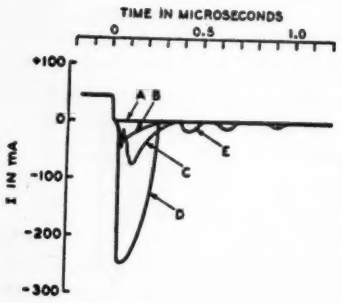

FIG. 2. Pulse study of germanium diodes.

the decay is approximately exponential. Curve D shows a curious case (not particularly rare, however) representing a momentary dissipation of over 10 watts. The decaying portion of the wave form is concave upward, reaching the zero line with a remarkably sharp discontinuity. This phenomenon may be explainable in terms of the Herring shock wave.[2] Some units represented by curve D also display "bubbles" of current (curve E). These bubbles are usually observed upon initial application of the test conditions, and commonly decrease in amplitude and vanish within five or ten seconds. The bubbles, or trains of them, recur with each applied pulse but may progress gradually toward the right or left on the time axis during their appearance.

The large bursts of power associated with these effects may be expected to change the characteristics of the units, and Mr. R. R. Blair has suggested that they may account for certain previously unexplained cases of damage to varistors in switching applications. Further studies using steep wave fronts backed by ample power appear likely to contribute to the basic understanding of semiconductors.

We wish to express our thanks to Mr. W. L. Shockley and other members of Bell Laboratories for helpful suggestions in connection with this work.

[1] W. Shockley, G. L. Pearson and J. R. Haynes, Bell Sys. Tech. J. **XXVIII**, 344 (1949).
[2] C. Herring, Bell Sys. Tech. J. **XXVIII**, 401 (1949).

The Elastic Constants of Germanium Single Crystals

W. L. BOND, W. P. MASON, H. J. MCSKIMIN, K. M. OLSEN, AND G. K. TEAL
Bell Telephone Laboratories, Murry Hill, New Jersey
February 27, 1950

THE interest in the properties of germanium single crystals arising from their use as semiconductors and transistors has led us to make measurements of the elastic constants of two single crystals.

One crystal (sample A) was grown from the melt, and two orientations were determined approximately by x-rays. Longitudinal and shear wave measurements of velocities were made along the 100 and 110 directions by the process described in an earlier communication.[1] This process determines the velocity within about

TABLE I. Elastic properties of sample A.

Direction of propagation	Direction of particle motion	Type of mode	Equation for velocity	Measured velocity cm/sec. $\times 10^{-5}$	Elastic constants dynes/cm^2 $\times 10^{-11}$
110	110	long	$v=\left(\frac{c_{11}+c_{12}+2c_{44}}{2\rho}\right)^{\frac{1}{2}}$	5.39	15.5
110	$1\bar{1}0$	shear	$v=\left(\frac{c_{11}-c_{12}}{2\rho}\right)^{\frac{1}{2}}$	2.75	4.06
110	001	shear	$v=(c_{44}/\rho)^{\frac{1}{2}}$	3.54	6.70
100	100	long	$v=(c_{11}/\rho)^{\frac{1}{2}}$	4.92	12.95
100	010	shear	$v=(c_{44}/\rho)^{\frac{1}{2}}$	3.54	6.70

½ percent. The longitudinal and shear-wave velocities are shown by Table I. The elastic constants are calculated from the velocity measurements using a density of 5.35. From these measurements we obtain the elastic constants (in dynes/cm^2)

$$c_{11}=12.92\pm0.12\times10^{11},\quad c_{12}=4.79\pm0.12\times10^{11},$$
$$c_{44}=6.70\pm0.07\times10^{11}.$$

The other crystal (sample B) was obtained by an improved method for growing pure germanium crystals[2] and a more accurate method was devised for measuring velocities for small samples.[3] Hence it was thought worth while to re-measure the elastic constants. A carefully oriented 110 section was used and the measured velocities are shown in Table II. From these values the three elastic constants are found to be (in dynes/cm^2)

TABLE II. Elastic properties of sample B.

Direction of propagation	Direction of particle motion	Type of wave	Equation for velocity	Measured velocity cm/sec. $\times 10^{-5}$	Elastic constants dynes/cm^2 $\times 10^{-11}$
110	110	long	$v=\left(\frac{c_{11}+c_{12}+2c_{44}}{2\rho}\right)^{\frac{1}{2}}$	5.410 ± 0.005	15.660 ± 0.03
110	$1\bar{1}0$	shear	$v=\left(\frac{c_{11}-c_{12}}{2\rho}\right)^{\frac{1}{2}}$	2.751 ± 0.002	4.049 ± 0.008
110	001	shear	$v=(c_{44}/\rho)^{\frac{1}{2}}$	3.547 ± 0.003	6.730 ± 0.01

$$c_{11}=(12.98\pm0.04)\times10^{11};\quad c_{12}=(4.88\pm0.04)\times10^{11};$$
$$c_{44}=(6.73\pm0.01)\times10^{11}.$$

[1] Bozorth, Mason, McSkimin, and Walker, Phys. Rev. **75**, 1954 (1949).
[2] This method is described by G. K. Teal and J. B. Little in a paper to be presented by title before the Oak Ridge meeting of the Physical Society (March, 1950).
[3] This method for measuring velocities by a phasing technique was described by H. J. McSkimin, J. Acous. Soc. Am. **22**, 86 (1950).

Energies of Some Gamma-Rays from ThC″, RaC, and Na^{24}

J. L. WOLFSON
Atomic Energy Project, National Research Council of Canada, Chalk River, Ontario, Canada
February 23, 1950

PRECISE values for the energies of the gamma-rays of nominal values 2.62 Mev from ThC″, and 2.2 Mev and 2.4 Mev from RaC, have recently become desirable in order to evaluate more accurately the binding energy of the deuteron.[1,2] Several measurements of the energies of these gamma-rays have been made and the results are presented in Tables I, II, and Fig. 3. In addition some measurements of the energy of the Na^{24} gamma-ray of nominal value 2.76 Mev, performed for another purpose, are given in Table II as they may be of interest in future disintegration studies.

TABLE I. Measurement of the 2.615-Mev ThC″ gamma-ray, using composite thin sources, by comparison of the "X" line from ThC″ with the K internal conversion line from the 0.4112±0.0001-Mev transition following Au^{198} decay.

Trial	X-line momentum (gauss-cm)	Gamma-ray energy (Mev)	Weight
1	9992	2.616	1
2	9992	2.616	1
3	9986	2.614	1
4	9990	2.615	1
5	9982	2.613	2
6	9989	2.615	2
Weighted mean	9988±13	2.615±0.004	

Previous studies of these gamma-rays have resulted in energy values ranging from 2.613 to 2.620 Mev for the ThC″ gamma-ray,[3,4] and energy values of 2.198 and 2.200 Mev,[5,6] and of 2.432 and 2.420 Mev for the two RaC gamma-rays,[5,6] while the most recent spectrometric determination of the Na^{24} gamma-ray energy has yielded the value[7] 2.758 Mev.

The measurements reported here are based upon comparisons of the gamma-rays with either the 0.4112±0.0001-Mev transition following Au^{198} decay[8] or the 1.3316±0.0010-Mev gamma-ray[9] from Co^{60}, utilizing internal or external conversion. The ThC″ gamma-ray energy has been found in both ways, while all other determinations employ the externally converted radiations. An iron-free single lens beta-ray spectrometer of focal length 9 cm was used, adjusted for line widths at half-maximum intensity ranging, in the different trials, from 1.6 to 1.9 percent in momentum. The supply current to the magnet was kept constant to within one part in 10^4, and was measured to the same accuracy by potentiometric determination of the potential drop across a single manganin resistor.

All sources and radiators used were 4 mm in diameter. The measurement of the ThC″ gamma-ray energy, as illustrated in Fig. 1, was effected using a composite thin source prepared by irradiating a disk of gold leaf, 0.2 mg/cm² thick, in the Chalk River pile to an activity of 0.2 to 0.3 mc. After transfer to the end of an aluminum rod of the same diameter, which then formed the source holder, RdTh active deposit was collected on the active gold over a period of 2 to 3 days. At the time of use the ThB activity present amounted to about 30 μc. Care was taken to confine the deposit to the gold surface, and visual inspection of autoradiographs using inactive gold showed the deposit to be uniform.

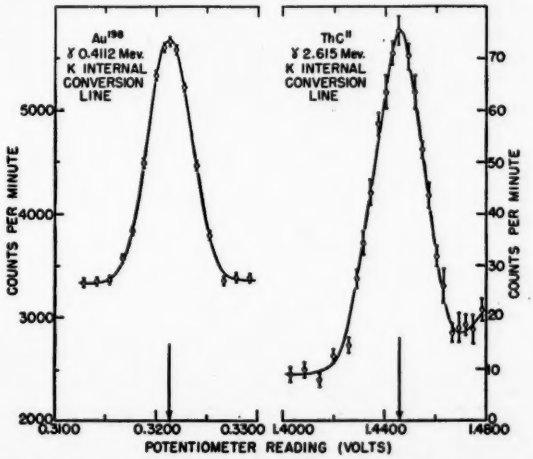

FIG. 1. (Left) K internal conversion line from the 0.4112±0.0001-Mev transition following Au^{198} decay. The continuum under the line includes 2040 counts per minute from the RdTh active deposit of the composite source. (Right) "X" line from ThC″. The rise at the high energy side is due to the neighboring L line. The vertical lines through the experimental points represent the standard deviations of the observed counting rates.

TABLE II. Gamma-ray measurements by comparison of external conversion K lines.

Gamma-ray nominal energy (Mev)	Comparison gamma-ray (Mev)	Trial	Weight	Radiator (mg/cm²)	Gamma-ray energy (Mev)	Weighted mean (Mev)
2.62 ThC″	1.3316 Co^{60}	1	1	25 U	2.615	
2.62 ThC″	1.3316 Co^{60}	2	1	25 U	2.617	2.616±0.006[a]
2.62 ThC″	1.3316 Co^{60}	1	1	8 Th	2.616	
2.62 ThC″	1.3316 Co^{60}	2	1	8 Th	2.614	2.615±0.005[a]
2.2 RaC	2.615 ThC″	1	2	43 U	2.208	
2.2 RaC	2.615 ThC″	2	2	25 U	2.209	
2.2 RaC	2.615 ThC″	3	1	25 U	2.205	2.208±0.006
2.76 Na^{24}	1.3316 Co^{60}	1	1	8 Th	2.756	
2.76 Na^{24}	1.3316 Co^{60}	2	2	8 Th	2.755	
2.76 Na^{24}	1.3316 Co^{60}	3	2	8 Th	2.755	2.755±0.005

[a] The value of 2.615 Mev as determined by the K line internal conversion comparisons of Table I is recommended over these results because of the superiority of the method with respect to thinness of source.

"Peak" measurements have been used in taking the ratio of momenta, the peak being taken as the axis of symmetry of the upper half of the line.

The series of external conversion measurements, one of which is plotted in Fig. 2, were made using U and Th radiators. The radiator, placed on the end of a brass or aluminum post, was left

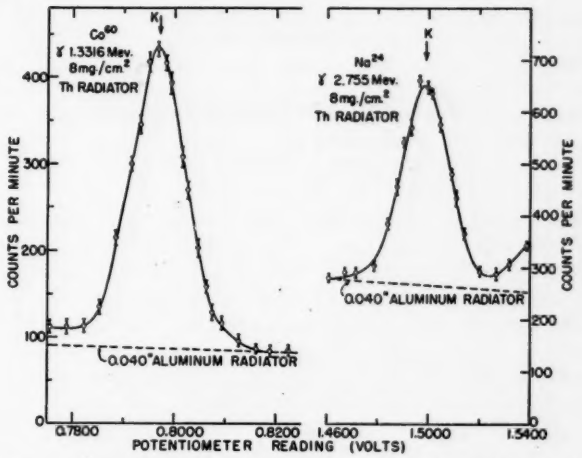

FIG. 2. (Left) K line from external conversion of the 1.3316±0.0010-Mev Co^{60} gamma-ray. The rise at the low energy side of the line is due to the L and M lines of the 1.172-Mev gamma-ray. (Right) K line from external conversion of the 2.755-Mev Na^{24} gamma-ray. The rise at the high energy side of the line is due to the neighboring L line.

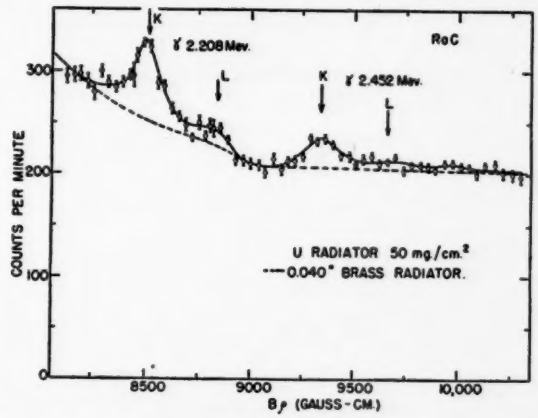

FIG. 3. Secondary electron spectrum of RaC above 2 Mev. The slight rise in the Compton distribution under the L line (2.208-Mev gamma-ray) is due to photoelectrons ejected from the thick brass radiator.

undisturbed during a trial. The post had been previously drilled out from the rear to within 0.040 in. of the radiator, and the sources were placed in position, alternately, from outside the vacuum chamber. Source strengths used were 3 mc RdTh, 7 mc Co^{60}, 5 to 10 mc Na^{24}, and 5 mc Ra. Peak determinations again were employed in taking the momentum ratios.

The secondary electron spectrum of RaC from 2.1 to 2.7 Mev is shown in Fig. 3. The second gamma-ray has an energy of 2.452 $\pm$0.012 Mev, and an intensity 35 to 40 percent of that of the 2.208-Mev gamma-ray. There is also some slight but inconclusive evidence of a weak gamma-ray of energy about 2.6 Mev.

Errors assigned include estimates of uncertainty in current measurement, relative peak shift, stray field correction, and location of the line peaks. The statistical accuracy and number of the experimental points form the basis for the weights assigned in column 4 of the Tables I and II.

It is a pleasure to acknowledge the aid and advice of Dr. L. G. Elliott, and the assistance rendered by Mr. D. W. Smellie.

[1] R. E. Bell and L. G. Elliott, Phys. Rev. **74**, 1552 (1948).
[2] P. Meyer, Zeits. f. Physik **126**, 336 (1949).
[3] C. D. Ellis, Proc. Roy. Soc. (London) **A138**, 318 (1932).
[4] Hornyak, Lauritsen, and Rasmussen, Phys. Rev. **76**, 731 (1949).
[5] C. D. Ellis, Proc. Roy. Soc. (London) **A143**, 350 (1934).
[6] A. Alichanov and G. Latyshev, Comptes Rendus U.R.S.S. **20**, 429 (1938).
[7] K. Siegbahn, Phys. Rev. **70**, 127 (1946).
[8] DuMond, Lind, and Watson, Phys. Rev. **73**, 1392 (1948).
[9] Lind, Brown, and DuMond, Phys. Rev. **76**, 1838 (1949).

Infra-Red Absorption of Silicon*

H. Y. Fan and M. Becker
Purdue University, Lafayette, Indiana
February 24, 1950

In a previous communication[1] the measurements on infra-red transmission through bulk silicon were reported. It was pointed out that for frequencies lower than that required for excitations across the forbidden energy gap the magnitude of absorption does not agree with the classical Drude theory for free charge carriers.

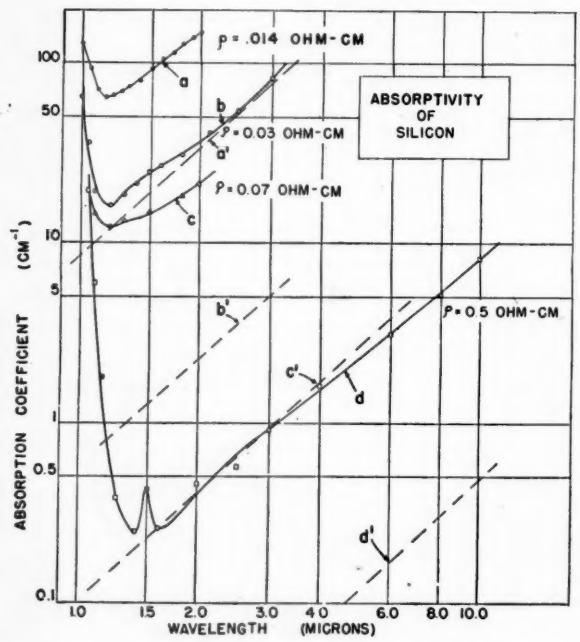

FIG. 1. Absorption coefficient as function of wave-length. The solid curves a, b, c, and d are determined experimentally. The corresponding dashed curves a', b', c', and d', are calculated from Eq. (2).

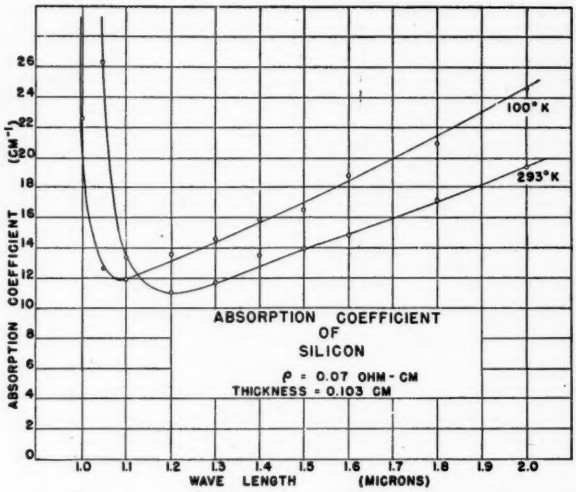

FIG. 2. Typical temperature dependence of absorption coefficient for samples with sloping Hall curves in the impurity range.

Results of further measurements on bulk samples of different resistivities are shown in Fig. 1. The dotted lines are calculated according to the Drude theory

$$\sigma = nk\nu = (e^2/2\pi m)[n_c\gamma/(\nu^2+\gamma^2)]. \quad (1)$$

In our measurements $\nu \gg \gamma$. In terms of the d.c. conductivity σ_0 and Hall constant R we have

$$\sigma = (e^2/4\pi^2m^2)(3\pi/8R^2\sigma_0\nu^2). \quad (2)$$

The absorption coefficient is

$$\mu = 4\pi k/\lambda = 4\pi\sigma/nc. \quad (3)$$

The calculated values are seen to be too low in all cases. As pointed out previously, the discrepancy is even larger for germanium. Quantum mechanically the absorption due to free carriers can be regarded as a broadening of the zero-frequency absorption line due to the scattering of electrons by the lattice. Such treatment gives an expression[2] idential to (1). However, for $\nu \gg \gamma$ the absorption should be regarded more appropriately as a two-stage process, the absorption of a photon leading to an intermediate state which goes over to a final state by interaction with the lattice.[3] In this case γ' determining the absorption will not be the same γ for d.c. conduction. This could be the reason for the discrepancy.

For a given frequency, μ of the different samples plotted against $n_c\gamma$ cannot be fitted well by a straight line. The plot of μ *versus* n_c seems to give a better fit to a straight line. Measurements on more samples of different varieties are being made to obtain a more reliable conclusion. If μ is really proportional to n_c, a possible explanation, is an overlapping of energy bands. Mullaney[4] has shown that silicon has two bands of zero width at the top of the group of filled bands below the conduction band. Absorptions producing transitions of holes at the top to the interior of the filled bands should therefore extent to very low frequencies. Such absorption without the aid of lattice interaction will be just proportional to the number of holes. Measurements on an N-type sample showed that the absorption is comparable with that expected of P-type samples of the same n_c. Although Mullaney's treatment does not give narrow bands at the bottom of the conduction bands the treatment is admittedly unsatisfactory for those bands.

Measurements at low temperatures revealed absorptions due to the ionization of the impurity centers. Figure 2 shows a typical case where the absorption at 100°K is *higher* than at room temperature. The impurity activation energy is 0.058 ev and the impurity concentration N is 1.1×10^{13} as calculated from the Hall

curve. At 100°K the hole concentration n_c is only one-tenth of the room temperature value; however, the absorption is increased. The absorption at the lower temperature must be, therefore, predominantly due to the ionization of the impurities, most of which are normally un-ionized at this temperature. On the other hand, the concentration of un-ionized impurities $(N-n_c)$ available for absorption at room temperature is one-fourth of that at 100°K but the absorption is reduced only by about 20 percent. Evidently the absorption at room temperature is largely due to the free holes. Samples with flat Hall curves, indicating no change in n_c and $(N-n_c)$, show a steady decrease in absorption with decreasing temperature,[1] which confirms the above explanation. Absorptions due to impurity centers introduced by nucleon bombardment have been reported[5] earlier and will be discussed in a future communication.

* Work assisted by a Signal Corps contract. A preliminary report was presented at the American Physical Society Meeting of November 26, 1949.
[1] M. Becker and H. Y. Fan, Phys. Rev. 76, 1531 (1949).
[2] R. de L. Kronig, Proc. Roy. Soc. 133, 255 (1931); Y. Fujioka, Zeits. f. Physik 76, 537 (1932).
[3] We are indebted to Professor H. Fröhlich for discussions on this point.
[4] J. F. Mullaney, Phys. Rev. 66, 326 (1944).
[5] Lark-Horovitz, Becker, Davis, and Fan, Bull. Am. Phys. Soc. 25, No. 1, 29 (1950).

Masses of Cr^{50}, Cr^{52}, and Fe^{54} *

HENRY E. DUCKWORTH AND HOWARD A. JOHNSON
Scott Laboratory, Wesleyan University, Middletown, Connecticut
February 28, 1950

A DOUBLE-FOCUSING mass spectrograph[1] has been used to photograph the doublets at mass number 25, 26, and 27 formed by doubly charged Cr^{50}, Cr^{52}, Fe^{54} and singly charged C_2H, C_2H_2, and C_2H_3. Typical $C_2H_2-Cr^{52}$ and $C_2H_3-Fe^{54}$ doublets are shown in Fig. 1. The metallic ions were obtained from a high frequency spark between stainless steel electrodes. The method by which the hydrocarbon ions were obtained is described below.

Source of hydrocarbon lines.—The hydrocarbon ions used in the present work were secured in a most fortuitous manner. Faint lines at mass numbers 24, 25, 26, 27, 28, and 29 were observed in the course of other work, and were attributed to C_2, $C_2H\cdots C_2H_5$ coming from the silicone in the diffusion pumps. These lines were intensified by removing the liquid air trap from the source vacuum system, and thereafter provided accurate and easily obtained standard masses. In addition to the group mentioned, two other series of suitable intensity have been observed, namely $C, CH\cdots CH_5$ and $C_3, C_3H\cdots C_3H_5$. These hydrocarbon molecules are ionized in the same high frequency spark which creates the metallic ions.

Mass of Cr^{50}.—The C_2H-Cr^{50} doublet at mass number 25 was photographed with an exposure time of ten minutes. From nine photographs of this doublet, the difference in packing fraction[2] between C_2H and Cr^{50} was found to be $\Delta f=14.26\pm0.03$, with extreme values of 14.09 and 14.43. The $Cr^{50}-Cr^{52}$ separation, assumed to be integral, served as the mass scale. Using Bainbridge's[3] recommended values of $H^1=1.0081283\pm0.0000028$ and $C^{12}=12.003856\pm0.000019$, the packing fraction of C_2H is $f=6.336\pm0.016$. This value, when combined with the above packing fraction difference, gives for Cr^{50} $f=-7.92\pm0.04$. The only other measurement of the mass of Cr^{50} has been made by Ogata,[4] using six photographs of the $C_4H_2-Cr^{50}$ doublet, who found the packing fraction of Cr^{50} to be $f=-7.11\pm0.08$. The present value of -7.92 ± 0.04 corresponds to a mass of $Cr^{50}=49.96040\pm0.00020$.

Mass of Cr^{52}.—The $C_2H_2-Cr^{52}$ doublet at mass number 26 was photographed with an exposure time of five minutes. From 14 photographs of this doublet, the packing fraction difference was found to be $\Delta f=17.41\pm0.025$ with extreme values of 17.22 and 17.62. The $Cr^{52}-Cr^{53}$ separation provided a suitable mass scale.

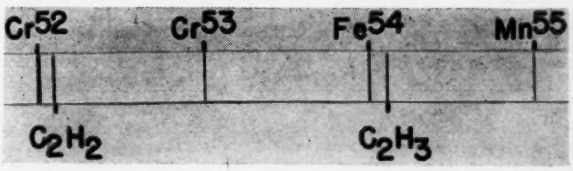

FIG. 1. Mass spectrum showing the doublets at mass numbers 26 and 27 formed by doubly charged Cr^{52}, Fe^{54} and singly charged C_2H_2, C_2H_3. Magnification 4×.

If the packing fraction of C_2H_2 is assumed to be $f=9.218\pm0.017$,[3] that of Cr^{52} is calculated to be $f=-8.19\pm0.04$. This is to be compared to Aston's value[5] of -8.18 ± 0.15 and Ogata's[4] value of -8.47 ± 0.08. The mass of Cr^{52} is calculated from the present packing fraction value of -8.19 ± 0.04 to be 51.95741 ± 0.00021.

Mass of Fe^{54}.—The exposure time for photographing the $C_2H_3-Fe^{54}$ doublet was also five minutes. Seventeen photographs of this doublet yielded a packing fraction difference $\Delta f=19.91\pm0.04$, with extreme values of 19.52 and 20.17. The separation between Fe^{54} and the overexposed Fe^{56}, assumed to be integral, served as the mass scale. With a packing fraction of C_2H_3 of 11.887 ± 0.018,[3] that of Fe^{54} is found to be -8.03 ± 0.05. Dempster[6] has measured this packing fraction to be -7.5 ± 0.8 while Ogata[4] has obtained -7.83 ± 0.09. The present value gives the mass of $Fe^{54}=53.95664\pm0.00027$.

In these experiments care has been taken to minimize the effect on the doublet spacing (a) of retardation of the ions by residual gas in the mass spectrograph, as observed by Dempster and Shaw,[7] and (b) of local inhomogeneities in the magnetic field. The first effect has been studied in this laboratory[8] in connection with the $Cu^{65}-Pt^{195}$ doublet, and has been found in that case to be negligible at pressures less than 9×10^{-6} mm Hg. In the present experiments the pressure was kept less than 5×10^{-6} mm Hg. The second effect, due to local inhomogeneities in the magnetic field, or to local electric fields in the magnetic analyzer arising from charged dust particles on the magnet pole faces, was minimized by photographing the doublets in several different positions on the photographic plate. The errors given in this Letter are probable errors based on the internal consistency of the data.

The authors appreciate the technical assistance of Mr. Clifford Gieselbreth. They are also grateful to Professor Carl Stearns who has allowed them the use of the comparator in the Van Vleck Observatory.

* This letter is based on work done at Wesleyan University under Contract AT (30-1)-451 with the AEC.
[1] H. E. Duckworth, Rev. Sci. Inst. 21, 54 (1950).
[2] The term "packing fraction" is defined as $f=(A-I)/I$, where A is the mass of the atom in question, and I is the nearest integer. In this letter the factor $\times10^{-4}$ is to be understood and is not written in expressing the numerical value of the packing fraction.
[3] K. T. Bainbridge, "Isotopic weights of the fundamental isotopes," Preliminary Report No. 1, National Research Council (June, 1948).
[4] K. Ogata, Phys. Rev. 75, 200 (1949).
[5] F. W. Aston, Nature 141, 1096 (1938).
[6] A. J. Dempster, Phys. Rev. 53, 64 (1938).
[7] A. J. Dempster and A. E. Shaw, Phys. Rev. 77, 746 (1950).
[8] Duckworth, Johnson, Preston, and Woodcock, Phys. Rev. (to be published).

On the Disintegration Scheme of I^{131}

I. FEISTER AND L. F. CURTISS
National Bureau of Standards, Washington, D. C.
February 10, 1950

SEVERAL different decay schemes have been proposed[1-3] for the important radioisotope I^{131}. In particular, Metzger and Deutsch[1] and Kern *et al.*[2] have published substantially different experimental results for the energy of the soft beta-component. In view of the importance of this component in determining the decay scheme, it seems worth while to report our measurement of the I^{131} beta-spectrum.[4]

TABLE I. Comparison of recent data on I^{131}, including our hitherto unpublished results. Gamma-intensities are given relative to that of the 364-kev gamma-ray arbitrarily taken as 100. Figures in parentheses were obtained from an assumed decay scheme, except for order of magnitude.

	Metzger and Deutsch[a]	Owen *et al.*[b]	Lind *et al.*[c]	Moe *et al.*[d]	Cork *et al.*[e]	Kern *et al.*[f]	Our values[g]
β-rays							
1. Energy (kev)	315±20	—	—	—	(259)	250±30	306±15
Intensity (%)	15	—	—	—	—	14	~20
2. Energy (kev)	600±5	597±5	—	—	(600)	605±5	606±5
Intensity (%)	85	—	—	—	—	86	~80
γ-rays							
1. Energy (kev)	80±1	83±2	80.133±0.005	—	80.1	80±2	80
Intensity	(7.6)	—	(8.7)	—	—	(22)	—
2. Energy (kev)	—	163±3	—	159	163.6	163	—
3. Energy (kev)	—	—	—	—	177.0	—	—
4. Energy (kev)	—	—	—	208(?)	—	—	—
5. Energy (kev)	283±3	286±6	284.13±0.1	284	284.1	282±1	284
Intensity	7.6	—	8.7	—	—	4.5	~9
6. Energy (kev)	363±3	368±7	364.18±0.1	364	364.2	363±2	364
Intensity	100	—	100	—	—	100	100
7. Energy (kev)	638±5	—	—	638	(625)	637±2	639±4
Intensity	19	—	—	—	—	17	~13

[a] See reference 1.
[b] Owen, Moe, and Cook, Phys. Rev. **74**, 1879 (1948).
[c] Lind, Brown, Klein, Muller, and DuMond, Phys. Rev. **75**, 1544 (1949).
[d] Moe, Owen, and Cook, Phys. Rev. **75**, 1270 (1949).
[e] See reference 2.
[f] See reference 3.
[g] The calibration of our spectrometer was checked against the accurate values of Lind *et al.* (reference c) for the 80-, 284-, and 364-kev γ-energies.

Figure 1 shows a Fermi plot of our beta-spectrum. The principal component is seen to have an end point at 606±5 kev, and the soft component at 306±15 kev. The latter value agrees within the limits of experimental error with that of Metzger and Deutsch, but cannot be easily reconciled with that of Kern *et al.*

The source[5] used was deposited on a 1.7 mg/cm² Al backing in the form of AgI with an average surface density of 0.5 mg/cm², and the counter window thickness was 1.0 mg/cm² mica. Our previous experience indicates that under these conditions the shape of the beta-spectrum is not appreciably affected above about 100 kev. The Fermi plot of the soft component was obtained using only points between 100 and 240 kev, since internal conversion lines distort the spectrum above 240 kev.

Table I summarizes the results of recent measurements on I^{131} by various authors, including our hitherto unpublished results. The 163-kev gamma-ray reported by several investigators has been identified as due to a 12-day isomer of Xe^{131} produced in about one percent of the I^{131} decay transitions.[6] It may be pointed out that the thicker the beta-source used the more likely it is that this radioactive Xe^{131} gas will be trapped in the source and its radiation observed.

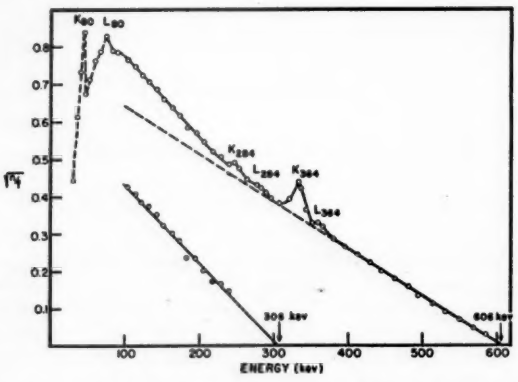

FIG. 1. Fermi plot of I^{131} beta-spectrum. The original relativistic Fermi function $f(Z,\eta)$ was used in making this plot.

On comparing the various decay schemes that have been proposed, our results tend to support that of Metzger and Deutsch. Further information of great value in deciding between these schemes would be a more accurate determination of the intensity of the 80-kev gamma-ray than has thus far been made.

We are indebted to the NBS Computation Laboratory for evaluation of the relativistic Fermi function $f(Z,\eta)$. This work was assisted by the AEC.

[1] F. Metzger and M. Deutsch, Phys. Rev. **74**, 1640 (1948).
[2] Cork, Keller, Sazynski, Rutledge, and Stoddard, Phys. Rev. **75**, 1621 (1949).
[3] Kern, Mitchell, and Zaffarano, Phys. Rev. **76**, 94 (1949).
[4] This investigation was carried out in the summer of 1948, and included a study of both beta- and gamma-spectra as well as beta-gamma- and gamma-gamma-coincidence absorption measurements. Publication was withheld, however, in the hope of determining the critical intensity of the 80-kev gamma-rays and the origin of the gamma-gamma-coincidences observed.
[5] The I^{131} used in this investigation was obtained from the Oak Ridge National Laboratory.
[6] Brosi, DeWitt, and Zeldes, Phys. Rev. **75**, 1615 (1949).

The Scattering of Electrons by Hydrogen Atoms

H. S. W. MASSEY AND B. L. MOISEIWITSCH
University College, London, England
February 27, 1950

IN a recent paper Hsuang[1] has applied a variational method to investigate the scattering of slow electrons by hydrogen atoms. His method does not allow for exchange effects. In the course of a systematic study of the usefulness of variational methods in atomic collision problems we have applied Hulthèn's variational method[2] to the hydrogen atom. The trial wave functions we have used are, in atomic units, of the form

$$\psi(r_1,r_2)=\exp(-r_1)f(r_2,r_{12})\pm\exp(-r_2)f(r_1,r_{12}), \qquad (1)$$

where

$$r_2f(r_2,r_{12})=\sin kr_2+\{a+\exp(-r_2)(b+cr_{12})\}(1-\exp(-r_2)\cos kr_2.$$

Here r_1, r_2, and r_{12} are the distances of the electrons from the nucleus and from each other, respectively, k is $2\pi mva_0/h$, and v the velocity of the incident electron. The second term of (1) allows for electron exchange, the ± signs corresponding to the cases in which the spins of the atomic and incident electrons are antiparallel and parallel, respectively. Except for the exchange terms the trial function is exactly the same as that used by Hsuang in his method which is, however, not the same as that of Hulthèn which we have employed. The term involving r_{12} allows for polarization of the atom by the incident electron, and the possibility of introducing such allowance is an important feature of the variation method.

We have, so far, determined the zero-order phase angle $\eta_0(=\tan^{-1}a)$, for the following cases (a) exchange neglected, no polarization correction (i.e., $c=0$), (b) exchange neglected, polarization correction included (i.e., c included as a variable parameter), (c) exchange included, no polarization correction (i.e., $c=0$), (d) exchange included, polarization correction included but $b=0$.

Cases (a) and (b) correspond to the cases considered by Hsuang. In general we reproduce his results in that η_0 tends to π as k tends to 0 in case (b), whereas in case (a) it tends to 0. On the other hand, our values of η_0 tend in both cases, as k increases, to those calculated by Macdougall[3] by numerical integration of the differential equation for the motion of electrons in the static field of a hydrogen atom.

The results for case (c) may be compared directly with those obtained by Morse and Allis[4] by exact numerical solution of the integro-differential equations which can be set up when polarization is ignored. Good agreement is found.

Finally, in case (d) the effect of including polarization in addition to exchange is found to be much less noticeable than when

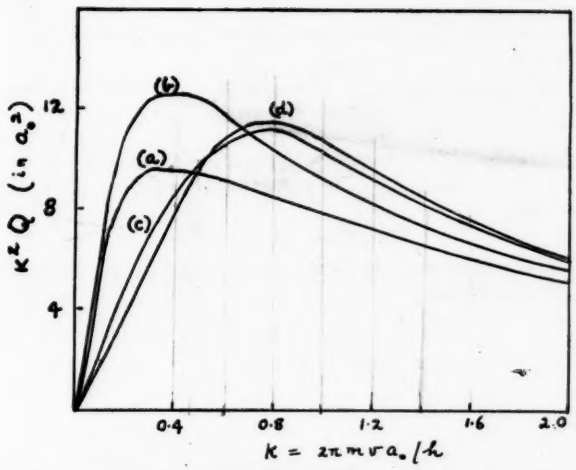

FIG. 1. The elastic scattering cross section Q for atomic hydrogen calculated by the Hulthèn variational method for the cases (a), (b), (c), (d) described in the text.

exchange is ignored. This is particularly true for the antisymmetric case, as would be expected. The antisymmetry already ensures that the two electrons are kept apart.

These results may be seen by reference to Fig. 1, in which the collision cross sections derived in the various cases are illustrated.

A full account of this work will be published later.

Our thanks are due Miss K. Blunt for carrying out many of the extensive numerical calculations involved.

[1] S. S. Hsuang, Phys. Rev. **76**, 477 (1949).
[2] L. Hulthèn, K. Fys. Sällsk, Lund Förhandl **14**, No. 21 (1944).
[3] J. McDougall, Proc. Roy. Soc. **A136**, 549 (1932).
[4] P. M. Morse and W. P. Allis, Phys. Rev. **44**, 269 (1933).

On the Sudden Increase in Cosmic-Ray Intensity on November 19, 1949

D. C. ROSE
National Research Council of Canada, Ottawa, Canada
March 2, 1950

CONTINUOUS recording of cosmic-ray intensities by Geiger-Müller counters is being carried on at Ottawa and at Resolute (latitude 74°41′ N; longitude 94°55′ W; geomagnetic latitude 83°). The equipment and arrangement of counters at both stations are identical. Four counter trays are used, three in a vertical line with 6 in. of lead between (1) and (2) and 8½ in. of lead between (2) and (3). The bottom tray (3) is surrounded with at least 4 in. of lead. A fourth counter tray, unshielded except for the building roof and $\frac{1}{16}$ in. of aluminum, is located nearby. At both stations coincidences are recorded between (1) and (2) and between (1) and (3) and the total counts in (3) are recorded. At Ottawa the total counts in all trays are recorded as well as the above coincidences.

At Ottawa on November 19 at 1048 GMT the intensity started to increase suddenly. It reached about 170 percent of the mean of the previous 12 hr. in about 6 min. The peak was narrow and sharp and reached roughly the same relative height in shielded counters, unshielded counters, and coincident pairs. The variation was so rapid at the peak that the necessity of counting over short intervals makes an accurate measure of its height impossible. The figures obtained vary from 50 to 90 percent with the different arrangements of counters. After the peak the intensity appears to decay roughly exponentially, though there are some significant irregularities in the decay curve. It returned to about 10 percent above the average in about an hour. A sudden increase on November 19 was first reported by Dauvillier[1] who found an increment of 3.6 percent at Bagneres, France. Forbush, Stinchcomb, and Schein[2] report a 43 percent increase at Cheltenham and Godhaven, a larger increase at Climax, and none at Huancayo. The time given by Forbush, Stinchcomb, and Schein is about 1045 and the Ottawa peak was obviously coincident with this. The increase found by Dauvillier occurred somewhat later and reached a maximum about 1200 hr. At Resolute the intensity started to rise at about 1100 GMT and the curve shows a broad peak 12 to 15 percent in height centered about 1145 hours, or approximately fifty minutes after the Ottawa peak. It was recorded by the shielded counter and both coincidence channels. This probably represents the same increase found by Dauvillier.

The delay in time and the significant irregularities in the Ottawa curve suggest that after the initial increase in intensity there were irregular subsequent bursts. If the subsequent bursts were composed of particles, then they might be expected to strike the earth at different localities because of their different energies or directions. Figure 1 shows a plot for eight days of the results from a shielded and an unshielded counter tray and a coincidence unit (6 in. of lead) at Ottawa, and from a similar coincidence unit and a shielded tray at Resolute. An expanded plot from an unshielded tray at Ottawa is also shown.

Previous observations of sudden increases[3,4] of this type have been associated with solar flares and have shown a decrease of 10 percent or more occurring some hours after the increase. After the increase on November 19 a sudden decrease did not occur. The decrease has been associated with the sudden commencement of a magnetic storm. An examination of magnetometer records taken at the same station at Ottawa does not show any strong sudden commencement but rather a gradually increasing magnetic disturbance starting about 1800 hr. On the days following November 19 the variations in intensity shown in Fig. 1 are probably meteorological.

On November 29 another unusual increase in intensity occurred at Ottawa. The unshielded trays showed an increase of about 35 percent lasting about 3 hr., centered about 1330 GMT. The shielded tray and the coincidence units indicated nothing irregular. A careful investigation eliminated any possibility of interference by radioactive sources in the neighborhood. Doan[5] and Wait and McNish[6] have reported increased ionization during rain, the former in an unshielded ionization chamber used for cosmic-ray

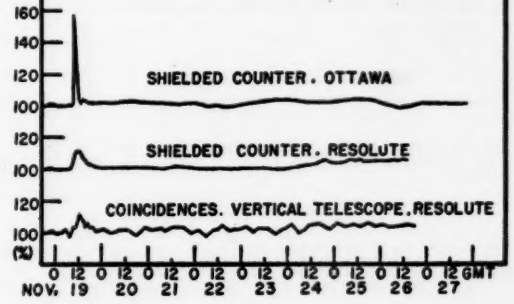
UNSHIELDED COUNTERS OTTAWA
A
A
NOV. 19
1100 1200 1300
GMT
COINCIDENCES. VERTICAL TELESCOPE. OTTAWA
SHIELDED COUNTER. OTTAWA
SHIELDED COUNTER. RESOLUTE
COINCIDENCES. VERTICAL TELESCOPE. RESOLUTE
(%)
0 12 0 12 0 12 0 12 0 12 0 12 0 12 0 12 0 12 GMT
NOV. 19 20 21 22 23 24 25 26 27

FIG. 1. Sudden increase in cosmic-ray intensity on November 19, 1949

studies and the latter in studying atmospheric ionization at ground level. These increases in ionization are considered to be due to radioactive matter brought down with the rain. Between 0935 and 1900 hr. GMT on November 29 at Ottawa precipitation was falling. The precipitation started as snow and changed to rain about 1400 hr. Compared with the results of Doan and Wait and McNish the 35 percent increase in the soft component registered at Ottawa by counters seems too high to be explained in the same way, unless there was an exceptionally high density of radioactive matter in the atmosphere at the time. An alternative, but not very likely explanation, might be that there was a burst of hard gamma-rays or some other radiation which would increase the number of soft shower particles without any appreciable effect on the hard component.

An interesting feature of the November 19 increase is the difference between the measurements at the various stations, particularly between Resolute and Godhaven (geomagnetic latitude 80°). These two stations are about 900 miles apart and the differences confirm previous indications that sudden increments in cosmic-ray intensity occur over a limited area. The lack of a sudden decrease after the increment is unusual, since a decrease has been reported on previous occasions.

The cooperation of the Department of Transport of the Government of Canada is appreciated for supplying facilities at Resolute and for weather information.

[1] A. Dauvillier, Comptes Rendus **229**, 1096 (1949).
[2] Forbush, Stinchcomb, and Schein, Bull. Am. Phys. Soc. **25**, No. 1, 15 (1950).
[3] I. L. Chakraborty and S. D. Chatterjee, Ind. J. Phys. **23**, 525 (1949).
[4] Forbush, Gill, and Vallarta, Rev. Mod. Phys. **21**, 44 (1949).
[5] R. L. Doan, Phys. Rev. **49**, 107 (1936).
[6] G. R. Wait and A. G. McNish, Monthly Weather Rev. **62**, 1 (1934).

An Identity in Quantum Electrodynamics

J. C. WARD
The Clarendon Laboratory, Oxford, England
February 27, 1950

IT has been recently proved by Dyson[1] that all divergencies in the S-matrix of electrodynamics may be removed by a renormalization of mass and charge. Dyson defines certain fundamental divergent operators Γ_μ, S_F', D_F' and gives a procedure for the calculation of their finite parts $\Gamma_{\mu 1}$, S_{F1}', D_{F1}' by a process of successive approximation. It is then shown that

$$\Gamma_\mu = Z_1^{-1}\Gamma_{\mu 1}(e_1), \quad S_F' = Z_2 S_{F1}(e_1), \quad D_F' = Z_3 D_{F1}(e_1), \qquad e_1 = Z_1^{-1} Z_2 Z_3^{\frac{1}{2}} e,$$

where Z_1, Z_2, and Z_3 are certain infinite constants and e_1 is the renormalized electronic charge. Dyson conjectured that $Z_1 = Z_2$, and it is proposed here to give a formal proof of this relation.

In the first place, with any proper electron self-energy part W, may be associated a set of proper vertex parts V^i obtained by inserting a photon line in one of the electron lines of W. Now consider the operators $\Lambda_\mu(V^i, p, p)$ in which the two external electron momentum variables p have been set equal, and the external photon variable made to vanish. Then $\Lambda_\mu(V^i, p, p)$ may be obtained from $\Sigma(W, p)$ by replacing S_F by $S_F\gamma_\mu S_F$ at one electron line of W. Because of the identity

$$-(1/2\pi)\partial S_F/\partial p_\mu = S_F\gamma_\mu S_F,$$

on summing $\Lambda_\mu(V^i, p, p)$ over all vertex parts V^i associated with W, one finds

$$\Sigma_{V^i}\Lambda_\mu(V^i, p, p) = -(1/2\pi)(\partial\Sigma(W, p)/\partial p_\mu).$$

(One can verify that any closed loop in W gives zero total effect.) Finally summing over all proper electron self-energy parts W, one finds

$$\Lambda_\mu(p, p) = -(1/2\pi)(\partial\Sigma^*(p)/\partial p_\mu).$$

Now substitute this identity into Eqs. (91) and (95) of reference 1. One finds

$$\Lambda_\mu = Z_1^{-1}[(1-Z_1)\gamma_\mu + \Lambda_\mu C], \quad \Sigma^* = Z_2^{-1}[(Z_2-1)S_F^{-1} + S_F^{-1}S_C/2\pi].$$

We have

$$-(1/2\pi)Z_2^{-1}\{(Z_2-1)2\pi\gamma_\mu + \gamma_\mu S_C + (\gamma_\lambda p_\lambda - iK_0)(\partial S_C/\partial p_\mu)\} = Z_1^{-1}\{(1-Z_1)\gamma_\mu + \Lambda_\mu C(p, p)\}.$$

Now put

$$\gamma_\lambda p_\lambda = iK_0, \quad (p_\lambda)^2 = -K_0^2.$$

The convergent parts of these equations then vanish and there is left the relation

$$-(1/2\pi)Z_2^{-1}(Z_2-1)2\pi\gamma_\mu = Z_1^{-1}(1-Z_1)\gamma_\mu$$

which reduces immediately to $Z_1 = Z_2$.

[1] F. J. Dyson, Phys. Rev. **75**, 1736 (1949).

The Partial Molal Entropy of Superfluid in Pure He⁴ below the λ-Point

O. K. RICE
Department of Chemistry, University of North Carolina, Chapel Hill, North Carolina
March 3, 1950

IN a recent article[1] (the notation of which is retained here, except that subscripts $4n$ and $4s$ refer to normal fluid and superfluid, respectively, in place of 1 and 2), I have considered the thermodynamics of liquid helium on the two-fluid theory, taking account of the fact that if two "phases" or "components," the normal fluid and the superfluid, exist together they must be in equilibrium with each other. On this basis, using the assumed relation[2] which states that the total molal entropy S at any temperature is the mole fraction x_{4n} of normal fluid times the molal entropy S_λ at the λ-point

$$S = x_{4n}S_\lambda = (1-x_{4s})S_\lambda, \tag{1}$$

using the empirical relation for S as a function of temperature

$$S = S_\lambda(T/T_\lambda)^r \tag{2}$$

(with $r \sim 5.6$), and assuming that the partial molal enthalpy of superfluid, $\bar{H}_{4s}$, is independent of temperature (at essentially constant pressure), and independent of x_{4s} (i.e., there is no heat of mixing), I derived the equation for the partial molal entropy of superfluid

$$\bar{S}_{4s} = S_\lambda x_{4n}/(r+1). \tag{3}$$

However, as I remarked in reference 1, there are some approximations involved in this procedure. Equation (1) is based on the assumption that below T_λ the entropy is contributed solely by the normal fluid, whose molal entropy is always set equal to the constant S_λ, thus neglecting any temperature dependence. Furthermore, there is an implied inconsistency, since Eq. (1) assumes no entropy of mixing while Eq. (3) implies that there is a mixing entropy. In fact, in the following letter we shall show that we may derive a somewhat different expression for S from Eq. (3). We shall, therefore, discard Eq. (1) and turn to a consideration of the enthalpies.

If $\bar{H}_{4s}$ is independent of x_{4s}, then $\bar{H}_{4n}$ must be also, and we have $\bar{H}_{4n} = H_{4n}$, where H_{4n} is the enthalpy of pure normal helium. We can write for the total molal enthalpy[3]

$$H = x_{4n}H_{4n}. \tag{4}$$

We will now proceed to derive an expression for $\bar{S}_{4s}$, in a somewhat more direct way than in reference 1, using Eq. (4) in place of Eq. (1). Since $F = H - TS$ and $\mu_{4s} = \bar{H}_{4s} - T\bar{S}_{4s} = -T\bar{S}_{4s}$ the condition for internal equilibrium, $F = \mu_{4s}$, gives

$$\bar{S}_{4s} = S - H/T. \tag{5}$$

Equation (2) implies, from the relation between S and H (see footnote 10 of reference 1) that

$$H/H_\lambda=(T/T_\lambda)^{r+1}, \tag{6}$$

with

$$H_\lambda=rS_\lambda T_\lambda/(r+1). \tag{7}$$

Using Eq. (4)

$$x_{4n}=(H_\lambda/H_{4n})(T/T_\lambda)^{r+1}. \tag{8}$$

From Eqs. (2), (5)–(7),

$$\bar{S}_{4s}=S_\lambda(T/T_\lambda)^r/(r+1). \tag{9}$$

This equation, of course, holds only at equilibrium. However, if H_{4n} were independent of T (hence equal to H_λ) we could write, using Eq. (8)

$$\bar{S}_{4s}=[S_\lambda/(r+1)]x_{4n}^{r/(r+1)}, \tag{10}$$

which expresses Δ_{4s} as a function of x_{4n} independent of T. If H_{4s} is temperature independent, then $(\partial S_{4s}/\partial T)x_{4n}=0$ (at constant pressure), so $\bar{S}_{4s}$ cannot depend explicitly on T. Equation (10), since it gives $\bar{S}_{4s}$ at all equilibrium concentrations, must thus be the correct general form for $\bar{S}_{4s}$, if H_{4n} is constant. If H_{4n} depends on T the proper equation for $\bar{S}_{4s}$ can still be obtained by eliminating T between Eqs. (8) and (9).

The determination of H_{4n} as a function of T offers some difficulty. I have suggested that the superfluid appeared above the λ-point in the form of globules, and below the λ-point principally in a sort of fibroid form. The fibroid form would not occur at all above T_λ but there would be some persistence of the globules below T_λ. The fibroid form only is actually included in the mole fraction x_{4s} below T_λ. Below the λ-point then the globules should be considered as part of the normal fluid, and they will alter its properties. However, it is unlikely that the globules are important at temperatures appreciably below T_λ, and it seems reasonable to suppose that we can get a good idea of the temperature dependence of H_{4n} by extrapolating the specific heat from above the temperature ($\sim$2.5°K) of appearance of the λ-anomaly.[4] If we do this we conclude that H_{4n} certainly does not vary much more rapidly that T itself, and the dependence of $\bar{S}_{4s}$ on x_{4n} probably lies somewhere between proportionality to $x_{4n}^{(r+1)/r}$ and $x_{4n}^{r/(r+1)}$. Equation (3), then, should give an approximation which may be used without fear of serious error.

[1] O. K. Rice, Phys. Rev. **76**, 1701 (1949). C. J. Gorter, Physica **15**, 523 (1949) has independently stated the basic principles, but we differ in subsidiary assumptions and in method.
[2] L. Tisza, Phys. Rev. **72**, 838 (1947).
[3] Compare W. Band and L. Meyer, Phys. Rev. **74**, 386 (1948), Eqs. (10) and (11).
[4] O. G. Engel and O. K. Rice, Phys. Rev. **78**, 55 (1950).

Thermodynamics of He^3-He^4 Solutions

O. K. Rice and Olive G. Engel
Department of Chemistry, University of North Carolina, Chapel Hill, North Carolina
March 3, 1950

In a recent letter Gorter and de Boer[1] have discussed mixtures of He^3 and He^4, modifying somewhat the earlier views of de Boer.[2] Their new formulation is in accord with the ideas of Rice,[3] but differs in one respect from what is found by a logical extension of his treatment of pure He^4.

Equation (3) of the preceding letter leads to the following expression for the total entropy of $m_{4n}+m_{4s}$ moles of pure He^4 below the λ-point.

$$S=m_{4n}S_{4n}-m_{4n}S_\lambda(r+1)^{-1}\ln[m_{4n}/(m_{4n}+m_{4s})]. \tag{1}$$

Here m_{4n} and m_{4s} are the number of moles of normal and superfluid, respectively. S_{4n}, the molal entropy of pure normal helium, cannot be directly determined below the λ-point, where pure normal He^4 is unstable, but its magnitude can be estimated. Equation (1) yields Eq. (3) of the preceding note by partial differentiation with respect to m_{4s}. It has the correct form (it is consistent with the Gibbs-Duhem relation for entropy) and fulfills the correct boundary condition for $m_{4s}=0$. It is thus uniquely determined by Eq. (3) of the preceding note.

Below the λ-point He^3 appears to be soluble only in the normal part[4] of He^4. There is therefore an entropy of mixing, S_{34}, which can be supposed to be independent of m_{4s}. Assuming Raoult's law

$$S_{34}=-m_{4n}R\ln[m_{4n}/(m_{4n}+m_3)]-m_3R\ln[m_3/(m_{4n}+m_3)]. \tag{2}$$

However, there is still a superimposed entropy of mixing, S_{ns}, of normal and superfluid. Rice's suggestion of a separation of normal superfluid in ordinary space makes it seem reasonable to suppose that S_{ns} will not depend on the relative amounts of He^3 and He^4 in the normal fluid. We simply substitute $m_{4n}+m_3$ for m_{4n} in the mixing term in Eq. (1):

$$S_{ns}=-(m_{4n}+m_3)S_\lambda(r+1)^{-1}\times\ln[(m_{4n}+m_3)/(m_{4n}+m_3+m_{4s})]. \tag{3}$$

S_λ has the same constant value; it is the entropy of pure He^4 at its λ-point. For the total Gibbs free energy of $m_{4n}+m_{4s}$ moles of He^4 and m_3 moles of He^3 we write

$$F=m_{4n}F_{4n}+m_3F_3-TS_{34}-TS_{ns}, \tag{4}$$

where F_3 and F_{4n} are molal free energies of pure He^3 and pure normal He^4 respectively; F_{4s} is zero. The terms m_3F_3 and $-TS_{34}$ are essentially like corresponding terms of Gorter and de Boer. However, these authors would make $(m_{4n}F_{4n}-TS_{ns})/m_{4n}$ (equivalent to their G_4) a function of T and $m_{4n}/(m_{4n}+m_{4s})$ instead of T and $(m_{4n}+m_3)/(m_{4n}+m_3+m_{4s})$.

From Eq. (4) with (2) and (3), we get the chemical potentials μ_{4n}, μ_{4s}, and μ_3 by partial differentiation with respect to m_{4n}, m_{4s}, and m_3, respectively. The μ's can be expressed as functions of T and the mole fractions x_{4n}, x_{4s}, and x_3, provided F_3 and F_{4n} are known as functions of T. F_{4n} cannot be obtained directly, but can be found if the specific heat of pure normal He^4 can be estimated (see preceding note). The values of x_{4n} and x_{4s} in an equilibrium mixture at any given T and x_3 can then be found by setting $\mu_{4n}=\mu_{4s}$ (or, alternatively,[1] by minimizing F), together with $x_{4n}+x_{4s}+x_3=1$. Thus the μ's become functions of T and x_3 only. The partial vapor pressures of He^3 and He^4 can then be found, provided the vapor pressures of pure He^3 and He^4 and the equations-of-state of their vapors are known.

A solution with properties determined by Eqs. (2)–(4) we shall call a "quasi-ideal" solution, since the mixture of He^3 and normal He^4 follows the ideal solution law, while the superimposed mixture of normal and superfluid follows the same law as pure He^4. If deviations occur in practice[5] it would seem reasonable to try first to explain them as deviations in the terms other than TS_{ns}. We may add terms

$$m_3RT\ln\gamma_3+m_{4n}RT\ln\gamma_{4n}$$

to Eq. (4), where γ_3 and γ_{4n} (activity coefficients for He^3 and normal He^4) depend only on $\rho=x_3/x_{4n}$, where $\gamma_3\to1$ and $d\gamma_3/d\rho^{-1}\to0$ as $x_{4n}\to0$, and $\gamma_{4n}\to1$ and $d\gamma_{4n}/d\rho\to0$ as $x_3\to0$, and where

$$m_3d\ln\gamma_3/d\rho+m_{4n}d\ln\gamma_{4n}/d\rho=0.$$

Such terms will not affect μ_{4s}, but will change the equilibrium between normal and superfluid He^4 because of the effect on μ_{4n}. However, this equilibrium would not be changed in sufficiently dilute solutions of He^3 and He^4 where He^4 obeys Raoult's law ($\gamma_{4n}=1$) even though He^3 obeys Henry's rather than Raoult's law. If there is heat of mixing of He^3 and He^4 it will be reflected in the temperature coefficients of $\ln\gamma_3$ and $\ln\gamma_{4n}$.

[1] C. J. Gorter and J. de Boer, Phys. Rev. **77**, 569 (1950).
[2] J. de Boer, Phys. Rev. **76**, 852 (1949).
[3] O. K. Rice, Phys. Rev. **76**, 1701 (1949); **77**, 142 (1950).
[4] Taconis, Beenakker, Nier, and Aldrich, Phys. Rev. **75**, 1966 (1949); Physica **15**, 733 (1949).
[5] Weinstock, Osborne, and Abraham, Phys. Rev. **77**, 400 (1950).

Erratum: Internal Pair Formation

[Phys. Rev. 76, 678 (1949)]

M. E. ROSE
Oak Ridge National Laboratory, Oak Ridge, Tennessee

IN transcribing to the manuscript an error occurred in the coefficient of J_{l-1} in Eq. (10a). This coefficient should be

$$l[\tfrac{1}{2}(W_+^2+W_-^2)+1]+1+W_+W_-.$$

All numerical results were obtained from the correct formula.

The H.F.S. Anomaly of the Potassium Isotopes*

S. A. OCHS, R. A. LOGAN, AND P. KUSCH
Columbia University, New York, New York

March 6, 1950

THE h.f.s. spectrum of atoms in a state for which $J=1/2$, and which results from the transitions $\Delta m_I=\pm 1$, $\Delta m_J=0$, contains doublets whose frequency separation is $2g_I\mu_0H/h$. One component of the doublet arises in the state $m_J=1/2$ and the other in the state $m_J=-1/2$. If the doublet separation is observed at some fixed field for each of two isotopes, the ratio of the nuclear g-values of the two isotopes can be found. At sufficiently high fields the mean frequency of the doublet is very nearly $\Delta\nu/(2I+1)$ and if the nuclear g-value is approximately known, it is possible to find $\Delta\nu$ very accurately from the mean frequency of the doublet.

We have observed the h.f.s. spectrum of both K^{39} and K^{41} at a magnetic field of about 12,000 gauss. At this field $g_J\mu_0H/h \cong 73(\Delta\nu^{39}) \cong 130(\Delta\nu^{41})$. The doublet separations are then about $2g_I^{39}\mu_0H/h=4.8\times10^6$ sec.$^{-1}$ and $2g_I^{41}\mu_0H/h=2.6\times10^6$ sec.$^{-1}$, and the mean frequencies of the doublets are about 115×10^6 sec.$^{-1}$ and 63×10^6 sec.$^{-1}$ for K^{39} and K^{41} respectively. The line-widths are about 2×10^3 sec.$^{-1}$ and measurements of the center of the lines can be made to about 100 sec.$^{-1}$.

From measurements of the frequencies of the components of each of two doublets for each isotope and by use of the result of Millman and Kusch for $g_I(K^{39})/g_J(^2S_{1/2})$, we find

$$(g_I^{39}/g_I^{41})=1.8218\pm0.0002$$

and

$$(\Delta\nu^{39}/\Delta\nu^{41})=1.81768\pm0.00001.$$

The h.f.s. ratio is in agreement with the value observed by Kusch, Millman, and Rabi,[2] 1.8178 ± 0.0002. As K^{39} and K^{41} have the same angular momentum, $(\Delta\nu^{39}/\Delta\nu^{41})_{\text{calc.}}=(g^{39}/g^{41})_{\text{obs.}}$, and

$$\Delta\equiv\frac{(\Delta\nu^{39}/\Delta\nu^{41})_{\text{obs}}-(\Delta\nu^{39}/\Delta\nu^{41})_{\text{calc}}}{(\Delta\nu^{39}/\Delta\nu^{41})_{\text{calc}}}=-(0.226\pm0.010)\text{ percent.}$$

If the nucleus is assumed to be a point dipole which interacts with the magnetic field produced by the electrons, then Δ should be equal to zero. However, if a nucleus of finite extent is considered, the interaction of the electron with the nucleus over that portion of the electron orbit which lies within the nucleus will depend upon the distribution of magnetic moment within the nucleus and an observable value of Δ may appear for two isotopes, since the distribution of moment may be different for the two nuclei. Bohr and Weisskopf[3] have calculated this effect for simple nuclear models. The nuclear magnetic moment may be considered as composed of two intrinsically different parts, a spin and an orbital moment. The h.f.s. anomaly can then, to the first approximation, be determined by g_S and g_L, the g-factors corresponding to these two moments, and by g_I, the g-factor of the total nuclear moment. The fractional change in the total h.f.s. separation, resulting from the finite nuclear volume, is then

$$\epsilon=(K_S)_{Nr}\frac{g_S}{g_I}\frac{g_L-g_I}{g_S-g_L}+(K_L)_{Nr}\frac{g_L}{g_I}\frac{g_I-g_S}{g_S-g_L},$$

where the contributions of the spin and orbital moments to the total interaction energy are decreased from the values corresponding to a point dipole, by the fractional amounts K_S and K_L, respectively. If two isotopes differ by an even number of neutrons, it seems reasonable to assume them to have the same g_S and g_L. Then, if $(K_S)_{Nr}$ and $(K_L)_{Nr}$ do not differ appreciably, the influence of the finite nuclear size on the h.f.s. ratio, becomes

$$\Delta\cong0.3b\frac{g_Sg_L}{g_S-g_L}\left(\frac{1}{g_I(1)}-\frac{1}{g_I(2)}\right),$$

where b, which depends on the atomic number, the nuclear radius, and the atomic state, has been tabulated by Bohr and Weisskopf.[3]

The case of K^{39} and K^{41} is of particular interest, since these two isotopes have the same total nuclear angular momentum. Their g_I values, however, are quite different ($g_I^{39}=-0.260$, $g_I^{41}=-0.143$), so that Δ is appreciable.

The above relationship for Δ predicts that the ratio $(\Delta\nu^{39}/\Delta\nu^{41})$ is smaller than the ratio (g_I^{39}/g_I^{41}) by approximately 0.18 $[g_Sg_L/(g_S-g_L)]$ percent. If for the spin g-factor that of the odd proton ($g_S=-5.6$) is used, there are two reasonable choices left for g_L. According to the model proposed by Schmidt,[4] the orbital momentum is that of the odd particle in the nucleus. Then $g_L=-1$ for Z odd and Δ is about -0.22 percent. Margenau and Wigner,[5] however, assume the orbital momentum to be due to the nuclear matter as a whole, and g_L becomes then equal to $-Z/A$ and Δ equal to about -0.097 percent. The experimental result of $\Delta=-0.23$ percent thus tends to support the single particle model of the nucleus. A similar phenomenon has been observed[6,7] for the Rb isotopes where the effect could also be best described by choosing $g_L=-1$.

* This research has been supported, in part, by the ONR.

[1] S. Millman and P. Kusch, Phys. Rev. **60**, 91 (1941).
[2] Kusch, Millman, and Rabi, Phys. Rev. **57**, 765 (1940).
[3] A. Bohr and V. F. Weisskopf, Phys. Rev. **77**, 94 (1950).
[4] T. Schmidt, Zeits. f. Physik **106**, 358 (1937).
[5] H. Margenau and E. Wigner, Phys. Rev. **58**, 103 (1940).
[6] S. Millman and P. Kusch, Phys. Rev. **58**, 438 (1940).
[7] F. Bitter, Phys. Rev. **75**, 1326 (1949).

Non-Local Fields

M. FIERZ
Seminar für theoretische Physik, Universität Basel, Switzerland

February 28, 1950

IN a paper entitled "Quantum Theory of Non-Local Fields,"[1] Yukawa remarks that such a field "may well happen to be approximately equivalent to some mixture of local fields." Now the solutions of his equations are superpositions of plane waves, which are identical with those describing particles of arbitrary spin. Yukawa's Eqs. (3) and (14) correspond to those which I used in my paper[2] of 1939; namely, my Eqs. (1.1) and (1.3)

$$\Box A_{ik\ldots l}=\kappa^2A_{ik\ldots l};\quad(\partial/\partial X_i)A_{ik\ldots l}=0.$$

One sees the correspondence immediately by comparing the properties of plane waves in their rest-systems in both theories. The coefficients $C(0,0,0,-\kappa;l,m)$ in Yukawa's Eq. (20) correspond to the amplitudes $A^0_{ik\ldots l}$,[3] describing a particle of spin l atrest (l is the number of indices of A^0).

From the equivalence of the solutions we may conclude that the theories are equivalent. It seems that we have the right to interpret the r_μ-space as spin-space, and the X_μ-space as a local space of the particle. In fact, as r_μ is bound to the equation $r_\mu r^\mu=\lambda^2$, and by this is an angular variable only, it seems rather questionable whether it describes a finite extension of the particle.

As all that can be said at the moment refers to the force-free case, it may be that one can introduce interactions in such a way that the equivalence of the two theories will be lost.

[1] H. Yukawa, Phys. Rev. **77**, 219 (1950).
[2] M. Fierz, Helv. Phys. Acta **12**, 3 (1939).
[3] See reference 2, p. 6.

Thermal Expansion in Silver Halides

A. W. LAWSON
Institute for the Study of Metals, University of Chicago, Chicago, Illinois
March 6, 1950

THE purpose of this letter is to call attention to some interesting data obtained by Strelkow[1] on the thermal expansion of the silver halides. Strelkow and his collaborators[1] have measured the thermal expansion of a large number of substances, including Bi, Zn, Cd, NaCl, AgCl, and AgBr, and find a rather striking anomalous expansion just below the melting points of these substances. The effects appear to be real pre-melting phenomena and not instrumental errors arising from creep.

The possibility of observing anomalous expansion in silver halides has been the subject of speculation by Mott and Gurney[2] and also by Seitz[3] who appear to be unacquainted with Strelkow's data. Accordingly, I present these data in a modified form in Fig. 1, in which I have plotted the logarithm of the anomalous increase in length as a function of the reciprocal of the absolute temperature. In this graph I have corrected Strelkow's data for the normal expansion of these solids by subtracting the change in length corresponding to an average expansion coefficient of 3.2×10^{-5}/°C for AgCl and 3.6×10^{-5}/°C for AgBr. These values are subject, however, to a certain amount of doubt. Nevertheless, the resultant points fall reasonably well on straight lines, suggesting the abnormal expansion arises from an activation process. The heats of activation derived from Fig. 1 are tabulated in Table I, where they are compared to the heats of activation

TABLE I. Heats of activation in cal./mole

	From expansion data	From conductivity data[a]
AgCl	7,100	12,500
AgBr	10,500	10,100

[a] Estimated by F. Seitz from the data of E. Koch and C. Wagner (Zeits. f. physik. Chemie **B38**, 295 (1937) on the conductivity of silver halides doped with lead halides.

determined from observations on the electrical conductivity of pure and doped salts.

In the case of AgBr, at least, the correlation is quite good and suggests that the anomalous expansion arises from the increase in the number of lattice defects which are responsible for the ionic conductivity. Since some doubt exists as to the nature of these defects (i.e., whether they are Frenkel or Schottky defects) it is of interest to ascertain whether the expansion data are capable of discriminating between the two possibilities.

Assuming a Frenkel mechanism and that the holes and interstitial Ag^+ atoms conduct equally, Seitz[3] has given the following relation for the fraction of defects in a AgBr lattice:

$$n/N = 29e^{-5050/T}.$$

For $T=690$°K we obtain a concentration of 2 percent defect lattice sites. If we assume that the increase in volume on the formation of a hole and an interstitial Ag^+ ion is about 0.25 times the volume originally occupied by the Ag^+ ion, and take into account the radii of the Ag^+ and Br^- ions, then the estimated increase in volume of the lattice at $T=690$°K is about 0.2 percent. On the other hand, if we assume that the defects are pairs of equally mobile Schottky holes and that the volume on the formation of such a pair is about 0.70 of the volume originally occupied by the Ag^+ and Br^- ions, then the estimated increase in volume at $T=690$°K is 1.4 percent. If one of the pair of Schottky holes is much more mobile than the other, the estimated increase in volume at this temperature would be 2.8 percent. Since the observed increase in volume in silver bromide at $T=690$°K is actually 2.9 percent, Strelkow's data would seem to favor the last model as the mechanism of conductivity in AgBr. This conclusion

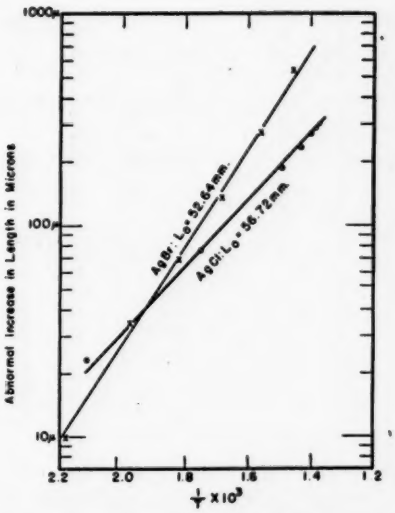

FIG. 1. Anomalous thermal expansion in AgBr and AgCl.

is not in conflict with the data of Breckenridge,[4] and recently arguments supporting this mechanism have been advanced by Mitchell.[5]

Unfortunately, the situation does not seem to be so clear cut in the case of AgCl. The heats of activation estimated from the expansion data and the conductivity data are in poor agreement. However, the expansion effect is much smaller in AgCl, and it is difficult to obtain a good estimate of the heat of activation from Strelkow's data. In fact there is some indication that the heat of activation is considerably higher just below the melting point of AgCl than the value given in Table I, but the data are insufficient to permit a definite statement on this point. The conclusion reached in the case of AgBr, however, suggests that further experiments on AgCl would cast considerable light on the mechanism of the conductivity in this case also.

[1] P. G. Strelkow, Physik. Zeits. Sowjetunion **12**, 77–82 (1937).
[2] Mott and Gurney, *Electronic Processes in Ionic Crystals* (Clarendon Press, Oxford, 1948).
[3] F. Seitz, Phys. Rev. **56**, 1063 (1939).
[4] R. G. Breckenridge, Technical Report 26, Laboratory for Insulation Research, M.I.T.
[5] J. W. Mitchell, Phil. Mag. **40**, 667 (1949).

Causes of Abnormal Efficiencies in Scintillation Counters*

W. G. CROSS**
Department of Physics, Harvard University, Cambridge, Massachusetts
March 6, 1950

IN the detection of beta- and gamma-rays with scintillation counters, numerous investigators have obtained efficiencies up to several times higher than those predicted theoretically.[1] The purpose of this note is to discuss some sources of these extra counts. Scattered gamma-rays, delayed pulses produced in the photo-multiplier tube or crystal, and multiple pulses from the amplifier when overloaded, have been suggested.[1]

For the Jordan-Bell amplifier[2] used with our counter, we observed a long second pulse to follow strong scintillation pulses, resulting in a sharp turn-up of the integral bias curve for small pulse heights (Fig. 1; the pulse height scale is a relative one, the smallest measured pulses being 10 volts high, to minimize the effect of any instability in the discrimination level). Tests with artificial pulses showed that these second pulses were due to overloading in the amplifier. When the detection of nearly all the

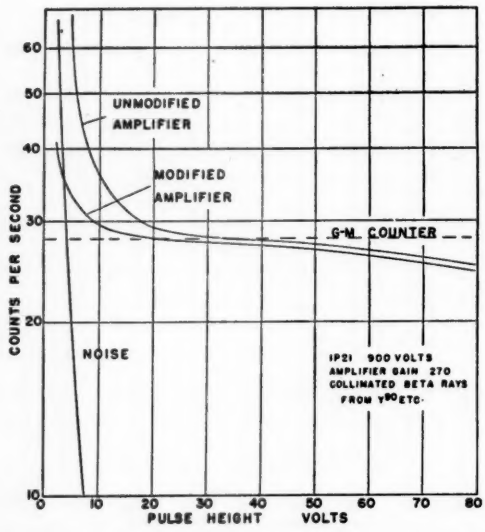

FIG. 1. The effect of spurious pulses on the low energy end of an integral bias curve.

Compton electrons produced in the crystal by gamma-rays is required, the range of energies of these electrons makes it essential that the amplifier be able to handle a wide range of pulse sizes.

When these second pulses had been eliminated by crystal diode clippers in the amplifier, the bias curve of pulses from an anthracene scintillation counter, illuminated by a well-collimated beam of beta-rays, still turned up sharply for pulse heights smaller than 10 volts, corresponding to 70-kev electrons (Fig. 1, noise rate subtracted). The correct beam strength shown was determined to within 1 percent with an end-window Geiger counter. An aluminum foil placed between the crystal and the photo-multiplier reduced the counting rate, at the lowest bias setting used, to less than 1 percent of that given by the crystal, showing that the extra counts were not due to beta-rays acting directly on the photo-multiplier. Similar results were obtained with anthracene purified by three independent methods[3] and with stilbene.

By introducing a variable deadtime it was shown that about half the extra pulses occurred within 200 microseconds of another pulse, and more small pulses were indeed observed on a scope during the 200 microseconds following large pulses than in an equal time 800 microseconds later. Pile-up of noise and signal pulses, which can lead to abnormal efficiencies, was not appreciable for the conditions used.

The crystal was removed and the same photo-multiplier illuminated by artificial flashes, 3 microseconds long and bright enough to give pulses larger than the largest ones from anthracene excited by Y^{90} beta-rays. At the minimum bias setting used the counting rate due to signal and noise together was equal, to within 1 percent, to the sum of the separate signal and noise rates. Hence under the conditions used, such light flashes produced no measurable secondary pulses in the photo-multiplier tube[4] or electronic equipment.

Except for the remote possibility that the much shorter flashes from anthracene, of about the same intensity, produce delayed pulses in the photo-multiplier, the extra pulses can only be delayed scintillations from phosphorescent decay in the anthracene.[5] The size of the extra pulses is compatible with their being produced by single electrons from the photo-multiplier cathode. That a weak, relatively long-period phosphorescence exists in anthracene and stilbene is demonstrated by removing a strong source from beside the scintillation counter. Counting continues for several seconds, while no such effect occurs with the photo-multiplier tube alone.

A much stronger long-period phosphorescence is exhibited by scheelite and artificial calcium tungstate crystals. By taking the counting rate at a sufficiently low bias, apparent efficiencies of several hundred percent can be obtained.

Because the delayed scintillations from anthracene extend over several hundred microseconds, we have usually found it impracticable to eliminate them by the use of an artificial deadtime. For incident gamma-rays of 2.5 Mev or less, they are apparently important only when electrons with energies less than about 70 kev must be measured. Projecting the straight part of gamma-ray integral bias curves (for organic crystals) back to zero pulse height has repeatedly given counting rates agreeing with the calculated rates to within 5 percent.

The advice of Professor N. F. Ramsey and suggestions and assistance of R. W. Birge, D. Bodansky and L. S. Lavatelli are gratefully acknowledged.

* Assisted by the joint program of the ONR and AEC.

** Now at the Chalk River Laboratory, National Research Council of Canada, Chalk River, Ontario, Canada.

[1] Rochester Conference on Scintillation and Crystal Counters (1948); R. Hofstadter, Phys. Rev. 75, 796 (1949); G. J. Hine, Science 110, 380 (1949).

[2] W. H. Jordan and P. R. Bell, Rev. Sci. Inst. 18, 703 (1947).

[3] By Professor J. A. Irvine of M.I.T., by the Harshaw Chemical Company and by the Reilly Tar and Chemical Company.

[4] With high photo-multiplier voltages, false pulses from photo-multiplier tubes have been reported. Oak Ridge Symposium on Scintillation Counters (1949); AECU 583.

[5] Delayed pulses from anthracene excited by very high energy protons were reported by L. Wouters, Oak Ridge Symposium on Scintillation Counters (1949).

Proceedings of the American Physical Society

MINUTES OF THE MEETING OF THE OHIO SECTION AT CINCINNATI, MARCH 4, 1950

THE 1950 Midwinter Meeting of the Ohio Section of the American Physical Society was held at the Department of Physics of the University of Cincinnati on Saturday, March 4. There was a very bad weather report the day preceding, so the attendance was small, only 50 being present. Dr. Isay A. Balinkin repeated his demonstration lecture on "Techniques of Color" and Dr. Alex E. S. Green gave a lecture on "Basic Principles of Atomic Energy." Dr. C. Harrison Dwight contributed a paper on the subject "Specialized Physics Courses" and five other contributed papers were presented, the abstracts of which are appended.

LEON E. SMITH, *Secretary*,
Denison University
Granville, Ohio

Formalistic vs. Realistic Theories. ALEX E. S. GREEN, *University of Cincinnati.*—The equivalence of the essential features of the Pauli-Villars regularization technique[1] with the writer's generalization procedure[2] is shown. The weighted superposition of fields so obtained is probably the only one powerful enough to offer hope of saving the framework of a linear local field theory. A realistic interpretation of all the fields has been criticized because in the quantum version negative energy bosons appear. Because of this some physicists have adopted a formalistic viewpoint and at the end of their calculations make all of the meson masses, but one, infinite. The procedure is then called a device without physical meaning. This confession unfortunately does not absolve the formalists from several important and inescapable consequences of their limiting process. We examine these and conclude that the formalists have replaced the realists difficulties by much greater difficulties. Apparently we must either try harder to find a satisfactory realistic interpretation or else give up the linear local field framework.

[1] W. Pauli and F. Villars, Rev. Mod. Phys. 21, 434 (1949).
[2] A. Green, Phys. Rev. 73, 519 (1948); 75, 1926 (1949).

Experimental and Theoretical Mesons. ALEX E. S. GREEN, *University of Cincinnati.*—Most of the arguments concerning the relative merits of a formalistic or realistic interpretation of a generalized (or regularized) field theory have been based upon working assumptions and perturbation methods which are at least as questionable as the basic aspects of the theory. It would thus seem wisest for the moment to look to nature for a verdict in the controversy. Recent experiments in electrodynamics can be explained with the Podolsky-Bopp theory (or a more generalized theory) in the manner suggested by Feynman without the formalistic limiting process but using instead the meson mass (or masses) of the μ-, π- or τ-mesons. The direct static effect of the meson field may indeed account for 2–7 Mc of the 11 ± 5-Mc discrepancy found by Bethe between the experimental and previously calculated Lamb shift. In meson theory we have already been presented with solid evidence for the existence of at least two *real* N.F. mesons which could not be accommodated if the formalistic limiting process were used without resorting to a monstrosity such as a regularized mixture theory. As soon as the number and properties of the very heavy mesons are determined we will know whether a realistic generalized theory can be more successful.

Multi-Layer Optical Interference Filters.* W. H. SHAFFER AND R. A. OETJEN, *Mendenhall Laboratory of Physics, Ohio State University.*—A multi-layer reflection interference filter is made by depositing on a good reflecting surface alternately layers of dielectric and thin metallic films. The theory has been developed for a two-layer filter, containing two dielectric layers separated by a metallic film, and such a filter has been constructed. The characteristics of this filter agree well with the theoretical predictions. Mulit-layer interference filters offer good promise of a method of producing relatively sharp and well-isolated pass bands with one filter plate.

* The work described in this paper was carried out, in part, under a contract between the Wright-Patterson Air Force Base of the Air Materiel Command and the Ohio State University Research Foundation.

Beta-Spectrum of Prometheum 147. WERNER S. EMMERICH AND J. D. KURBATOV, *Ohio State University.*—Prometheum 147 disintegrating by beta-emission of 223 kev[1] has been obtained from the Oak Ridge National Laboratory, AEC. A sample on Zapon film was mounted in a helium filled cloud chamber operated with a magnetic field of 220 gauss. The beta-spectrum obtained from electron tracks showed the shape of an allowed transition with an end point of 225 ± 10 kev.[2] In addition, three groups of monochromatic electrons in the range of energies of 60, 150, and 200 kev were observed, which have not been reported previously. The number of monochromatic electrons is about five percent of the total electrons in the continuous spectrum. The presence of monochromatic electrons suggests the existence of long-lived metastable states in the prometheum region. The nuclear species is not yet established with certainty. A grant-in-aid for research given by the Graduate School of the Ohio State University is gratefully acknowledged.

[1] P. W. Levy, Plut. Proj. MonP-314, 84, June 1947.
[2] Compare also: Price, Motz, and Langer, Phys. Rev. 77, 744 (1950), and Lidofsky, Macklin, and Wu, Phys. Rev. 76, 1888 (1949).

A Heat Conduction Problem. BORIS PODOLSKY.—The problem of determining the temperature distribution generated by a sinusoidally varying point heat source within a moving medium is considered, and the temperature wave remaining after the disappearance of the transients is found.